

Aus dem Universitätsklinikum Heidelberg
Zentrum für Orthopädie, Unfallchirurgie und Paraplegiologie

Forschungszentrum für Experimentelle Orthopädie
Leitung: Prof. Dr. rer. biol. hum. Wiltrud Richter

**Physicochemical stimuli to enhance the quality of human engineered cartilage:
The role of osmolarity and calcium**

Inauguraldissertation
zur Erlangung des Doctor scientiarum humanarum (Dr. sc. hum.)
an der
Medizinischen Fakultät Heidelberg
der
Ruprecht-Karls-Universität

vorgelegt von
Tim Dieter Hammersen

aus
Frankfurt a.M. (Höchst)

2023

Dekan:

Prof. Dr. med. Dr. h.c. Hans-Georg Kräusslich

Doktormutter:

Frau Prof. Dr. rer. biol. hum. Wiltrud Richter

TABLE OF CONTENTS

TABLE OF CONTENTS	I
ABBREVIATIONS	V
1 Introduction	1
1.1 Structure and function of articular cartilage.....	1
1.2 Cartilage defects and regenerative approaches.....	3
1.3 Molecular regulators of cartilage homeostasis.....	5
1.4 Regulation of cartilage homeostasis by mechanical loading.....	6
1.5 Mechanisms of mechanical signal transduction.....	7
1.6 Osmolarity.....	10
1.6.1 Osmotic pressure in articular cartilage.....	11
1.6.2 The role of FCD for the level of osmotic pressure in articular cartilage.....	11
1.7 Response of chondrocytes to acute hyperosmotic challenge.....	13
1.7.1 Regulation of GAG synthesis by acute hyperosmotic challenge.....	13
1.7.2 Regulation of SOX9 by acute hyperosmotic challenge.....	15
1.7.3 Regulation of <i>COL2A1</i> and <i>ACAN</i> gene expression by acute hyperosmotic challenge.....	15
1.8 Response of chondrocytes to long-term hyperosmotic challenge.....	17
1.8.1 Regulation of GAG synthesis by long-term hyperosmotic stimulation.....	17
1.8.2 Regulation of SOX9 by long-term hyperosmotic stimulation.....	17
1.8.3 Regulation of <i>COL2A1</i> and <i>ACAN</i> expression and GAG deposition by long-term hyperosmotic stimulation.....	17
1.9 Signal transduction after hyperosmotic stimulation of chondrocytes.....	19
1.9.1 Regulation of MAPK signaling by hyperosmotic challenge.....	19
1.9.2 Regulation of the osmo-sensitive transcription factor NFAT5.....	20
1.10 The role of different cations for hyperosmotic stimulation of chondrocytes.....	21
1.11 Relevance of extracellular calcium for clinically significant neocartilage maturation.....	23
1.11.1 Relevance of extracellular calcium for neocartilage maturation in osteochondral defects.....	24
1.11.2 Effect of extracellular calcium on cartilage formation by AC and MSC.....	26
1.12 Aim of the study.....	28
2 Materials	29
2.1 Chemical reagents.....	29
2.2 Cell culture supplements.....	31
2.3 Consumables.....	31
2.4 Radioactive isotopes.....	32
2.5 Kits & ELISA.....	32
2.6 Histological staining reagents.....	32

TABLE OF CONTENTS

2.7 Enzymes	33
2.8 Biomaterials	33
2.9 Growth factors	33
2.10 Agonists/Inhibitors.....	33
2.11 Antibodies	33
2.12 Plasmids	34
2.13 Cells	34
2.14 Primers	35
2.15 Equipment/Devices.....	35
2.16 Software.....	36
2.17 Buffers and media.....	37
2.17.1 Agarose-gel electrophoresis	37
2.17.2 Cell culture	37
2.17.3 Assay buffer	39
2.17.4 SDS Page.....	39
2.17.5 Western blot	40
2.17.6 Histology	40
2.17.7 Bacteria growth media.....	41
3 Methods	41
3.1 Legal and ethical aspects of the study	41
3.2 Cell culture	42
3.2.1 Isolation and expansion of AC.....	42
3.2.2 Isolation and expansion of MSC.....	42
3.2.3 Seeding and maturation of AC and MSC in collagen scaffolds	43
3.2.4 Hyperosmotic stimulation of cartilage TE constructs	43
3.2.5 Calcium, Niclosamide and PTHrP stimulation of cartilage TE constructs	44
3.2.6 Expansion of cell lines	44
3.3 Plasmid amplification and preparation.....	44
3.4 Transfection and overexpression.....	45
3.5 Histological analyses	45
3.5.1 Embedding of cartilage TE constructs.....	45
3.5.2 Preparation of tissue sections for histological staining	46
3.5.3 Safranin Orange staining.....	46
3.5.4 Immunohistochemical staining.....	46
3.5.5 Alizarin Red S staining	47
3.5.6 Mounting of stained tissue sections	47
3.6 Collection of human blood plasma	47
3.7 Biochemical analyses	48
3.7.1 DNA quantification.....	48
3.7.2 Glycosaminoglycan quantification (DMMB Assay)	48
3.7.3 Protein quantification	49
3.7.4 Alkaline phosphatase activity assay.....	49

3.7.5 Calcium quantification assay	50
3.8 Radiolabel incorporation for quantification of <i>de novo</i> GAG synthesis.....	50
3.9 Molecular biological analyses.....	51
3.9.1 Isolation of total RNA	51
3.9.2 Quantification of RNA concentration	51
3.9.3 Purification of total RNA.....	51
3.9.4 Reverse transcription	52
3.9.5 Quantitative PCR	52
3.9.6 DNA gel electrophoresis	54
3.10 Protein analyses	54
3.10.1 Generation of whole cell protein lysates	54
3.10.2 Generation of pepsin-digested collagen lysates	55
3.10.3 SDS gel electrophoresis	55
3.10.4 Western blotting	56
3.10.5 Western blotting for collagen detection	56
3.10.6 Enzyme-linked immunosorbent assay (ELISA).....	56
3.10.7 PTHrP Immunoradiometric assay.....	58
3.11 Statistical analysis.....	59
4 Results.....	60
4.1 Acute hyperosmotic stimulation of cartilage tissue engineering constructs.....	60
4.1.1 Maturation of engineered cartilage	60
4.1.2 Regulation of ERK and p38 pathways by acute hyperosmotic stimulation at low FCD	61
4.1.3 Regulation of pERK and p38 pathways by acute hyperosmotic stimulation at high FCD	63
4.1.4 Expression of osmo-response genes after acute hyperosmotic stimulation at low versus high FCD	64
4.1.5 Regulation of SOX9 by acute hyperosmotic stimulation at low versus high FCD	65
4.1.6 Regulation of <i>COL2A1</i> and <i>ACAN</i> expression by acute hyperosmotic challenge at low versus high FCD	66
4.1.7 Regulation of TGF β and BMP pathways by acute hyperosmotic stimulation at low versus high FCD	67
4.1.8 Regulation of GAG synthesis by hyperosmotic stimulation at low vs high FCD.....	69
4.1.9 Effect of hyperosmotic stimulation on the expression of mechano-response genes	70
4.2 Long-term hyperosmotic stimulation of cartilage tissue engineering constructs	72
4.2.1 Evaluation of calcium concentrations in the medium.....	72
4.2.2 Effect of long-term hyperosmotic stimulation on DNA content of AC and MSC-based TE constructs	74
4.2.3 Effect of long-term hyperosmotic stimulation on the expression of differentiation markers in AC and MSC-derived chondrocytes.....	75
4.2.4 Effect of long-term hyperosmotic stimulation of AC on GAG synthesis and GAG deposition	76
4.2.5 Effect of long-term hyperosmotic stimulation of MSC-derived chondrocytes on GAG synthesis and GAG deposition	78

4.2.6	Effect of long-term hyperosmotic stimulation of AC and MSC-derived chondrocytes on type II collagen deposition.....	79
4.2.7	Effect of long-term hyperosmotic stimulation on GAG synthesis of AC and MSC-derived chondrocytes using different osmolytes	81
4.2.8	Influence of long-term extracellular calcium stimulation on the phenotype of AC and MSC-derived chondrocytes	82
4.2.9	The effect of long-term extracellular calcium stimulation of AC and MSC-derived chondrocytes on the regulation of anabolic signaling mechanisms	84
4.2.10	The regulation of catabolic signaling mechanisms in AC and MSC-derived chondrocytes after long-term extracellular calcium stimulation	87
4.2.11	The effect of long-term extracellular calcium stimulation of AC and MSC-derived chondrocytes on PTHrP signaling	90
4.2.12	Effect of long-term extracellular calcium stimulation on cAMP levels in AC and MSC-derived chondrocytes.....	98
4.2.13	Effect of PTHrP stimulation on differentiation marker expression, GAG synthesis and GAG deposition in AC-based TE constructs	99
4.2.14	Comparison of calcium sensing receptor levels in AC and MSC-derived chondrocytes	101
5	Discussion	103
5.1	Effects of acute hyperosmotic stimulation on cartilage homeostasis	103
5.1.1	Establishment of AC-based cartilage TE constructs with low and high FCD.....	103
5.1.2	Establishment of acute hyperosmotic response markers for engineered cartilage replacement tissue	105
5.1.3	Acute hyperosmotic regulation of pro-chondrogenic signaling pathways.....	107
5.1.4	The role of acute hyperosmotic stimulation as a sub-parameter of mechanical compression.....	109
5.2	Effects of long-term high extracellular calcium stimulation on cartilage matrix formation	111
5.2.1	Comparison of AC- and MSC-based cartilage TE constructs at control conditions	112
5.2.2	Inverse regulation of cartilage ECM formation after long-term extracellular calcium stimulation.....	113
5.2.3	Role of anabolic and catabolic signaling mechanisms for calcium-regulated changes in GAG synthesis and cartilage ECM formation.....	115
5.2.4	Influence of high extracellular calcium concentrations on the phenotype of AC and MSC-derived chondrocytes	119
5.2.5	Implications for osteochondral tissue engineering	120
5.3	Limitations of the study	121
5.4	Conclusion and outlook	124
6	Summary	125
7	Zusammenfassung	127
8	References	129
	EIGENANTEIL AN DER DATENERHEBUNG UND -AUSWERTUNG	VI
	EIGENE VERÖFFENTLICHUNGEN UND BEITRÄGE.....	VI
	APPENDIX.....	VIII
	LEBENS LAUF	X
	DANKSAGUNG	XI
	EIDESSTÄTLICHE VERSICHERUNG	XIII

ABBREVIATIONS

3D	Three-dimensional
AC	Articular chondrocytes
ACAN	Aggrecan
ACI	Autologous chondrocyte implantation
ALP	Alkaline phosphatase
BMP	Bone morphogenetic protein
bp	Base pair
BSA	Bovine serum albumin
Ca ²⁺	Calcium ion
[Ca ²⁺] _e	Extracellular calcium concentration
cDNA	Complementary DNA
CPM	Counts per minute
Cq	Quantification cycle (threshold cycle, Ct)
COL2A1	Type II collagen
COL10A1	Type X Collagen
Da	Dalton
DMEM	Dulbecco's Modified Eagle's Medium
DMMB	1,9-Dimethylmethylene Blue
DMSO	Dimethyl sulfoxide
DNA	Deoxyribonucleic acid
dNTP	Deoxynucleotide triphosphate
dT-primer	Deoxythymidin primer
ECM	Extracellular matrix
EDTA	Ethylenediamine tetraacetic acid
ERK	Extracellular signal-regulated kinase
FCD	Fixed charge density
FCS	Fetal calf serum
FGF	Fibroblast growth factor
GAG	Glycosaminoglycan
HA	Hydroxyapatite

ABBREVIATIONS

HRP	Horseradish peroxidase
IF	Immuno-fluorescence
IHC	Immuno-histochemistry
IRMA	Immunoradiometric assay
K ⁺	Potassium ion
MAPK	Mitogen-activated protein kinase
mAb	Monoclonal antibody
MMP	Matrix metalloproteinase
mRNA	Messenger ribonucleic acid
MSC	Mesenchymal stromal cells
Na ⁺	Sodium ion
OA	Osteoarthritis
p	Prefix for phosphorylated proteins
pAb	Polyclonal antibody
PAGE	Polyacrylamide gel electrophoresis
PBS	Phosphate-buffered saline
PCR	Polymerase chain reaction
PG	Proteoglycan
PTHrP	Parathyroid hormone-related protein
RT	Room temperature
RT-qPCR	Reverse transcription quantitative PCR
SafO	Safranin-Orange
SDS	Sodium dodecyl sulfate
SEM	Standard error of the mean
SOX9	Sex determining region Y-box 9
TBS	Tris-buffered saline
TCP	Tricalcium phosphate
TE	Tissue engineering
TGFβ	Transforming growth factor β
WB	Western blot

1 Introduction

1.1 Structure and function of articular cartilage

Articular cartilage is a subtype of hyaline cartilage that is found in diarthrodial joints at the surface of long bones, where it functions as a shock absorbing and protective layer to withstand high mechanical forces that arise from skeletal movement. Together with the surrounding lubricating synovial fluid it enables a frictionless movement of the joint. To achieve these properties, articular cartilage has a highly organized structure and molecular composition in which each individual component significantly contributes to the function of the tissue.

Articular cartilage is organized in four different layers that are characterized by a specific composition of the main molecular components of the tissue's extracellular matrix (ECM): Collagens and proteoglycans (PG, see below). Chondrocytes are the only cell type in articular cartilage and are embedded in a dense mesh of highly organized ECM.

The uppermost layer of articular cartilage, facing the joint space, is called *superficial zone*. In this layer, chondrocytes have a flat morphology and are embedded in a mesh of thin collagen fibrils that run almost exclusively parallel to the surface. In the subsequent *middle zone*, the number of chondrocytes decreases and the cells have a characteristic round morphology. The collagen fibers are thicker in size and are oriented randomly. In the *deep zone*, chondrocytes are small and round in morphology and reside in vertically oriented stacks of multiple chondrocytes, called chondrons. The collagen concentration is reduced in this zone but contains thick fibrils that are oriented perpendicular to the surface. The concentration of PG is lowest in the superficial zone and increases with depth of the tissue. Articular cartilage is connected to the subchondral bone via a transition zone of *calcified cartilage* in which chondrocytes become hypertrophic and start to secrete specific molecules to induce matrix mineralization (Buckwalter and Mankin 1998).

Collagens make up 60% of the dry mass of articular cartilage and with 95% of total collagen, type II collagen is by far the most abundant collagen in the tissue. Type II collagen is organized as a homotrimer of $\alpha_1(\text{II})$ chains, encoded by the gene *COL2A1*, that form a characteristic triple helix structure. Other collagens include type IX collagen and type XI collagen, which together with type II collagen form a porous mesh of collagen fibrils that provide the typical tensile strength of the tissue. Type X collagen is exclusively secreted by hypertrophic chondrocytes in the deep and

calcified cartilage zone. It consists of a homotrimer of $\alpha_1(X)$ chains, encoded by the gene *COL10A1* and is involved in matrix mineralization (Gahunia et al. 2020).

Proteoglycans (PG) present 30% of the tissue's dry weight. PG are large molecules composed of a core protein to which glycosaminoglycan (GAG) chains are covalently attached. The most abundant PG in articular cartilage is aggrecan which is encoded by the gene *ACAN*. The covalently attached GAG side chains consist of highly sulfated polysaccharides, of which chondroitin sulfate is the most common one in articular cartilage (Gahunia et al. 2020). By binding to hyaluronic acid via a link protein, several hundreds of aggrecans can form large aggregating clusters (Figure 1). Due to the high degree of sulfation, synthesis of newly formed GAGs can be monitored via measurement of incorporation of radiolabeled ^{35}S -sulfate into the ECM. The high degree of sulfation also provides a high negative fixed charge density (FCD) to the tissue, which, by attracting positively charged counter ions, creates the characteristic osmotic pressure of the tissue. As a result of the high FCD, water is attracted to the tissue and stored in the ECM. Besides collagens and PG, water is the main constituent of articular cartilage which presents 80% of the wet weight of the tissue. Together, PG and water create the high compressive strength of the tissue.

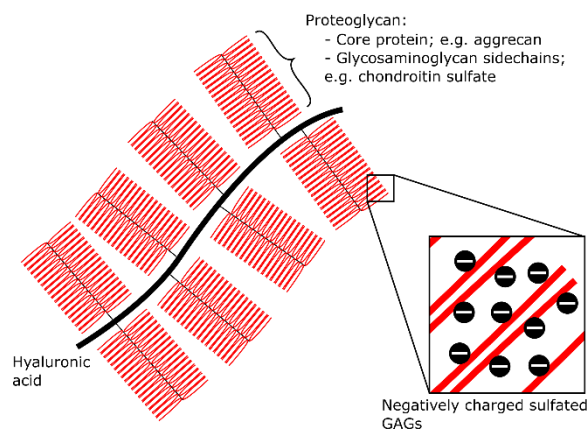


Figure 1 Schematic structure of proteoglycans. Several proteoglycans composed of a core protein such as aggrecan and sulfated glycosaminoglycan (GAG) side chains are attached to a hyaluronic acid molecule. Sulfate residues of GAGs provide high negative charge to the complex.

Articular chondrocytes represent only 1% of the dry mass of the tissue (Stockwell 1967). Due to their post-mitotic nature and their isolated location surrounded by a densely packed mesh of ECM, chondrocytes cannot divide or migrate within the tissue. Nevertheless, chondrocytes can sense and respond to external stimuli and their main task is to maintain a healthy articular cartilage matrix by regulating synthesis and degradation of ECM molecules, referred to as cartilage homeostasis.

Macroscopically, articular cartilage is a non-innervated, avascular and alymphatic tissue and supply of the tissue is maintained predominantly via passive diffusion, resulting in a low regeneration capacity. Therefore, cartilage defects induced by mechanical overuse, traumatic injury or as a result of genetic predisposition do not heal spontaneously but lead to progressive deterioration of the tissue, ultimately developing into the degenerative whole joint disease osteoarthritis (OA) (Litwic et al. 2013; Visser et al. 2015). Thus, identification and treatment of cartilage defects is essential to prevent disease progression and restore the function of the tissue (Gelber et al. 2000).

1.2 Cartilage defects and regenerative approaches

OA is the most prevalent joint disease in developed countries, affecting nearly 50% of women (48.1%) and one third of men (31%) over the age of 65 in Germany (Fuchs et al. 2017). Clinical symptoms of OA include pain, joint stiffness and instability. As a consequence, reduced quality of life and physical inactivity result in the development of several comorbidities (Dantas et al. 2021). Thus, OA and OA-related diseases create an enormous economic burden for the healthcare system and effective regenerative treatments are highly desired. In order to treat articular cartilage defects and to restore the function of the tissue, several clinical approaches have evolved, including the use of biomaterials (Garrigues et al. 2014; Levorson et al. 2013), cartilage transplantation (LaPrade et al. 2009) and cell-based regenerative therapies (Al Faqeh et al. 2012). Since chondrocytes cannot self-renew or migrate in the tissue, cell-based approaches have become particularly relevant to restore the vital aspect of the tissue.

Due to a cost-effective and minimally invasive procedure, first choice for chondral defect treatment is the **microfracture** technique, aiming at the stimulation of the self-healing capacity of the tissue. For this purpose, drilling into the subchondral bone is performed which leads to bleeding into the defect and blood clot formation (Steadman et al. 1997). This allows recruitment of progenitor cells from the bone marrow into the defect to stimulate cartilage repair. Although this technique provides functional improvement in the short-term, in the long-term the formation of fibro cartilage instead of hyaline articular cartilage limits the tissues resistance to mechanical deterioration (Goyal et al. 2013; Kreuz et al. 2006). While microfracture is typically applied to small lesions below 2-4 cm² in size, larger defects are treated by **autologous chondrocyte implantation (ACI)** (Evans 2013). ACI was introduced in 1989 for the treatment of rabbit patellar focal defects and in 1994 applied to patients to treat full thickness chondral defects (Brittberg et al. 1994; Grande et al. 1989). In the first generation of ACI, isolation and *in vitro* expansion of autologous chondrocytes harvested from the defect side or from non-weight bearing areas of the patient

served as cell source for implantation into a debrided lesion under a periosteal cover. Although promising results regarding clinical symptoms in long-term follow up studies of 10 to 20 years have been observed (Peterson et al. 2010), the disadvantages of ACI are a cost-intensive two-step procedure, a high rate of revision and donor side morbidity at the area of chondrocyte harvest (Richter et al. 2016). Subsequently, **matrix assisted autologous chondrocyte implantation** evolved, in which a type I/III collagen scaffold served to support cartilage neogenesis in the defect (Behrens et al. 2006). ACI thereby entered the field of cartilage **tissue engineering** (TE).

TE is an interdisciplinary field that combines approaches from life science and engineering to generate tissues outside of the body that can then be implanted into the defective areas of the body (Langer and Vacanti 1993). Research in cartilage TE, therefore, attempts to provide a permanent treatment option by *ex vivo* formation of engineered tissue with similar properties compared to the native tissue. For this purpose, a combination of cells, biomaterials, bioactive factors and physical stimuli is used. More specifically, TE includes the isolation and *in vitro* cultivation of cells which are then seeded onto tissue scaffolds where they proliferate, migrate, and differentiate using appropriate nutrients and growth factors. Stimulation of cells with physical or chemical stimuli can be used to further guide tissue development towards the desired phenotype (Zhang et al. 2009).

In order to generate functional cartilage TE constructs with similar properties to native articular cartilage, it is important to ensure the deposition of the main components of the cartilage ECM (type II collagen and PG) in the constructs. Together, type II collagen and PG provide the crucial architecture of the tissue that is needed to exert its function in the joint. However, a general drawback of engineered cartilage is that it does not reach similar type II collagen and PG levels like native tissue (Eyrich et al. 2007; Hu and Athanasiou 2006) and therefore presents itself with an inappropriate composition of the ECM that cannot adequately respond to the demanding mechanical conditions in the joint (Hunziker 2009). In order to generate TE constructs that can resist the challenging mechanical conditions in the joint in the long term, it is necessary to guide engineered cartilage towards a high PG and type II collagen content. For this purpose, it is important to understand the response of chondrocytes to mechanical challenge in more detail. Thus, the basic molecular processes that determine cartilage homeostasis and its regulation by mechanical stimuli is an active field of investigation (Glatt et al. 2019; O'Connor et al. 2013; Responde et al. 2012).

1.3 Molecular regulators of cartilage homeostasis

To counteract mechano-induced wear and tear processes and to maintain the structural composition of the tissue, chondrocytes modulate the cartilage ECM throughout life by keeping the synthesis and degradation of the ECM in balance.

Cartilage matrix production is regulated by the expression of ECM-related genes, including those encoding for type II collagen (*COL2A1*) and aggrecan (*ACAN*). Main molecular pathways for the regulation of cartilage matrix homeostasis include the growth factor networks of the transforming growth factor β (TGF β) family, including the bone morphogenic protein (BMP) pathway (Thielen et al. 2019). TGF β and BMP pathway activity is regulated via binding of TGF β and BMP ligands to specific type II serine threonine-protein kinase receptors to recruit the corresponding type I receptors, forming a heteromeric receptor complex (Thielen et al. 2019). Each ligand of the TGF β superfamily binds to a characteristic combination of type I and type II receptors (Heldin et al. 1997). During canonical TGF β signaling, TGF β binds to TGF β receptor II (TGFBR2) which forms a heterodimer with TGF β receptor I (TGFBR1, also known as ALK5) resulting in the phosphorylation of SMAD2/3 proteins (Heldin et al. 1997). Phosphorylated SMAD2/3 proteins then bind SMAD4 and translocate into the nucleus to induce the expression of ECM-related molecules (Zawel et al. 1998). TGF β is essential for *in vitro* redifferentiation of chondrocytes via induction of sex determining region Y-box 9 (SOX9) (Furumatsu et al. 2005), the transcriptional master regulator of chondrocyte development *in vivo* (Healy et al. 1999) which is involved in upregulation of ECM-associated genes *COL2A1* and *ACAN in vitro* (Dexheimer et al. 2016; Hellingman et al. 2011). To a certain extent, TGF β can also induce SMAD1/5/9 phosphorylation, which is typically associated with the canonical BMP signaling pathway (Thielen et al. 2019; Wu et al. 2016).

BMPs belong to the TGF β superfamily of proteins. They were also shown to stimulate cartilage formation via induction of SOX9 *in vivo* (Healy et al. 1999) and induce proteoglycan and type II collagen production *in vitro* (Flechtenmacher et al. 1996). BMP ligands bind to BMP receptor I (ALK3) which forms a complex with BMP receptor II, ALK2 or ALK6 to induce SMAD1/5/9 phosphorylation (Heldin et al. 1997). Upon complex formation with SMAD4 and translocation to the nucleus, SMAD1/5/9 binds to BMP responsive elements to regulate the expression of cartilage ECM-related molecules (Blaney Davidson et al. 2009; Kusanagi et al. 2000). In addition to regulating the expression of cartilage ECM-related genes, TGF β and BMPs were also shown to induce de novo synthesis of proteoglycans and collagens *in vitro* (Luyten et al. 1994; Redini et al. 1988; van der Kraan et al. 1992) and *in vivo* (van Beuningen et al. 1998; van Beuningen et al. 1994).

Cartilage matrix destruction is mediated via collagen-degrading enzymes such as matrix metalloproteinases (MMPs) or aggrecan-degrading enzymes such as ADAMTS-5, inducing net loss of collagens and GAGs (Billinghurst et al. 1997; Hurskainen et al. 1999). Molecular pathways involved in cartilage matrix degradation are the NF- κ B and COX2-PGE₂ signaling networks. Induction of NF- κ B signaling using IL-1 β or TNF α reduced the GAG and collagen content of human articular chondrocytes *in vitro* (Bassleer et al. 1998) and inhibited Col2a1 expression in rat articular chondrocytes (Seguin and Bernier 2003). COX2/PGE₂ signaling has been described as a downstream mediator of the NF- κ B signaling pathways (Park et al. 2006; Tanabe and Tohnai 2002) and IL-1 β -mediated reduction of PG synthesis and induction of matrix degradation was dependent on COX2 and PGE₂ activity in human OA chondrocytes (Attur et al. 2008).

Thus, while net increase in cartilage ECM is characterized by increased synthesis as well as deposition of GAGs and type II collagen, cartilage degradation occurs due to the activity of matrix degrading enzymes. In order to deposit natural amounts of type II collagen and PG in cartilage replacement tissue, a high ECM synthesis is desired. Regulation of ECM synthesis should, therefore, be a main read out parameter in studies aiming to improve cartilage replacement tissue. Since cartilage homeostasis is determined by a tight regulation of the pro-anabolic growth factors TGF β and BMP via regulation of SOX9 and expression of cartilage ECM molecules *COL2A1* and *ACAN*, these molecules should also be a focus as read out parameters.

1.4 Regulation of cartilage homeostasis by mechanical loading

During daily activities articular cartilage is exposed to mechanical loading of different natures, including compression, shear stress and hydrostatic pressure. Originally considered an inert tissue, it is now known that cartilage, specifically chondrocytes embedded in the ECM, respond to diverse physical stimuli. The dense ECM around chondrocytes thereby serves as a transducer of biomechanical and biochemical signals (Chen et al. 2013; Guilak et al. 2006). In healthy participants, physical activity showed a protective effect on cartilage volume (Foley et al. 2007; Racunica et al. 2007) and resulted in increased PG synthesis (Kiviranta et al. 1987; Parkkinen et al. 1993), whereas lack of mechanical signals due to immobilization can lead to degradation of the cartilage ECM (Brady et al. 2015). Likewise, supraphysiological levels of loading by mechanical overuse are one of the main risk factors for OA development and cartilage degradation (Arden and Nevitt 2006; Fahy et al. 2018; Ramage et al. 2009), demonstrating the relevance of mechanical loading for cartilage homeostasis. Due to limitations of *in vivo* studies to determine the mechano-induced biochemical pathways during cartilage homeostasis, *in vitro* studies have been performed to evaluate molecular aspects of load-induced articular cartilage homeostasis.

Upon mechanical challenge of cartilage, forces are transduced via the ECM and subsequently perceived by the chondrocytes. The arriving mechanical signals are then translated into intracellular signaling cascades, to regulate anabolic or catabolic processes (Chowdhury et al. 2004). It is known that dynamic mechanical compression of bovine articular cartilage explants induced the expression of *COL2A1* and *ACAN* mRNA (Fitzgerald et al. 2008) and mechano-induced activation of TGF β signaling was suggested by induction of *ALK5* and TGF β gene expression in bovine cartilage explants (Madej et al. 2014). Moreover, dynamic mechanical loading also stimulated ECM synthesis in several studies using bovine articular chondrocytes (Kim et al. 1994; Quinn et al. 1998; Sah et al. 1989).

In an attempt to determine the contribution of mechanical loading to cartilage homeostasis in human articular chondrocytes, our group has unraveled molecular details of the mechano-response of chondrocytes in a relevant three-dimensional (3D) model of human articular cartilage (Hecht et al. 2019; Lückgen et al. 2022; Praxenthaler et al. 2018; Scholtes et al. 2018). Importantly, we demonstrated that the response of chondrocytes to mechanical loading depended on the amount of ECM that was present in the loaded tissue (Praxenthaler et al. 2018). Three hours of cyclic unconfined compression at low GAG content resulted in a catabolic response of chondrocytes, demonstrated by reduced GAG synthesis and lower *ACAN* and *COL2A1* expression, while *SOX9* mRNA and protein levels remained unaffected. In contrast, mechanical loading at high GAG content increased GAG synthesis along with *SOX9* mRNA and protein levels and maintained *ACAN* and *COL2A1* expression. Mechanical loading also increased the expression of BMP ligands *BMP2* and *BMP6* independent of the GAG content of the tissue. No changes in *SMAD2/3* and *SMAD1/5/9* signaling were observed after mechanical loading (Praxenthaler et al. 2018). Moreover, the GAG synthesis rate after mechanical loading positively correlated with the GAG content of the construct, demonstrating that the response of chondrocytes to mechanical loading depends on the amount of GAG present in the tissue (Farnsworth et al. 2014; Praxenthaler et al. 2018). Overall, these data emphasized that the tissues' GAG content is a main determinant of its mechanical competence.

1.5 Mechanisms of mechanical signal transduction

To better understand how mechanical loading regulates cartilage homeostasis, it is necessary to take the multimodal nature of physical stimuli into consideration (O'Connor et al. 2013). While mechanical forces induce a variety of strains, tension and compression, which lead to cellular and nuclear deformations, in addition, also indirect biophysical factors are generated, including changes in hydrostatic pressure, fluid flow, local ion composition and osmotic pressure which are

each tightly connected to each other (Graceffa et al. 2019; Guilak and Mow 2000; Mow et al. 1999; Wilusz et al. 2014) (Figure 2).

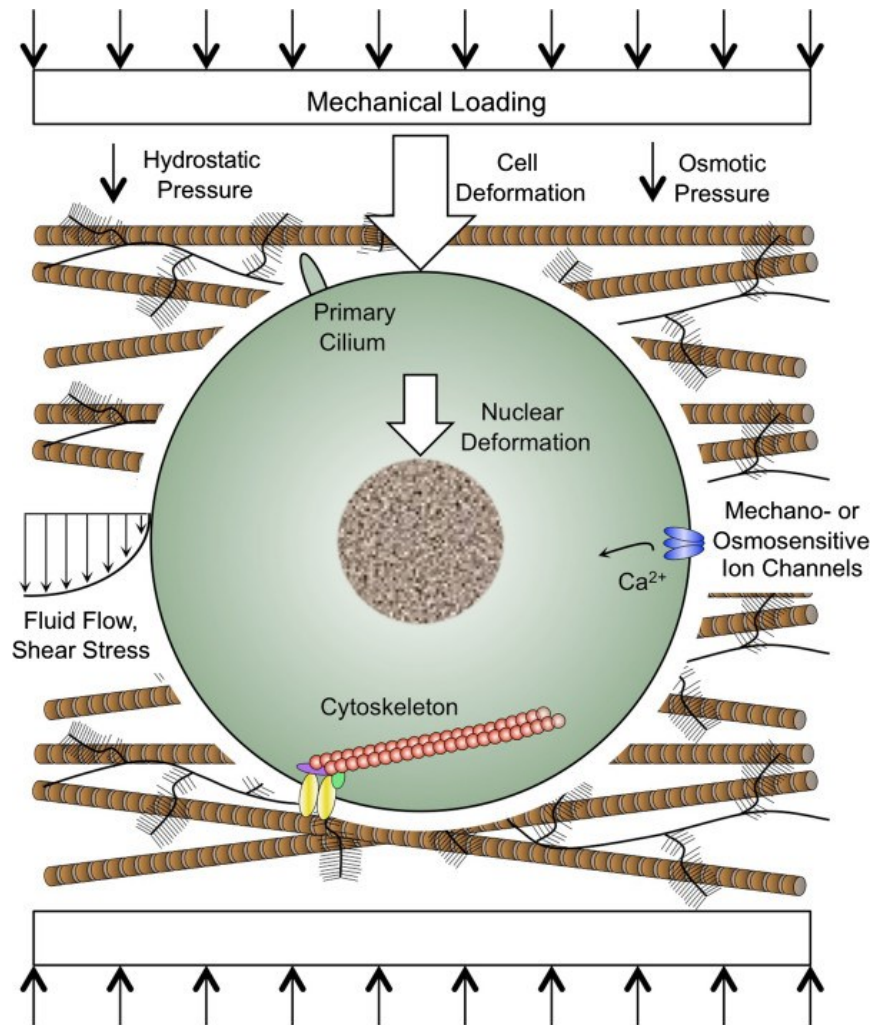


Figure 2 Mechanisms of mechanotransduction in chondrocytes. Mechanical loading (ML) of cartilage induces deformations of the ECM and subsequently provokes cellular and nuclear deformations. Secondary to mechanical deformations, ML exerts hydrostatic pressure, fluid flow shear stress and changes in local osmotic pressure. Translation of mechanical signals into intracellular signaling mechanisms occurs via integrins that are connected to the cytoskeleton, mechano- or osmo-sensitive ion channels or the primary cilium. Figure adapted from O'Connor et al 2013.

During mechanical loading of the joint, the primary force transmission occurs via the ECM to the chondrocytes and leads to cellular and nuclear deformations (Guilak 1995). These physical deformations can, among other factors, influence chromatin remodeling in the nucleus and thereby alter gene expression (Chen et al. 2016). Furthermore, force transmission via the ECM is translated into intracellular signaling mechanism via several mechano-sensory cellular structures, including integrins, mechano-sensitive ion channels and the primary cilium. Integrins are the main

class of mechano-sensitive molecules, which are transmembrane receptors that connect the cytoskeleton of chondrocytes with the surrounding ECM molecules (Loeser 2014). Via these connections, deformations of the ECM are transduced to the cytoskeleton and initiate intracellular signaling pathways. Mechano-sensitive ion channels include potassium channels, calcium channels, non-selective cation channels and chloride channels which are activated in response to cellular deformation and subsequently cause disturbance of intracellular ion composition and activation of molecular signaling pathways (Barrett-Jolley et al. 2010; Han et al. 2012). The primary cilium is a non-motile cellular organ that extends from the cellular surface of chondrocytes where it senses mechano-induced deformations of the ECM via integrins (Muhammad et al. 2012; Whitfield 2008). In addition, excitation may also occur via compression-induced flow of the interstitial fluid which arises secondary to mechanical forces (McGlashan et al. 2006).

Such secondary stimuli are indirectly induced as a result of the mechano-induced compressive, tensile or shear forces and in turn induce a number of physicochemical stimuli, including hydrostatic pressure, fluid flow and changes in osmotic pressure. Hydrostatic pressure occurs as a result of fluid pressurization. In contrast to mechanical pressure, hydrostatic pressure does not induce cellular deformations (Bachrach et al. 1998). Nevertheless, the regulation of cartilage homeostasis by hydrostatic pressure was demonstrated in several studies (Angele et al. 2003; Elder and Athanasiou 2008; Toyoda et al. 2003). Fluid flow arises from mechano-induced extrusion of interstitial fluid from the tissue and leads to enhanced exchange and availability of nutrients and growth factors around chondrocytes (Albro et al. 2012). Importantly, the outflow of water from the tissue also alters the local ion concentration in the tissue and thereby induces changes in local tissue osmolarity (Urban et al. 1993). Thus, besides purely mechanical forces, the response of chondrocytes to mechanical loading is determined by an interplay of several physicochemical challenges.

Understanding the individual sub-stimuli that contribute to load-induced cartilage homeostasis provides the opportunity to develop precisely targeted treatments for *de novo* cartilage formation in TE constructs. Engineered cartilage tissue with a sufficiently high ECM content could then withstand the demanding mechanical conditions in the joint in the long-term. Since the load-induced sub-stimuli may have overlapping or opposing consequences for cartilage homeostasis, it is important to identify the decisive factor that contributes to load-induced enhancement of cartilage matrix synthesis. This would enable researchers to optimize cartilage TE constructs easier and faster. Therefore, research should focus on two important aspects: 1) To identify the acute contribution of individual mechano-induced sub-stimuli to GAG synthesis and 2) to test whether

long-term application of such sub-stimuli can optimize the GAG content and, thus, the mechanical quality of TE constructs over a long time.

Many studies already reported an effect of short-term (hours) and long-term (days to weeks) dynamic mechanical compression on the GAG synthesis rate of human chondrocytes (Diao et al. 2017; Hecht et al. 2019; Jeon et al. 2012; Lückgen et al. 2022; Nebelung et al. 2011; Praxenthaler et al. 2018; Scholtes et al. 2018). However, none of these studies so far considered the specific contribution of individual sub-stimuli for the acute and long-term outcome with the intent to develop cheaper, reproducible and easy to apply protocols. Since the function of articular cartilage, including its resistance to mechanical loads, is greatly determined by its osmotic swelling pressure, changes in local tissue osmolarity appear as a promising sub-parameter of load-induced changes in cartilage matrix synthesis. Mechanical loading experiments do not allow to separate the mechanical stimulus from the osmotic stimulus. Thus, to shed light on this and learn more about the contribution of acute osmotic changes to cartilage matrix synthesis it is necessary to investigate the effect of acute hyperosmotic stimulation independent of other mechano-induced stimuli. In addition, long-term hyperosmotic stimulation may also be used as a simple approach to optimize the GAG content of TE constructs over time. To this end, current knowledge on osmolarity and osmotic pressure in articular cartilage and the contribution of osmotic challenge to the regulation of cartilage homeostasis is summarized in the following sections.

1.6 Osmolarity

Per definition *osmolarity* (or osmotic concentration) is the number of moles of osmotic active molecules in a solution and is expressed as osmoles per liter, i.e., Osm (Baltz 2012). When two solutions are separated by a membrane that is permeable for all molecules including the solvent, at equilibrium the concentration of all molecules and therefore the osmotic concentration will be equal in both solutions. When however, the membrane is selectively permeable for some of the molecules, an imbalance between osmotic active molecules on the two sides of the membrane occurs and the osmolarity of the two solutions is different. If the membrane that separates the two solutions is permeable for the pure solvent, molecules of the solvent will flow from the side of lower osmolarity (hypoosmotic solution) to the side of higher osmolarity (hyperosmotic solution) until an equilibrium is reached. *Osmotic pressure* is defined as the minimal pressure needed to prevent the inflow of solvent across this semipermeable membrane (Lodish et al. 2000). In biological systems such semipermeable membranes are represented for example by the phospholipid bilayer of cell membranes (Hoffmann et al. 2009). A solution outside of a cell is called *hypotonic* when the concentration of solutes is lower than inside the cell. When a cell is immersed

in a hypotonic solution, the osmotic pressure will cause water to flow into the cell in order to balance the concentration of solutes on both sides of the cell membrane. In contrast, when the concentration of solutes is higher outside the cell this is referred to as a *hypertonic* solution and will cause an outflow of water from the cell. As a result, cells undergo cell volume changes in response to different osmotic pressures, with hypotonic solutions causing cells to swell and hypertonic solutions causing cells to shrink (Hoffmann et al. 2009). A solution is called *isotonic* when no difference in osmolarity exists between the cell and its surrounding and therefore no change in cell volume occurs (Hoffmann et al. 2009). In biological systems, osmotic pressure is an important factor affecting function and phenotype of cells and tissues. The origin of osmotic pressure can be of different nature. In the case of cells, the separation of two solutions occurs across the cell membrane (Hoffmann et al. 2009). However, in biological tissues, osmotic pressure between the tissue and its surrounding fluid can arise in the absence of a selectively permeable membrane. This is the result of locally fixed electrostatic charges in the ECM which is most prominently known for biological tissues related to articular cartilage.

1.6.1 Osmotic pressure in articular cartilage

Articular cartilage consists of type II collagen that is organized in a fibrillar mesh to provide elastic and tensile strength to the tissue. The porous mesh of collagen fibrils is filled by PG. PG and their covalently attached GAGs are rich in free SO_3^- and COO^- groups, which provide the so called fixed charged density (FCD) of the tissue. Consequently, a positive correlation between GAG content and FCD was reported by Lu et al. (Lu et al. 2004). The negative FCD attracts positively charged counter ions such as Na^+ , K^+ and Ca^{2+} into the tissue in order to gain electro-neutrality (Hall et al. 1996a). Thereby, the FCD creates an osmotic imbalance and leads to the characteristic hyperosmotic nature of articular cartilage compared to its surrounding fluid. When such differences in osmolarity arise from electrostatic charges rather than separation of solutes via a semipermeable membrane, this is referred to as *Donnan osmotic pressure*. As a result of Donnan osmotic pressure, water flows into the tissue to balance the osmotic disequilibrium (Maroudas 1976). The hydrophilic properties of PGs thereby create the characteristic swelling of articular cartilage that provides a high resistance to mechanical compression to the tissue. The intervening collagen fibers limit the swelling of the tissue and thereby determine the physiological osmolarity of cartilage, which is hypertonic with respect to the surrounding interstitial fluid (Maroudas 1976).

1.6.2 The role of FCD for the level of osmotic pressure in articular cartilage

The classical theoretical attempt to determine the osmolarity of cartilage is the triphasic theory that describes cartilage as a mixture of a charged solid phase (FCD network), a neutral liquid phase

(water) and dissolved ions (simplified: Na^+ and Cl^-) (Lai et al. 1991). Derived from this theoretical model and later confirmed in experimental approaches, the osmolarity of healthy articular cartilage was determined to vary from 350 to 480 mOsm, depending on the depth of the tissue (Urban et al. 1993; Zimmerman et al. 2021). Due to an increased concentration of FCD with the depth of cartilage tissue, osmolarity is lowest in the superficial zone and increases with depth of the tissue (Hall et al. 1996a). In contrast, the osmolarity of human blood plasma was determined at 290 mOsm (Cheuvront et al. 2014) and that of synovial fluid at approximately 400 mOsm (Baumgarten et al. 1985). Upon mechanical compression and shearing of cartilage, as provoked during joint motion, cartilage is compressed and water is squeezed out of the tissue. Consequently, the FCD in the tissue raises and the local ion concentration increases, thus further raising the osmotic pressure in the tissue (Figure 3). Upon unloading of the joint, water flows back into the tissue, creating a dynamic osmotic environment within the tissue. Thus, load-induced osmotic pressure is dynamic and can be in the range of 350-550 mOsm (Schneiderman et al. 1986; Stockwell 1991).

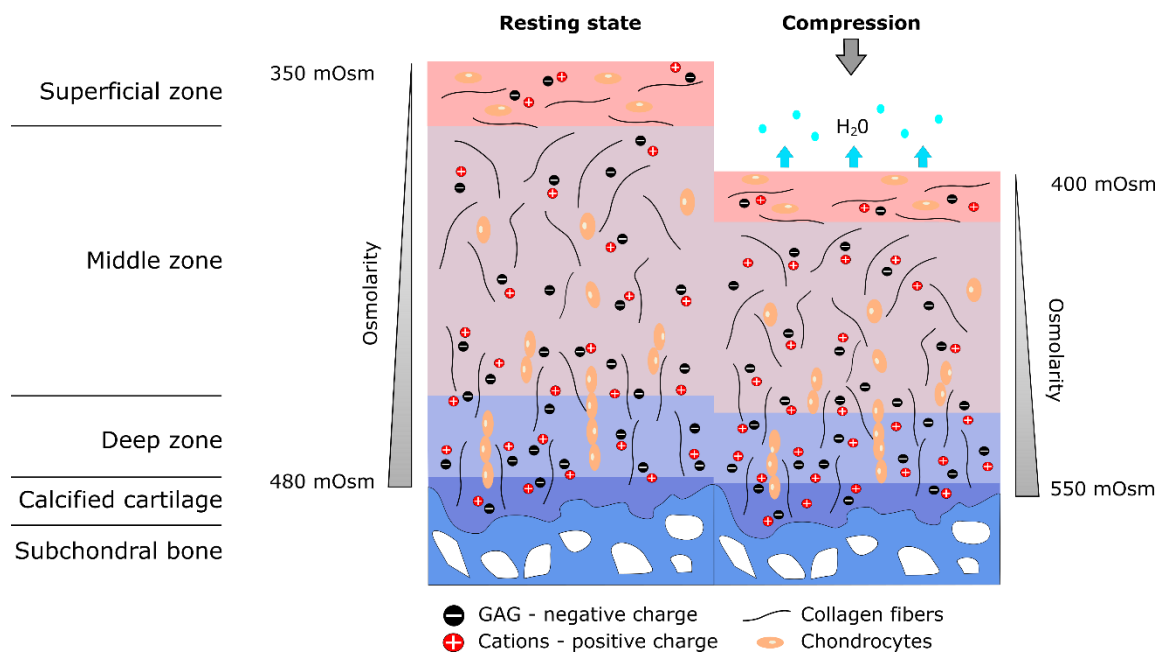


Figure 3 Schematic structure of articular cartilage. Zonal architecture of articular cartilage at rest (left) and under mechanical compression (right). The distribution of charges associated with negatively charged GAGs (-) and positively charged counter ions (+) and the resulting osmolarity varies with depth and compression of the tissue.

During degenerative diseases such as OA or in response to mechanical overload or disuse, ECM is degraded and therefore FCD and tissue osmolarity declines (Maroudas et al. 1985). In contrast, during *de novo* cartilage formation or regeneration, ECM is deposited, increasing the FCD and thus

tissue osmolarity (Lu et al. 2004). Therefore, beyond acute load-induced changes of osmolarity, osmotic pressure can change gradually over several days to weeks or even months with deposition or loss of FCD in the tissue (Hall 2019).

Overall, the FCD determines the osmotic pressure in articular cartilage. Changes in FCD can occur acutely as provoked by mechanical compression or gradually over a long time as a result of ECM formation or degradation. Hence, to identify the contribution of osmotic stimuli to the acute mechano-induced loading response, it is necessary to investigate the regulation of cartilage matrix homeostasis after acute hyperosmotic challenge independent of other stimuli. Furthermore, to optimize cartilage TE constructs in the long-term, effects of long-term hyperosmotic stimulation should be tested. For this purpose, the current literature on osmo-induced changes on cartilage matrix homeostasis is summarized in the following sections with focus on acute or long-term hyperosmotic challenge.

1.7 Response of chondrocytes to acute hyperosmotic challenge

So far, GAG synthesis (Hopewell and Urban 2003; Urban et al. 1993; Villanueva et al. 2009), SOX9 levels (Erndt-Marino et al. 2019; Peffers et al. 2010; Tew et al. 2009) and ECM marker gene expression (Caron et al. 2013; Palmer et al. 2001; Tew et al. 2009) were identified as relevant read-out parameters after acute hyperosmotic stimulation. In addition, these are also essential parameters of a mechanical loading response of 3D neocartilage (Praxenthaler et al. 2018; Scholtes et al. 2018).

Chondrocytes in suspension or monolayer culture lack a proper ECM-rich 3D environment. This precludes drawing any conclusions about whether hyperosmotic changes are a relevant sub-parameter for compression-related alterations in GAG synthesis, SOX9 and ECM marker gene expression in neocartilage. Therefore, studies are needed which assess the osmo-response of chondrocytes embedded in a cartilage-relevant 3D environment such as 3D neocartilage tissue. Current knowledge on the effects of acute hyperosmotic challenge on GAG synthesis, SOX9 and cartilage ECM marker gene expression will help to understand to what extent the culture model determines the acute osmo-response of chondrocytes.

1.7.1 Regulation of GAG synthesis by acute hyperosmotic challenge

During **suspension culture**, bovine articular chondrocytes were exposed to a broad set of extracellular osmolarities and the GAG synthesis rate, measured as incorporation of radio-labeled sulfate-35, was assessed. After 24 hours of treatment, a maximal synthesis rate was observed around 380 mOsm, while above and below this level the synthesis rate declined (Urban et al.

1993). Interestingly, this corresponded to the osmolarity that chondrocytes would experience under physiological conditions *in vivo*, later referred to as physosmotic environment (Jahr et al. 2022). However, when in the same study a 24-hours osmotic stimulation was applied after an overnight pre-incubation in standard chondrocyte medium at 250 mOsm, the GAG synthesis rate was highest at 250 mOsm and declined with increase in osmolarity, suggesting that isolated chondrocytes adapt to their extracellular osmolarity within 24 hours after which further changes in osmolarity impair matrix production (Urban et al. 1993). These data highlight that isolated chondrocytes respond to changes in osmolarity quickly and subsequently adjust the rate of ECM synthesis to the new conditions.

Using **cartilage explants**, Urban et al. further investigated whether chondrocytes embedded in their native tissue, and therefore exposed to physosmotic conditions, showed a different response to hyperosmolarity compared to isolated chondrocytes. Interestingly, 24 hours of osmotic stimulation shifted the highest GAG synthesis rate in cartilage explants to slightly lower osmolarity of 310-350 mOsm compared to chondrocytes in suspension culture (380 mOsm, see above) (Urban et al. 1993). This indicated that the presence of native ECM alters the response of chondrocytes to osmotic challenge. Thus, chondrocytes in suspension culture, which are isolated from their native niche, are in an untypical physiological state which may critically contribute to the observed differences between isolated and *in situ* chondrocytes.

In **3D cultures** using alginate beads or PEG gels chondrocytes reside as isolated cells with a typical round morphology. Importantly, without chondrogenic pre-maturation, these gels lack a cartilage-typical ECM and have virtually no FCD. Only upon pre-maturation, chondrocytes deposit a cartilage-like ECM in the gels and a FCD develops. In 3D-cultured chondrocytes, the effect of acute hyperosmotic stimulation was so far only investigated without pre-maturation of the cells. The authors, therefore, neglected the effects of a cartilage-relevant FCD in the tissue for the osmo-response. Under these conditions, acute hyperosmotic stimulation for 24 hours or more enhanced the GAG synthesis rate (Hopewell and Urban 2003; Villanueva et al. 2009), which was also described for chondrocytes in suspension culture (Urban et al. 1993).

Overall, this suggested a similar response of isolated chondrocytes in suspension culture and in 3D without chondrogenic pre-maturation. However, current literature provides no information on the response of chondrocytes to acute hyperosmotic stimulation under cartilage relevant-conditions at high FCD.

1.7.2 Regulation of SOX9 by acute hyperosmotic challenge

Production of cartilage ECM is controlled by the transcription factor SOX9. In human articular chondrocytes cultured in monolayer or in 3D alginate gels without pre-maturation, acute hyperosmotic stimulation at 550 mOsm for 5 hours induced *SOX9* mRNA expression (Tew et al. 2009). Interestingly, *SOX9* mRNA induction depended on the absence of actin stress fibers. While monolayer chondrocytes form actin stress fibers during adherence culture, the formation is naturally inhibited in alginate culture. Therefore, in monolayer culture, induction of *SOX9* expression after hyperosmotic stimulation was only observed after inhibition of stress fiber formation, whereas in freshly embedded chondrocytes in 3D alginate culture hyperosmolarity induced *SOX9* expression without further treatment (Tew et al. 2009). These data emphasized the importance to determine the SOX9 osmo-response in rounded cells rather than in monolayer attached chondrocytes. In addition, hyperosmotic stimulation at 550 mOsm for 5 hours post-transcriptionally increased *SOX9* mRNA stability in monolayer culture of human (Tew et al. 2009) and equine (Peffer et al. 2010) articular chondrocytes. Consequently, an increase in SOX9 protein levels was observed. An induction of *SOX9* mRNA expression was also found in human articular chondrocytes in 3D alginate culture without pre-maturation after hyperosmotic stimulation at 490 mOsm for 24 hours (Erndt-Marino et al. 2019).

In conclusion, acute hyperosmotic stimulation induced SOX9 mRNA and protein levels in monolayer as well as in freshly embedded 3D-cultured chondrocytes. However, the lack of tissue pre-maturation in these studies does not provide information on the response of chondrocytes to acute hyperosmotic stimulation under cartilage-relevant conditions at high FCD.

1.7.3 Regulation of *COL2A1* and *ACAN* gene expression by acute hyperosmotic challenge

In monolayer culture of the murine chondrogenic ATDC5 cell line as well as human MSC-derived chondrocytes, 21 days of consecutive 380 mOsm hyperosmotic stimulation upregulated the expression of ECM-related genes *COL2A1* and *ACAN*. Knockdown of SOX9 using siRNA abolished the hyperosmotic induction of *Col2a1* and *Acan* expression in ATDC5 cells (Caron et al. 2013), indicating that hyperosmolarity-induced *Col2a1* and *Acan* expression was regulated via SOX9.

Acute hyperosmotic stimulation of freshly isolated human articular chondrocytes in monolayer culture at 550 mOsm for 24 hours induced *COL2A1* promoter activity, while *COL2A1* mRNA expression and half-life was reduced. This indicated increased transcription but also turnover of *COL2A1* mRNA in monolayer chondrocytes (Tew et al. 2009). In a similar setup of bovine articular chondrocytes, stimulated at 580 mOsm for 24 hours, *ACAN* promoter activity was reduced along

with *ACAN* mRNA expression (Palmer et al. 2001). Likewise, acute hyperosmotic stimulation at 550 mOsm for 5 hours reduced *ACAN* and *COL2A1* expression in monolayer-cultured equine articular chondrocytes (Peffer et al. 2010). In human articular chondrocytes in 3D alginate culture without pre-maturation, 24 hours of acute hyperosmotic stimulation resulted in no alteration of *ACAN* and *COL2A1* expression (Erndt-Marino et al. 2019).

Unfortunately, the effect of acute hyperosmotic stimulation was so far not investigated in pre-matured engineered cartilage and thus, no data are available on whether *COL2A1* and *ACAN* expression changes upon acute hyperosmotic stimulation in a cartilage-relevant environment at high FCD.

Altogether, although several authors investigated the effects of acute hyperosmotic stimulation on 3D-cultured chondrocytes, all of these studies were performed without pre-maturation of the tissue and therefore neglected the effects of a cartilage-relevant FCD. Considering the importance of the FCD for maintaining the osmotic pressure in cartilage, the lack of FCD in these studies questions whether these models can accurately depict the response of chondrocytes to hyperosmotic stimulation under cartilage-relevant conditions. Importantly, due to its role for maintaining the osmotic pressure in cartilage, FCD may also be crucial for chondrocytes to respond to external stimuli. For example, it was shown that load-induced GAG synthesis changes at low versus high GAG content and differences in FCD associated with GAGs in the tissue may be the reason for this (Praxenthaler et al. 2018). Likewise, incorporation of FCD by crosslinking chondroitin sulfate into PEG hydrogels significantly altered the mechano-response of chondrocytes (Farnsworth et al. 2014). An importance of FCD for the response of chondrocytes to mechanical stimuli is also suggested from *in vivo* studies. Topographical variations in FCD and biochemical composition of human articular cartilage between high or low weight-bearing areas (Rogers et al. 2006) indicates that high FCD correlates with areas of high mechanical loads. Opposite, a loss of FCD during OA-related ECM degradation correlates with an impaired mechano-competence of the tissue (Knecht et al. 2006). Taken together, these studies highlight that FCD may be important for the response of chondrocytes to external stimuli such as mechanical loading. Therefore, to elucidate whether acute hyperosmotic stimulation is a sub-parameter of load-induced stimulation of GAG synthesis, a model is required that takes FCD into consideration.

1.8 Response of chondrocytes to long-term hyperosmotic challenge

1.8.1 Regulation of GAG synthesis by long-term hyperosmotic stimulation

To determine the effect of long-term hyperosmotic stimulation on GAG synthesis, Negoro et al. encapsulated bovine articular chondrocytes in alginate gels and matured them at 270, 370, 470 or 570 mOsm. After 6 days of maturation, the GAG synthesis rate was increased at 370 and 470 mOsm compared to 270 mOsm, reaching significance only at 370 mOsm (Negoro et al. 2008). These data indicated that long-term hyperosmotic stimulation increased the GAG synthesis rate of 3D-cultured bovine articular chondrocytes. Interestingly, the effect was strongest at a moderately enhanced osmolarity. So far, it remained unclear whether long-term hyperosmotic stimulation also regulates the GAG synthesis rate of human chondrocytes.

1.8.2 Regulation of SOX9 by long-term hyperosmotic stimulation

The regulation of *SOX9* expression by long-term hyperosmotic stimulation was addressed in several studies in monolayer- and 3D-cultured chondrocytes. In monolayer-cultured murine chondrogenic ATDC5 cells, long-term hyperosmotic stimulation for 14 days enhanced *SOX9* mRNA expression (Caron et al. 2013; Jahr et al. 2022). In 3D-cultured human articular chondrocytes in alginate gels, long-term hyperosmotic stimulation at 490 mOsm for 7 days also induced *SOX9* expression (Erndt-Marino et al. 2019). Even longer hyperosmotic stimulation at 430 mOsm for 5 weeks induced *SOX9* expression in high density micromass pellets of porcine articular chondrocytes (Sieber et al. 2020).

Thus, at defined conditions, long-term hyperosmotic challenge for several weeks can stimulate *SOX9* expression in monolayer- and 3D-cultured chondrocytes. Whether long-term hyperosmotic stimulation regulates *SOX9* at the protein level has so far never been addressed.

1.8.3 Regulation of *COL2A1* and *ACAN* expression and GAG deposition by long-term hyperosmotic stimulation

Long-term hyperosmotic stimulation of monolayer-cultured ATDC5 cells at 380 mOsm for 14 days significantly increased *Acan* and *Col2a1* expression and enhanced GAG deposition (Caron et al. 2013; Jahr et al. 2022). A similar induction of *COL2A1* and *ACAN* expression was also observed after long-term hyperosmotic stimulation at 380 mOsm for 7 days in monolayer-cultured human articular chondrocytes (Jahr et al. 2022; Tan Timur et al. 2019). This indicated enhanced ECM marker expression and GAG deposition in monolayer-cultured chondrocytes.

During 3D culture of human articular chondrocytes in alginate gels at 490 mOsm for 7 days, *COL2A1* and *ACAN* expression were significantly increased compared to controls (Erndt-Marino et al. 2019). Using bovine articular chondrocytes encapsulated in alginate gels, hyperosmotic stimulation at 370 mOsm for 6 days (Negoro et al. 2008) or 380 mOsm for 12 days (Xu et al. 2010) also enhanced GAG deposition in the gels. Long-term hyperosmotic stimulation of porcine articular chondrocytes in micromass-culture at 430 mOsm for 5 weeks induced *ACAN*, but not *COL2A1* expression. However, no effect on GAG and type II collagen deposition was observed in this study (Sieber et al. 2020). In contrast, after 4 weeks of hyperosmotic stimulation at 400 mOsm, Sampat et al. demonstrated enhanced total GAG levels in alginate gels seeded with bovine articular chondrocytes. Importantly, at the same time, also the DNA content per gel raised significantly, indicating more GAG but also more cells in the gel (Sampat et al. 2013). Likewise, O'Connor et al. showed increased total GAG but not GAG/DNA levels after 2 weeks of hyperosmotic stimulation of porcine articular chondrocytes in agarose gels at 600 mOsm (O'Connor et al. 2014), indicating that hyperosmolarity may stimulate chondrocyte proliferation.

Overall, long-term hyperosmotic stimulation enhanced ECM-related marker expression in monolayer- and 3D-cultured chondrocytes. While some studies reported a stimulation of GAG deposition after long-term hyperosmotic stimulation, other studies found no such effects. Whether long-term hyperosmotic stimulation can also enhance the deposition of GAGs in human 3D neocartilage remained so far unclear.

In summary, although several studies investigated the effect of long-term hyperosmotic stimulation on bovine and porcine chondrocytes in 3D culture, no studies were performed using cartilage-relevant models of human 3D engineered neocartilage. Long-term hyperosmotic stimulation induced *SOX9* expression and ECM-related marker gene expression in 2D and 3D culture. An enhanced GAG synthesis and GAG deposition was observed at moderately enhanced osmolarities. This suggests moderate long-term hyperosmotic challenge as a promising stimulus to enhance the quality of human cartilage replacement tissue in the long-term. Thus, to elucidate the role of long-term hyperosmotic stimulation as a clinically relevant stimulus to enhance the quality of cartilage replacement tissue, studies are needed which assess the long-term osmo-response of human chondrocytes embedded in a cartilage-relevant 3D environment such as 3D neocartilage tissue.

1.9 Signal transduction after hyperosmotic stimulation of chondrocytes

Several mechanisms have been proposed on how chondrocytes translate osmotic changes into the activation of intracellular signaling cascades, referred to as osmotransduction (Liedtke 2007). Upstream of osmo-induced changes in GAG synthesis and cartilage matrix associated gene expression, mitogen-activated protein kinase (MAPK) signaling (Hdud et al. 2014; Racz et al. 2007; Tew et al. 2009) and nuclear factor of activated T-cells 5 (NFAT5) (Caron et al. 2013; Jahr et al. 2022; van der Windt et al. 2010) were suggested to act as important osmo-signaling molecules in chondrocytes. Their regulation in 2D- and 3D-cultured chondrocytes was demonstrated in several studies.

1.9.1 Regulation of MAPK signaling by hyperosmotic challenge

Upon perception of altered osmotic conditions by chondrocytes, the stimuli are transduced into chemical signals by the activation of intracellular signaling cascades. The MAPK signaling pathways are among the most prominent osmo-sensitive signaling pathways and activation of MAPK in response to hyperosmotic stress is known from several cell types (Sheikh-Hamad and Gustin 2004; Watts et al. 1998) including chondrocytes (Hdud et al. 2014; Racz et al. 2007; Tew et al. 2009). In mammalian cells three subfamilies of MAPK have been identified: Extracellular signal-regulated kinase-p44/42 MAPK (ERK1/2), p38 MAPK (p38) and c-Jun N-terminal kinase (JNK). External signals are transduced via a phosphorylation cascade and ultimately lead to phosphorylation of ERK1/2, p38 or JNK.

Acute hyperosmotic stimulation at 450 mOsm induced ERK1/2 phosphorylation in monolayer rat intervertebral disc cells, which naturally reside in a similar cartilaginous matrix compared to articular chondrocytes. In their study, Tsai et al. observed ERK1/2 phosphorylation already after 5 minutes of hyperosmotic stimulation and levels remained elevated after long-term stimulation for 24 hours (Tsai et al. 2007). In isolated equine chondrocytes, ERK1/2 was phosphorylated after hypoosmotic stimulation (280 mOsm) and de-phosphorylated after hyperosmotic stimulation (480 mOsm) while p38 phosphorylation was observed specifically after hyperosmotic stimulation (Hdud et al. 2014). Phosphorylation of all three MAPKs was observed in isolated porcine articular chondrocytes treated on day 3 after isolation for 6 hours at 600 mOsm (Racz et al. 2007). In monolayer culture of freshly isolated human articular chondrocytes, hyperosmotic challenge at 550 mOsm phosphorylated p38 MAPK, which was evident 10 minutes after the start of stimulation and lasted for the entire treatment period of 5 hours (Tew et al. 2009). These data indicate that hyperosmotic stimulation of monolayer chondrocytes induced MAPKs within several minutes and maintained their activation for several hours. Furthermore, inhibition of ERK1/2 or p38 activity

prevented hyperosmotic induction of ECM-associated genes in nucleus pulposus cells (Tsai et al. 2007) and p38 inhibition prevented the hyperosmotic induction of *SOX9* expression and *COL2* promoter activity in human articular chondrocytes, suggesting the involvement of p38 and ERK1/2 activation in osmo-induced regulation of ECM homeostasis (Tew et al. 2009).

Thus, in monolayer culture, phosphorylation of ERK1/2 and p38 can serve as a potent marker of intracellular signal transduction upon hyperosmotic stimulation. However, whether MAPKs are activated by osmotic stress in 3D-cultured human articular chondrocytes and whether the response depends on a low versus high FCD remains unknown. Importantly, induction of MAPK activity and expression of its downstream targets *FOS*, *FOSB* and *DUSP* is also known from mechanical loading studies (Praxenthaler et al. 2018). Therefore, in order to elucidate whether the induction of MAPK activity and expression of its downstream targets is a unique event of mechanical loading or may be caused by load-induced alterations in local osmolarity, experiments to address the regulation of these pathways after purely osmotic stimulation at low vs high FCD are needed.

1.9.2 Regulation of the osmo-sensitive transcription factor NFAT5

NFAT5, also referred to as tonicity enhanced binding protein (TonEBP) or osmo-responsive element binding protein (OREBP), is well recognized for its upregulation upon changes in osmolarity in non-cartilaginous cell types (Morancho et al. 2008). Upon hyperosmotic stress, NFAT5 forms homo dimers in the nucleus and binds to the tonicity responsive enhancer (TonE) binding site of target gene promoters (Stroud et al. 2002), including those of ion channels and transporters that control the uptake or release of osmolytes in order to regulate cell volume. Acknowledged NFAT5 target genes include sodium-/myo-inositol channel (*SLC5A3*) (Na et al. 2003), sodium/chloride-coupled acid transporter (*SLC6A12*) (Lopez-Rodriguez et al. 2004) and calcium-binding proteins (*S100A4*) (Chen et al. 2009).

The relevance of NFAT5 for osmotransduction in cartilaginous cells was demonstrated by hyperosmotic induction of NFAT5 in intervertebral disk cells (Tsai et al. 2007). Besides from its role in adjusting the level of intracellular osmolarity, NFAT5 is a key regulator of ECM homeostasis in cartilaginous connective tissue as indicated by the presence of a functional active TonE site in the promoter of the *ACAN* gene in cells of the intervertebral disk (Tsai et al. 2007). In human articular chondrocytes, long-term monolayer culture at physosmotic conditions increased *NFAT5* gene expression along with its target genes *S100A4* and *SLC6A12*. Knock down of NFAT5 prevented the induction of its target genes and also abolished osmo-induced upregulation of cartilage matrix-related genes *ACAN*, *COL2* and *SOX9* (van der Windt et al. 2010). Using the murine chondrogenic

cell line ATDC5, Caron et al. showed that NFAT5 acts upstream of SOX9 to regulate downstream cartilage ECM-associated genes (Caron et al. 2013). These data indicated that NFAT5 is involved in osmo-regulated ECM homeostasis in chondrocytes.

Thus, expression of *NFAT5* and its target genes *SLC6A12* and *S100A4* was reported in response to long-term hyperosmotic stimulation of monolayer chondrocytes. However, whether acute osmotic stimulation induces NFAT5 in 3D-cultured chondrocytes is still an open question.

In summary, monolayer data indicate that after hyperosmotic stimulation of chondrocytes, osmotransduction occurs via the phosphorylation of MAPKs, the activation of the osmo-sensitive transcription factor NFAT5 and the expression of its transcriptional downstream targets to induce an anabolic expression pattern. However, whether hyperosmotic stimulation activates MAPKs and stimulates *NFAT5* expression in 3D-cultured chondrocytes and human engineered cartilage and whether they can be used as osmo-response markers remained so far unknown.

1.10 The role of different cations for hyperosmotic stimulation of chondrocytes

Due to the attraction of positively charged ions to the negative FCD of the proteoglycans, increased osmolarity is also inevitably accompanied by an accumulation of cations. Sodium, potassium and calcium ions are among the most abundant cations in cartilage (Hall et al. 1996a). In addition to their osmotic activity, cations also affect the membrane potential of cells, can bind to specific ion channels and interact with other ions and biomolecules. Therefore, the above-described translation of osmotic signals into cellular signaling mechanisms may vary according to the type of cations that is present. This is important for the selection of appropriate ions for future studies on acute versus long-term osmotic stimulation of chondrocytes.

Sodium ions (Na^+) are the most abundant cations in articular cartilage reaching levels of 240-350 mM (Hall et al. 1996a). Therefore, sodium chloride is most often used for experimental manipulation of the osmotic environment. A comparison of osmotic stimulation using sodium chloride as ionic or sucrose as non-ionic osmolyte showed similar effects on GAG synthesis (Urban et al. 1993), induction of *SOX9* mRNA (Tew et al. 2009) and *ACAN* promoter activation (Palmer et al. 2001) after hyperosmotic stimulation of isolated chondrocytes, suggesting that chondrocytes primarily respond to the change in osmolarity rather than ionic effects induced by Na^+ . Recently, the use of standard ringer's saline as routine irrigation solution during joint arthroscopic surgery was challenged by the use of more hyperosmotic solutions due to their chondroprotective properties (Howard et al. 2020). While Na^+ is widely used in irrigation solutions, recent data

proposed a pro-inflammatory role of Na⁺ ions in macrophages and thus its role for osmotic adjustment of irrigation solution was questioned and potassium was suggested as an alternative ion source (Binger et al. 2015; Erndt-Marino et al. 2019; Kleinewietfeld et al. 2013).

The concentration of **Potassium ions** (K⁺) in cartilage is approximately 7-12 mM (Hall et al. 1996a). Comparing the effect of increased osmolarity by K⁺, Na⁺ or sucrose, it was demonstrated that K⁺ was more efficient in reducing protein levels of OA-related catabolic markers as well as inflammatory markers compared to Na⁺ or sucrose, suggesting the use of K⁺ in joint arthroscopic surgery (Erndt-Marino et al. 2019). At the same time expression of anabolic ECM-related markers *COL2A1*, *ACAN* and *SOX9* was observed with hyperosmotic K⁺ treatment, which is in line with other studies using Na⁺. However, for ECM-related markers no direct comparison of K⁺ and Na⁺ or sucrose was performed in this study (Erndt-Marino et al. 2019).

Extracellular **calcium ion** (Ca²⁺) levels in articular cartilage are in the range of 4-20 mM depending on the density of fixed negative charges within the depth of the tissue. This is unusual compared to other tissues, blood plasma or tissue culture medium where the Ca²⁺ concentration is around 1.8 mM (Maroudas 1980). Due to its divalent nature, the electrostatic interaction between Ca²⁺ and the cartilage ECM is stronger than for monovalent ions such as Na⁺ or K⁺. As a result, the activity coefficient of Ca²⁺ in cartilage is reduced and Ca²⁺ can occur at higher concentrations in cartilage than in solution before it precipitates (Maroudas 1980). Though present in cartilage tissue at much lower concentrations compared to Na⁺, Ca²⁺ ions are of major importance for cellular signaling activity in chondrocytes in response to various external stimuli, including mechanical (Guilak et al. 1999), electrical (Xu et al. 2009) and osmotic stimulation (Erickson et al. 2001). The cellular response of chondrocytes to osmotic stress includes the induction of intracellular calcium transients which regulate changes in cell volume (Erickson et al. 2001; Phan et al. 2009; Zhou et al. 2016). The importance of extracellular Ca²⁺ to evoke intracellular calcium transients was demonstrated by the inflow of extracellular calcium via calcium-permeable ion channels (Erickson et al. 2001; Erickson et al. 2003). Physiological levels of intracellular calcium concentrations are typically < 1 μM, resulting in a strong gradient between intra- and extracellular Ca²⁺ levels and influx of Ca²⁺ through calcium-permeable ion channels can occur along this gradient. Intracellular Ca²⁺ is a highly versatile second messenger with a multitude of intracellular signaling activities and deviations in temporal and local calcium regulation can lead to serious cell malfunctions and even cell death.

Besides its role as an intracellular second messenger, Ca²⁺ can also act as a first messenger by directly binding to cell membrane-bound receptors. It was shown, that cells can sense fluctuations of the extracellular Ca²⁺ environment via the calcium-sensing receptor (CaSR) and translate the

signal into the activation of intracellular signaling cascades. CaSR is a member of the group of G-protein coupled receptors and activation of CaSR in the parathyroid gland is associated with the regulation of systemic body calcium homeostasis (Shoback et al. 1984). In chondrocytes, CaSR knock out was shown to be involved in mouse callus formation by delaying the chondrogenic to osteogenic transition, suggesting a role of extracellular Ca^{2+} during long-term *in vivo* chondrocyte differentiation (Cheng et al. 2020).

In summary, the high abundance of sodium ions in articular cartilage compared to potassium and calcium ions suggest sodium as the most relevant ion to mediate the acute load-induced changes in osmolarity which are in the order of several 100 mOsm. In addition, GAG synthesis and ECM-related marker expression remained constant under ionic Na^+ , non-ionic sucrose and PEG as osmolytes (Erndt-Marino et al. 2019; Urban et al. 1993). Therefore, Na^+ is an ideal osmolyte in acute hyperosmotic stimulation experiments.

In contrast, to investigate the long-term effect of increased osmolarity to optimize the quality of cartilage TE constructs, studies suggested a stimulation of GAG synthesis and GAG deposition at moderately enhanced hyperosmolarities. Since extracellular calcium concentrations are moderately enhanced in articular cartilage compared to the surrounding tissue (Maroudas 1980), calcium appears as a promising ion to mediate long-term effects on the quality of cartilage replacement tissue. In addition, in the above-described literature, Cheng et al. suggest a role for extracellular Ca^{2+} during long-term chondrocyte differentiation. Thus, calcium appears as a relevant osmolyte to be chosen for long-term hyperosmotic stimulation experiments.

1.11 Relevance of extracellular calcium for clinically significant neocartilage maturation

The relevance of extracellular calcium for neocartilage maturation was first suggested by results from developmental chondrocyte models of chicken limb bud mesenchyme (San Antonio and Tuan 1986) and mouse growth plate chondrocytes (Rodriguez et al. 2005). For the application to clinically relevant TE approaches, other studies also identified a role of resorbable calcium-containing bone-replacement materials for osteogenic (Barradas et al. 2012; Yuan et al. 2010) and chondrogenic (Brocher et al. 2013; Sarem et al. 2018) differentiation of progenitor cells. During osteochondral TE, cartilage maturation occurs in close vicinity to calcified structures. Thus, a more detailed understanding of the composition of osteochondral TE constructs will help to elucidate the relevance of extracellular calcium as a long-term hyperosmotic stimulus during maturation of clinically relevant 3D neocartilage tissue.

1.11.1 Relevance of extracellular calcium for neocartilage maturation in osteochondral defects

Cartilage defects can be divided (i) into partial thickness chondral defects, (ii) full thickness chondral defects and (iii) osteochondral defects depending on the depth of the lesion. While partial thickness chondral defects only affect the articular cartilage without calcified cartilage, full thickness chondral defects include damage of the calcified zone. In osteochondral defects, damage of articular and calcified cartilage extends to injury of the subchondral bone (Lopa and Madry 2014). For the repair of purely chondral defects, a one-phase cartilage replacement tissue is usually applied. For osteochondral defects, bi-phasic (Getgood et al. 2012; Gotterbarm et al. 2006; Lopa and Madry 2014) or even tri-phasic (Kunisch et al. 2018; St-Pierre et al. 2012) constructs were designed in which a cellular cartilage phase is attached to an acellular bone replacement material in order to create an osteochondral unit.

Cartilage phase

Articular chondrocytes and mesenchymal stromal cells are the most commonly used cell types to create the cellular cartilage phase.

Articular chondrocytes (AC) are the native cell type in articular cartilage and therefore exhibit a high cartilage formation potential *in vivo* and *in vitro* (Dreher et al. 2020; Pelttari et al. 2008). The classical model to form 3D cartilage tissue *in vitro* is high density culture of AC to form cartilaginous pellets (Schulze-Tanzil et al. 2002; Zhang et al. 2004), but the combination of AC with biomaterials is commonly performed in order to further support the deposition of cartilage ECM. For this purpose, a porcine type I/III collagen-based scaffold seeded with human AC was established in our lab which demonstrated formation of stable hyaline-like articular cartilage *in vitro*, characteristic of a dense type II collagen- and PG-rich ECM, reaching mechanical properties similar to that of native cartilage (Hecht et al. 2019; Praxenthaler et al. 2018; Scholtes et al. 2018). Despite the promising progress as mentioned above, AC availability is limited and harvest of chondrocytes includes injury of intact cartilage tissue. This leads to donor side morbidity and creates potential sites of progressive cartilage destruction. Therefore, alternative cell sources are sought.

Mesenchymal stromal cells (MSC) are available in large quantities and due to their self-renewal capacity provide high expansion potential *in vitro* (Pittenger et al. 1999). MSC are typically isolated from bone marrow and are characterized by a fibroblast-like phenotype and the ability to adhere to plastic. Initially, the term *mesenchymal stem cells* was introduced by Arnold I. Caplan and refers to cells from the bone marrow of mesenchymal origin, capable to differentiate into all tissues of the mesenchymal lineage (Caplan 1991). However, since their stem cell potential was initially not

convincingly demonstrated in *in vivo* ectopic implantation models, the International Society for Cell Therapy (ISCT) defined MSC in 2005 as mesenchymal stromal cells. Under appropriate differentiation protocols, MSC differentiate into cartilage, classically performed during 3D high-density pellet culture (Johnstone et al. 1998). Stimulation with the growth factor TGF β is essential for chondrogenic differentiation during which MSC, similar to AC, upregulate ECM-related genes *COL2A1* and *ACAN* and deposit a type II collagen- and PG-rich ECM during pellet culture (Winter et al. 2003) as well as in porcine type I/III collagen scaffolds (Lückgen et al. 2022). However, chondrogenic differentiation of MSC follows the endochondral lineage, typically observed in the growth plate of developing long bones (Yoo et al. 1998). Therefore, cartilage formed by MSC is only transient, accompanied by trans-differentiation into a hypertrophic phenotype. MSC-derived hypertrophic chondrocytes start to express hypertrophic markers such as type X collagen and upregulate terminal differentiation marker matrix metalloproteinase 13 (MMP13) and osteogenic markers bone sialoprotein (IBSP) and alkaline phosphates (ALP) to induce matrix mineralization (Dreher et al. 2020; Pelttari et al. 2006). After ectopic implantation in mice, MSC-derived cartilage develops into bone which is unfavorable for cartilage defect repair. Recent TE-approaches however, succeeded in the suppression of this undesired change in phenotype using a MSC-based heparin-augmented cartilaginous 3D hydrogel (Chasan et al. 2022). Therefore, MSC present a promising alternative cell source for cartilage TE approaches.

Bone replacement phase

In the acellular bone replacement layer, various calcium-phosphate ceramics such as tricalcium phosphate (TCP) or hydroxyapatite (HA) have been used for osteochondral TE constructs as their chemical composition closely resembles that of native bone. Importantly, calcium ceramics degrade *in vitro* and *in vivo*, releasing calcium-phosphates which stimulate osteogenic differentiation of progenitor cells *in vitro* and bone formation *in vivo* (Yuan et al. 2010). Differences between bone replacement materials arise from their calcium to phosphate ration (Ca/P), with lower Ca/P ratio resulting in a higher dissolution rate. For example, TCP with a Ca/P ratio of 1.5 dissolves faster than HA with a Ca/P ratio of 1.67 (Barradas et al. 2013; Hoppe et al. 2011). Strikingly, enhanced expression of osteogenic differentiation markers was observed by human bone marrow-derived MSC cultured under osteogenic conditions in the presence of fast resolving TCP compared to slow resolving HA *in vitro* and *in vivo* (Yuan et al. 2010), an effect that could be mimicked *in vitro* by the addition of calcium ions to the osteogenic culture medium of MSC (Barradas et al. 2012). Likewise, the presence of TCP (Brocher et al. 2013) or HA (Sarem et al. 2018) was also shown to promote the chondrogenic differentiation of MSC.

Thus, these data demonstrate a crucial role of calcium ions to impact the osteogenic and chondrogenic differentiation of progenitor cells. This is of particular interest for the treatment of osteochondral defects, where the design of multi-phasic TE constructs requires cartilage ECM deposition in close vicinity to calcified structures. While the release of calcium ions from bone replacement materials is variable, the addition of soluble calcium ions into the medium allows to precisely manipulate calcium concentrations in the culture medium. Current knowledge on soluble extracellular calcium ions during chondrogenic maturation of AC and MSC, the two commonly used cell types for osteochondral TE, is therefore summarized below.

1.11.2 Effect of extracellular calcium on cartilage formation by AC and MSC

When driving AC re-differentiation and MSC chondrogenesis towards the expression of a cartilage-specific, type II collagen- and PG-rich extracellular matrix (ECM), a variety of intracellular signaling mechanisms are critical to modulate chondrogenic (re-)differentiation, including TGF- β /SMAD2/3, BMP/SMAD1/5/9 and parathyroid hormone-related peptide (PTHrP) signaling (Goldring et al. 2006; Weiss et al. 2010). Importantly, the regulation of these pathways is calcium-sensitive, suggesting calcium signaling as an eminent stimulus to be considered for the study of AC and MSC chondrogenic (re-)differentiation (Matta and Zakany 2013). Extracellular calcium-induced CaSR activation was particularly shown to regulate PTHrP signaling in several cell types, including murine GPC (Rodriguez et al. 2005) and bovine articular chondrocytes (Burton et al. 2005), suggesting an involvement of PTHrP in calcium-induced regulations of chondrocyte (re-)differentiation and matrix formation. Whether long-term application of calcium ions as hyperosmotic stimulus can enhance the quality of TE constructs, composed of AC or MSC is so far unclear.

1.11.2.1 Effect of extracellular calcium on redifferentiation of AC

The effect of elevated extracellular Ca^{2+} concentration ($[\text{Ca}^{2+}]_e$) on AC re-differentiation is yet poorly investigated. While there are no data available on the effect of extracellular calcium on re-differentiation of primary human ACs, Koyano and colleagues described that in monolayer-cultured bovine AC variations in extracellular calcium affected total collagen but not proteoglycan deposition (Koyano et al. 1996). In their study, alterations from basal (1.8 mM) $[\text{Ca}^{2+}]_e$ to higher (10 mM) $[\text{Ca}^{2+}]_e$ showed only mild induction of type II collagen deposition which was accompanied by a strong induction of type X collagen. In contrast, lowering the $[\text{Ca}^{2+}]_e$ to 0.1 mM significantly increased type II collagen synthesis independent of type X collagen, suggesting that low, but not high extracellular calcium promotes bovine chondrocyte re-differentiation. While no effect of extracellular calcium concentration on GAG synthesis was observed in isolated bovine

chondrocytes in suspension culture over the range of 0-10 mM (Urban et al. 1993) others have found increased GAG synthesis in cartilage explants from 12 day-old chicken embryo vertebra at increased extracellular $[Ca^{2+}]$ of 5 mM (Shulman and Opler 1974).

Overall, beyond some contradictory data on animal chondrocytes, no studies are available on the effect of extracellular calcium on cartilage matrix synthesis and deposition by human AC in 3D culture.

1.11.2.2 Effect of extracellular calcium on chondrogenesis of MSC

The effect of high extracellular calcium on chondrogenesis of MSC-like cells was first investigated in the 1980s in developmental chicken embryo studies in monolayer culture, where alcian blue-positive nodule formation as well as proteoglycan synthesis was increased at elevated calcium concentration in the culture medium (San Antonio and Tuan 1986). Opposite results were reported in monolayer culture of MSC-like rat chondrogenic cells (Chang et al. 1999a) and mouse growth plate chondrocytes (Rodriguez et al. 2005), where proteoglycan deposition was significantly decreased at elevated (3.0 mM) $[Ca^{2+}]_e$. Likewise, 3D cultured human bone marrow and adipose tissue-derived MSC cultured at high extracellular calcium concentrations during chondrogenesis showed reduced proteoglycan deposition (Mellor et al. 2015; Sarem et al. 2018). However, the employment of BMP or L-thyroxin during chondrogenesis may have considerably influenced the outcome by driving cells into hypertrophic differentiation. Thus, high extracellular calcium induced or decreased cartilage matrix formation in MSC-like cells, depending on the species of cells and the applied culture conditions.

Overall, to elucidate whether long-term hyperosmotic stimulation can be a relevant stimulus to enhance the quality of cartilage replacement tissue, these data highlight the importance of the calcium microenvironment for cartilage ECM synthesis and deposition. However, it is currently unknown whether higher extracellular calcium stimulates or inhibits the cartilage ECM formation in cartilage TE constructs. Since AC and MSC are often used cell types for cartilage TE, the response of both cell types to long-term hyperosmotic stimulation using extracellular calcium should be investigated in terms of GAG synthesis, GAG deposition and type II collagen deposition.

1.12 Aim of the study

An insufficient deposition of type II collagen and PG presents a general drawback of culture-grown human cartilage replacement tissue. Recent studies of our group achieved a stimulation of cartilage matrix synthesis by a defined mechanical loading protocol which depended on a high fixed charge density (FCD) of the tissue. However, the decisive physicochemical parameter of the multimodal loading encounter which induced cartilage matrix synthesis in the chondrocytes remained unclear. Identifying the individual sub-parameter that contributes to load-induced cartilage homeostasis may provide an easily applicable stimulus to optimize the ECM content of cartilage replacement tissue. Due to the essential role of osmotic pressure for cartilage function, osmotic challenge appears as a very important parameter of the loading-response. However, the contribution of acute hyperosmotic pressure to homeostasis of engineered cartilage is unclear and models that take a cartilage typical FCD into consideration are required. Interestingly, long-term maturation of animal chondrocytes under hyperosmotic conditions enhanced the ECM content of 3D-engineered cartilage, but this was so far never investigated for human 3D-cultured cartilage.

Therefore, the aim of this study was 1) to find out whether acute hyperosmotic pressure, as a sub-parameter of mechanical compression, influences cartilage matrix synthesis in a human 3D engineered cartilage model at low and high FCD and 2) to elucidate whether long-term hyperosmotic challenge can enhance cartilage ECM synthesis and deposition of matrix in human engineered cartilage.

For this purpose, human 3D engineered cartilage replacement tissue was pre-matured for 3 or 35 days to develop a cartilage-like ECM of low and high FCD. After hyperosmotic challenge for 3 to 24 hours, induction of osmo-sensitive pathways ERK1/2 and p38, and of several osmo-response genes was determined and the activity of pro-chondrogenic pathways and GAG synthesis was investigated. Long-term hyperosmotic calcium stimulation was realized with AC and MSC-based cartilage replacement tissue exposed for 35 days. GAG synthesis as well as GAG- and type II collagen deposition were assessed via radiolabel-incorporation, ELISA, (immuno-)histochemistry, qPCR and Western blotting. Underlying pro- and anti-chondrogenic signaling mechanisms were investigated using ELISA, Western blot, qPCR and immunoradiometric assay.

2 Materials

2.1 Chemical reagents

Table 1 Chemical reagents

Chemical	Supplier
Acetic acid	Carl Roth (Karlsruhe, DE)
Acetone	Carl Roth (Karlsruhe, DE)
Ammonium persulfate (APS)	Sigma-Aldrich (St. Louis, US)
Aquatex	Merck (Darmstadt, DE)
ATX Ponceau S red staining solution	Sigma-Aldrich (St. Louis, US)
Boric acid	Sigma-Aldrich (St. Louis, US)
Bouin's solution	Sigma-Aldrich (St. Louis, US)
Bovine serum albumin (BSA)	Sigma-Aldrich (St. Louis, US)
Bradford reagent	Sigma-Aldrich (St. Louis, US)
Bromophenol blue	Sigma-Aldrich (St. Louis, US)
Calcium chloride (CaCl ₂)	Sigma-Aldrich (St. Louis, US)
Chloroform	Carl Roth (Karlsruhe, DE)
Chondroitin Sulfate A	Sigma-Aldrich (St. Louis, US)
Coomassie brilliant blue	Sigma-Aldrich (St. Louis, US)
1,9-Dimethylmethylene blue	Sigma-Aldrich (St. Louis, US)
Dimethylsulfoxide (DMSO)	Sigma-Aldrich (St. Louis, US)
Disodium hydrogen phosphate (Na ₂ HPO ₄)	Merck (Darmstadt, DE)
DNA Loading Dye 6x	Thermo Fisher Scientific (Waltham, US)
Ethanol	Carl Roth (Karlsruhe, DE)
Ethylenediaminetetraacetic acid (EDTA)	Sigma-Aldrich (St. Louis, US)
Ficoll Paque Plus	Cytiva (Uppsala, SE)
Gelatin	Sigma-Aldrich (St. Louis, US)
GeneRuler™ 100 bp DNA Ladder (100 ng/μl)	Thermo Fisher Scientific (Waltham, US)
Glycerol	Carl Roth (Karlsruhe, DE)
β-Glycerophosphat	Sigma-Aldrich (St. Louis, USA)
Glycine	Carl Roth (Karlsruhe, DE)
Hydrochloric acid (HCl)	Carl Roth (Karlsruhe, DE)
Indomethacin	Sigma-Aldrich (St. Louis, US)
Isobutylmethylxanthin (IBMX)	Sigma-Aldrich (St. Louis, US)
Isopropanol	Carl Roth (Karlsruhe, DE)
Kanamycin	Carl Roth (Karlsruhe, DE)
LB-Agar (Lennox)	Carl Roth (Karlsruhe, DE)
LB-Medium (Lennox)	Carl Roth (Karlsruhe, DE)
Lumi-Light Western Blotting Substrate	Roche (Mannheim, DE)
Magnesium chloride (MgCl ₂)	Sigma-Aldrich (St. Louis, US)
Methanol	Carl Roth (Karlsruhe, DE)
β-Mercaptoethanol	Gibco/Life Techn. (Carlsbad, US)

Chemical	Supplier
Neo-Mount	Merck (Darmstadt, DE)
Oligo (dT) primer	Eurofins MWG Operon (Huntsville, US)
Paraffin Paraplast X-Tra®	Leica Biosystems (Nussloch, DE)
Paraformaldehyde	Merck (Darmstadt, DE)
Pefabloc®	Sigma-Aldrich (St. Louis, US)
peqGOLD TriFast	PEQLAB Biotechnologie (Erlangen, DE)
peqGreen DNA/RNA dye	PEQLAB Biotechnologie (Erlangen, DE)
PhosphoSafe™ Extraction Reagent	Merck (Darmstadt, DE)
p-Nitrophenylphosphat	Sigma-Aldrich (St. Louis, US)
p-Nitrophenol standard	Sigma-Aldrich (St. Louis, US)
Potassium chloride (KCl)	Merck (Darmstadt, DE)
Potassium dihydrogen phosphate (KH ₂ PO ₄)	AppliChem (Darmstadt, DE)
Precision Plus Protein Standards™ Dual Color	Bio-Rad (Hercules, US)
Restore™ PLUS WB Stripping Buffer	Thermo Fisher Scientific (Waltham, US)
RNaseOut™ Ribonuclease Inhibitor	Invitrogen/Life Techn. (Carlsbad, US)
Roti® Histol	Carl Roth (Karlsruhe, DE)
Roti®-Mount FluorCare	Carl Roth (Karlsruhe, DE)
Rotiphorese® 30 acrylamide solution	Carl Roth (Karlsruhe, DE)
Skim milk powder	Sigma-Aldrich (St. Louis, US)
SOC Medium	Thermo Fisher Scientific (Waltham, US)
Sodium chloride (NaCl)	Carl Roth (Karlsruhe, DE)
Sodium dodecyl sulfate (SDS)	Sigma-Aldrich (St. Louis, US)
Sodium hydroxide	Sigma-Aldrich (St. Louis, US)
Sucrose	Sigma-Aldrich (St. Louis, US)
Tetramethylethylenediamine (TEMED)	AppliChem (Darmstadt, DE)
Tris	Sigma-Aldrich (St. Louis, US)
Tris base	Merck (Darmstadt, DE)
Tris HCl	Sigma-Aldrich (St. Louis, US)
Triton X-100	Sigma-Aldrich (St. Louis, US)
Trizol	Ambion/Life Technologies (Carlsbad, US)
Trypan blue solution 0.4%	Sigma-Aldrich (St. Louis, US)
Turk's solution	Merck (Darmstadt, DE)
Tween® 20	Sigma-Aldrich (St. Louis, US)
Ultima Gold™ liquid scintillation cocktail	Perkin Elmer (Waltham, US)
UltraPure DNase/RNase-free distilled water	Invitrogen/Life Techn. (Carlsbad, US)
WesternBright® Quantum HRP substrate	Advanta (Menlo Park, US)
X-tremeGENE™ 9 transfection reagent	Roche (Mannheim, DE)
Xylene cyanol	Sigma-Aldrich (St. Louis, US)

2.2 Cell culture supplements

Table 2 Cell culture supplements

Medium Component	Supplier
L-Ascorbic acid-2-phosphate	Sigma-Aldrich (St. Louis, US)
Dexamethasone	Sigma-Aldrich (St. Louis, US)
Dimethyl sulfoxide (DMSO)	Sigma-Aldrich (St. Louis, US)
Dulbecco's Modified Eagle Medium (DMEM) high / low glucose	Gibco/Life Techn. (Carlsbad, US)
Fetal calf serum (FCS)	Gibco/Life Techn. (Carlsbad, US)
Insulin glARGine 100 U/mL	Sanofi-Aventis (Frankfurt am Main, DE)
ITS+ Premix	Corning Life Sciences (New York, US)
Non-essential amino acids	Gibco/Life Techn. (Carlsbad, US)
Penicillin/Streptomycin	Invitrogen/Life Techn. (Carlsbad, US)
L-Prolin	Sigma-Aldrich (St. Louis, US)
Sodium-pyruvate	Gibco/Life Techn. (Carlsbad, US)
Sodium-selenite	Sigma-Aldrich (St. Louis, US)
Transferrin, human	Sigma-Aldrich (St. Louis, US)

2.3 Consumables

Table 3 Consumables

Consumable	Supplier
Adhesion Slides SuperFrost Plus™	Thermo Fisher Scientific (Waltham, US)
Amersham Hybond ECL Nitrocellulose Membrane	GE Healthcare (Chalfont St. Giles, UK)
Biopsy-punches 4 mm, round	Stiefel (Brentford, UK)
Cell culture flasks Cellstar T25, T75, T175	Nunc (Wiesbaden, DE)
Cell culture plates for suspension culture	Nunc (Wiesbaden, DE)
Cryo-tubes	Simport (Saint-Mathieu-de-Beloeil, CAN)
Filter paper Whatman 3 mm	GE Healthcare (Chalfont St Giles UK)
Flat-bottom plate 96-well, black	Greiner Bio One (Kremsmünster, AT)
Flat-bottom plate 96-well, transparent	Greiner Bio One (Kremsmünster, AT)
Glass measurement vial 0.15 ml	Knauer (Berlin, DE)
Gloves, one-way	Peha-Soft Hartmann (Heidenheim, DE)
Lightcycler 8-tube stripes, white	Roche Applied Science (Basel, CH)
Lightcycler 96-well plate, white	Roche Applied Science (Basel, CH)
Nylon strainer (40 µm)	BD Falcon (Franklin Lakes, US)
Parafilm M	Pechiney Plastic Packaging (Chicago, US)
Pipet tips	Eppendorf (Hamburg, DE)
Pipets, one-way	Becton Dickinson (Heidelberg, DE)
Reaction tubes 0.5 ml, 1.5 ml, 2 ml	Eppendorf (Hamburg, DE)
Reaction tubes 15 ml, 50 ml	Becton Dickinson (Heidelberg, DE)

Consumable	Supplier
Reaction tubes, RNase-free 0.5 ml, 1 ml, 2 ml	Steinbrenner Laborsysteme (Wiesenbach, DE)
Scalpel	Feather (Osaka, JP)
Steritop Express™ Plus (0.22 µm)	Merck (Darmstadt, DE)
TissueCut® Microtome Blade	Medite (Burgdorf, DE)

2.4 Radioactive isotopes

Table 4 Radioactive isotopes

Radioactive isotopes	Supplier
[³⁵ S]-Sulfate	Hartmann Analytics (Braunschweig, DE)

2.5 Kits & ELISA

Table 5 Kits and ELISA

Kit	Supplier
Absolute QPCR SYBR Green Mix, 2x	Thermo Fisher Scientific (Waltham, US)
cAMP Enzyme-Linked Immunosorbent Assay (ELISA) Kit	Enzo Life Sciences (Lörrach, DE)
Infinity Calcium Arsenazo III	Thermo Fisher Scientific (Waltham, US)
OmniScript RT Kit	Qiagen (Hilden, DE)
PGE2 ELISA Kit	Enzo Life Sciences (Lörrach, DE)
Quant-iT PicoGreen dsDNA Assay Kit	Thermo Fisher Scientific (Waltham, US)
QIAGEN Plasmid Maxi Kit	Qiagen (Hilden, DE)
QIAquick Gel Extraction Kit	Qiagen (Hilden, DE)
Type II Collagen Detection Kit, 6018 (ELISA)	Chondrex Inc. (Woodinville, US)
Zymoclean™ GEL DNA Recovery Kit	Zymo Research (Irvine, US)

2.6 Histological staining reagents

Table 6 Histological staining reagents

Staining Solution / Dye	Supplier
Alizarin red S	Chroma (Münster, DE)
Certistain Fast Green FCF	Merck (Darmstadt, DE)
Eosin 2% aqueous	Waldeck (Münster, DE)
Impact® Vector® Red AP substrate	Vector labs (Burlingame, US)
Meyer's hemalum solution	Chroma (Münster, DE)
Safranin-Orange	Fluka/Sigma-Aldrich (St. Louis, US)

2.7 Enzymes

Table 7 Enzymes

Enzyme	Supplier
Collagenase B	Roche (Mannheim, DE)
Hyaluronidase	Sigma-Aldrich (St. Louis, US)
Omniscript Reverse Transcriptase	Qiagen (Hilden, DE)
Pronase	Sigma-Aldrich (St. Louis, US)
Proteinase K, recombinant	Thermo Fisher Scientific (Waltham, US)
RNaseOUT	Invitrogen/Life Techn. (Carlsbad, US)
10x Trypsin/EDTA	Biochrom/Merck (Darmstadt, DE)

2.8 Biomaterials

Table 8 Biomaterials

Biomaterial	Supplier
Optimaix 3D collagen carrier	Matricel (Herzogenrath, DE)

2.9 Growth factors

Table 9 Growth factors

Component	Supplier
FGF2, recombinant human	Active Bioscience (Hamburg, DE)
TGF β 1, recombinant human	Miltenyi Biotec (Bergisch-Gladbach, DE), Biomol (Hamburg, DE)

2.10 Agonists/Inhibitors

Table 10 Agonists/Inhibitors

Compound	Supplier
IBMX	Sigma-Aldrich (St. Louis, US)
Niclosamide	Sigma-Aldrich (St. Louis, US)
PTHrP ₁₋₃₄	Bachem (CH)
PTHrP ₇₋₃₄	Bachem (CH)

2.11 Antibodies

Table 11 Antibodies

Primary Antibody	Supplier	Dilution
β -Actin mouse mAb (clone AC-15)	GeneTex (Irvine, US)	WB, 1:10000
BSP II (IBSP) mouse mAb (clone LFMb-24)	Santa Cruz (Dallas, US)	WB, 1:500

Primary Antibody	Supplier	Dilution
CaSR mouse mAb (clone 5C10, ADD)	Invitrogen/Life Techn. (Carlsbad, US)	WB, 1:500
Collagen type II mouse mAb (clone II-4CII)	ICN Biomedicals (Eschwege, DE)	IHC, 1:1000
Collagen type X mouse mAb (clone X53)	Quartett (Berlin, DE)	WB, 1:500
ERK1/2 rabbit (rb) pAb	Cell Signaling (Danvers, US)	WB, 1:1000
P38 MAPK rabbit pAb	Cell Signaling (Danvers, US)	WB, 1:1000
p65 (active) mouse mAb (clone 12H11)	Merck (Darmstadt, DE)	WB, 1:500
p65 rabbit mAb (clone D14E12)	Cell Signaling (Danvers, US)	WB, 1:1000
Phospho-ERK1/2 mouse mAb (clone E-4)	Santa Cruz (Dallas, US)	WB, 1:1000
Phospho-P38 mouse mAb (clone D3F9)	Cell Signaling (Danvers, US)	WB, 1:1000
Phospho-SMAD1/5/9 rabbit mAb (clone D5B10)	Cell Signaling (Danvers, US)	WB, 1:250
Phospho-SMAD2 rabbit mAb (clone 138D4)	Cell Signaling (Danvers, US)	WB, 1:250
PTHLH rabbit pAb	Abcam (Cambridge, UK)	WB, 1:1000
SMAD1 rabbit mAb (clone EP565Y)	Abcam (Cambridge, UK)	WB, 1:500
SMAD2/3 rabbit mAb (clone D7G7)	Cell Signaling (Danvers, US)	WB, 1:1000
SMAD5 rabbit mAb (clone EP619Y)	Abcam (Cambridge, UK)	WB, 1:1000
SOX9 rabbit pAb	Merck (Darmstadt, DE)	WB, 1:2000

Secondary Antibody	Supplier	Dilution
Anti-Mouse HRP goat (gt) pAb	Jackson ImmunoRes. (West Grove, US)	WB, 1:5000
Anti-Rabbit HRP gt pAb	Jackson ImmunoRes. (West Grove, US)	WB, 1:10000
Brightvision, 1 step goat anti-mouse/rabbit AP	Immunologic (Duiven, NL)	IHC, undiluted

2.12 Plasmids

Table 12 Plasmids

Plasmid	Catalog #	Supplier
Parathyroid hormone related protein (PTHLH) (NM_198965) Human Tagged ORF Clone	RC223709	OriGeneTechnologies, Inc. (Rockville, US)
pCMS-EGFP	6101-1	Takara Bio USA, Inc. (San Jose, US)

2.13 Cells

Table 13 Cells

Cell	Catalog #	Supplier
OneShot TOP10 Chemically Competent E. coli	C4040	Invitrogen/Life Technologies (Carlsbad, US)

2.14 Primers

Table 14 Primers

Gene	Forward Sequence 5' – 3'	Reverse Sequence 5' – 3'	T _A [°C]
18S	GTAACCCGTTGAACCCATT	CCATCCAATCGGTAGTAGCG	58
ACAN	GGAACCACTTGGGTCACG	GCACATGCCTTCTGCTT	58
ALP	CACCAACGTGGCTAAGAATG	ATCTCCAGCCTGGTCTCCTC	58
BMP2	ACGAGGTCCTGAGCGAGTTC	GAAGCTCTGCTGAGGTGATAA	58
BMP4	GGATCTTTACCGGCTTCAGTC	CCTGGGATGTTCTCCAGATG	58
BMP6	ATTACAACAGCAGTGAATTGA	TTCATGTGTGCGTTGAGTG	58
BMP7	CCAGAACCCTCCAAGAC	GTTGGTGGCGTTCATGTAG	58
COL2A1	TGGCCTGAGACAGCATGAC	AGTGTTGGGAGCCAGATTGT	58
COL10A1	TTTACGCTGAACGATACCAAA	TTGCTCTCCTCTTACTGCTAT	58
COX2	TTCAAATGAGATTGTGGAAAATTGCT	AGATCATCTCTGCCTGAGTATCTT	58
DUSP5	CTCCCACTTTCAAGAAGCAA	GGCAGGATCTCAGATTCGTA	60
FOS	TCCAGTGCCAACTTCATTCC	GCTGCAGCCATCTTATTCTT	60
FOSB	CCAGGGAAATGTTTCAGGCT	GAAGAGATGAGGGTGGGTTG	60
GAPDH	CCACCCATGGCAAATCCATGGCA	TCTAGACGGCAGGTCAGGTCCACC	58
GREM1	CCGCACTCAGCGCCAC	AGGGCTCCCACCGTGTGA	60
IBSP	CAGGGCAGTAGTGACTCATCC	TCGATTCTTCATTGTTTTCTCCT	59
ID1	ATCAGGGACCTTCAGTTGGAGC	AGACCCACAGAGCACGTAATTCC	62
MMP13	CTGGAGATATGATGATACTAAC	CACGCATAGTCATATAGATACT	58
NFAT5	TCCCCTCAGAACAACATGCC	CTGCAACAAGCAGCATAGGTG	60
PTHLH	CGGTGTTCTGCTGAGCTA	TGCGATCAGATGGTGAAGGA	58
RPL13	CATTTCTGGCAATTTCTACAG	CAGGCAACGCATGAGGAAT	58
S100A4	TCTTGGTTTGATCCTGACTGCT	TCGTTGTCCCTGTTGCTGTC	60
SLC5A3	CGCTACGAGCTGGCTTTAATC	CAGCATTTACTCAGGTGCTGG	60
SLC6A12	ACACAGAGCATTGCACGGACT	CCAGAACTCGTCTCTCCAGAA	62
SOX9	GTACCCGCACTTGCAACAAC	TCGCTCTCGTTCAGAAGTCTC	60

2.15 Equipment/Devices

Table 15 Equipment and devices

Technical Device	Supplier
Agarose gel electrophoresis chamber	Bio-Rad (Hercules, US)
Agarose gel imaging system	PEQlab/VWR (Erlangen, DE)
Centrifuge Rotina 420	Hettich (Tuttlingen, DE)
Centrifuge Universal 320	Hettich (Tuttlingen, DE)
DNA/RNA UV Cleaner Hood	Kisker Biotech (Steinfurt, DE)
FluoStar Omega	BMG Labtech (Offenburg, DE)
Fusion-SL 3500-WL (Western Blot imager)	PEQlab/VWR (Erlangen, DE)
Gel casting system for SDS-Gels	Bio-Rad (Hercules, US)
Heated tweezers	Vogel (Fernwald, DE)

Technical Device	Supplier
Heating plate for paraffin sections	Medax (Neumünster, DE)
Hybrid2000 (hybridization oven)	H. Saur (Reutlingen, DE)
Incubator for paraffin embedding	Heraeus (Hanau, DE)
Incubator, cell culture	Heraeus (Hanau, DE)
LightCycler® 96	Roche Applied Science (Basel, CH)
Microscope Axioplan2 Imaging + AxioCam HRC	Zeiss (Oberkochen, DE)
Mini PROTEAN® II xi Cell	Bio-Rad (Hercules, US)
Mini Trans-Blot® Cell	Bio-Rad (Hercules, US)
Mixer mill MM 400	Retsch (Haan, DE)
NanoDrop ND-1000 Spectrophotometer	Thermo Fisher Scientific (Waltham, US)
Neubauer counting chamber	Karl Hecht (Sondheim an der Röhn, DE)
Orbital shaker 3015	GFL (Burgwedel, DE)
Paraffin oven EG1120	Leica (Wetzlar, DE)
pH Meter PB-11, pH electrode PY-P11	Sartorius (Göttingen, DE)
Pipets	Eppendorf (Hamburg, DE)
Polytron PT-MR 2100	Kinematika (Luzern, CH)
Power Supply Pac 3000	Bio-Rad (Hercules, US)
Roller slide KWEM9-G2/A_V1 and rail	Schaeffler (Herzogenaurach, DE)
Shatterproof plexiglass transport box	Biostep (Burkhardtsdorf, DE)
Semi-Micro Osmometer K7400	Knauer (Berlin, DE)
Short and spacer plates 1.5 mm	Bio-Rad (Hercules, US)
Sliding microtome Jung Histoslide 2000R	Leica (Wetzlar, DE)
Steel balls 5 mm	Retsch (Haan, DE)
Sunrise Magellan, micro plate reader	Tecan (Männedorf, CH)
Thermomixer comfort 1.5ml	Eppendorf (Hamburg, DE)
ThermoStat plus 1.5ml	Eppendorf (Hamburg, DE)
Vacuum pump RZ 2.5	Vacuubrand (Weinheim, DE)
Wallac 1420 Victor2 micro plate reader	PerkinElmer Life Sciences (Waltham, US)
Wallac MicroBeta-Counter	PerkinElmer Life Sciences (Waltham, US)
Water bath, cell culture	GFL (Burgwedel, DE)
Water bath, paraffin sections	Medax (Neumünster, DE)

2.16 Software

Table 16 Software

Software	Supplier
Axiovision Rel 4.6.3.0	Zeiss (Oberkochen, DE)
Bio-1D	Vilber Lourmat (Eberhardzell, DE)
BioCapt 11.02	Vilber Lourmat (Eberhardzell, DE)
Fusion Molecular Imaging	Vilber Lourmat (Eberhardzell, DE)
GraphPad Prism	GraphPad Software, Inc. (La Jolla, US)
ImageJ 1.48v	National Institute of Health (New York, US)
LightCycler® 96 Software	Roche Applied Science (Basel, CH)

Software	Supplier
Magellan 6.6	Tecan (Männedorf, CH)
MS Office	Microsoft (Redmont, US)
ND_1000 V3.8.1	Thermo Fisher Scientific (Waltham, US)
Photoshop CS2	Adobe Systems Software, (Dublin, IE)
SPSS Statistics 25	IBM (Armonk, US)
Wallac 1420 Manager	PerkinElmer Life Sciences (Waltham, US)

2.17 Buffers and media

2.17.1 Agarose-gel electrophoresis

Table 17 Agarose-gel electrophoresis buffers

<u>50x TAE buffer</u>		<u>2x DNA loading buffer</u>	
Ingredient	Concentration	Ingredient	Concentration
Tris base	2 M	Glycerol	10% (v/v)
Acetic acid	6% (v/v)	Bromophenol blue	0.083% (w/v)
EDTA	50 mM	Xylen cyanole	0.083% (w/v)
Prepared in water. Diluted 1:50 before use.		Prepared in water.	

2.17.2 Cell culture

Table 18 Cell culture buffers and medium

<u>10x PBS for cell culture</u>		<u>Expansion medium for MSC</u>	
Ingredient	Concentration	Ingredient	Concentration
NaCl	1.37 M	Fetal calf serum (FCS)	12.5% (v/v)
KCl	27 mM	Penicillin /Streptomycin	1% (v/v)
KH ₂ PO ₄	18 mM	L-Glutamine	2mM
Na ₂ HPO ₄ ·2H ₂ O	101 mM	Non-essential amino acids	2 mM
Prepared in water. Adjusted to pH 7.4, diluted 1:10 and autoclaved before use.		β-Mercaptoethanol	50 μM
		FGF2	4 ng/ml
		Prepared in DMEM (4.5 g/l glucose); FGF2 added freshly before use; stored at 4°C and only used up to one week after supplementation.	
<u>Expansion medium for AC</u>		<u>Expansion medium for cell lines</u>	
Ingredient	Concentration	Ingredient	Concentration
Fetal calf serum (FCS)	10% (v/v)	Fetal calf serum (FCS)	10% (v/v)
Penicillin /Streptomycin	1% (v/v)	Penicillin /Streptomycin	1% (v/v)
Prepared in DMEM (1 g/l glucose).		Prepared in DMEM (4.5 g/l glucose).	

Differentiation medium for MSC

Ingredient	Concentration
Sodium pyruvate	1 mM
L-Ascorbic acid-2-phosphate	0.17 mM
Dexamethasone	0.1 μ M
L-Proline	0.35 mM
Penicillin /Streptomycin	1% (v/v)
ITS+ Premix	1% (v/v)
TGF β 1	10 ng/ml

Prepared in DMEM (4.5 g/l glucose), filtered sterile, stored at -20°; TGF β 1 and ITS+ added freshly before use; stored at 4°C and only used up to one week after supplementation.

NaCl stock solution

Ingredient	Concentration
NaCl	4.2 M

Prepared in water.

MgCl₂ stock solution

Ingredient	Concentration
MgCl ₂	1.25 M

Prepared in water.

Niclosamide stock and working solution

Ingredient	Concentration
Niclosamide	10 mM

Stock solution prepared in DMSO. Dilute stock solution 1:1000 in water to obtain 100 μ M working solution.

TGF β stock solution

5 μ g TGF β 1 were solved in 100 μ l 10 mM citric acid pH 3.0 and diluted in 400 μ l of PBS to a final concentration of 10 μ g/ml.

Re-differentiation medium for AC

Ingredient	Concentration
Sodium pyruvate	1 mM
L-Ascorbic acid-2-phosphate	0.17 mM
Dexamethasone	0.1 μ M
L-Proline	0.35 mM
Penicillin /Streptomycin	1% (v/v)
Insulin	5 μ g/ml
Sodium selenite	5 ng/ml
Transferrin	5 μ g/ml
BSA	1.25 mg/ml
TGF β 1	10 ng/ml

Prepared in DMEM (4.5 g/l glucose), filtered sterile, stored at -20°; TGF β 1 and Insulin added freshly before use; stored at 4°C and only used up to one week after supplementation.

CaCl₂ stock solution

Ingredient	Concentration
CaCl ₂	1.25 M

Prepared in water.

Sucrose stock solution

Ingredient	Concentration
Sucrose	3.75 M

Prepared in water.

PTHrP₁₋₃₄ stock solution

Ingredient	Concentration
PTHrP ₁₋₃₄	10 μ g/ml

Prepared in water.

FGF2 stock solution

50 μ g FGF2 were solved in 500 μ l 1% BSA in PBS and diluted in water to a final concentration of 10 μ g/ml.

2.17.3 Assay buffer

Table 19 Assay buffers

Proteinase K digestion buffer

Ingredient	Concentration
Tris-HCl	50 mM
CaCl ₂	1 mM

Prepared in water. Adjusted to pH 8.

ALP buffer

Ingredient	Concentration
Glycin	0.1 M
MgCl ₂	1 mM
ZnCl ₂	1 mM

Prepared in water. Adjusted to pH 9.6

DMMB staining solution

Ingredient	Concentration
Glycine	1.45 M
NaCl	27 mM
Dimethylmethylen blue	20 g/l

Prepared in water. Adjusted to pH 3; stored in the dark.

2.17.4 SDS Page

Table 20 SDS-Page buffers

4x Sample buffer

Ingredient	Concentration
Tris-HCl, 1 M pH 6.8	25% (v/v)
Glycerol	10% (v/v)
SDS	8% (v/v)
Bromophenol blue	0.02% (w/v)
β-Mercaptoethanol	10% (v/v)

Prepared in water.

10x Stacking gel buffer

Ingredient	Concentration
Tris	1 M

Prepared in water. Adjusted to pH 6.8

5% Stacking gel

Ingredient	Volume
Stacking Gel Buffer pH 6.8	3.0 ml
Rotiphorese® 30 acrylamide	2.0 ml
Water	7.0 ml
SDS 10% (w/v)	122 µl
APS 10% (w/v)	100 µl
TEMED	10 µl

10x Running buffer

Ingredient	Concentration
Tris base	0.25 M
Glycine	2 M
SDS	1% (w/v)

Prepared in water. Diluted 1:10 before use.

10x Separating gel buffer

Ingredient	Concentration
Tris	1.5 M

Prepared in water. Adjusted to pH 8.8

10% Separating gel

Ingredient	Volume
Separating Gel Buffer pH 8.8	5.0 ml
Rotiphorese® 30 acrylamide	6.7 ml
Water	7.9 ml
SDS 10% (w/v)	200 µl
APS 10% (w/v)	200 µl
TEMED	8 µl

2.17.5 Western blot

Table 21 Western blot buffers

10x Transfer buffer

Ingredient	Concentration
Glycine	2.4 mM
Tris-Base	313 mM
SDS	1.25% (w/v)

Diluted 1:10 in 650 ml water and 250 ml MeOH before use

Coomassie staining solution

Ingredient	Concentration
Methanol	50% (v/v)
Acetic acid	10% (v/v)
Coomassie brilliant blue	0.25% (w/v)

Prepared in water.

10x TBE buffer

Ingredient	Concentration
Tris base	1 M
Boric acid	1 M
0.5 M EDTA pH 8.0	2% (v/v)

Prepared in water. Dilute 1:10 in water before use.

10x TBS

Ingredient	Concentration
NaCl	1.45 M
KCl	27 mM
Tris-HCl	25 mM

Adjusted to pH 7.6, diluted 1:10 before use

Coomassie De-Staining Solution

Ingredient	Concentration
Methanol	25.0% (v/v)
Acetic acid	7.5% (v/v)

Prepared in water.

Blocking solution (Western blot)

5% (w/v) Skim Milk in TBS-T

TBS-T

0.1% (v/v) Tween20 in TBS

2.17.6 Histology

Table 22 Histology buffers

10x PBS for histology

Ingredient	Concentration
NaCl	1.37 M
KCl	1.07 M
KH ₂ PO ₄	15 mM
Na ₂ HPO ₄ ·2H ₂ O	37 mM

Prepared in water. Diluted 1:10 before use

Safranin-Orange stain

Ingredient	Concentration
Safranin-O	0.2% (w/v)
Acetic acid	1% (v/v)

Prepared in water. Filtered before use

10x TBS for histology

Ingredient	Concentration
NaCl	5 M
Tris	35 mM
Tris-HCl	165 mM

Prepared in water. Diluted 1:10 before use

Fast-Green stain

Ingredient	Concentration
Fast green	0.04% (w/v)
Acetic acid	0.2% (v/v)

Prepared in water. Filtered before use

PBS pH 5,5

Ingredient	Concentration
NaCl	137 mM
KCl	2.68 mM
Na ₂ HPO ₄	10.14 mM
KH ₂ PO ₄	1.76 mM

Prepared in water. Adjusted to pH 5.5

4% Paraformaldehyde

Ingredient	Concentration
Paraformaldehyde	4% (w/v)

Prepare in 1x PBS for histology, gently shake, resolve in microwave. Don't let boil. Store at -20°C

Blocking solution

Ingredient	Concentration
BSA	5% (w/v) in PBS

Alizarin Red S stain

Ingredient	Concentration
Alizarin Red S	5 g/l in H ₂ O

2.17.7 Bacterial growth media

Table 23 Bacterial growth media

LB-Medium

Ingredient	Concentration
LB-Medium (Lennox)	20 g/l

Prepared in water. Sterilized in autoclave for 20 minutes. Store medium at 4°C.

LB-Agar plates

Ingredient	Concentration
LB-Agar (Lennox)	35g/l

Prepared in water. Sterilized in autoclave for 15 minutes. Antibiotics were added after cooling to 50°C. Poured in sterile culture plates. Store plates at 4°C.

3 Methods**3.1 Legal and ethical aspects of the study**

This study was carried out in accordance with the current version of the Declaration of Helsinki. The study concept was reviewed and approved by the ethics committee of the medical faculty of the University of Heidelberg (ethical approval: S-117/2014, S-609/2019 and S-058/2020) and written informed consent was obtained from all individuals included in the study. The participation of the patients was voluntary with the right to withdraw from the study at any time.

3.2 Cell culture

3.2.1 Isolation and expansion of AC

Samples of human articular cartilage were obtained from a total of 21 patients at the age of 40 to 87 years (mean age: 65 ± 9 years, 11 male and 10 female patients) undergoing total knee replacement surgery. Using a scalpel, hyaline cartilage from regions with no evident degeneration was gently separated from the subchondral bone, without transferring the mineralized layer. The total amount of the removed cartilage was weighed, minced and subsequently digested overnight for 16-20 hours at 37°C in a digestion mixture of 10 ml/g cartilage, consisting of 1.5 mg/ml collagenase B and 100 µg/ml hyaluronidase in chondrocyte expansion medium to remove the ECM from the cells. After digestion, isolated chondrocytes were separated from the undigested tissue by filtration through a 40 µm nylon mesh and the cells from the filtrate were pelleted by centrifugation at $300 \times g$ for 10 min. Chondrocytes were then washed, plated at 5,700 cells/cm² and expanded for 2 passages in chondrocyte expansion medium at 37°C, 6% CO₂. Medium was changed twice a week.

3.2.2 Isolation and expansion of MSC

Human bone marrow aspirates were obtained from a total of 15 patients at the age of 27 to 83 years (mean age: 61 ± 14 years, 8 male and 7 female patients) undergoing total hip replacement surgery. The mononuclear cell fraction was separated from bone marrow aspirates by Ficoll-Paque™ density gradient. For this, the freshly collected bone marrow aspirate was washed twice with PBS followed by centrifugation for 10 minutes at $650 \times g$ to remove remaining fat and bone tissue. The washed bone marrow suspension was then carefully pipetted on top of Ficoll-Paque™ reagent. The two separated layers were then centrifuged for 35 minutes at $1460 \times g$. No break was applied to centrifugation at the end of the run. During the density gradient centrifugation, the different cell types are separated based on their density. While the non-nucleated erythrocytes aggregate at the bottom of the tube, the overlying phase mainly contains granulocytes. MSC are located in the interphase between Ficoll-Paque™ solution and PBS, where the mononucleated cells form a macroscopically visible ring. After the PBS phase was carefully removed, the visible ring of mononucleated cells was collected using a pipette and washed three times with PBS at decreasing centrifugation steps of 650, 450, 250 $\times g$ for 10 minutes. The resulting cell pellet was seeded into 0.1% gelatin-coated culture flasks at a density of 125,000 to 150,000 cells per cm² and cultured in MSC expansion medium at 37°C in a humidified atmosphere and 6% CO₂. After 24 hours non-adherent cells were removed by washing with PBS and cells were expanded for 3

passages under identical conditions as described above. Medium was refreshed three times a week.

In accordance with the generally accepted surface marker profile (Dominici et al. 2006), MSCs were routinely tested and found positive for CD90, CD105, CD73 and CD146, and negative for CD34 and CD45 (Diederichs et al. 2019).

3.2.3 Seeding and maturation of AC and MSC in collagen scaffolds

For the generation of AC or MSC cartilage TE-constructs, AC from passage 2 or MSC from passage 3 were seeded into a type I/III collagen scaffold. The scaffolds consist of parallel oriented porcine type I and type III collagen fibers, which form the basis for storing secreted matrix molecules. The time-dependent increase in deposition of GAGs in the scaffold was demonstrated for both human AC and human MSC (Lückgen et al. 2022). For seeding cells into the scaffold, 500,000 AC or MSC were centrifuged in a 1.5 ml reaction tube at $300 \times g$ for 10 minutes. The supernatant was removed except for about 20 μ l and the cells were resuspended in the remaining volume. 10 μ l of the cell suspension were added into a well of a 24-well suspension culture plate and a cylindrical collagen scaffold (\emptyset 4 mm \times 1.5 mm) was placed on top. The remaining cell suspension was then pipetted onto the top of the scaffold to achieve a homogenous seeding of the construct from both sides. To ensure a sufficient attachment of the cells to the scaffold, the plates were incubated for 2 hours at 37°C and 6% CO₂ before medium was added. After 40 minutes of incubation, the scaffolds were rotated using a forceps to promote even attachment. After 2 hours, the AC- or MSC-seeded scaffolds were immersed in 1.5 ml of AC redifferentiation or MSC differentiation medium, respectively. Constructs were matured at 37°C, 6% CO₂, for the indicated time points with medium being changed three times a week.

3.2.4 Hyperosmotic stimulation of cartilage TE constructs

For hyperosmotic stimulation experiments 10, 15, 22, 34 or 49 μ l of NaCl stock solution were added directly to the culture well, containing 1.5 ml medium, to achieve final osmolarities of 350, 400, 450, 500 or 550 mOsm, respectively. Equal amounts of water were added to control wells. Hyperosmotic stimulation was terminated after 3, 6 or 24 hours by snap freezing constructs in liquid nitrogen.

Medium osmolarity was confirmed using a freezing point osmometer (Semi-Micro Osmometer K7400, Knauer). In brief, 150 μ l of medium were added into a glass measurement vial, fixed in the measurement adapter and placed in the cooling cavity of the device.

3.2.5 Calcium, Niclosamide and PTHrP stimulation of cartilage TE constructs

For calcium stimulation experiments, AC- or MSC-based cartilage TE constructs were cultured in AC or MSC (re)differentiation medium with or without the addition of CaCl₂ throughout the complete (re)differentiation. Before each medium exchange, 12 µl or 50 µl CaCl₂ stock solution were freshly added to 10 ml of AC or MSC (re)differentiation medium to achieve final concentrations of 3.3 mM or 8.0 mM Ca²⁺ in the medium, respectively. Calcium concentration in the medium was confirmed at indicated timepoints using, the Infinity Calcium Arsenazo III assay kit (see section 3.7.5). For ionic controls, equal volume of MgCl₂ stock solution were added. For osmotic controls, equal volume of sucrose stock solution was added. On day 35, samples were harvested by snap freezing constructs in liquid nitrogen.

For Niclosamide stimulation experiments, Niclosamide was solved in DMSO and added to the culture medium of constructs cultured with or without the addition of CaCl₂. Niclosamide working solution was pre-diluted in a dilution series and 10 µl of the respective dilution series were added to 1 ml of culture medium to achieve final concentrations of 0.1 µM [33 ng/ml], 0.5 µM [162 ng/ml] or 1 µM [327 ng/ml] throughout the complete (re)differentiation. Equal volume of DMSO was added to separate controls.

In the case of PTHrP stimulation, constructs were treated with 10 ng/ml PTHrP₁₋₃₄ in the culture medium at indicated time points and conditions. For this, 10 µl of PTHrP₁₋₃₄ stock solution were added to 10 ml of culture medium.

3.2.6 Expansion of cell lines

The osteosarcoma cell line SaOS-2, the chondrosarcoma cell line SW1353, and human embryonal kidney cells HEK293 were acquired commercially. HepG2 and HCT116 cell lines were a kind gift from Dr. Jörg Fellenberg (Heidelberg University Hospital). All cell lines were cultured in expansion medium for cell lines at 37°C and 6% CO₂. At 80% confluency, cells were passaged at a ratio of 1:10.

3.3 Plasmid amplification and preparation

For amplification of plasmids, competent *E. coli* cells were used. Cells were slowly thawed on ice and 2 µL of plasmid DNA in the concentration of 1 ng/µL was added. Cells and DNA were mix by gentle tapping. The mixture was then incubated for 5 minutes on ice before incubation for 30 seconds in a water bath at 42°C and placed back on ice for 5 minutes. 300 µl of SOC medium was added to the bacteria and the sample was incubated for 1 hour at 37°C with constant shaking at 225 rpm. Selection for bacteria that had taken up the plasmid was achieved by spreading 50 µL of

the cells on self-poured, prewarmed LB agar plates containing 50 µg/mL kanamycin. Plates were incubated at 37°C overnight to allow bacterial colonies to form. For amplification, kanamycin-resistant single colonies were inoculated into 5 ml LB-medium containing 50 µg/ml kanamycin and grown for 8 hours at 37°C with constant shaking at 225 rpm. After this selective growth, bacteria were further amplified by adding 4 ml of bacterial suspension into 200 ml of LB-Medium, containing 50 µg/ml kanamycin and incubated overnight at 37°C and 225 rpm. The resulting bacterial suspension was then centrifuged at 600 x g for 15 minutes and plasmids were isolated using the QIAGEN Plasmid Maxi Kit according to the manufacturers protocol.

3.4 Transfection and overexpression

For PTHLH overexpression, 3×10^5 HEK293 cells were seeded into one well of a 6-well plate and cultured overnight in DMEM low-glucose, 10% FCS, 100 U/ml penicillin, 100 mg/ml streptomycin (complete medium) at 37°C, 6% CO₂. On the next day, cells were serum-starved for 6 hours before start of transfection. Transfection was performed using X-tremeGENE™ 9 DNA transfection reagent. Transfection reagent was brought to room temperature and mixed using vortex for one second before 3 µl of transfection reagent and 1 ng of plasmid DNA were added to a final volume of 100 µl of serum-free DMEM. The transfection reagent/DNA complex was incubated at room temperature for 15 minutes and then added dropwise to the cells (100 µl per well of a 6-well plate). Following transfection, cells were incubated for 72 hours at 37°C and the medium was replaced with fresh complete medium 24 hours after transfection. Transfection efficiency was monitored using fluorescence microscopy. After 72 hours cells were harvested for subsequent analyses (see section 3.10.1).

3.5 Histological analyses

3.5.1 Embedding of cartilage TE constructs

Snap frozen cartilage constructs were fixed in 500 µl 4% paraformaldehyde for 4 hours at room temperature (RT). After rinsing in 1 ml PBS, the tissue was stepwise dehydrated for 3 hours in 70%, 3 hours in 96% and overnight in 100% isopropanol, followed by 2 hours in 100% acetone. Dehydrated tissues were then incubated for at least 4 hours or overnight in paraffin at 65°C. Cylindrical cartilage TE constructs were embedded vertically in paraffin with the cutting surface facing down to allow for frontal sectioning in the microtome.

3.5.2 Preparation of tissue sections for histological staining

For staining and microscopic analysis, paraffin blocks containing the embedded tissue were cooled down to 4°C and sectioned in slices of 5 µm using a sliding microtome. Serial sections from the center region of the constructs were cut and transferred onto the surface of a 38°C warm water bath to allow for stretching of the sections. Two to three sections were taken up per glass slide and dried for 2 hours on a 38°C warm heating plate, followed by full drying at 42°C for 48 hours. Sections were then processed for staining by incubating four times for 5 minutes in Rotihistol, followed by stepwise rehydration in 100, 96, 70 and 50% isopropanol for 5 minutes each. After a final incubation for 5 minutes in demineralized water, sections were ready for staining.

3.5.3 Safranin Orange staining

The maturity of the engineered cartilage TE constructs was judged according to Safranin Orange (SafO) staining. SafO is a cationic dye which stains anionic tissue components such as sulfate residues. Due to the poly-anionic sulfated GAGs in mature cartilage, SafO staining intensity can be used as a measurement of GAG deposition in the construct.

For SafO staining, rehydrated tissue sections were incubated in 0.2% SafO for 25 minutes. After rinsing the sections three times in demineralized water, the tissue was counter-stained in 0.04% Fast-Green solution for 25 seconds. After final rinsing for three times in demineralized water, samples were dehydrated and mounted according to protocol 3.5.6.

3.5.4 Immunohistochemical staining

Immunohistological staining was performed to detect type II collagen deposition in the constructs via an indirect detection system using primary and ALP-conjugated secondary antibodies.

For enzymatic antigen retrieval, rehydrated tissue sections were incubated for 15 minutes with hyaluronidase [4 mg/mL] in PBS (pH 5.5), followed by incubation for 30 minutes with pronase [1 mg/mL] in PBS (pH 7.4) at 37°C in a humid chamber. After each digest, sections were washed three times for 5 minutes in PBS. To reduce unspecific binding of antibodies, sections were then blocked in 5% BSA in PBS for 30 minutes. Tissue sections were then incubated overnight at 4°C with mouse anti-human type II collagen antibody (1:1000), washed three times for 5 minutes in phosphate-free TBS, followed by incubation with BrightVision alkaline phosphatase-coupled goat anti-mouse/anti-rabbit IgG secondary antibody for 30 minutes. After washing three times for 5 minutes in TBS, detection was performed using ImmPACT® Vector® Red substrate for alkaline phosphatase. Slides were then washed three times for 5 minutes in TBS and nuclei were stained

by incubation with Mayer's hemalum solution for 3 minutes, followed by rinsing in tap water for 15 minutes. Sections were then mounted according to protocol 3.5.6.

3.5.5 Alizarin Red S staining

Alizarin Red S is an anthraquinone derivative that complexes with calcium ions. To investigate the precipitation of calcium from the medium during differentiation, the bottom of the plate and the TE constructs were stained with Alizarin Red S to visualize calcium deposits.

For staining of tissue sections, rehydrated sections were washed for 5 minutes in demineralized water, followed by staining with 0.5% Alizarin Red S solution for 5 minutes. After rinsing the sections three times in demineralized water, the tissue was counter-stained in 0.04% Fast-Green solution for 15 seconds. After final rinsing for three times in demineralized water, samples were dehydrated and mounted according to the protocol in section 3.5.6.

For staining the bottom of the plate, the empty wells were washed three times with PBS, fixed with 70% ice-cold ethanol for 20 minutes at 4°C and washed with demineralized water. The bottom of the plate was then stained with 0.5% Alizarin Red S solution for 10 minutes and washed five times with demineralized water.

3.5.6 Mounting of stained tissue sections

After staining, sections were mounted permanently under glass slides to allow for long-term storage for several years.

Sections stained with SafO or Alizarin Red S were dehydrated by sequential incubation for 30 seconds, once in 96% isopropanol and twice in 100% isopropanol, followed by four times 5 minutes in Rotihistol. Sections were mounted in anhydrous Neomount under glass slides. Immunohistochemically stained sections were rinsed in demineralized water and directly mounted in hydrous Aquatex under glass slides.

3.6 Collection of human blood plasma

Human blood plasma was obtained from healthy donors. Written informed consent was obtained from all individuals included in the study. Whole blood was collected in EDTA collection tubes and centrifuged at 2,500 x g for 10 minutes. The clear supernatant was transferred to fresh 1.5 ml reaction tubes and stored at -20°C.

3.7 Biochemical analyses

3.7.1 DNA quantification

For quantification of the DNA content of cartilage TE constructs, the Quant-iT PicoGreen dsDNA Assay Kit was used according to the manufacturer's instructions. The principle of the assay kit is based on the intercalation of fluorescein into double-stranded DNA and subsequent photometric quantification of fluorescence activity.

In brief, snap frozen constructs were digested overnight in 1 ml Proteinase K digestion buffer with 0.5 mg/ml Proteinase-K at 65°C while shaking at 800 rpm. Digests were diluted 1:20 in Proteinase K digestion buffer. For the standard curve, a 1:2 serial dilution of the DNA standard included in the kit was prepared in Proteinase K digestion buffer, ranging from 1 µg/ml to 15.6 ng/ml and Proteinase K digestion buffer serving as a blank. In a black flat-bottomed 96-well plate, 20 µl sample or 8 µl DNA standard was added to 80 µl or 92 µl Proteinase K digestion buffer, respectively, to reach a total volume of 100 µl. To each well, 100 µl fluorescein-solution (stock diluted 1:200 in Proteinase K digestion buffer) was added and incubated for 5 minutes at RT in the dark. Upon excitation at 485 nm wavelength, the fluorescence emission was measured at 535 nm in a microplate reader. DNA concentrations were calculated from technical duplicates according to values deducted from the standard curve.

3.7.2 Glycosaminoglycan quantification (DMMB Assay)

The content of glycosaminoglycans in cartilage TE constructs was determined by the Dimethylmethylene Blue (DMMB) assay (Farndale et al. 1986). The assay is based on the photometric quantification of the shift of the absorption spectrum of DMMB upon binding to sulfated GAGs.

Snap frozen constructs were digested using Proteinase K as described above (section 3.7.1) and digests were diluted 1:10 in Proteinase K digestion buffer. For the standard curve, a 1:2 serial dilution row of Chondroitin sulfate-A (CS) in Proteinase K digestion buffer was prepared ranging from 500 to 7.8 µg/ml and Proteinase K digestion buffer served as blank. 30 µl of sample or CS standard was pipetted into a clear flat bottom 96-well plate and 200 µl of DMMB staining solution was added to each well, followed by incubation for 5 minutes at RT in the dark. Absorption at 530 nm was measured using a microplate reader. GAG concentrations were calculated from technical duplicates according to values deducted from the standard curve and normalized to the DNA content determined as described above (section 3.7.1).

3.7.3 Protein quantification

The quantification of protein concentration in protein lysates was determined according to the method described by Bradford (Bradford 1976). The used dye, Coomassie Brilliant Blue G-250, exists in an anionic (blue), neutral (green), and a cationic (red) form. Complexation of proteins with the dye stabilizes its anionic form via hydrophobic and ionic interactions, shifting its absorption maximum to 595 nm wavelength.

For quantification of protein content, cell lysates were diluted 1:10 in demineralized water. A standard curve was generated from a 1:2 serial dilution of BSA in distilled water ranging from 1 mg/ml to 15.6 µg/ml and distilled water served as blank. 10 µl of sample or BSA standard were pipetted into a clear flat bottom 96-well plate and 200 µl Bradford solution was added, followed by incubation for 5 minutes at RT in the dark. Absorption at 595 nm was measured in a microplate reader. Protein concentrations were calculated from technical duplicates according to values deducted from the standard curve.

3.7.4 Alkaline phosphatase activity assay

The alkaline phosphatase (ALP) enzyme is a major regulator of bone mineralization by hydrolyzing inorganic pyrophosphate which is a naturally occurring inhibitor of mineralization. In addition, ALP also provides inorganic phosphate from pyrophosphate and organic phosphomonoesters for the synthesis of hydroxyapatite which is a major constituent of mammalian bones. The principle of the assay is based on the hydrolyzing activity of ALP to convert the non-proteinaceous chromogenic substrate para-Nitrophenylphosphate (pNPP) to para-Nitrophenol (pNP), inducing a color shift towards yellow. This can be detected photometrically at a wavelength of 405/490 nm. ALP activity was measured in a standardized volume of culture supernatant. Culture supernatants conditioned for 48 hours were pooled from two constructs and stored at -80°C before the measurement. For measurement, conditioned medium was thawed, vortexed and spun down. A standard curve was generated from a 1:2 serial dilution of p-NP in unconditioned culture medium ranging from 200 µg/ml to 3.125 µg/ml and unconditioned culture medium served as blank. 100 µL of conditioned supernatant or p-NP standard were pipetted into a clear flat bottom 96-well plate and 100 µL substrate solution (10 mg/ml p-NPP in ALP buffer) was added. ALP activity was measured photometrically at 405/490 nm wavelength every 30 minutes for up to 3 hours using a plate reader. ALP activity was calculated from technical triplicates according to values deducted from the standard curve and expressed as ng/ml/min.

3.7.5 Calcium quantification assay

For quantification of calcium concentrations in the medium, the Infinity Calcium Arsenazo III assay kit was used according to the manufacturer's instructions. The principle of the assay kit is based on the reaction of calcium ions with Arsenazo III to form a purple-colored complex and subsequent photometric quantification.

In brief, culture supernatants were collected as described for ALP Assay and incubated with calcium Arsenazo III solution. For the standard curve, a CaCl_2 stock solution [100 mM] was prepared in distilled water. The stock solution was diluted 1:10, followed by 1:2 serial dilution in distilled water, resulting in a standard curve ranging from 5 mM to 0.16 mM. Distilled water served as blank. For measurement, 2 μl of culture supernatant or CaCl_2 standard were pipetted into clear flat bottom 96-well plate and 100 μl Arsenazo III solution was added. Calcium concentrations were measured photometrically at 650 nm from technical duplicates and quantified according to values deduced from the standard curve.

3.8 Radiolabel incorporation for quantification of *de novo* GAG synthesis

GAG synthesis was measured after 21 and 35 days of culture. At the end of culture, engineered cartilage was placed on a nylon mesh in a 48-well plate to allow labeling from all sides. Samples were immersed in 500 μl chondrogenic medium containing 4 μCi $^{35}\text{SO}_4$. The well plate with the constructs was then transferred into a shatterproof transport box which was placed in a cell culture incubator. Samples were incubated at 37°C 6% CO_2 for 24 hours to allow for glycosaminoglycan synthesis. For hyperosmotic stimulation studies, sulfate incorporation was performed in standard chondrogenic medium at 330 mOsm for 24 hours immediately following stimulation at 330 or 550 mOsm. For calcium stimulation studies, label incorporation was performed under standard chondrogenic conditions with or without addition of CaCl_2 for 24 hours. Samples were then washed five times in 500 μl Na_2SO_4 [1 mM] in PBS for 20 minutes on a shaker at 200 rpm to remove free ^{35}S . For analysis, constructs were digested in 1 ml Proteinase K digestion buffer with 0.5 mg/ml Proteinase-K at 60°C overnight. The incorporated label was quantified by adding 25 μl of digest in 2 ml of Ultima Gold scintillation liquid and measuring β -scintillation counting using Wallac MicroBeta-Counter and the program Winspectral. Radioactive count was normalized to its DNA content.

3.9 Molecular biological analyses

3.9.1 Isolation of total RNA

Total RNA from cartilage TE constructs is isolated using a single-phase phenol-guanidine isothiocyanate solution (TriFast/Trizol), which lyses the cells, denatures proteins and stabilizes the RNA at the same time. While proteins and DNA will be found in the organic phenol-chloroform phase, RNA stays in the aqueous phase and can thus be separated.

Samples were taken up in 1 ml Trifast/Trizol. To allow for sufficient cell lysis in the presence of a high matrix content in the constructs, the samples were mechanically crushed using a Polytron. The polytron knife was cleaned before each new sample by serial washing with 1 ml of 0.5 M NaOH, RNase-free distilled water and TriFast/Trizol. The lysates were then transferred to new 1.5 ml reaction tubes and frozen at -80°C for at least 2 hours. They were then thawed and brought to room temperature for 10 minutes. 200 μl of chloroform were added and the samples were vortexed for 30 seconds and incubated again for 10 minutes at room temperature. For phase separation, the samples were centrifuged for 5 minutes at $13,000 \times g$ and the aqueous phase containing the RNA was transferred to a new 1.5 ml reaction tube. The RNA was precipitated by adding 500 μl isopropanol and mixing the samples using vortex for 30 seconds and subsequent incubation on ice for 15 minutes. After an additional round of centrifugation for 15 minutes at $13,000 \times g$ and 4°C , the isopropanol was discarded and the precipitate was washed twice with 1 ml ice-cold 70% ethanol and centrifuged. Residual ethanol was completely removed by evaporation and total RNA was resuspended in 20 μl of 10 mM Tris-HCl.

3.9.2 Quantification of RNA concentration

To determine the RNA concentration, 1 μl of total RNA was measured by UV light absorbance at 260 nm (UV260) using a NanoDrop ND-1000 spectrophotometer. In contrast, proteins have an absorption maximum at 280 nm (UV280) and phenols at 230 nm (UV230). Thus, purity of RNA samples was estimated by the absorbance ratios UV260/UV280 (contamination by proteins) and UV260/UV230 (contamination by phenol or guanidine). RNA samples with UV260/UV280 ratios of 1.8-2.0 and UV260/UV230 ratios over 2.0 were considered pure.

3.9.3 Purification of total RNA

Due to the high deposition of proteoglycan-rich matrix that can contaminate RNA isolation, total RNA had to be purified for quantitative transcriptome analysis. For this purpose, the Zymoclean Gel DNA Recovery Kit was used, in which 4 μg of total RNA were transferred into a 1.5 mL reaction

tube and filled up to a total volume of 60 μl with RNase-free water. Three times the volume of agarose dissolving buffer (ADB) was then added and the samples were centrifuged in Zymo-Spin columns for 1 minute at 13,000 \times g and 4°C. Two washing steps were carried out, each with 200 μl washing buffer with centrifugation for 1 minute at 13,000 \times g and 4°C. After the last washing step, the samples were dry centrifuged for 1 minute to remove ethanol residues. RNA was eluted in 15 μl of RNase-free water after 10 minutes of incubation at room temperature before the eluate was collected by centrifugation at 13,000 \times g for 1 minute into a new 1.5 ml reaction tube. The RNA concentration was determined according to the protocol in section 3.9.2 and the samples were stored at -80°C until further use.

3.9.4 Reverse transcription

To create a DNA template for polymerase chain reaction (PCR), mRNA was reverse-transcribed into more stable complementary DNA (cDNA) using reverse transcriptase (RT), an RNA-dependent DNA polymerase. For this purpose, 500 ng of purified total RNA were filled up to a total volume of 9 μl with RNase-free water. After addition of 1 μl oligo(dT) primer (0.5 $\mu\text{g}/\text{ml}$), denaturation was carried out at 70°C for 10 minutes. After a short incubation on ice, a master mix of 2 μl RT buffer, 1 μl RNaseOUT, 1 μl dNTPs (5 mM), 1 μl Omniscript RT (4 units) and 5 μl water was added per sample. This mixture was then incubated at 37°C for 60 minutes and the reverse transcription was terminated by heating at 93°C for 5 minutes. Samples were diluted 1:10 with RNase-free water and stored at -20°C until further use.

3.9.5 Quantitative PCR

The quantitative real-time polymerase chain reaction (qRT-PCR) is based on DNA replication with an additional real-time measurement of the relative increase in DNA molecules after each amplification step. Using a DNA polymerase, sequence-specific primers, and dNTPs, a DNA template can be amplified through iterative cycles of denaturation (breaking of the double strand), annealing (attachment of specific primers), and elongation (by dNTPs and DNA polymerase). Quantification is performed using an intercalating dye (here SYBR® Green) that binds to double-stranded DNA during amplification. After each cycle the dye is excited and the intensity of the emitted light is detected by the device. When the measured signal intensity exceeds the background signals for the first time, this value is referred to as the cycle threshold (CT value). It serves as the relative initial amount in the sample. For quantification of relative expression of the target gene, the cycle difference (ΔCT) between the linear amplification curves of the target sequence and the chosen house-keeping genes is calculated. Thus, qRT-qPCR is a relative measure comparing the expression of genes of interest to selected reference genes. Subsequently, a

melting curve analysis is carried out. The specificity of the amplified product can be determined by separating the double-stranded DNA by continuously increasing the temperature which will reduce the emitted light from intercalated dye. Depending on the G/C content of the product and the decreasing fluorescence signal, a specific melting curve is thus obtained for each product.

if possible, qRT-PCR was performed using at least one exon-spanning primer, to avoid amplification of genomic DNA. Alternatively, primer pairs were separated by at least one large intron on the corresponding genomic DNA. Per reaction, 5 μ l SYBR Green Mix, 2 μ l RNase-free water, 0.5 μ l forward primer and 0.5 μ l reverse primer were pipetted as master mix into the well of a white 96-well plate. Then, 2 μ l cDNA were added per well. The plate was sealed with sealing foil and centrifuged at 50 rpm for 1 minute to ensure that all of the reaction mixture went to the bottom of the well. Amplification in a Light cycler was performed according to the protocol in Table 24. Specific annealing temperatures (T_A) for each cycle can be derived from section 2.14 of this study.

Table 24 qRT-PCR reaction protocol

	Step	Temperature [°C]	Time [s]
	Initial Denaturation	95	600
Amplification cycles (40x)	Denaturation	95	15
	Primer annealing	T_A	20
	Elongation	72	30
	Denaturation	95	10
Melting curve analysis 5 readings/°C	Annealing	65	60
	Denaturation	97	1
	Storage	4	∞

Analysis of qRT-PCR results was carried out using the ΔCT method. Therefore, the CT values were normalized to that of internal, constantly expressed reference genes GAPDH, 18S and RPL13 that were not regulated by osmotic or calcium stimuli. Relative mRNA expression was calculated by subtracting the CT value of the sample from the mean of the CT values of the reference genes (ΔCT) and corrected for a PCR efficiency of $E=1.8$ according to the manufacturer's recommendations. The percentage of relative gene expression was as follows:

$$\Delta CT = CT_{target} - CT_{reference}$$

$$Rel. gene expression = 1.8^{\Delta CT} \times 100\%$$

3.9.6 DNA gel electrophoresis

As an additional quality control, agarose gel electrophoresis of the amplified product was performed to validate that the amplified product showed only one distinct band at the expected running height.

For agarose gel electrophoresis, a 1.5% agarose solution was prepared by boiling 2.25 g agarose in 250 μ l TAE buffer, cooling it to approx. 60°C and adding 4.5 μ l of the intercalating dye PeqGreen before pouring the gel. When the gel became solid, the gel was immersed in TAE buffer. The PCR products were prepared for electrophoresis by mixing 10 μ l of PCR product with 10 μ l of 2x DNA loading buffer. A volume of 10 μ l was then loaded into the pouches of the agarose gel. For reference of band size, 5 μ l of GeneRuler 100 bp Plus DNA Ladder were loaded as a base pair standard. Gel electrophoresis was performed for 35 minutes at 120 V in TAE buffer and DNA bands were visualized using UV light.

3.10 Protein analyses

3.10.1 Generation of whole cell protein lysates

To produce whole-cell lysates from cartilage TE constructs, snap frozen constructs were transferred to a pre-cooled 2 ml Safe-Lock reaction tube. For lysis, 150 μ l of Phosphosafe lysis buffer, which inhibits the enzymatic degradation of the phosphate groups of the proteins, and 1.5 μ l Pefabloc, a serine protease inhibitor, were added to the constructs. The tissue was then mechanically disintegrated by placing an ice-cooled metal ball in the tube and grinding the tissue in a ball mill (MixerMill 400) for 2 x 2 minutes at 30Hz. The whole cell lysates were then centrifuged at 13,000 x g for 20 minutes at 4°C and the supernatants were transferred to a new reaction tube. Before storing at -80°C for further analysis, protein concentration was determined according to the protocol in section 3.7.3.

To produce whole-cell lysates from transfected monolayer HEK293T cells (see section 3.4), cells were gently washed with TBS, 100 μ l of TBS were added per well and cells were collected into a 1.5 ml reaction tube using a cell scraper. After spinning down cells for 3 minutes at 3,000 x g, cells were lysed in 100 μ l phosphosafe lysis buffer + 1 μ l pefabloc on ice for 15 minutes. The lysates were then centrifuged at 13,000 x g for 20 minutes at 4°C and the supernatants were transferred to a new reaction tube and stored at -80°C for further analysis.

3.10.2 Generation of pepsin-digested collagen lysates

For detection of collagens, cartilage TE constructs are digested using pepsin. When digested with pepsin, components of the extracellular matrix are digested and the cells detach from the 3D structure. However, pepsin is not able to break down collagens and is therefore suitable for extracting collagens from the tissues. Furthermore, the extraction is based on the salt-based precipitation of collagens from the digestion solution.

For isolation of collagens from cartilage TE constructs, snap frozen constructs were digested at room temperature for at least 16 hours with pepsin solution (2.5 mg/ml pepsin in 0.5 M acetic acid, 0.2 M NaCl) to degrade all proteins except collagens. The pH was then adjusted to pH 7 using 1 M Tris Base and collagens were extracted by stepwise addition of NaCl salt to the digest with intermittent inverting to avoid precipitation of NaCl. NaCl was added to a final concentration of 4.5 M NaCl, followed by incubation overnight at 4°C. After centrifugation for 30 minutes at 13,000 x g and 4°C, pellets were resuspended in 400 µl precipitation buffer (0.1 M Tris Base, 0.4 M NaCl) and collagens were precipitated for 4 hours at -20°C with 100% ethanol. After centrifugation for 30 minutes at 13,000 x g and 4°C, the pellets were resuspended in 100µl of lysis buffer (50 mM Tris, 150 mM NaCl, 1% Triton X-100) and stored at -20°C.

3.10.3 SDS gel electrophoresis

In sodium dodecyl sulfate-polyacrylamide gel electrophoresis (SDS-PAGE) proteins are separated based on their molecular weight. Therefore, proteins are heat-denatured in sample buffer, containing reducing agent, detergent (SDS) and mercaptoethanol to support the denaturation of proteins. Upon denaturation, the native conformation of proteins is destroyed the negatively charged SDS binds to the proteins. Hence, depending on their size, the denatured proteins move in the electrical field at different speeds through a polyacrylamide gel. In addition, sample buffer contains bromophenol blue that moves the fastest through the gel and enables to visualize the running front.

For SDS-PAGE, 25-30 µg protein per sample were diluted in H₂O to the same concentration and were then mixed 1:4 with 4x sample buffer and denatured for 5 minutes at 95°C. Denatured proteins were then loaded into a 5% stacking gel in combination with a 10% separating gel, embedded in a 1x running buffer. For size marker, 5 µl of the Precision Plus Protein Standard Dual Color from BIORAD were loaded in the gel. The proteins were first concentrated in the stacking gel at a voltage of 80 V and then separated at 120 V. SDS-PAGE was stopped just before the running front reached the bottom of the gel. At the end of the run, the stacking gel was discarded and the separating gel was used for Western blot analysis as described below.

3.10.4 Western blotting

Proteins were transferred from the SDS gel to a nitrocellulose membrane by Western blotting. Using specific primary antibodies and horseradish peroxidase (HRP)-labeled secondary antibodies, specific proteins were detected on the membrane. Detection via HRP is achieved via a chemiluminescence signal emitted by a substrate when oxidized by HRP.

Protein transfer from the SDS gel to an Amersham Hybond ECL nitrocellulose membrane was performed either in a wet blot chamber (Mini Trans-Blott Cell, Bio-Rad) at 100 V for 1 hour in transfer buffer or using the semi-dry method for 10 minutes at 1.3 A (up to 25 V) with 1x TBE buffer using a Turboblot (Bio-Rad) device. To check whether the transfer of the proteins was successful, the gel was stained in Coomassie staining solution for 5 minutes and then washed in destaining solution in order to detect remaining proteins in the gel. In addition, the membrane was stained in Ponceau S staining solution for 10 minutes to confirm binding of proteins to the membrane before further processing. The membrane was destained by washing in TBS-T for 2 minutes. To block unspecific binding sites, the membrane was blocked in 5% skim milk in TBS-T for 1 hour at room temperature. For detection of specific proteins, the membrane was incubated with the respective primary antibodies (section 2.11) at 4°C overnight, followed by washing three times for 5 minutes in TBS-T. The membrane was then incubated with secondary antibody for 1 hour at room temperature and washed again in TBS-T for three times 5 minutes before detection. For detection, HRP substrate (Lumi-Light Western Blotting Substrate) was evenly distributed on the membrane. The chemiluminescence-signal was detected in a Fusion-SL 3500-WL detection chamber, and images of luminescence and marker bands were superimposed using Photoshop.

3.10.5 Western blotting for collagen detection

For analysis of collagens using Western blotting, pepsin-digested collagen lysates (see section 3.10.2) were used instead of whole cell protein lysates. The processing of SDS-PAGE and Western blotting was identical for collagen detection and cellular proteins. Wet blot transfer was used for collagen detection.

3.10.6 Enzyme-linked immunosorbent assay (ELISA)

3.10.6.1 Type II collagen ELISA

The type II collagen content in cartilage TE constructs was measured in pepsin-digested collagen lysates (see section 3.10.2) using a native type II collagen ELISA detection kit according to the manufacturer's instructions. The type II collagen ELISA is a sandwich immunoassay in which a

capture antibody is coated onto the wells of the plate to which binds the antigen of interest. Detection is performed using a streptavidin peroxidase conjugated secondary detection antibody. For type II collagen ELISA, 100 μ l of diluted capture antibody was pipetted into each well and incubated overnight at 4°C. The wells were washed three times with washing buffer and after the last washing step, the washing buffer was completely removed by tapping on paper towels. For the standard curve, a 1:2 serial dilution of the type II collagen standard provided by the kit was prepared in sample dilution buffer, ranging from 2 μ g/ml to 3.1 ng/ml. Samples were diluted 1:200 to 1:1000 depending on the estimated collagen content of the construct. Then 50 μ l of sample, standard or blank were pipetted into the appropriate wells of the plate and 50 μ l of diluted detection antibody were added and the plate was covered with sealing foil. After incubation for 2 hours at RT, the plate was washed three times with washing buffer and 100 μ l of streptavidin peroxidase solution were added to each well. After incubation for 1 hour at RT, the plate was washed 3 times and 100 μ l of the chromogen OPD was added to each well. After 30 minutes of incubation at RT, the reaction was terminated by adding 50 μ l of stop solution to each well and absorption at 490 nm wavelength was measured using a microplate reader. Type II collagen concentrations were calculated from technical duplicates according to values deducted from the standard curve.

3.10.6.2 cAMP ELISA

The intracellular cAMP concentration in whole cell lysates was measured using cAMP ELISA according to the manufacturer's instructions. The cAMP ELISA is a competitive immunoassay in which an ALP-conjugated cAMP competes with the cAMP present in the samples for the binding of a monoclonal antibody. To enable the measurement of cAMP, 1 mM IBMX, a phosphodiesterase inhibitor that prevents the rapid breakdown of cAMP, was added to the cultured constructs 30 minutes before the start of the experiment and during treatments of up to 24 hours.

For cAMP ELISA, snap frozen TE constructs were thawed on ice and then chemically digested in a 2 ml Safe-Lock reaction vessel in 0.1 M HCl provided by the kit and mechanically disintegrated by placing an ice-cooled metal ball in the tube and grinding the tissue in a ball mill (MixerMill 400) for 2 x 2 minutes at 30Hz. The samples were then centrifuged for 15 minutes at 13,000 \times g and 4°C and the supernatants were transferred to fresh reaction vessels. For the standard curve, a 1:2 serial dilution of the cAMP standard provided by the kit was prepared in 0.1 M HCl, ranging from 20 pmol/ml to 0.078 pmol/ml. After pretreatment with 50 μ l of a neutralization solution, 100 μ l of sample, standard or blank were pipetted into the wells of an IgG-coated plate and 50 μ l of cAMP-ALP conjugate and 50 μ l of cAMP antibody were added. The plate was covered with sealing

foil and incubated for 2 hours at room temperature on a plate shaker at 500 rpm. The wells were washed three times with washing buffer and after the last washing step, the washing buffer was completely removed by tapping on paper towels. Then, 200 μ l of pNPP substrate solution were immediately pipetted into the wells and the plate was incubated for 1-2 h at 37°C without shaking. The reaction was stopped by adding 50 μ l of stop solution before detection in a micro plate reader at 405 nm wavelength. The measured optical density (OD) is inversely proportional to the cAMP concentration in the samples. cAMP concentrations were calculated from technical duplicates according to values deducted from the standard curve.

3.10.6.3 PGE₂ ELISA

The secretion of PGE₂ into the culture supernatant was measured using PGE₂ ELISA (Enzo Life Sciences) according to the manufacturer's instructions. This is a competitive immunoassay in which an ALP-conjugated PGE₂ competes with the PGE₂ present in the samples for the binding of a monoclonal antibody.

In brief, the conditioned medium was thawed on ice and centrifuged for 5 minutes at 13,000 x g to remove cell debris. For the standard curve, a 1:2 serial dilution of the PGE₂ standard provided by the kit was prepared in assay buffer, ranging from 2.5 ng/ml to 39.1 pg/ml. Then 100 μ l of sample, standard or blank were pipetted into the wells of an IgG-coated plate and 50 μ l PGE₂-ALP conjugate and 50 μ l of PGE₂ antibody were added and the plate was covered with foil. After incubation for 2 hours at room temperature on a plate shaker at about 500 rpm, the plate was washed three times with washing buffer. After the last washing step, the washing buffer was completely removed by tapping on paper towels. Then, 200 μ l of para-nitrophenyl phosphate (pNPP) substrate solution were immediately pipetted into the wells and the plate was incubated for 45 minutes at room temperature without shaking. The reaction was stopped by adding 50 μ l of stop solution before detection in a micro plate reader at 405 nm wavelength with a correction wavelength of 580 nm. The measured optical density is inversely proportional to the PGE₂ concentration in the samples. PGE₂ concentrations were calculated from technical duplicates according to values deducted from the standard curve.

3.10.7 PTHrP Immunoradiometric assay

PTHrP Immunoradiometric assay (IRMA) was performed by Laboratory Dr. Limbach (Heidelberg, Germany) using active PTHrP immunoradiometric assay (Immunotech) on whole-cell lysates from transfected monolayer HEK293 cells or cartilage TE constructs (for lysis protocol see section 3.10.1). Sample preparation was performed to remove traces of extraction reagent. For this purpose, proteins were precipitated from the lysates using acetone. In detail, twice the volume

(300 μ l) of ice-cold acetone was added to the lysate and mixed by inverting, followed by incubation for 15 minutes on ice with occasional inverting. After centrifugation for 20 minutes at 13,000 x g at 4°C, the supernatant was removed and the pellet was dried for 1-2 minutes. Care was taken to not let the pellet dry too long. The pellet was then resuspended in human blood plasma collected according to protocol in section 3.6 (250 μ l per TE construct or 100 μ l per well of a 6-well plate). To avoid loss of PTHrP protein due to repetitive freeze-thaw cycles, sample preparation was performed immediately following cell lysis. Prepared samples were stored at -80°C and transferred on dry ice to the measurement facility. PTHrP values were determined for one technical replicate per sample.

3.11 Statistical analysis

Data analysis was performed using Graph Pad Prism. Mean values and standard error of the mean (SEM) were calculated with each TE construct considered as independent biological replicate. For visualization, the data were presented as bar chart with the mean and SEM or as lines of individual control samples and the corresponding treatment sample. Differences between control and treatment groups were tested using paired Student's two-tailed t-test with pairs defined by the donor cell population. In the case of multiple groups, only the scientifically meaningful group comparisons were assessed using the Student's two-tailed t-test and a post hoc Bonferroni correction to adjust for multiple comparison when necessary. Comparisons between different cell types were tested using the unpaired Student's two-tailed t-test. $P \leq 0.05$ was considered as statistically significant.

4 Results

4.1 Acute hyperosmotic stimulation of cartilage tissue engineering constructs

4.1.1 Maturation of engineered cartilage

In order to investigate whether acute hyperosmotic stimulation is a relevant factor for the regulation of GAG synthesis in our engineered cartilage model, a type I/III collagen scaffold was seeded with 5×10^5 human AC. Constructs were allowed to mature for 3 to 35 days under chondrogenic conditions to accumulate an articular cartilage-like ECM. Chondrocyte redifferentiation was determined on tissue sections stained with Safranin O to visualize the presence of sulfated GAGs throughout the tissue (Figure 4 A). Three days after seeding of AC into the carrier, Safranin O staining was negative, indicating low GAG content. After 21 and 35 days of chondrocyte maturation, constructs stained positive for Safranin O. GAG deposition on day 35 appeared homogeneous throughout the construct in samples from 3 out of 4 donors, whereas staining intensity for GAGs was slightly reduced in the peripheral region with AC from 1 donor (see

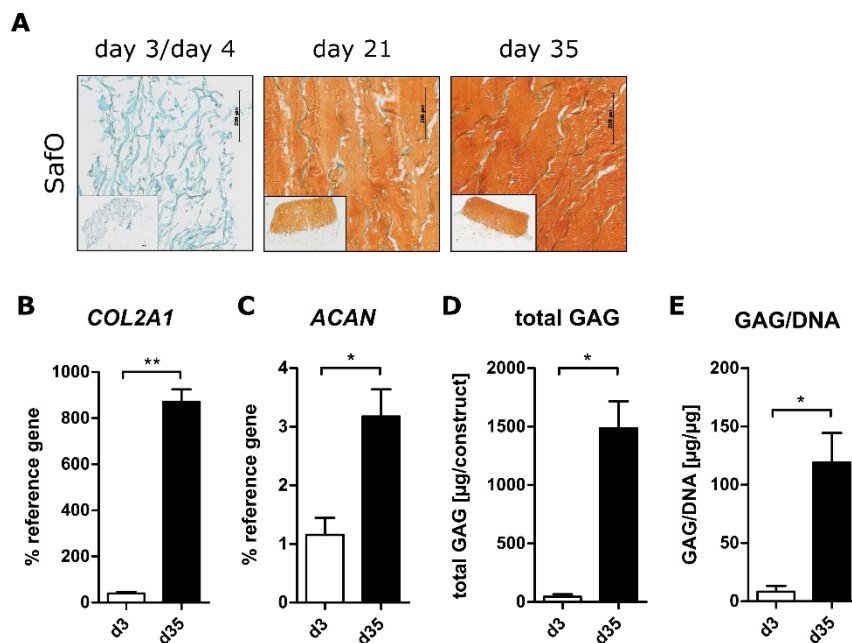


Figure 4 GAG quantification in AC-based TE-constructs. 5×10^5 AC were seeded in a type I/III collagen carrier and subjected to chondrocyte redifferentiation medium for up to 35 days **A)** Tissue sections from day 3 or 4, day 21 and day 35 were stained using Safranin O to visualize sulfated GAGs in the tissue. Fast green staining served as counterstaining. Scale bars indicate 200 μm . Insets show Safranin O staining of full-size constructs at 5x magnification. Expression of **(B)** *COL2A1* and **(C)** *ACAN* was determined by qPCR. Gene expression levels were normalized to the mean expression of reference genes *18S*, *GAPDH* and *RPL13*. **D)** Quantification of total GAG content in the tissue using DMMB assay. **E)** Total GAG levels were normalized to DNA content. Data are presented as mean \pm SEM from $n=3$ donors. * $p < 0.05$, ** $p < 0.01$, paired Student's t-test, d3 vs d35.

also Figure 7). Along with cartilage-like GAG deposition, a strong upregulation of *COL2A1* and *ACAN* mRNA expression was observed between day 3 and day 35 (Figure 4 B+C). Also, the GAG content per construct raised significantly from $44.68 \mu\text{g} \pm 21.66 \mu\text{g}$ on day 3 to $1487.13 \mu\text{g} \pm 229.8 \mu\text{g}$ on day 35 (33.3-fold, $p=0.02$) according to quantification of total GAG deposition using the DMMB assay (Figure 4 D). Total GAG levels referred to the DNA content of the construct significantly increased between day 3 ($8.30 \pm 4.95 \mu\text{g}/\mu\text{g}$) and day 35 ($119.10 \pm 25.33 \mu\text{g}/\mu\text{g}$, 14.4-fold, $p=0.03$) (Figure 4 E). Since qualitative and quantitative assessment of GAGs using Safranin O staining and DMMB assay is based on the detection of negative sulfate residues in the tissue, neocartilage on day 3 was defined to have a low FCD whereas neocartilage on day 35 was defined as having a high FCD.

4.1.2 Regulation of ERK and p38 pathways by acute hyperosmotic stimulation at low FCD

In order to select a valid hyperosmotic stimulation regime for our 3D cartilage model, osmo-response markers were needed to confirm that cells are responding. Thus, the molecular response of chondrocytes to acute hyperosmotic stimulation at low FCD was investigated in a pilot experiment. Since we asked whether osmotic pressure is a relevant physicochemical sub-parameter of mechano-induced changes in GAG synthesis, a three hour stimulation period was selected in adaptation to 3 hours of mechanical loading applied in our previous studies (Praxenthaler et al. 2018; Scholtes et al. 2018). Stimulation parameters were selected according to the physiologically relevant changes in local osmolarity in native articular cartilage, ranging from 350 to 550 mOsm. Acute hyperosmotic stimulation was applied by the addition of NaCl-solution to the culture medium to increase medium osmolarity from 330 mOsm in the basal chondrocyte redifferentiation medium to up to 550 mOsm in the hyperosmotic groups. Medium osmolarity was confirmed once using a freezing point osmometer.

Phosphorylation of p38 and ERK1/2 is a common immediate response of human articular chondrocytes to hyperosmotic treatment periods of 10 minutes up to 6 hours. It was therefore investigated whether p38 and ERK1/2 also serve as valid immediate osmo-response markers in our model of 3D cultured engineered cartilage.

Immediately after acute hyperosmotic stimulation of day 3 constructs over a broad set of hyperosmotic concentrations of 330-550 mOsm, the activation of p38 and ERK1/2 was assessed by Western blotting. At control conditions, phosphorylation of ERK1/2 was weak. Acute hyperosmotic stimulation for 3 hours at 350 and 400 mOsm did not change pERK1/2 levels compared to untreated controls. However, pERK1/2 signal intensity gradually increased from 400

to 550 mOsm, showing a strong pERK1/2 signal at 550 mOsm (Figure 5 A). Likewise, p38 phosphorylation was low at 330-400 mOsm and gradually increased from above 400 to 550 mOsm (Figure 5 B). Phospho-p38 levels appeared slightly reduced at 330-400 mOsm post-stimulation compared to before the treatment. Due to weak signal intensities and low sample size this may reflect variations around the basal level.

Overall, the pilot experiment suggested that in 3D-cultured human articular chondrocytes 3 hours of acute hyperosmotic stimulation above 400 mOsm induced p38 and ERK1/2 signaling activity. Since the strongest induction of p38 and ERK1/2 phosphorylation was observed at 550 mOsm, this osmolarity was selected for further treatments. This is in the physiological range of osmolarity in the joint after mechanical compression.

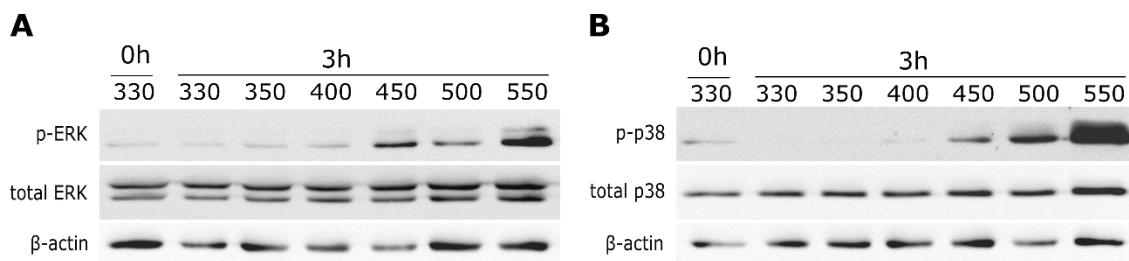


Figure 5 Induction of p38 and pERK after increasing hyperosmotic stimulation in AC at low FCD. 5×10^5 AC were seeded in a type I/III collagen carrier and subjected to chondrocyte redifferentiation medium for 3 days. Acute hyperosmotic stimulation at 330-550 mOsm was applied by the addition of NaCl to the culture medium for 3 hours on day 3. Immunoblotting was performed against **A)** phosphorylated and total ERK1/2 and **B)** phosphorylated and total p38. Immunoblotting against β -actin served as loading control. Results of this pilot experiment were obtained from AC from n=1 donor.

Next, samples from additional AC donors were stimulated with 550 mOsm. To investigate whether ERK1/2 and p38 activation in 3D cultured chondrocytes was specific to short stimulation time of 3 hours or will also occur after hyperosmotic challenge of up to 24 hours, low FCD constructs were exposed to hyperosmotic stimulation at 550 mOsm for 3, 6 or 24 hours. Hyperosmotic stimulation for 3 hours at 550 mOsm confirmed a strong induction of pERK and p-p38 signals in samples from three additional donors (Figure 6). While pERK1/2 levels were elevated over 3, 6 and 24 hours of hyperosmotic stimulation (Figure 6 A), induction of p38 phosphorylation was observed after 3 and 6 hours of hyperosmotic stimulation but returned back to baseline levels after 24 hours of constant hyperosmotic stimulation (Figure 6 B), indicating cell adaptation.

Thus, also longer stimulation times induced p38 and ERK1/2 signaling, qualifying them as valid osmo-response markers in our model at low FCD.

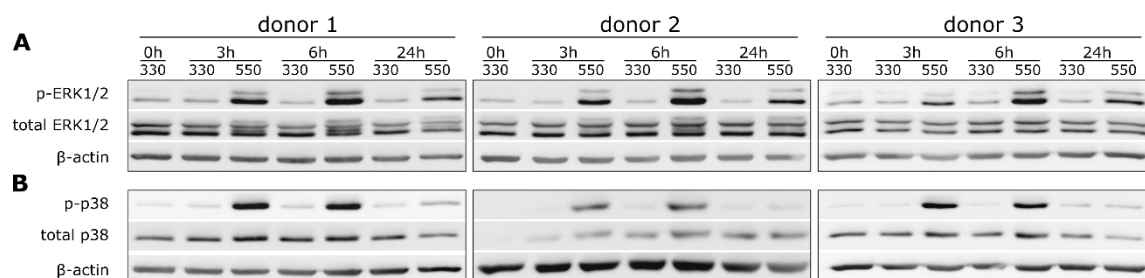


Figure 6 Hyperosmotic induction of p38 and pERK after 3, 6 and 24 hours in AC at low FCD. 5×10^5 AC were seeded in a type I/III collagen carrier and subjected to chondrocyte redifferentiation medium for 3 days. Acute hyperosmotic stimulation at 550 mOsm was applied by the addition of NaCl to the culture medium for 3, 6 or 24 hours on day 3. Immunoblotting was performed against **A)** total and phosphorylated ERK1/2 as well as **B)** total and phosphorylated p38. Immunoblotting against β -actin served as loading control. Results are shown for AC from $n=3$ independent donors.

4.1.3 Regulation of pERK and p38 pathways by acute hyperosmotic stimulation at high FCD

In order to determine whether the FCD of engineered cartilage influences the acute hyperosmotic induction of p38 and ERK1/2 signaling, day 35 constructs were exposed to hyperosmotic stimulation at 550 mOsm for 3, 6 or 24 hours and phosphorylation of osmo-response markers p38 and ERK1/2 was investigated. Hyperosmotic induction of ERK1/2 phosphorylation was detected after 3, 6 and 24 hours in samples from 2 out of 3 donors (Figure 7 A, donor 1+3). In samples from 1 out of 3 donors, induction of ERK1/2 phosphorylation was only observed after 6 hours (Figure 7 A, donor p 2). Hyperosmotic stimulation induced p38 phosphorylation after 3 and 6 hours but not

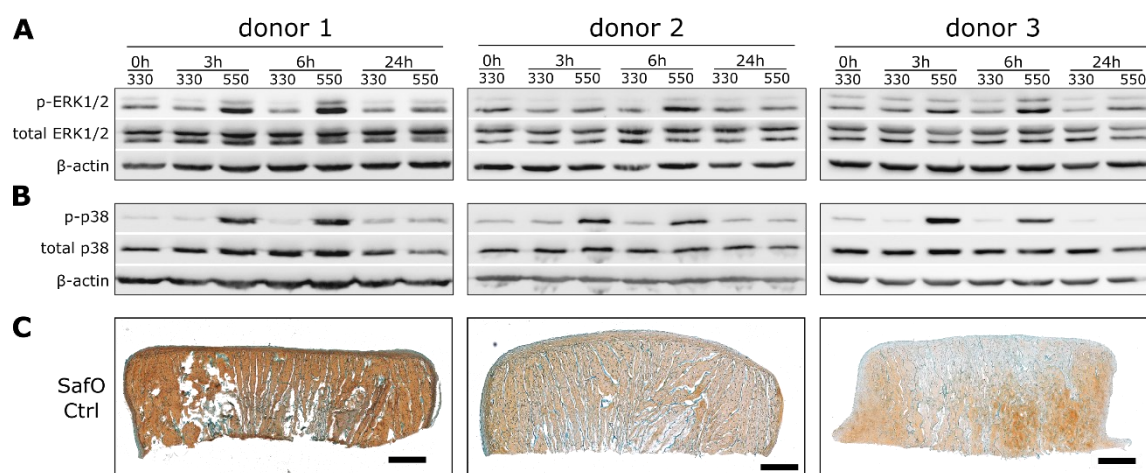


Figure 7 Hyperosmotic induction of p38 and pERK after 3, 6 and 24 hours in AC at high FCD. 5×10^5 AC were seeded in a type I/III collagen carrier and subjected to chondrocyte redifferentiation medium for 35 days. Acute hyperosmotic stimulation at 550 mOsm was applied by the addition of NaCl to the culture medium for 3, 6 or 24 hours on day 35. Immunoblotting was performed against **A)** total and phosphorylated ERK1/2 as well as **B)** total and phosphorylated p38. Immunoblotting against β -actin served as loading control. **C)** Tissue sections of day 35 neocartilage were stained using Safranin O to visualize sulfated GAGs in the tissue. Fast green staining served as counterstaining. Scale bars indicate 500 μ m. Results are shown for AC from $n=3$ independent donors.

after 24 hours (Figure 7 B). Safranin O staining of control constructs on day 35 was performed to compare the FCD of parallel samples between donors and showed clear variability (Figure 7 C). Thus, this demonstrated for the first time that 3D-cultured chondrocytes responded to 3 to 6 hours of acute hyperosmotic stimulation by phosphorylation of p38 and ERK1/2 and this occurred independent of the FCD of the tissue. The FCD did therefore not alter the acute hyperosmotic induction of p38 and ERK1/2 in 3D engineered cartilage, qualifying them as valid osmo-response markers in our model at low and at high FCD.

4.1.4 Expression of osmo-response genes after acute hyperosmotic stimulation at low versus high FCD

In order to identify additional molecular osmo-response markers for our model, the regulation of known molecular targets was investigated at mRNA level. In previous studies, enhanced expression of the osmo-responsive transcription factor *NFAT5* and its target genes *SLC6A12*, *SLC5A3* and *S100A4* was reported after hyperosmotic stimulation in monolayer chondrocytes. Therefore, expression of these markers was tested in maturing engineered cartilage after hyperosmotic stimulation at 550 mOsm for 3, 6 or 24 hours using qPCR. Hyperosmolarity moderately induced the expression of the osmo-sensitive transcription factor *NFAT5* on day 3 and day 35. This reached significance after 24 hours on day 3 (1.86 ± 0.06 -fold, $p=0.005$) and after 3 hours (1.21 ± 0.02 -fold, $p=0.006$) and 6 hours (1.88 ± 0.21 -fold, $p=0.05$) on day 35 compared to control cultures at the same time point (Figure 8 A). Again, the regulation of *NFAT5* appeared similar at low and high FCD. Expression of *NFAT5* target genes *SLC6A12* and *SLC5A3* was unaltered after 3 hours and 6 hours at all conditions and a mild but significant reduction of *S100A4* expression was observed after 6 hours of hyperosmotic stimulation on day 35 (0.70 ± 0.07 -fold, $p=0.05$) (Figure 8 B-D). The expression of all three target genes was strongly induced after 24 hours of hyperosmotic stimulation independent of the FCD. However, due to the small sample size and large standard deviation, this regulation reached significance only for *SLC6A12* (41.06 ± 8.29 -fold, $p=0.04$) and *SLC5A3* (12.36 ± 2.26 -fold, $p=0.03$) on day 3 and for *S100A4* (3.21 ± 0.07 -fold, $p=0.001$) on day 35. Nevertheless, the osmo-induced expression of *SLC6A12*, *SLC5A3* and *S100A4* after 24 hours was obvious in neocartilage of low and high FCD, suggesting an upregulation of *NFAT5* target genes after hyperosmotic stimulation for 24 hours independent of FCD.

These data indicated for the first time that in our model of 3D-cultured chondrocytes acute hyperosmotic stimulation at 550 mOsm led to early induction of osmo-sensitive *NFAT5* gene expression, followed by late upregulation of its transcriptional targets *SLC6A12*, *SLC5A3* and *S100A4* after 24 hours of stimulation. Thus, expression of *NFAT5* qualifies as additional immediate

osmo-response marker, whereas expression of *SLC6A12*, *SLC5A3* and *S100A4* can only be used as late osmo-response markers.

In summary, the FCD was not relevant for the induction of osmo-sensitive markers ERK1/2, p38, *NFAT5* and *NFAT5* target genes after acute hyperosmotic stimulation of human 3D engineered cartilage.

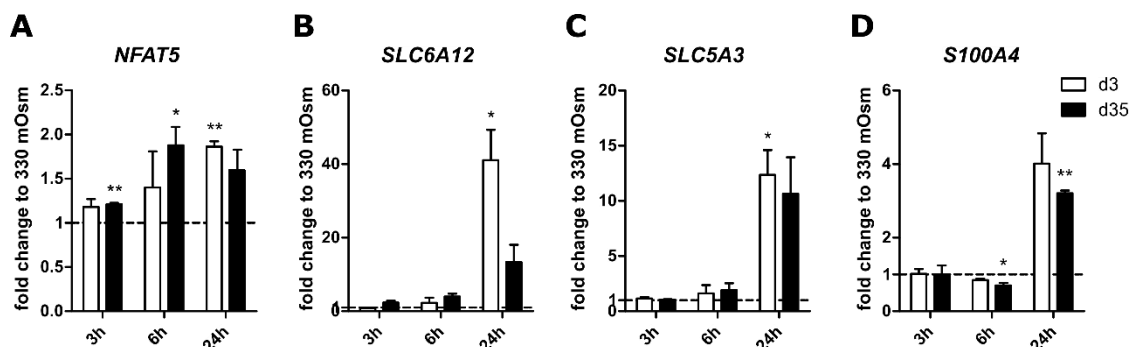


Figure 8 Gene expression of osmo-response markers after acute hyperosmotic stimulation. 5×10^5 AC were seeded in a type I/III collagen carrier and subjected to chondrocyte redifferentiation medium for 3 or 35 days. Acute hyperosmotic stimulation at 550 mOsm was applied by the addition of NaCl to the culture medium for 3, 6 or 24 hours on day 3 or day 35. Expression of (A) *NFAT5*, (B) *SLC6A12*, (C) *SLC5A3* and (D) *S100A4* was determined by qPCR. Gene expression levels were normalized to the mean expression of reference genes *18S*, *GAPDH* and *RPL13*. Data are presented as mean \pm SEM fold change difference between 550 mOsm and control constructs of the same time point (dashed line at 1) of AC from $n=3$ donors. * $p < 0.05$, ** $p < 0.01$, paired Student's t-test.

4.1.5 Regulation of SOX9 by acute hyperosmotic stimulation at low versus high FCD

Hyperosmotic stimulation studies on human articular chondrocytes in monolayer suggested a regulation of the expression of cartilage ECM-related markers *SOX9*, *COL2A1* and *ACAN*, but their regulation under cartilage relevant conditions at high FCD was never addressed. Whether hyperosmotic stimulation regulates *SOX9* in pre-matured 3D-cultured articular chondrocytes and whether FCD is a relevant parameter was, therefore, investigated next. When *SOX9* mRNA and protein levels were investigated after acute hyperosmotic stimulation at 550 mOsm for 3, 6 or 24 hours on day 3 and day 35, no significant effect on *SOX9* mRNA expression was observed (Figure 9 A). *SOX9* protein levels were inconsistently affected in samples from three donors on day 3. In samples from donor 1, *SOX9* levels increased from the start of stimulation over 24 hours already in control cultures, while treatment with 550 mOsm showed no regulation. In samples from donor 2 and 3, *SOX9* levels remained unaltered at control conditions. Hyperosmotic stimulation, however, reduced *SOX9* levels at all time points in samples from donor 2, but enhanced *SOX9* levels after 24 hours hyperosmotic stimulation in samples from donor 3, indicating inconsistent regulation of *SOX9* protein levels on day 3 (Figure 9 B). On day 35, *SOX9* levels were consistently downregulated by hyperosmotic stimulation in all 3 donors at all time points (Figure 9 C).

In summary, hyperosmolarity regulated SOX9 protein levels inconsistently at low FCD but a uniform reduction in SOX9 protein levels was observed at high FCD. Thus, the FCD obviously influenced the hyperosmotic regulation of SOX9 protein, which may be of relevance for cartilage matrix production.

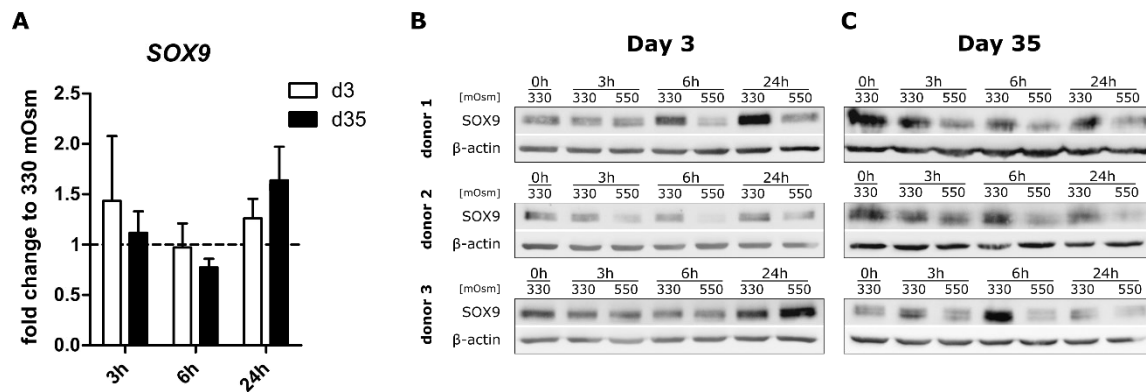


Figure 9 Effect of acute hyperosmotic stimulation on the expression of SOX9. 5×10^5 AC were seeded in a type I/III collagen carrier and subjected to chondrocyte redifferentiation medium for 3 or 35 days. Acute hyperosmotic stimulation at 550 mOsm was applied by the addition of NaCl to the culture medium for 3, 6 or 24 hours on day 3 or day 35. **(A)** Expression of SOX9 was determined on day 3 or day 35 by qPCR. Gene expression levels were normalized to the mean expression of reference genes *18S*, *GAPDH* and *RPL13*. Data are presented as mean \pm SEM fold change difference between 550 mOsm and control constructs of the same time point (dashed line at 1) of $n=3$ donors, paired Student's *t*-test. **(B)** Immunoblotting against SOX9 was performed on day 3 (left panels) and day 35 (right panels). β -actin served as loading control. Results are shown for AC from $n=3$ independent donors.

4.1.6 Regulation of *COL2A1* and *ACAN* expression by acute hyperosmotic challenge at low versus high FCD

To elucidate whether the reduced SOX9 protein levels on day 35 correlated with a reduced expression of its transcriptional targets *COL2A1* and *ACAN* after osmotic challenge, hyperosmotic stimulation was performed on day 3 and day 35 for 3, 6 or 24 hours and *COL2A1* and *ACAN* expression were determined by qPCR. A slight mean reduction of *COL2A1* expression was observed after 6 hours (0.69 ± 0.23 -fold, $p=0.30$) and 24 hours (0.59 ± 0.20 -fold, $p=0.17$) on day 3, which did not reach significance (Figure 10 A). On day 35, no regulation of *COL2A1* expression was obvious. Likewise, hyperosmotic stimulation showed no significant effect on *ACAN* expression after 3, 6 and 24 hours at low and high FCD (Figure 10 B).

These results indicated that acute hyperosmotic stimulation of 3D-cultured chondrocytes for up to 24 hours had no immediate effect on the expression of cartilage ECM-related genes *COL2A1* and *ACAN* at either FCD. Reduction of SOX9 protein levels at high FCD did, therefore, not lead to instant changes in *COL2A1* and *ACAN* expression.

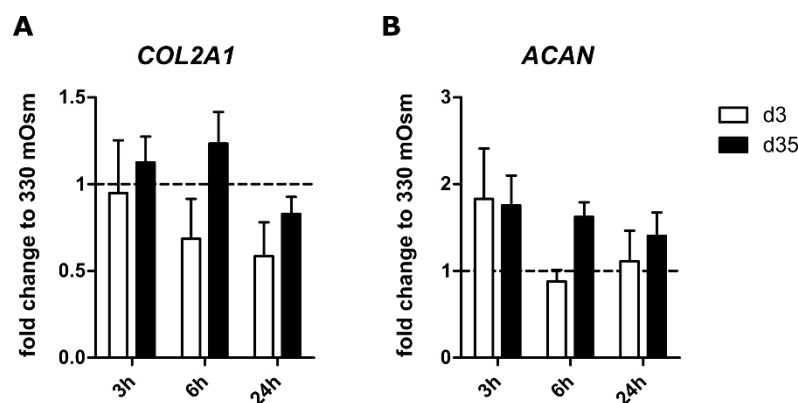


Figure 10 Effect of acute hyperosmotic stimulation on the gene expression of chondrocyte differentiation markers. 5×10^5 AC were seeded in a type I/III collagen carrier and subjected to chondrocyte redifferentiation medium for 3 or 35 days. Acute hyperosmotic stimulation at 550 mOsm was applied by the addition of NaCl to the culture medium for 3, 6 or 24 hours on day 3 or day 35. Expression of (A) *COL2A1* and (B) *ACAN* was determined on day 3 or day 35 by qPCR. Gene expression levels were normalized to the mean expression of reference genes *18S*, *GAPDH* and *RPL13*. Data are presented as mean \pm SEM fold change difference between 550 mOsm and control constructs of the same time point (dashed line at 1) of AC from $n=3$ donors, paired Student's t-test.

4.1.7 Regulation of TGF β and BMP pathways by acute hyperosmotic stimulation at low versus high FCD

To determine mechanisms that may contribute to hyperosmotic reduction of SOX9 protein levels at high but not at low FCD, the activity of regulatory pathways that are upstream of SOX9 was analyzed. For this purpose, the regulation of chondrocyte redifferentiation pathways TGF β -SMAD2/3 and BMP-SMAD1/5/9 was investigated after hyperosmotic stimulation at low and high FCD. Hyperosmotic stimulation was performed for 3, 6 or 24 hours and osmo-induced SMAD2/3

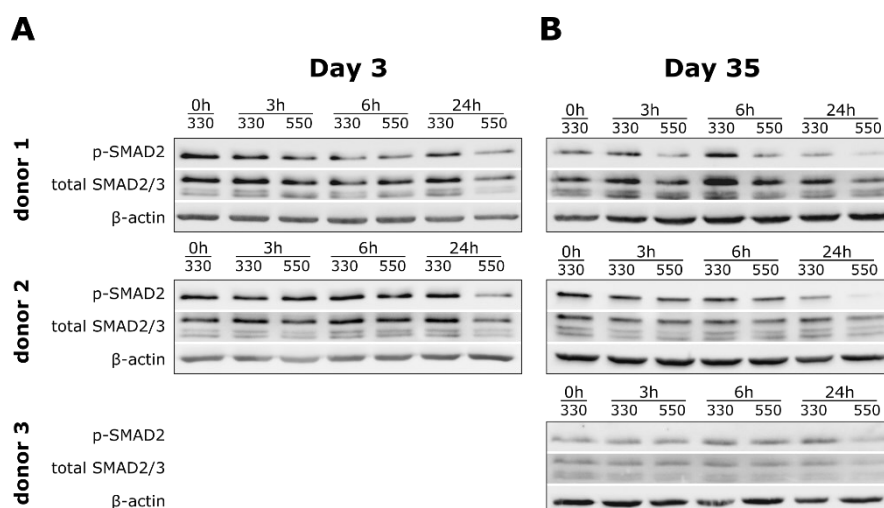


Figure 11 Effect of acute hyperosmotic stimulation on SMAD2 phosphorylation. 5×10^5 AC were seeded in a type I/III collagen carrier and subjected to chondrocyte redifferentiation medium for 3 or 35 days. Acute hyperosmotic stimulation at 550 mOsm was applied by the addition of NaCl to the culture medium for 3, 6 or 24 hours on day 3 or day 35. Immunoblotting against total SMAD2/3 and phosphorylated SMAD2 was performed on (A) day 3 and (B) day 35. Immunoblotting against β -actin served as loading control. Results are shown for AC from $n=2$ (day 3) and $n=3$ (day 35) independent donors.

and SMAD1/5/9 phosphorylation were evaluated in AC constructs on day 3 and day 35 using Western blotting. On day 3, hyperosmotic stimulation for 3 or 6 hours showed no regulation of SMAD2/3 activity. However, stimulation for 24 hours consistently downregulated pSMAD2 signals in neocartilage from all donors (Figure 11 A). Likewise, on day 35, no regulation of pSMAD2 levels was observed after 3 hours of hyperosmotic stimulation in samples from two donors (Figure 11 B, donor 2+3). In neocartilage from one donor, downregulation of pSMAD2 was already observed after 3 hours of stimulation (Figure 11 B, donor 1). pSMAD2 levels were consistently reduced after 24 hours of hyperosmotic challenge in all donors (Figure 11 B). Thus, only 24 hours of hyperosmotic stimulation consistently suppressed SMAD2/3 signaling activity.

Hyperosmotic stimulation inconsistently downregulated pSMAD1/5/9 levels in samples from 3 donors on day 3 (Figure 12 A). While hyperosmotic stimulation reduced pSMAD1/5/9 levels after 6 and 24 hours in samples from donor 1, pSMAD1/5/9 levels were reduced after 3 and 6 hours, but not after 24 hours of stimulation in samples from donor 2. In samples from donor 3, pSMAD1/5/9 was reduced after 3 and 24 hours, but not after 6 hours of stimulation. On day 35, hyperosmotic stimulation consistently downregulated pSMAD1/5/9 levels at all time points (Figure 12 B).

Thus, while the hyperosmotic reduction of SMAD2/3 pathway activity was independent of the FCD, SMAD1/5/9 signaling activity was consistently reduced only at high FCD. De-phosphorylation of SMAD1/5/9 at low FCD showed a similar trend compared to high FCD, but was inconsistent. Therefore, the inconsistent regulation of SOX9 and BMP-SMAD1/5/9 signaling at low FCD and the

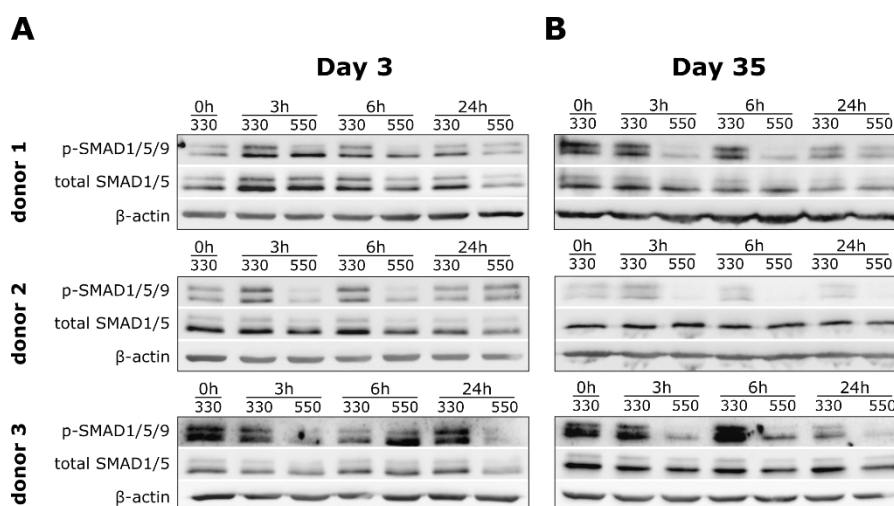


Figure 12 Effect of acute hyperosmotic stimulation on SMAD1/5/9 phosphorylation. 5×10^5 AC were seeded in a type I/III collagen carrier and subjected to chondrocyte redifferentiation medium for 3 or 35 days. Acute hyperosmotic stimulation at 550 mOsm was applied by the addition of NaCl to the culture medium for 3, 6 or 24 hours on day 3 or day 35. Immunoblotting against total SMAD1/5 and phosphorylated SMAD1/5/9 was performed on (A) day 3 and (B) day 35. Immunoblotting against β -actin served as loading control. Results are shown for AC from $n=3$ independent donors.

strong downregulation of both after 3, 6 and 24 hours at high FCD suggest that the regulation of SOX9 protein levels is under the control of the BMP pathway.

4.1.8 Regulation of GAG synthesis by hyperosmotic stimulation at low vs high FCD

Previous data from our group demonstrated a reduced GAG synthesis after dynamic compressive loading for 3 hours at low FCD (day 3) while GAG synthesis was stimulated in neocartilage of high FCD (d35). To analyze whether acute hyperosmotic stimulation is a sub-parameter of mechanical compression that is relevant for GAG synthesis, the GAG synthesis rate was measured after 3 hours of acute hyperosmotic stimulation at low versus high FCD. For this purpose, radiolabeled ^{35}S -sulfate incorporation was measured over 24 hours after the end of hyperosmotic stimulation on day 3 or day 35. Radio incorporation was referred to the DNA content of the construct to normalize for differences in cell number. Acute hyperosmotic stimulation for 3 hours by trend reduced the GAG synthesis rate of day 3 constructs (0.72 ± 0.01 -fold, $n=2$), which would be in line with negative effects seen after mechanical loading on day 3 in the same model. However, due to the low sample size, this did not reach statistical significance. No significant regulation of GAG synthesis was observed after hyperosmotic stimulation on day 35 (1.10 ± 0.10 -fold, $n=4$) (Figure 13).

Thus, while acute hyperosmotic stimulation may reproduce the load-induced changes in GAG synthesis at low FCD, no difference in GAG synthesis was observed after acute hyperosmotic challenge at high FCD.

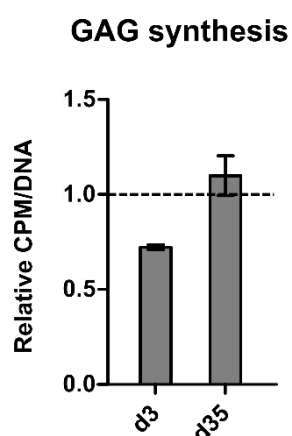


Figure 13 Effect of acute hyperosmotic stimulation on GAG synthesis rate. 5×10^5 AC were seeded in a type I/III collagen carrier and subjected to chondrocyte redifferentiation medium for 3 or 35 days. Acute hyperosmotic stimulation at 550 mOsm was applied by the addition of NaCl to the culture medium for 3 hours on day 3 or day 35. GAG synthesis rate was measured as radiolabeled ^{35}S -sulfate incorporation during 24 hours after end of stimulation. Radiolabel-incorporation was normalized to the DNA content of the TE-constructs and control samples were set to one. Data are presented as mean \pm SEM for AC from $n=2$ (day 3) or $n=4$ (day 35) donors, paired Student's t-test.

4.1.9 Effect of hyperosmotic stimulation on the expression of mechano-response genes

Several genes from the MAPK pathway (*FOS*, *FOSB* and *DUSP*) and BMP pathway (*BMP2* and *BMP6*) were established as robust mechano-response genes in previous studies from our group (Hecht et al. 2019; Lückgen et al. 2022; Praxenthaler et al. 2018; Scholtes et al. 2018). It was now asked whether acute hyperosmotic signals as possible relevant sub-parameters of our mechanical compression protocol may be able to induce these genes.

When the expression of these mechano-response genes was investigated after hyperosmotic stimulation for 3, 6 or 24 hours at low and high FCD, an induction of *FOS* was obvious after 3 and 6 hours on day 3 and day 35, reaching significance after 6 hours on day 3 (5.74 ± 1.07 -fold, $p=0.04$). Stimulation for 24 hours significantly decreased *FOS* expression on day 35 (0.81 ± 0.04 -fold, $p=0.04$) while no change was observed on day 3 (Figure 14 A). Thus, hyperosmotic stimulation increased expression of *FOS* predominantly at short stimulation times of 3 or 6 hours at either FCD, while longer stimulation for 24 hours reduced *FOS* expression at high FCD.

Hyperosmotic stimulation by trend upregulated *FOSB* expression on day 3, reaching significance at 3 hours (6.11 ± 0.76 -fold, $p=0.02$). On day 35, *FOSB* expression was by trend higher at 3 and 6 hours but was unchanged after 24 hours of hyperosmotic stimulation (Figure 14 B). Thus, *FOSB* expression may respond to hyperosmotic stimulation similar to *FOS* and both together may qualify as early osmo-response markers.

Expression of *DUSP5* showed a different pattern than *FOS* and *FOSB* after hyperosmotic stimulation and raised significantly only after 6 hours of stimulation of day 35 samples ($1.88 \pm$

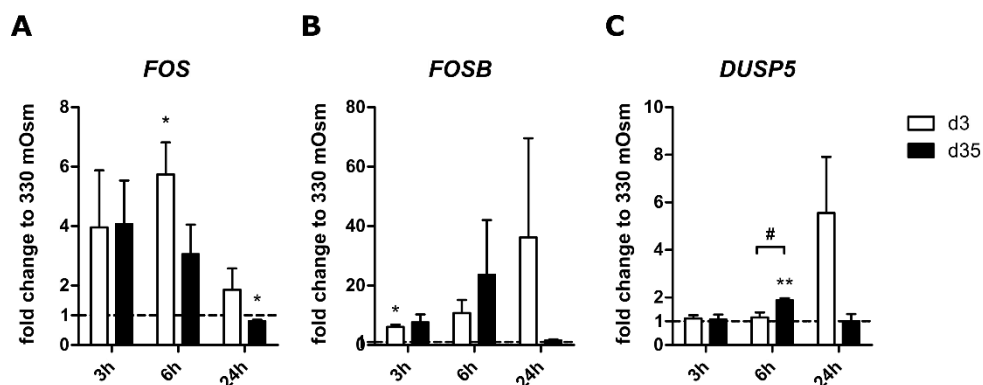


Figure 14 Effect of hyperosmotic stimulation on the expression of mechano-response genes from the MAPK family. AC-laden TE-constructs were subjected to chondrocyte redifferentiation medium for 35 days and 550 mOsm hyperosmotic stimulation was performed on day 3 or day 35 for 3, 6 or 24 hours. Expression of (A) *FOS*, (B) *FOSB* and (C) *DUSP5* was determined by qPCR. Gene expression levels were normalized to the mean expression of reference genes *18S*, *GAPDH* and *RPL13*. Data are presented as mean \pm SEM difference between 550 mOsm and control constructs. For each donor cell population, the control was set to 1 (dashed line at 1). $n=3$ donors. * $p<0.05$, ** $p<0.01$, paired Student's t-test, 330 vs 550 mOsm; # $p<0.05$, paired Student's t-test, d3 vs d35.

0.09-fold, $p=0.01$) (Figure 14 C), indicating that *DUSP5* is less sensitive to acute hyperosmotic stimulation. Due to the low sample size and large standard deviation, the regulations reached significance only at selected time points and further experiments will be needed to confirm the observed trends.

Overall, hyperosmotic conditions induced *FOS* and *FOSB* expression, suggesting hyperosmotic pressure may be a relevant sub-parameter for their upregulation after mechanical challenge. In contrast, *DUSP5* and its induction was less sensitive to hyperosmotic stimulation and appears to be a unique event of mechanical loading.

When the expression of mechano-response genes *BMP2* and *BMP6* was analyzed after hyperosmotic stimulation on day 3, no regulation was observed after 3 and 6 hours of stimulation. A clear trend to increased expression of *BMP2* (7.65 ± 2.62 -fold, $p=0.13$) and *BMP6* (20.09 ± 7.29 -fold, $p=0.12$) was obvious after 24 hours of stimulation. On day 35, no regulation of *BMP2* and *BMP6* was observed after 3 and 6 hours of stimulation. Hyperosmotic challenge for 24 hours showed only slight induction of *BMP6* (5.09 ± 2.42 -fold, $p=0.23$) (Figure 15).

Thus, while hyperosmotic induction of *BMP2* and *BMP6* was unchanged at short stimulation times at either FCD, only long hyperosmotic stimulation times of 24 hours enhanced *BMP2* and *BMP6* expression especially at low FCD. Hyperosmotic effects may, therefore, not or only little contribute to the robust mechano-induction of *BMP2* and *BMP6*.

It was therefore concluded that hyperosmotic stimulation reproduced the upregulation of mechano-response genes *FOS* and *FOSB*, independent of the FCD. The common induction of *FOS* and *FOSB* expression after mechanical and osmotic challenge indicates that mechanical and osmotic stresses partly induce similar response patterns.

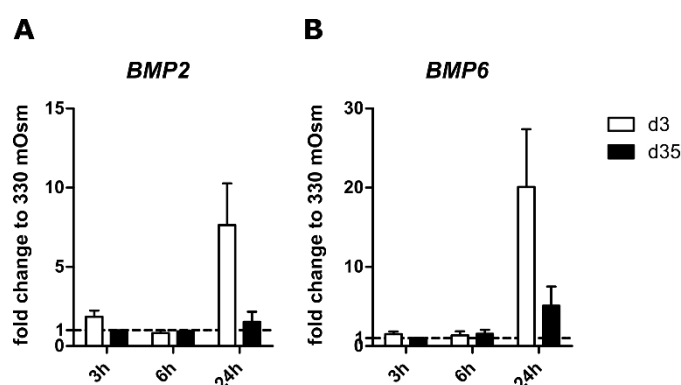


Figure 15 Effect of hyperosmotic stimulation on the expression of BMP ligands. AC-laden TE-constructs were subjected to chondrocyte redifferentiation medium for 35 days and 550 mOsm hyperosmotic stimulation was performed on day 3 or day 35 for 3, 6 or 24 hours. Expression of (A) *BMP2* and (B) *BMP6* was determined by qPCR. Gene expression levels were normalized to the mean expression of reference genes *18S*, *GAPDH* and *RPL13*. Data are presented as mean \pm SEM difference between 550 mOsm and control constructs. For Each donor cell population, the control was set to 1 (dashed line at 1). $n=3$ donors, paired Student's t-test.

Overall, molecular characterization of the hyperosmotic response of human 3D-cultured articular chondrocytes after different times of pre-maturation culture established ERK1/2 and p38 as well as *NFAT5*, *FOS* and *FOSB* as immediate osmo-response markers, irrespective of FCD. In addition, *SLC6A12*, *SLC5A3* and *S100A4* were identified as osmo-response markers after hyperosmotic stimulation for 24 hours independent of FCD. A downregulation of pro-chondrogenic SMAD1/5/9 and SOX9 protein was demonstrated specifically at high FCD, but a trend to less GAG synthesis was only observed after hyperosmotic stimulation for 3 hours at low FCD. Thus, acute hyperosmotic pressure appeared not as relevant sub-parameter of load-induced GAG synthesis in our model of mature human 3D engineered cartilage.

4.2 Long-term hyperosmotic stimulation of cartilage tissue engineering constructs

So far, 3D engineered cartilage tissue lacks a sufficiently high ECM content to withstand the demanding mechanical conditions in the joint in the long-term. A moderate long-term hyperosmotic stimulation was suggested to increase the GAG synthesis rate and enhance the ECM deposition in 3D engineered cartilage from various animal species. Whether a long-term hyperosmotic stimulation may also provide a cheap and simple stimulus to enhance the cartilage matrix deposition in our model of human 3D engineered neocartilage was therefore addressed next. To elucidate whether long-term hyperosmotic stimulation can be a relevant stimulus to enhance the quality of cartilage replacement tissue, several studies highlighted the importance of the calcium microenvironment for cartilage ECM synthesis and deposition. However, it is currently unknown whether high extracellular calcium stimulates or inhibits the cartilage ECM formation in cartilage TE constructs. Since AC and MSC are often used cell types for cartilage TE, the response of both cell types to long-term hyperosmotic stimulation using extracellular calcium was investigated. For this purpose, AC and MSC-derived chondrocytes were matured to form neocartilage under control or high extracellular calcium conditions. The quality of the tissue was assessed by its DNA content, expression of differentiation markers, GAG synthesis as well as GAG deposition and type II collagen deposition.

4.2.1 Evaluation of calcium concentrations in the medium

To investigate whether long-term hyperosmotic stimulation of AC and MSC-derived chondrocytes can enhance the type II collagen and PG deposition in 3D engineered cartilage, a promising calcium

stimulation regime has to be selected. For this purpose, 5×10^5 human AC or MSC were seeded into type I/III collagen scaffolds and allowed to mature under chondrogenic conditions for up to 35 days. Previous studies observed changes in GAG and type II collagen deposition in adipose tissue-derived MSC at extracellular calcium concentrations of 8.0 mM (Mellor et al. 2015). Based on these studies, calcium concentration in the medium was adjusted from 1.8 mM in the standard chondrocyte differentiation medium over 3.3 mM to 8.0 mM in the calcium stimulation groups. This corresponds to a moderate hyperosmotic stimulation of 10 mOsm or 24 mOsm, respectively. CaCl_2 -solution was freshly added to the culture medium at each medium change. Calcium levels in the medium were confirmed on day 1 of culture and at weekly intervals from day 7 to day 35 using Infinity Calcium Arsenazo III kit. While measurements on day 1 had to be performed 24 hours after medium change, measurements on day 7 to 35 were performed 48 hours after medium change. On day 1, mean medium calcium concentration after 1.8, 3.3 and 8.0 mM $[\text{Ca}^{2+}]_e$ treatment was at 1.94 mM, 3.39 mM and 7.57 mM in the AC-group and at 1.79 mM, 3.28 mM and 7.94 mM in the MSC-group, respectively (Figure 16 A). 48 hours after medium change on day 7 to

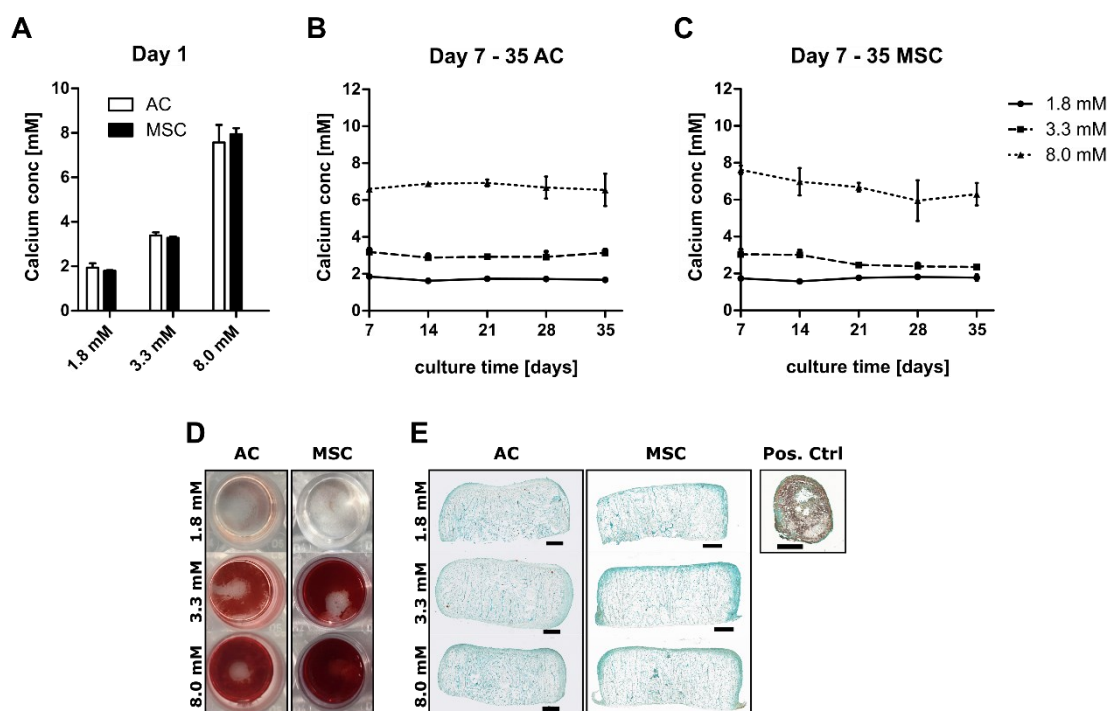


Figure 16 Evaluation of medium calcium concentrations. 5×10^5 AC or MSC were seeded in a type I/III collagen carrier and subjected to chondrocyte (re)differentiation medium for up to 35 days. Long-term hyperosmotic stimulation was applied by the addition of CaCl_2 to the culture medium throughout the complete maturation to reach 3.3 mM or 8.0 mM $[\text{Ca}^{2+}]_e$, corresponding to +10 mOsm or +24 mOsm. **(A-C)** Calcium medium concentrations were determined in culture supernatants pooled from two constructs of $n=2-4$ AC and MSC donors. Measurements were performed on (A) day 1 or (B-C) over the time course of 5 weeks for (B) AC- and (C) MSC-laden constructs. Data are depicted as mean \pm SEM. **(D)** Alizarin red S staining of the well bottom of the culture dish after 35 days of culture from $n=3$ AC and MSC donors. Unstained area in the 3.3 mM and 8.0 mM group presents the position of the TE-construct during culture. **(E)** Alizarin red S staining of tissue sections from AC or MSC TE-constructs cultured for 35 days at different $[\text{Ca}^{2+}]_e$. Representative images from $n=5$ AC and $n=6$ MSC donors are depicted. Mineralized MSC pellets after ectopic implantation in mice for 56 days served as positive control.

35, calcium concentrations were slightly lower in the 3.3 mM and 8.0 mM group compared to measurement at the 24 hour time-point on day 1. Mean calcium concentrations in the medium over 35 days were 3.07 mM and 6.87 mM in the AC-group and 2.75 mM and 6.91 mM in the MSC-group, respectively (Figure 16 A+B). To investigate whether a slight decline of the mean medium calcium concentration was accompanied by a precipitation of calcium, the bottom of the culture well was stained for the presence of a calcium-precipitate using Alizarin Red S. On day 35, a strong Alizarin Red S-positive precipitate was observed at the bottom of the well in the 3.3 mM and 8.0 mM groups of AC and MSC. No staining was detected at control conditions (Figure 16 D). To ensure that the calcium precipitation did not lead to calcification of the construct, day 35 AC- and MSC tissue was stained using Alizarin Red S. No staining was observed in tissue sections after 35 days at all conditions, indicating that calcium precipitation was restricted to the bottom of the well and did not lead to calcification of the tissue (Figure 16 D).

Overall, elevation of extracellular calcium concentrations was confirmed in the high $[Ca^{2+}]_e$ -groups. Thus, 3.3 mM and 8.0 mM $[Ca^{2+}]_e$ were selected as promising treatments for long-term hyperosmotic stimulation.

4.2.2 Effect of long-term hyperosmotic stimulation on DNA content of AC and MSC-based TE constructs

Increased DNA levels were previously reported after long-term hyperosmotic stimulation in bovine and porcine 3D-cultured chondrocytes (O'Connor et al. 2014; Sampat et al. 2013). In order to investigate whether long-term hyperosmotic stimulation induces changes in cell numbers in our model of human 3D neocartilage, the DNA content in AC and MSC-based TE constructs was determined after initial seeding on day 0 and on day 35. Similar DNA levels were detected in AC and MSC-based TE constructs on day 0 (AC: $5.08 \pm 0.33 \mu\text{g}$; MSC: $6.42 \pm 1.08 \mu\text{g}$), indicating that equal amounts of AC and MSC were seeded into the carrier. Over 35 days, the mean DNA content nearly doubled in AC control constructs, reaching $9.51 \pm 0.58 \mu\text{g}$. Extracellular calcium stimulation at 8.0 mM significantly enhanced the DNA levels in AC on day 35 ($11.23 \pm 0.82 \mu\text{g}$, $p=0.008$, $n=14$) (Figure 17 A). In contrast, DNA levels in MSC-based TE constructs remained unchanged at all time points and conditions (Figure 17 B).

Thus, long-term hyperosmotic stimulation at 8.0 mM $[Ca^{2+}]_e$ significantly enhanced the DNA levels of AC constructs, while no such effect was observed in MSC constructs. This indicated that quantification of cartilage matrix components in the construct should be referred to its DNA content in order to correct for altered cell numbers after calcium treatment.

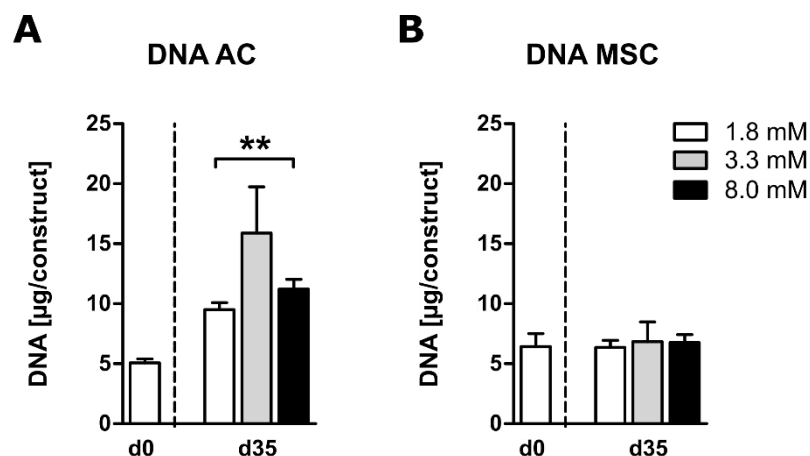


Figure 17 Effect of long-term hyperosmotic stimulation on the DNA content of AC- and MSC-based TE-constructs. 5×10^5 AC or MSC were seeded in a type I/III collagen carrier and subjected to chondrocyte (re)differentiation medium for up to 35 days. Long-term hyperosmotic stimulation was applied by the addition of CaCl_2 to the culture medium throughout the complete maturation to reach 3.3 mM or 8.0 mM $[\text{Ca}^{2+}]_e$. DNA per construct was quantified on day 0 or day 35 of culture in (A) AC- or (B) MSC-laden constructs. All data are expressed as mean \pm SEM in AC- or MSC samples from $n=5$ (day 0) or $n=3-4$ (3.3 mM) and $n=10-14$ (8.0 mM) donors. * $p < 0.05$, ** $p < 0.01$, paired Student's t-test, vs. 1.8 mM on day 35.

4.2.3 Effect of long-term hyperosmotic stimulation on the expression of differentiation markers in AC and MSC-derived chondrocytes

To investigate whether long-term hyperosmotic stimulation promotes the chondrogenic differentiation of cartilage TE constructs, the expression of differentiation markers was investigated. For this purpose, AC and MSC-derived chondrocytes were stimulated with 3.3 mM or 8.0 mM $[\text{Ca}^{2+}]_e$ for 35 days and *COL2A1*, *ACAN* and *SOX9* mRNA levels were determined using qPCR. On day 35 of AC redifferentiation, mean expression levels were slightly lower at 3.3 mM $[\text{Ca}^{2+}]_e$ compared to control constructs at the same time point, reaching significance only for *ACAN* (Figure 18 A). Stimulation of AC at 8.0 mM $[\text{Ca}^{2+}]_e$ led to significantly lower expression of all three differentiation markers (Figure 18 A). In MSC-derived chondrocytes, 3.3 mM and 8.0 mM extracellular calcium treatment did not change the expression of differentiation markers *COL2A1*, *ACAN* and *SOX9* (Figure 18 B).

Overall, significantly lower *COL2A1*, *ACAN* and *SOX9* mRNA expression in AC at 8.0 mM $[\text{Ca}^{2+}]_e$ indicated that long-term hyperosmotic stimulation reduced the redifferentiation of AC, especially at 8.0 mM $[\text{Ca}^{2+}]_e$ whereas chondrogenic differentiation of MSC appeared unaffected.

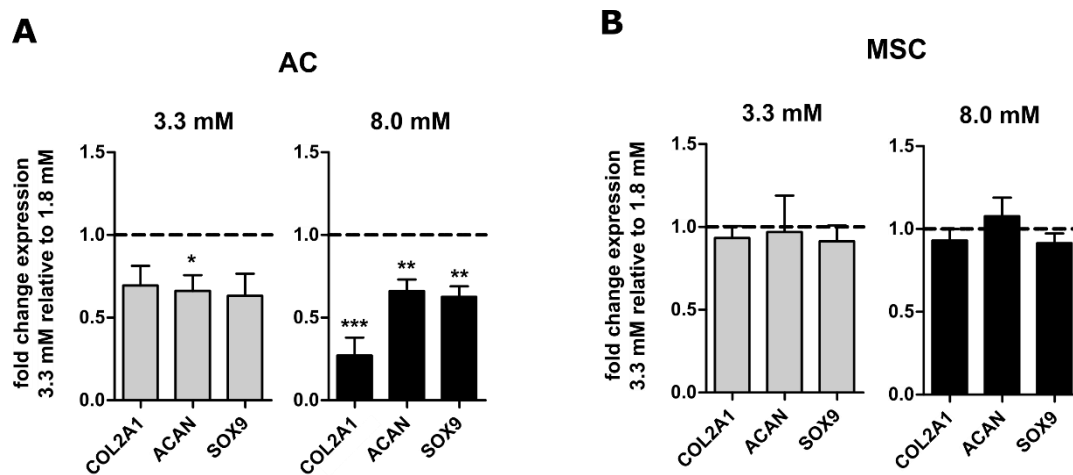


Figure 18 Effect of long-term hyperosmotic stimulation on differentiation marker expression by AC and MSC-derived chondrocytes. 5×10^5 AC or MSC were seeded in a type I/III collagen carrier and subjected to chondrocyte (re)differentiation medium for up to 35 days. Long-term hyperosmotic stimulation was applied by the addition of CaCl_2 to the culture medium throughout the complete maturation to reach 3.3 mM or 8.0 mM $[\text{Ca}^{2+}]_e$. *COL2A1*, *ACAN* and *SOX9* mRNA levels were determined by qPCR. Gene expression levels were normalized to the mean expression of reference genes *18S*, *GAPDH* and *RPL13* and 1.8 mM $[\text{Ca}^{2+}]_e$ control samples were set to one (dashed line at 1.0). **A)** AC- or **B)** MSC-laden constructs were cultured at 3.3 mM $[\text{Ca}^{2+}]_e$ (grey bars) or 8.0 mM $[\text{Ca}^{2+}]_e$ (black bars) and differentiation marker expression was determined on day 35. All data are expressed as mean \pm SEM in AC- and MSC samples from $n=3-4$ (3.3 mM) or $n=8-9$ (8.0 mM) donors. * $p < 0.05$, ** $p < 0.01$, *** $p < 0.001$, paired Student's t-test, vs. 1.8 mM.

4.2.4 Effect of long-term hyperosmotic stimulation of AC on GAG synthesis and GAG deposition

To investigate whether the lower expression of differentiation markers by AC was accompanied by reduced GAG formation in the construct, GAG synthesis and GAG deposition by AC was analyzed after long-term hyperosmotic stimulation at 3.3 mM or 8.0 mM $[\text{Ca}^{2+}]_e$ for 35 days. To allow the detection of positive and negative calcium-dependent effects on GAG formation, only experiments from donor populations with strong chondrocyte redifferentiation under control conditions were included. Tissue sections from 18 experiments were stained with Safranin O to visualize the presence of sulfated GAGs throughout the tissue. Only constructs in which the control sample showed more than 70% stained area according to Safranin O were included in the analysis ($n=11$ samples from 10 donors, see Appendix Figure 1 and Figure 19 A). Treatment with 3.3 mM $[\text{Ca}^{2+}]_e$ did not change the staining intensity in samples from two out of 3 donors but reduced the staining intensity in samples from one donor. At 8.0 mM $[\text{Ca}^{2+}]_e$, Safranin O staining intensity was strongly reduced in samples from 5 donors, slightly reduced in samples from 1 donor and unchanged in samples from 4 donors. Quantitative evaluation of the GAG deposition on day 35 revealed no difference in the GAG/DNA content between controls and samples cultured at 3.3 mM $[\text{Ca}^{2+}]_e$ (Figure 19 B). In contrast, 8.0 mM $[\text{Ca}^{2+}]_e$ treatment for 35 days significantly reduced the GAG/DNA content from $43.10 \pm 4.58 \mu\text{g}/\mu\text{g}$ in control constructs to $27.79 \pm 3.68 \mu\text{g}/\mu\text{g}$

($p=0.0031$, $n=11$) in the 8.0 $[Ca^{2+}]_e$ group. Remarkably, a reduced GAG deposition was obvious in 10 out of 11 samples (Figure 19 C). The GAG synthesis rate was measured by incorporation of radio-labeled ^{35}S -sulfate over the last 24 hours of culture on day 35 and referred to the DNA content of the construct. Lower GAG synthesis was observed in 2 out of 2 experiments at 3.3 mM $[Ca^{2+}]_e$ (Figure 19 D) and 8 out of 9 donor populations tested at 8.0 mM $[Ca^{2+}]_e$ (Figure 19 E). On average, the mean GAG synthesis rate was by trend reduced at 3.3 mM $[Ca^{2+}]_e$ compared to control constructs (0.58 ± 0.02 -fold, $n=2$), but this did not reach significance due to a low sample size. At 8.0 mM $[Ca^{2+}]_e$, the GAG synthesis rate dropped significantly to 70% of control levels (0.70 ± 0.09 -fold, $p=0.01$, $n=9$).

Overall, this demonstrated that in human 3D-cultured AC, a reduced expression of differentiation markers after long-term hyperosmotic stimulation was accompanied by a significantly reduced GAG synthesis and GAG/DNA deposition. Similar to differentiation marker expression (Figure 18 A), regulation of GAG synthesis and deposition reached significance only at 8.0 mM $[Ca^{2+}]_e$.

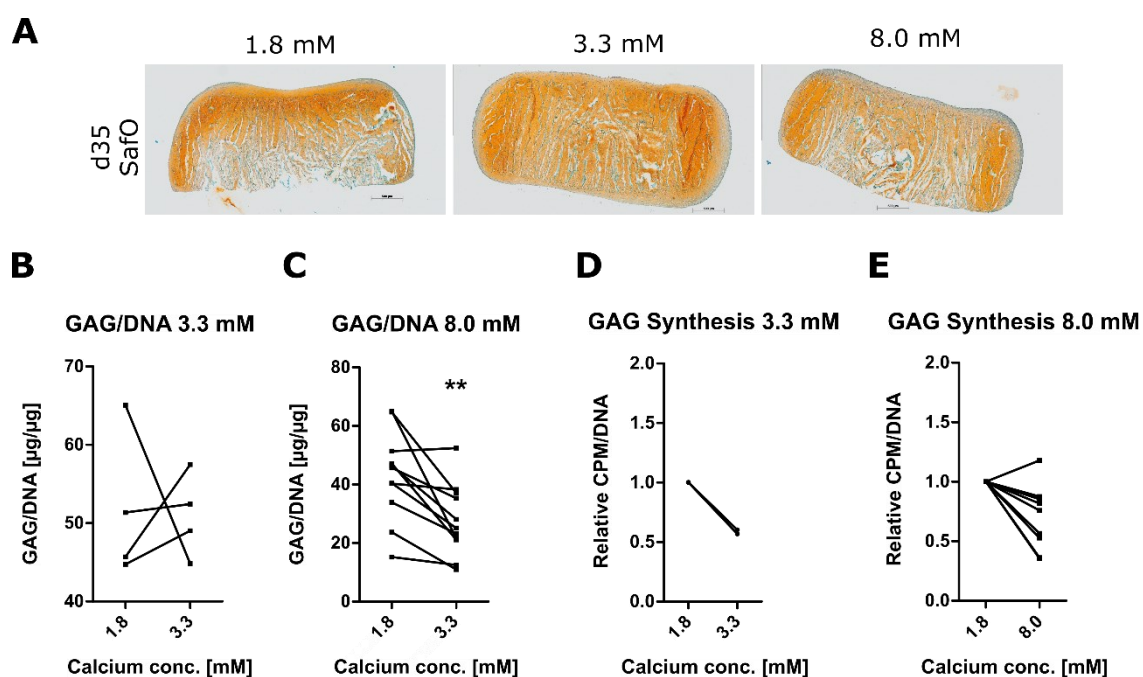


Figure 19 Effect of long-term hyperosmotic stimulation on GAG formation by AC. 5×10^5 AC were seeded in a type I/III collagen carrier and subjected to chondrocyte (re)differentiation medium for up to 35 days. Long-term hyperosmotic stimulation was applied by the addition of $CaCl_2$ to the culture medium throughout the complete maturation to reach 3.3 mM or 8.0 mM $[Ca^{2+}]_e$. **(A)** Standard paraffin sections from day 35 TE-constructs were stained with Safranin O/Fast green to visualize GAGs. Representative images are depicted for AC from $n=3$ (3.3 mM) or $n=10$ (8.0 mM) donors. **(B+C)** GAG content measured by DMMB assay after culture at 3.3 mM (B) or 8.0 mM (C) $[Ca^{2+}]_e$ for 35 days. Values were normalized to the DNA-content. **(D+E)** GAG synthesis rate measured as ^{35}S -sulfate incorporation during the last 24 hours of culture on day 35 in constructs cultured at 3.3 mM (D) or 8.0 mM (E) $[Ca^{2+}]_e$. Values were normalized to DNA-content and 1.8 mM $[Ca^{2+}]_e$ control samples were set to one. All data are depicted as individual donor matched pairs of the control and the corresponding treatment group for AC from B) $n=4$ constructs from 3 donors, C) $n=11$ constructs from 10 donors, D) $n=2$ constructs from 2 donors and E) $n=9$ constructs from 9 donors $**p<0.001$, paired Student's t-test, 1.8 mM vs. 8.0 mM.

4.2.5 Effect of long-term hyperosmotic stimulation of MSC-derived chondrocytes on GAG synthesis and GAG deposition

To investigate whether the unchanged expression of differentiation markers in MSC-derived chondrocytes after long-term hyperosmotic stimulation correlated with an unaltered GAG formation in the construct, GAG synthesis and GAG deposition were determined. For this purpose, MSC-laden constructs were cultured at 3.3 mM or 8.0 mM $[Ca^{2+}]_e$ for 35 days. Similar to AC, MSC experiments were only included in the analysis when tissue sections of control samples on day 35 stained more than 70% positive for Safranin O (n=10 samples from 9 donors, see Appendix Figure 2 and Figure 20 A). Treatment with 3.3 mM $[Ca^{2+}]_e$ slightly enhanced the staining intensity for Safranin O in samples from 2 out of 4 donors whereas no change was observed in samples from two donors. At 8.0 mM $[Ca^{2+}]_e$, Safranin O staining intensity was enhanced in samples from 4 donors, no change was observed in samples from 3 donors and staining intensity was reduced in samples from 2 donors. Quantification of GAG/DNA content showed increased GAG/DNA values

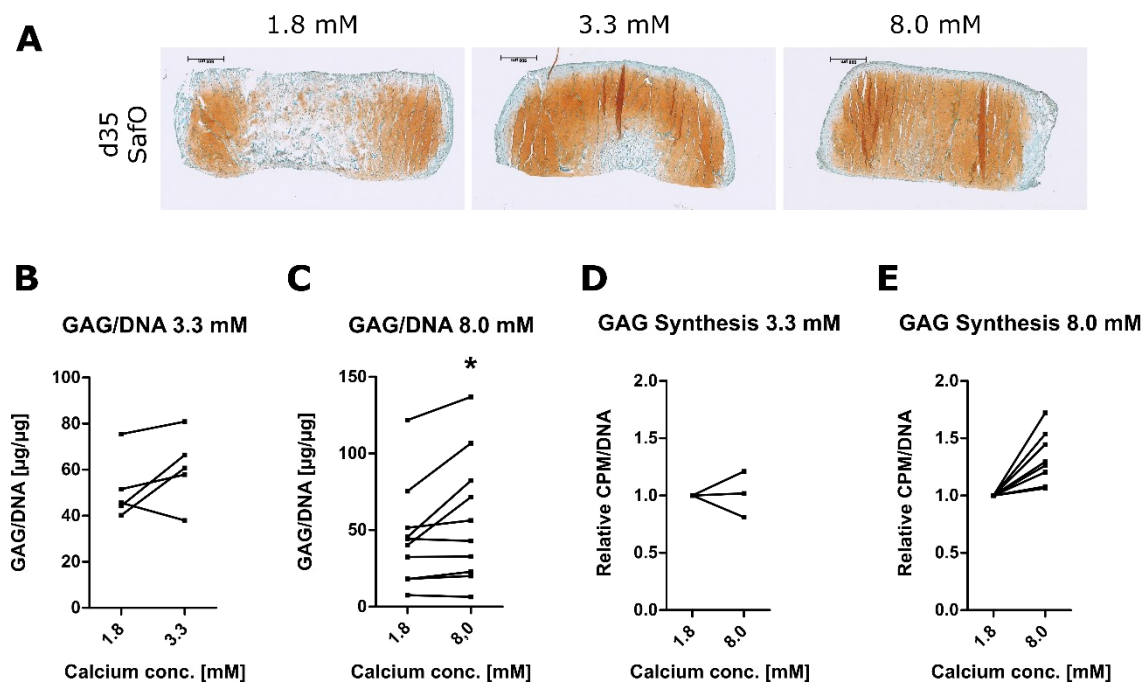


Figure 20 Effect of long-term hyperosmotic stimulation on GAG formation by MSC-derived chondrocytes. 5×10^5 MSC were seeded in a type I/III collagen carrier and subjected to chondrocyte (re)differentiation medium for up to 35 days. Long-term hyperosmotic stimulation was applied by the addition of $CaCl_2$ to the culture medium throughout the complete maturation to reach 3.3 mM or 8.0 mM $[Ca^{2+}]_e$. **(A)** Standard paraffin sections from day 35 TE-constructs were stained with Safranin O/ Fast green to visualize GAGs. Representative images are depicted for MSC from n=4 (3.3 mM) or n=9 (8.0 mM) donors. **(B+C)** GAG content measured by DMMB assay after culture at 3.3 mM (B) or 8.0 mM (C) $[Ca^{2+}]_e$ for 35 days. Values were normalized to the DNA-content. **(D+E)** GAG synthesis rate measured as ^{35}S -sulfate incorporation during the last 24 hours of culture on day 35 in constructs cultured at 3.3 mM (D) or 8.0 mM (E) $[Ca^{2+}]_e$. Values were normalized to DNA-content and 1.8 mM $[Ca^{2+}]_e$ control samples were set to one. All data are depicted as individual donor matched pairs of the control and the corresponding treatment group for MSC from B) n=5 constructs from 4 donors, C) n=10 constructs from 9 donors, D) n=3 constructs from 3 donors and E) n=8 constructs from 8 donors. * $p < 0.05$, paired Student's t-test, 1.8 mM vs. 8.0 mM.

in 4 out of 5 experiments (Figure 20 B). At 8.0 mM $[Ca^{2+}]_e$, the GAG/DNA content was enhanced in 8 out of 10 samples (Figure 20 C). Overall, long-term hyperosmotic stimulation significantly enhanced the GAG/DNA content from $45.52 \pm 10.48 \mu\text{g}/\mu\text{g}$ in controls to $57.89 \pm 13.16 \mu\text{g}/\mu\text{g}$ ($p=0.029$, $n=10$) in the 8.0 mM $[Ca^{2+}]_e$ group. No significant change was observed in the 3.3 mM $[Ca^{2+}]_e$ -group. Long-term hyperosmotic stimulation at 3.3 mM $[Ca^{2+}]_e$ enhanced the GAG synthesis rate on day 35 in samples from 2 out of 3 donors (Figure 20 D). 8.0 mM $[Ca^{2+}]_e$ treatment increased the GAG synthesis rate in samples from all MSC donors (Figure 20 E). While the mean GAG synthesis rate was unchanged at 3.3 mM $[Ca^{2+}]_e$ (1.01 ± 0.12 -fold, $p=0.92$, $n=3$), it increased significantly under stimulation with 8.0 mM $[Ca^{2+}]_e$ (1.33 ± 0.08 -fold, $p=0.0049$, $n=8$).

Thus, despite unchanged differentiation marker expression, long-term hyperosmotic stimulation significantly enhanced the GAG deposition and GAG synthesis at 8.0 mM $[Ca^{2+}]_e$ in MSC-based TE constructs. Overall, long-term hyperosmotic stimulation at 8.0 mM $[Ca^{2+}]_e$ induced an inverse regulation of GAG formation by AC and MSC-derived chondrocytes.

4.2.6 Effect of long-term hyperosmotic stimulation of AC and MSC-derived chondrocytes on type II collagen deposition

To test whether long-term hyperosmotic stimulation induced a regulation of type II collagen protein levels by AC and MSC-derived chondrocytes, immunohistochemical staining and ELISA against type II collagen were performed on day 35. Due to a limited availability of cells, only one calcium concentration was included in the following experiments. Since the strongest effects on differentiation marker expression of AC (Figure 18 A) as well as GAG synthesis and GAG deposition (Figure 19 and Figure 20) were observed at 8.0 mM $[Ca^{2+}]_e$, this concentration was selected for further experiments.

In AC constructs, high calcium treatment for 35 days slightly reduced the staining intensity against type II collagen (Figure 21 A). Quantification of type II collagen using an ELISA revealed a reduced type II collagen content per construct in samples from all AC donors (Figure 21 B). In MSC-constructs, type II collagen immunostaining was slightly stronger at 8.0 mM $[Ca^{2+}]_e$ (Figure 21 C) and type II collagen ELISA revealed a higher type II collagen deposition in 8.0 mM samples from all MSC donors compared to the corresponding controls (Figure 21 D). On average, the mean type II collagen content in AC constructs on day 35 was reduced from $28.62 \pm 10.14 \mu\text{g}$ in controls to $5.91 \pm 2.87 \mu\text{g}$ (4.84-fold, $p=0.069$, $n=4$) in the high calcium-group. In MSC constructs, mean type II collagen content increased from $40.34 \pm 11.72 \mu\text{g}$ in controls to $70.45 \pm 17.10 \mu\text{g}$ (1.75-fold, $p=0.061$, $n=6$) at 8.0 mM $[Ca^{2+}]_e$. However, statistical analysis revealed no significant difference by calcium stimulation of AC- and MSC-groups.

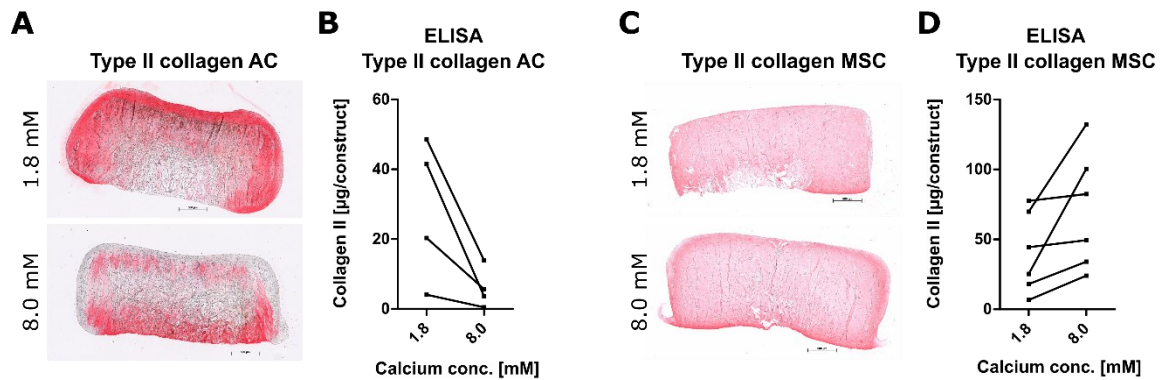


Figure 21 Effect of long-term hyperosmotic stimulation on type II collagen deposition by AC and MSC-derived chondrocytes. AC- or MSC-laden TE-constructs were cultured in chondrocyte differentiation medium for 35 days at 1.8 mM or 8.0 mM $[\text{Ca}^{2+}]_e$. **(A+C)** Type II collagen deposition was detected by immunohistochemistry in paraffin sections from (A) AC- and (C) MSC-based TE constructs. Representative images are depicted for samples from $n=6$ AC and $n=7$ MSC donors. **(B+D)** Type II collagen deposition was quantified on d35 via type II collagen ELISA in samples from $n=4$ AC (B) and $n=6$ MSC (D) donors. Data are depicted as individual donor matched pairs of the control and the corresponding treatment group. No statistical significance according to paired Student's t-test, 1.8 mM vs. 8.0 mM.

Thus, long-term hyperosmotic calcium stimulation at 8.0 mM did not significantly change the mean type II collagen deposition by AC and MSC-derived chondrocytes.

Overall, while long-term hyperosmotic stimulation by extracellular calcium promoted cartilage matrix formation in MSC-based cartilage TE constructs, it compromised cartilage matrix formation during AC-based cartilage neogenesis.

Since higher extracellular calcium concentrations cannot be avoided under certain conditions, such as during osteochondral TE, it was of interest whether AC and MSC were equally suited to deposit GAG and type II collagen under elevated calcium conditions. Therefore, the data depicted in Figure 19 C (GAG/DNA content of AC samples), Figure 20 C (GAG/DNA content of MSC samples), Figure 21 B (type II collagen content of AC samples) and Figure 21 D (type II collagen content of MSC samples) were subjected to a comparative statistical analysis. At control conditions on day 35, AC and MSC-derived chondrocytes deposited a similar amount of GAG/DNA ($p=0.83$) as well as of type II collagen ($p=0.22$) in the construct. In contrast, at 8.0 mM $[\text{Ca}^{2+}]_e$ on day 35, MSC-based constructs reached significantly higher GAG/DNA values than AC-constructs ($p=0.03$) (Figure 22 A). Likewise, type II collagen levels were significantly higher in MSC- compared to AC-based TE constructs at high extracellular calcium concentrations ($p=0.013$) (Figure 22 B).

Thus, MSC-derived chondrocytes showed a robust cartilage matrix production also under high calcium conditions, depositing significantly more GAG/DNA and type II collagen than AC.

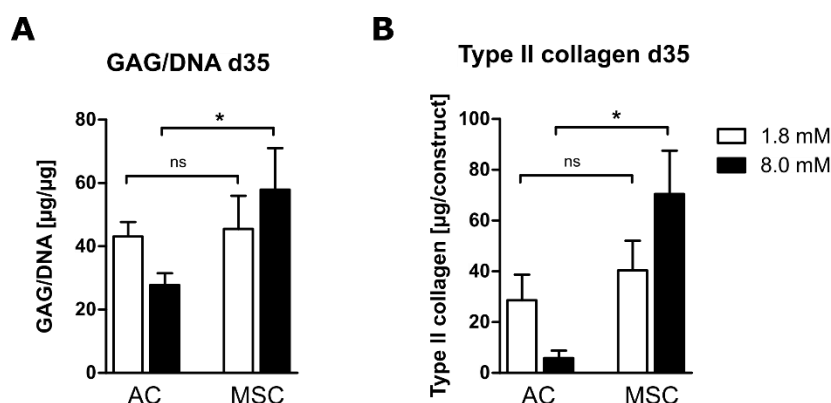


Figure 22 Comparison of GAG and type II collagen levels in AC- versus MSC-based TE-constructs after long-term high extracellular calcium stimulation. AC- or MSC-laden TE-constructs were cultured in chondrocyte differentiation medium for 35 days at 1.8 or 8.0 mM [Ca²⁺]_e. **(A)** GAG content measured by DMMB assay on day 35. Values were normalized to DNA-content. **(B)** Type II collagen deposition was quantified on d35 via type II collagen ELISA. All data are expressed as mean ± SEM in samples from n=11 AC- and n=10 MSC donors (GAG/DNA) or n=4 AC- and n=6 MSC donors (type II collagen ELISA). *p<0.05, unpaired Student's t-test, AC vs MSC.

4.2.7 Effect of long-term hyperosmotic stimulation on GAG synthesis of AC and MSC-derived chondrocytes using different osmolytes

Whether the inverse regulation of GAG synthesis by calcium-stimulated AC and MSC-derived chondrocytes was specific to CaCl₂-treatment was assessed using MgCl₂ or sucrose as ionic or osmotic controls, respectively. For this purpose, AC and MSC-based TE constructs were stimulated for 35 days with equimolar concentrations of MgCl₂ or equiosmolar concentrations of sucrose in

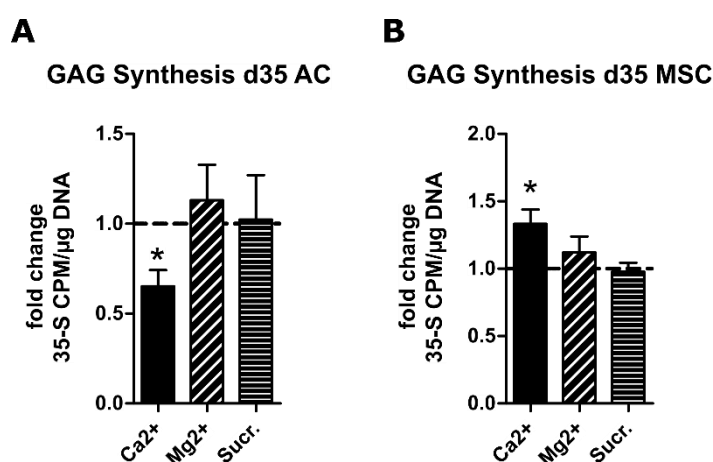


Figure 23 Effect of different osmolytes on GAG synthesis of AC and MSC-derived chondrocytes. AC- or MSC-laden TE-constructs were cultured in chondrocyte differentiation medium for 35 days. Medium calcium concentration was adjusted to 8.0 mM [Ca²⁺]_e by the addition of CaCl₂ to the culture medium in the calcium-group. Equimolar addition of MgCl₂ was performed as ionic control in the magnesium-group. Equiosmolar concentration of sucrose was added as osmotic control in the sucrose group. GAG synthesis rate was measured as ³⁵S-sulfate incorporation during the last 24 hours of culture on day 35 by AC **(A)** or MSC **(B)**. Values were normalized to DNA-content and control samples were set to one (dashed line at 1.0). All data are expressed as mean ± SEM in samples from n=6 AC- and n=4 MSC donors. *p<0.05, paired Student's t-test vs control.

the medium and the GAG synthesis rate was measured. In AC and MSC-derived chondrocytes, neither 8.0 mM $[Mg^{2+}]_e$ nor +24 mOsm sucrose induced alterations in GAG synthesis (Figure 23). It was therefore concluded that the regulation of GAG synthesis after long-term hyperosmotic stimulation was specific to treatment with high extracellular calcium.

Overall, this argues in favor of calcium-specific rather than general hyperosmotic effects on cartilage ECM synthesis.

4.2.8 Influence of long-term extracellular calcium stimulation on the phenotype of AC and MSC-derived chondrocytes

While re-differentiation of AC results in the formation of hyaline-like articular chondrocytes, MSC follow the endochondral differentiation pathway and develop into hypertrophic chondrocytes. Previous studies indicated that during chondrogenic differentiation of adipose tissue-derived MSC, high extracellular calcium treatment shifted the phenotype from cartilage-like cells at 1.8 mM $[Ca^{2+}]_e$ to osteoblast-like cells at 8.0 mM $[Ca^{2+}]_e$ (Mellor et al. 2015). To determine whether the reduced cartilage ECM formation by AC at high calcium levels was due to mis-differentiation towards a pro-hypertrophic phenotype, the expression of hypertrophic and osteogenic markers was examined on mRNA and protein level. Furthermore, it was investigated whether the increased GAG formation by MSC-derived chondrocytes occurred at reduced hypertrophic differentiation. For this purpose, AC- and MSC-laden TE constructs were cultured at control or 8.0 mM $[Ca^{2+}]_e$ for 35 days and gene expression of *COL10A1*, *IBSP* and *ALPL* was detected using qPCR. ALP enzyme activity was determined in culture supernatant on day 35 and type X collagen and IBSP protein were detected using Western blot.

In AC constructs cultured at control conditions for 35 days, a low expression of *COL10A1*, *IBSP* and *ALPL* was detected (Figure 24 A-C). This did not translate into detectable levels of the respective protein as indicated by the absence of ALP enzyme activity in the supernatant (Figure 24 D) and type X collagen and IBSP in Western blots (Figure 24 E+F). Furthermore, an unchanged expression of hypertrophic and osteogenic markers after extracellular calcium treatment demonstrated that AC did not mis-differentiate into a pro-hypertrophic phenotype.

As expected, MSC-derived chondrocytes underwent hypertrophic differentiation under control conditions, indicated by strong expression of *COL10A1*, *IBSP* and *ALPL* mRNA (Figure 24 A-C). While calcium stimulation did not change the expression of *COL10A1* and *IBSP* (Figure 24 A+B), *ALPL* expression was significantly increased (Figure 24 C). At the protein level, MSC-derived chondrocytes showed high ALP enzyme activity in the supernatant which did not change upon calcium treatment (Figure 24 D). This indicated that calcium-induced upregulation of *ALPL* mRNA

expression did not translate into higher ALP enzyme activity. In MSC-derived chondrocytes, type X collagen was detected at control and high calcium conditions. While extracellular calcium treatment reduced type X collagen levels in samples from two donors, the signal was increased in samples from one donor (Figure 24 E). IBSP protein was detected in control samples from one MSC donor on day 35. At high calcium conditions, IBSP protein was detected in samples from all three donors, however, in 2 out of 3 donors IBSP levels were still very faint (Figure 24 F). This indicated that MSC-derived chondrocytes still follow the endochondral differentiation pathway under high calcium conditions. However, no consistent regulation of hypertrophic markers was observed after calcium treatment.

Overall, this indicated that long-term extracellular calcium stimulation did not lead to pro-hypertrophic mis-differentiation of AC. The enhanced GAG synthesis and GAG deposition of MSC-derived chondrocytes at 8.0 mM $[Ca^{2+}]_e$ occurred at maintained hypertrophic differentiation.

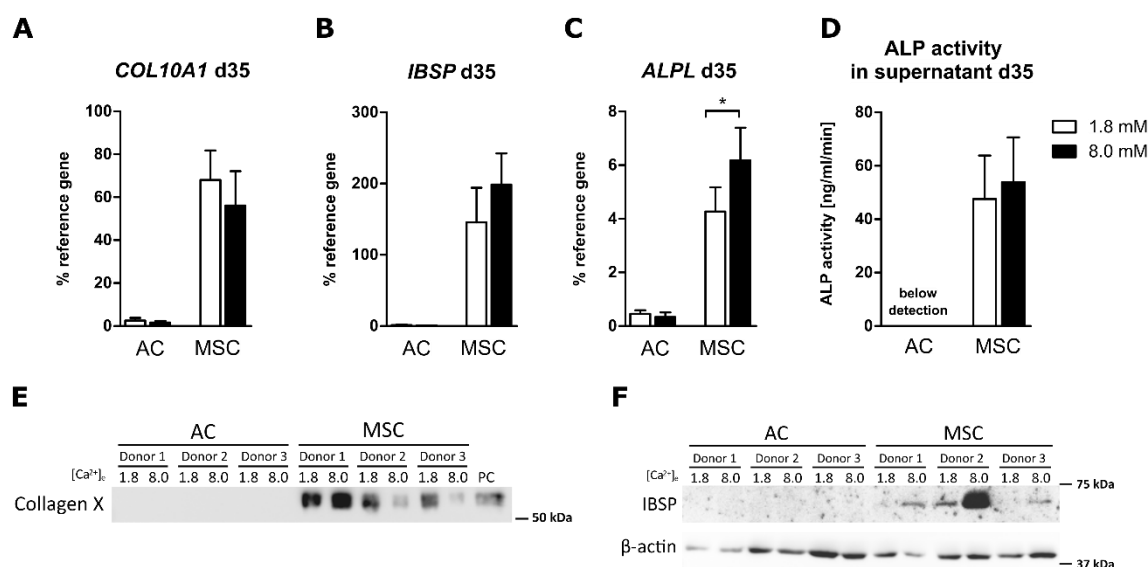


Figure 24 Regulation of endochondral differentiation markers by extracellular calcium stimulation in AC and MSC-derived chondrocytes. AC- or MSC-laden TE-constructs were cultured in chondrocyte differentiation medium for 35 days at 1.8 or 8.0 mM $[Ca^{2+}]_e$. **A-C)** *COL10A1*, *IBSP* and *ALPL* mRNA levels were determined by qPCR. Gene expression levels were normalized to the mean expression of reference genes *18S*, *GAPDH* and *RPL13*. All data are expressed as mean \pm SEM of n=6 AC and n=6 MSC donors. * p<0.05, paired Student's t-test, 1.8 mM vs. 8.0 mM. **D)** Alkaline phosphatase activity was determined in culture supernatants from AC and MSC-derived chondrocytes on day 35. Data are depicted as mean \pm SEM of n=6 AC and n=7 MSC donors. **E)** Immunoblotting against type X collagen was performed on pepsin digest from AC and MSC-derived chondrocytes on day 35. Results are shown for samples from n=3 AC and n=3 MSC donors. Pepsin digest from day 42 MSC micromass pellets served as positive control. **F)** Immunoblotting against IBSP was performed on whole cell protein lysate from AC and MSC-derived chondrocytes on day 35. β -actin served as loading control. Results are shown for samples from n=3 AC and n=3 MSC donors.

4.2.9 The effect of long-term extracellular calcium stimulation of AC and MSC-derived chondrocytes on the regulation of anabolic signaling mechanisms

Next, it was of interest to find out whether the calcium-dependent inverse regulation of GAG formation by AC and MSC-derived chondrocytes was accompanied by an inverse regulation of prominent pro-chondrogenic signaling pathways. Therefore, the regulation of pro-chondrogenic SOX9 protein as well as TGF β - and BMP pathway activity by high calcium treatment were investigated. For this purpose, AC or MSC-based TE-constructs were cultured at control or 8.0 mM [Ca²⁺]_e for 35 days and SOX9 protein, SMAD2/3 and SMAD1/5/9 phosphorylation were analyzed using Western blot. Moreover, expression of genes from the BMP signaling pathway were determined by qPCR.

4.2.9.1 Effect of long-term extracellular calcium stimulation of AC and MSC-derived chondrocytes on SOX9 protein and SMAD2/3 pathway activity

To investigate whether extracellular calcium stimulation inversely regulated pro-chondrogenic SOX9 protein or TGF β -SMAD2/3 pathway activity in AC and MSC-derived chondrocytes, SOX9 protein and SMAD2/3 phosphorylation were analyzed on day 35. In AC, 8.0 mM [Ca²⁺]_e did not consistently alter SOX9 levels among samples from three donors (Figure 25). While samples from 2 donors showed no change, SOX9 levels were slightly enhanced in samples from 1 donor. In MSC-derived chondrocytes, high calcium treatment inconsistently regulated SOX9 levels in samples from 5 donors. While high calcium slightly reduced SOX9 levels in samples from 3 donors, SOX9 levels were slightly increased in samples from 1 other donor. Samples from 1 MSC donor showed no regulation of SOX9 protein (Figure 25). This indicated that SOX9 protein was not consistently regulated at high extracellular calcium concentration in AC and MSC-derived chondrocytes.

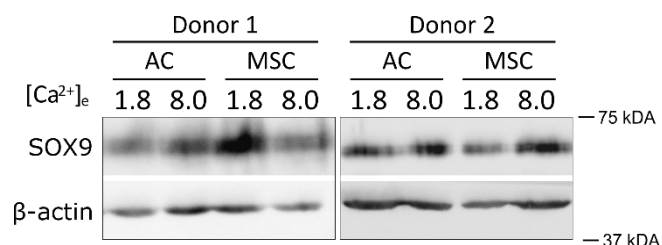


Figure 25 Effect of long-term extracellular calcium stimulation on SOX9 protein levels in AC and MSC-derived chondrocytes. AC- or MSC-laden TE-constructs were cultured in chondrocyte differentiation medium for 35 days at 1.8 or 8.0 mM [Ca²⁺]_e. Immunoblotting against SOX9 was performed on whole cell protein lysate from AC and MSC-derived chondrocytes on day 35. β -actin served as loading control. Representative blots are shown for n=3 AC and n=5 MSC donors.

Investigation of TGF β pathway activity revealed that extracellular calcium stimulation of AC and MSC-derived chondrocytes for 35 days did not alter SMAD2/3 phosphorylation in either cell type or condition (Figure 26).

Thus, the inverse regulation of GAG deposition after long-term extracellular calcium stimulation in AC and MSC-based TE constructs was not associated with changes in SOX9 protein levels or TGF β -SMAD2/3 pathway activity. Regulation of SOX9 levels and TGF β -SMAD2/3 pathway activity is therefore no likely reason for the calcium-mediated inverse regulation of cartilage matrix formation.

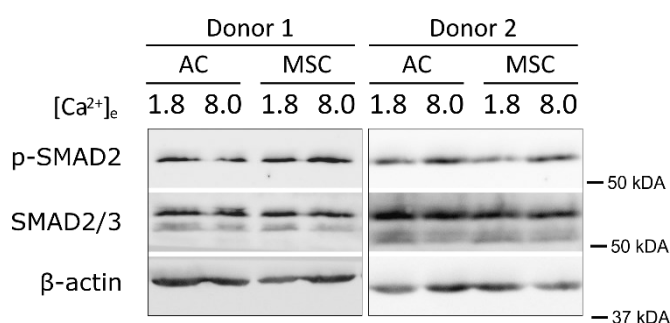


Figure 26 Effect of long-term extracellular calcium stimulation on SMAD2/3 levels in AC and MSC-derived chondrocytes. AC- or MSC-laden TE-constructs were cultured in chondrocyte differentiation medium for 35 days at 1.8 or 8.0 mM [Ca²⁺]_e. Immunoblotting against total SMAD2/3 and phosphorylated SMAD2 was performed on whole cell protein lysate from AC and MSC-derived chondrocytes on day 35. β -actin served as loading control. Representative blots are shown for n=3 AC and n=5 MSC donors.

4.2.9.2 Effect of long-term extracellular calcium stimulation of AC and MSC-derived chondrocytes on BMP pathway activity

Whether the inverse regulation of GAG formation in AC and MSC-based constructs correlated with an inverse regulation of the BMP pathway was addressed next. For this purpose, AC and MSC-derived chondrocytes were stimulated at 8.0 mM [Ca²⁺]_e for 35 days and the expression of BMP ligands *BMP2*, *-4*, *-6* and *-7* was determined using qPCR. In AC constructs on day 35, calcium treatment significantly enhanced the expression of *BMP2* and *BMP6* and reduced the expression of *BMP4*. In MSC-derived chondrocytes, calcium stimulation enhanced the expression of *BMP6* and *BMP7* (Figure 27). Although the regulation of BMP ligands *BMP2*, *-4* and *-7* reached significance only in specific cell types, by trend a similar regulation pattern of BMP ligand expression was observed in AC and MSC-derived chondrocytes.

Thus, calcium stimulation did not differentially regulate BMP ligand expression in AC and MSC-derived chondrocytes.

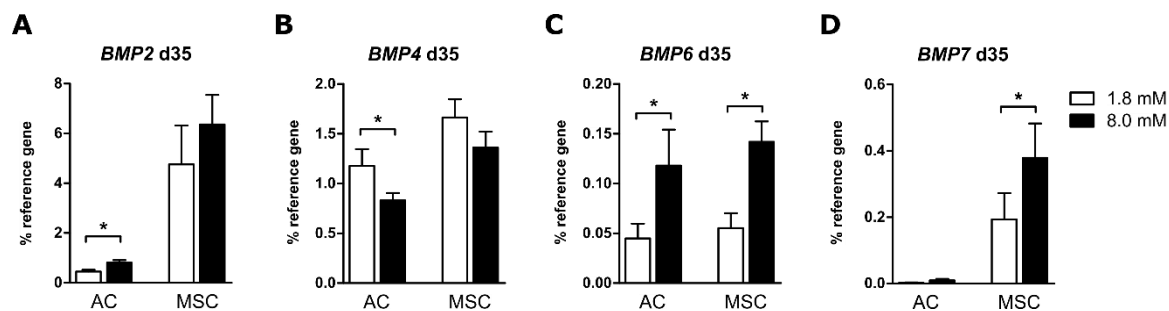


Figure 27 Effect of long-term extracellular calcium stimulation on BMP ligand expression by AC and MSC-derived chondrocytes. AC- or MSC-laden TE-constructs were cultured in chondrocyte differentiation medium for 35 days at 1.8 or 8.0 mM $[Ca^{2+}]_e$. *BMP2*, *BMP4*, *BMP6* and *BMP7* mRNA levels were determined by qPCR. Gene expression levels were normalized to the mean expression of reference genes *18S*, *GAPDH* and *RPL13*. All data are expressed as mean \pm SEM of n=8 AC and MSC donors. * $p < 0.05$, paired Student's t-test, 1.8 mM vs. 8.0 mM.

To further elucidate the effect of calcium stimulation on BMP signaling, the expression of the endogenous BMP inhibitor *GREM1* as well as BMP response gene *ID1* was investigated. In both cell types, 8.0 mM calcium treatment did not change the expression of *GREM1*. However, in MSC-derived chondrocytes, *GREM1* was significantly lower expressed compared to AC (Figure 28 A), an effect that was previously reported by our group (Dexheimer et al. 2016). No regulation of *ID1* expression was observed by calcium treatment in both cell types (Figure 28 B).

Thus, in AC and MSC-derived chondrocytes, long-term extracellular calcium treatment did not differentially regulate the expression of *GREM1* and *ID1*. However, higher expression of BMP inhibitor *GREM1* was observed in AC compared to MSC-derived chondrocytes.

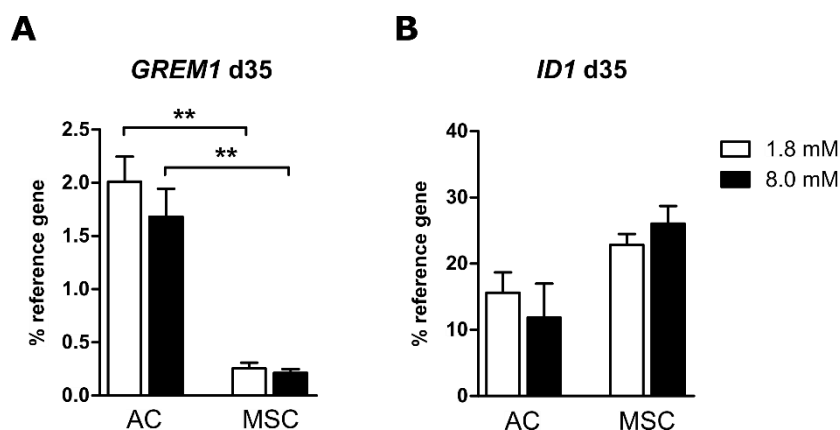


Figure 28 Effect of long-term extracellular calcium stimulation on *GREM1* and *ID1* gene expression in AC and MSC-derived chondrocytes. AC- or MSC-laden TE-constructs were cultured in chondrocyte differentiation medium for 35 days at 1.8 or 8.0 mM $[Ca^{2+}]_e$. *GREM1* and *ID1* mRNA levels were determined by qPCR. Gene expression levels were normalized to the mean expression of reference genes *18S*, *GAPDH* and *RPL13*. All data are expressed as mean \pm SEM of n=6 AC and n=7 MSC donors. * $p < 0.05$, unpaired Student's t-test, AC vs. MSC.

To further investigate the effects of long-term extracellular calcium stimulation on BMP pathway activity in AC and MSC-derived chondrocytes, phosphorylation of SMAD1/5/9 was assessed using Western blotting. While extracellular calcium stimulation enhanced pSMAD1/5/9 levels in samples from one AC- and one MSC donor, no change was observed in samples from 2 AC- and 4 MSC donors (Figure 29 A). This indicated that extracellular calcium stimulation did not affect the phosphorylation of SMAD1/5/9 in both cell types. However, in line with higher expression of BMP inhibitor *GREM1* in AC, SMAD1/5/9 phosphorylation was higher in MSC-derived chondrocytes compared to AC, irrespective of calcium treatment. This effect was observed among samples from 4 MSC donors. SMAD1/5/9 phosphorylation from one MSC donor showed comparable levels to AC.

Thus, the inverse regulation of cartilage matrix formation in AC- versus MSC-based TE constructs after extracellular calcium treatment was not mirrored by a differential regulation of BMP pathway activity.

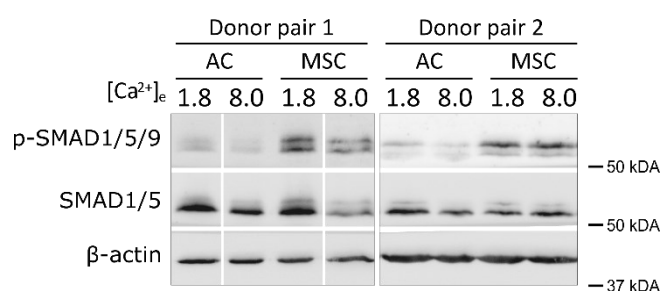


Figure 29 Analysis of BMP signaling activity in response to long-term extracellular calcium stimulation in AC and MSC-derived chondrocytes. AC- or MSC-laden TE-constructs were cultured in chondrocyte differentiation medium for 35 days at 1.8 or 8.0 mM [Ca²⁺]_e. Immunoblotting against total SMAD1/5 and phosphorylated SMAD1/5/9 was performed on whole cell protein lysate from AC and MSC-derived chondrocytes on day 35. Immunoblotting against β-actin served as loading control. Representative blots are shown for n=3 AC and n=5 MSC donors. Samples from a donor pair were run on the same gel.

4.2.10 The regulation of catabolic signaling mechanisms in AC and MSC-derived chondrocytes after long-term extracellular calcium stimulation

4.2.10.1 Effect of long-term extracellular calcium stimulation of AC and MSC-derived chondrocytes on *S100A4* and *MMP13* expression

To further elucidate the molecular mechanisms underlying the calcium-related inverse regulation of GAG deposition and GAG synthesis in AC- and MSC-based TE constructs, a possible catabolic signaling mechanism was investigated. S100-proteins are known to be crucially involved in the transduction of calcium signaling responses in many cell types, including chondrocytes (Donato et al. 2013). Especially S100A4 was proposed as a calcium-dependent regulator of matrix degrading

MMP13 gene and protein levels as well as catabolic NF- κ B signaling in human articular chondrocytes in monolayer (Yammani et al. 2006). It was therefore asked next, whether the high calcium-mediated compromised cartilage matrix formation by AC may occur parallel to S100A4 regulation and subsequent induction of catabolic marker expression. To test a differential regulation of S100A4 in both cell types, AC- and MSC-based TE-constructs were exposed to long-term extracellular calcium stimulation for 35 days and the induction of S100A4 expression was investigated using qPCR. In addition, the expression of the catabolic marker MMP13 was determined by qPCR.

On day 35, long-term extracellular calcium stimulation significantly increased the expression of S100A4 by AC (2.33-fold, $p=0.03$, $n=6$), while no regulation was observed in MSC-derived chondrocytes (Figure 30 A). Likewise, high $[Ca^{2+}]_e$ increased MMP13 expression by AC (7.37-fold, $p=0.05$, $n=6$) but not by MSC-derived chondrocytes (Figure 30 B).

Thus, calcium stimulation specifically enhanced the expression of S100A4 and MMP13 in AC. Induction of S100A4 and MMP13 expression, therefore, occurred parallel to a reduced GAG synthesis rate and GAG deposition in AC constructs.

With the intention to establish a causal relationship between S100A4 and cartilage matrix formation, S100A4 was inhibited using the S100A4 transcriptional inhibitor Niclosamide. Unfortunately, treatment of AC- and MSC constructs with established concentrations of Niclosamide ranging from 100 nM to 1 μ M for 35 days in the presence or absence of high $[Ca^{2+}]_e$ completely halted AC and MSC (re)differentiation (data not shown). Thus, no conclusion about a possible causal relationship between high calcium-induced S100A4 expression and compromised cartilage ECM formation was possible. Nevertheless, a significantly increased expression of S100A4 in high calcium-stimulated AC but not in MSC-derived chondrocytes encourages future

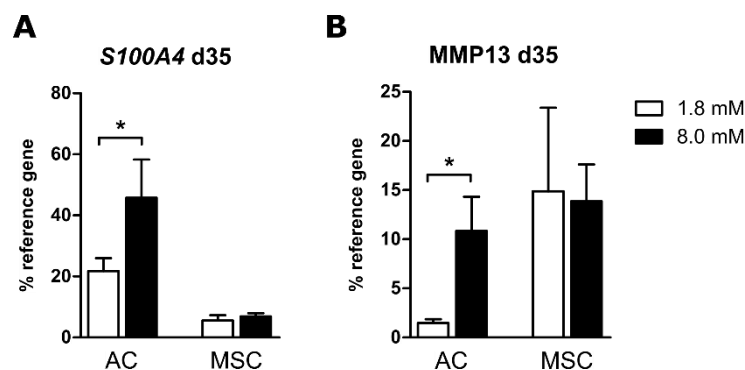


Figure 30 Effect of long-term extracellular calcium stimulation on S100A4 and MMP13 mRNA expression in AC and MSC-derived chondrocytes. AC- or MSC-laden TE-constructs were cultured in chondrocyte differentiation medium for 35 days at 1.8 or 8.0 mM $[Ca^{2+}]_e$. S100A4 and MMP13 mRNA levels were determined by qPCR. Gene expression levels were normalized to the mean expression of reference genes 18S, GAPDH and RPL13. All data are expressed as mean \pm SEM in samples from $n=6$ AC- and $n=7$ MSC donors. * $p<0.05$, paired Student's t-test, 1.8 mM vs. 8.0 mM.

experiments on forced *S100A4* expression in AC to investigate its role for cartilage matrix production.

Since *S100A4* was reported to induce NF- κ B signaling activity in human chondrocytes (Yammani et al. 2006), the regulation of NF- κ B pathway activity was investigated as a putative downstream target of calcium-induced *S100A4* expression. Specifically, it was addressed whether high calcium treatment also led to a specific induction of NF- κ B pathway activity in AC. For this purpose, AC and MSC-derived chondrocytes were subjected to 8.0 mM $[\text{Ca}^{2+}]_e$ for 35 days and NF- κ B pathway activity was assessed by detection of an active p65 sub-unit using Western blot. Unfortunately, AC- and MSC constructs of this experiment showed insufficient maturation according to safranin O staining. Therefore, no conclusion was possible about the induction of NF- κ B by high calcium treatment in AC and MSC-derived chondrocytes.

Overall, the specific induction of *S100A4* and *MMP13* expression by exogenous calcium treatment occurred exclusively in the AC-group and indicated the activation of some catabolic molecules whose closer connection to impaired GAG formation should further be established.

4.2.10.1 The effect of long-term extracellular calcium stimulation on the regulation of *COX2* expression and PGE_2 secretion in AC and MSC-derived chondrocytes

In human OA chondrocytes, *COX2* and PGE_2 inhibit GAG synthesis and induce cartilage matrix degradation (Attur et al. 2008). In addition, *COX2* and PGE_2 were induced by high extracellular calcium concentrations in murine osteoblasts (Choudhary et al. 2004; Choudhary et al. 2003). It was therefore asked next, whether the calcium-mediated reduction of cartilage matrix formation by AC was associated with a regulation of *COX2* expression and PGE_2 secretion. For this purpose, the effect of long-term 8.0 mM extracellular calcium stimulation on *COX2* expression was analyzed in AC and MSC-derived chondrocytes using qPCR. After 35 days of calcium stimulation, no change in *COX2* expression was observed in both cell types. Mean *COX2* expression levels were higher in MSC-derived chondrocytes compared to AC, irrespective of calcium treatment, but no statistical significance was reached (Figure 31 A). When PGE_2 release into the culture supernatant over 48 hours before termination of culture was measured using a PGE_2 ELISA, PGE_2 concentration in the conditioned culture supernatant was significantly enhanced in MSC-derived chondrocytes from 4811 ± 3115 pg/ml in the control to 13611 ± 5120 pg/ml ($p=0.012$, $n=10$) at 8.0 mM $[\text{Ca}^{2+}]_e$. Although calcium treatment almost doubled the mean PGE_2 levels in AC from 12 ± 2 pg/ml in control samples to 20 ± 7 pg/ml ($p=0.28$, $n=6$) in the calcium group, no significant difference in PGE_2 levels was reached (Figure 31 B). In line with previous data from our group, mean PGE_2 levels were clearly higher in MSC-derived chondrocytes compared to AC (Lückgen et al. 2022). However,

due to a large standard deviation, this significance was lost after correction for multiple comparisons.

Thus, while calcium stimulation did not change the expression of *COX2* in both cell types, PGE₂ levels were significantly enhanced only in MSC-derived chondrocytes. Catabolism-associated *COX2* expression and PGE₂ secretion, therefore, did not correlate with the calcium-related reduction of GAG synthesis and GAG deposition in AC constructs.

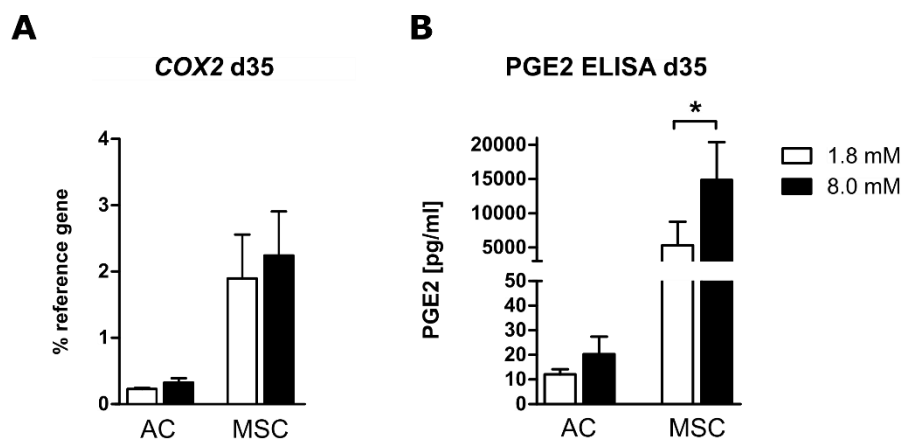


Figure 31 Effect of long-term extracellular calcium stimulation on *COX2* and PGE₂ in AC and MSC-derived chondrocytes. AC- or MSC-laden TE-constructs were cultured in chondrocyte differentiation medium for 35 days at 1.8 or 8.0 mM [Ca²⁺]_e. **(A)** *COX2* mRNA expression was determined by qPCR. Gene expression levels were normalized to the mean expression of reference genes *18S*, *GAPDH* and *RPL13* (n=6 AC- and n=5 MSC donors). **(B)** Culture supernatant was conditioned for 48 hours before the end of culture and PGE₂ levels were measured via PGE₂ ELISA (n=6 AC- and n=10 MSC donors). All data are expressed as mean ± SEM. * p<0.05, *** p<0.001, paired Student's t-test, 1.8 mM vs. 8.0 mM.

4.2.11 The effect of long-term extracellular calcium stimulation of AC and MSC-derived chondrocytes on PTHrP signaling

During *in vitro* MSC chondrogenesis, PTHrP can have pro-chondrogenic (Fischer et al. 2014) or anti-chondrogenic (Fischer et al. 2014; Mueller et al. 2013; Weiss et al. 2010) effects. In addition, in bovine articular chondrocytes, the regulation of PTHrP was calcium-sensitive (Burton et al. 2005), suggesting that the induction of PTHrP may change under high calcium conditions. It was therefore investigated, whether the calcium-dependent inverse regulation of cartilage matrix formation in AC- and MSC-based TE constructs, was associated with a differential regulation of PTHrP mRNA expression and protein levels.

4.2.11.1 The regulation of *PTHLH* expression in AC and MSC-derived chondrocytes after long-term extracellular calcium stimulation

To elucidate the regulation of the calcium-sensitive PTHrP pathway during long-term extracellular calcium stimulation, AC and MSC-derived chondrocytes were cultured at control or 8.0 mM $[Ca^{2+}]_e$ for up to 35 days and *PTHLH* mRNA expression was analyzed. Expression of *PTHLH* was investigated at regular intervals during the course of (re)differentiation on day 7, 21 and 35 using qPCR. In AC, high $[Ca^{2+}]_e$ did not change the expression of *PTHLH* on day 7 (n=3), but *PTHLH* expression was significantly induced on day 21 (6.62-fold, p=0.02, n=6) and on day 35 (9.88-fold, p=0.04, n=6) (Figure 32 A). Remarkably, in MSC-derived chondrocytes, *PTHLH* expression remained low at day 21 and 35 at control and high calcium conditions (Figure 32 B).

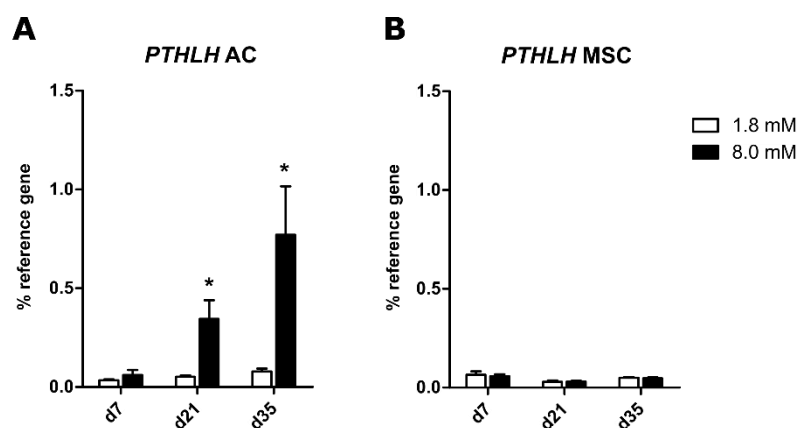


Figure 32 Effect of long-term extracellular calcium stimulation on *PTHrP* mRNA expression in AC and MSC-derived chondrocytes. AC- or MSC-laden TE-constructs were cultured in chondrocyte differentiation medium for 7, 21 or 35 days at 1.8 or 8.0 mM $[Ca^{2+}]_e$. *PTHrP* mRNA levels were determined by qPCR. Gene expression levels were normalized to the mean expression of reference genes *18S*, *GAPDH* and *RPL13*. All data are expressed as mean \pm SEM of n=3 (day 7) and n=6 (day 21 and day 35) AC donors and n=5 (day 7), n=3 (day 21) and n=8 (day 35) MSC donors. * p<0.05, paired Student's t-test, 1.8 mM vs 8.0 mM $[Ca^{2+}]_e$.

Thus, long-term extracellular calcium stimulation enhanced the expression of *PTHLH* in AC whereas no regulation was observed in MSC-derived chondrocytes. Due to a differential regulation of *PTHLH* expression by calcium in AC and MSC-derived chondrocytes, PTHrP represents an interesting molecule involved in the inverse regulation of GAG synthesis and GAG deposition by both cell types.

4.2.11.2 Establishment of PTHrP protein detection using Western blotting

To test whether an AC-specific enhancement of *PTHLH* mRNA expression by high $[Ca^{2+}]_e$ was translated into higher PTHrP protein levels, a detection method was needed to measure PTHrP protein. For this purpose, a PTHrP antibody should be established to detect PTHrP protein using Western blotting. A flow chart describing the necessary steps to establish a PTHrP-specific

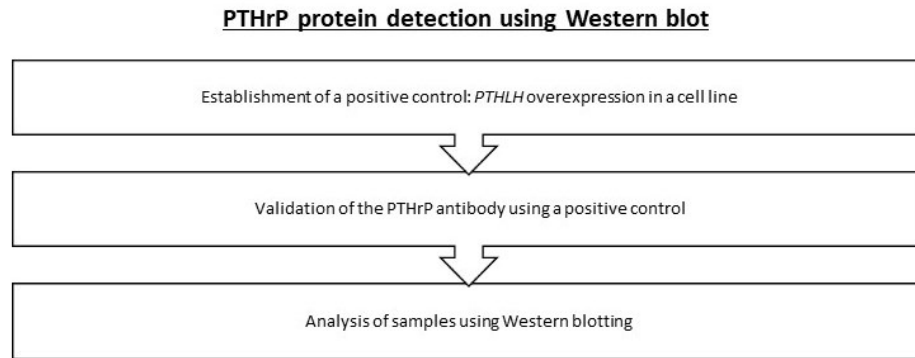


Figure 33 Flow chart of PTHrP protein detection using Western blotting. Overview of the main steps during the establishment of Western blotting as an analysis method to detect PTHrP protein levels.

antibody is depicted in Figure 33. Initially, positive control samples with high PTHrP levels had to be generated by overexpressing *PTHLH* in a human cell line. This positive control was then used to validate the specificity of the antibody to detect human PTHrP protein via Western blotting. Subsequently, high calcium-stimulated samples were assessed for the regulation of PTHrP levels in AC and MSC-derived chondrocytes.

To generate a positive control for the validation of the specificity of the PTHrP antibody, three human cell lines (HEK293T, SaOS-2, SW1353) were transfected with a *PTHLH* overexpression

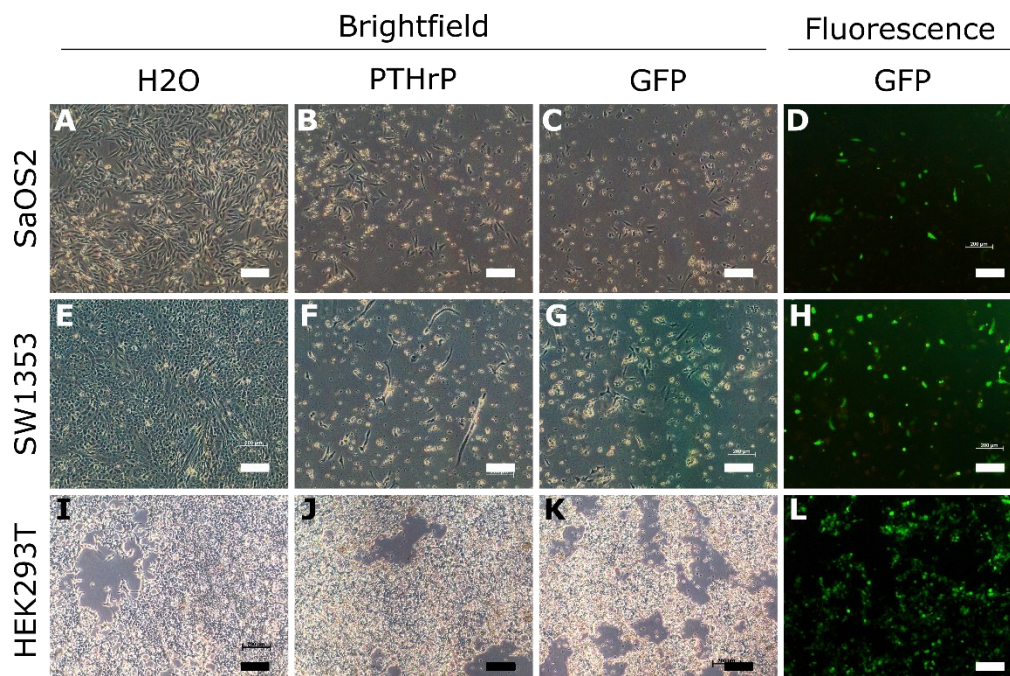


Figure 34 Transfection of cell lines with PTHrP overexpression plasmid. 3×10^5 SaOS-2 (A-D), SW1353 (E-H) or HEK293T (I-L) cells were seeded into 6 well plates and attached over night. Cells were transfected with PTHrP overexpression plasmid, GFP control plasmid or without DNA using X-tremeGENE™ 9 transfection reagent for 24 hours. 72 hours after transfection, cell loss and transfection efficacy were assessed via bright field microscopy and fluorescence microscopy, respectively. Representative images of $n=4$ wells from two separate transfection rounds are shown. Scale bar indicates 200 μm .

plasmid to constitutively overexpress human *PTH1LH*. Cells transfected with a GFP plasmid served as negative control for PTHrP protein detection and as a measurement of transfection efficiency. Among the three tested cell lines, significant cell loss was observed in SaOS-2 and SW1353 cells 72 hours after transfection with PTHrP and GFP plasmid compared to cells transfected without plasmid (Figure 34A-C and E-G). No cell-loss was observed after transfection in HEK293T cells (Figure 34 I-K). Fluorescence imaging for the presence of GFP proved a high transfection efficiency in HEK293T cells (Figure 34L). Thus, HEK293T cells were selected to generate lysates with high PTHrP levels (HEK^{PTHrP}) to be used as a positive control for PTHrP antibody validation using Western blotting. Protein lysate from GFP-transfected HEK cells (HEK^{GFP}) was used as negative control. For the validation of the PTHrP antibody via Western blotting, protein lysates from HEK^{PTHrP} or HEK^{GFP} cells were collected 72 hours after transfection. In HEK^{PTHrP} overexpression lysate, a positive band was detected at the expected band size of 20 kDa (Figure 35 A). No signal was detected in lysates from HEK^{GFP} cells, confirming the specificity of the antibody. Dilution of HEK^{PTHrP} lysate at 1:2, 1:4 and 1:8 in water confirmed a PTHrP-positive band at a dilution factor of 1:2 and 1:4, while 1:8 dilution showed no visible signal for PTHrP. Of note, sample dilution of up to 1:8 showed not visible dilution of band intensities for the β -actin loading control. Since β -actin is a highly abundant protein, it was obvious from other experiments, that dilution factors of 1:16 or higher are necessary before changes in β -actin levels become visible in the studies blots (see page 96). Unfortunately, no PTHrP signal was detected using protein lysates from monolayer cultured HCT116 cells and in HepG2 cells for which high endogenous PTHrP levels had been reported (Li et al. 1996) (Figure 35 A). Likewise, no band was observed in protein lysates from AC constructs cultured at control or high $[Ca^{2+}]_e$ for 35 days, indicating that endogenous PTHrP levels were too low for detection using Western blotting (Figure 35 A). This finding was confirmed in samples from two additional AC- and MSC-donors (Figure 35 B). Thus, Western blot was not sensitive enough to detect endogenous levels of PTHrP in AC and MSC-derived chondrocytes.

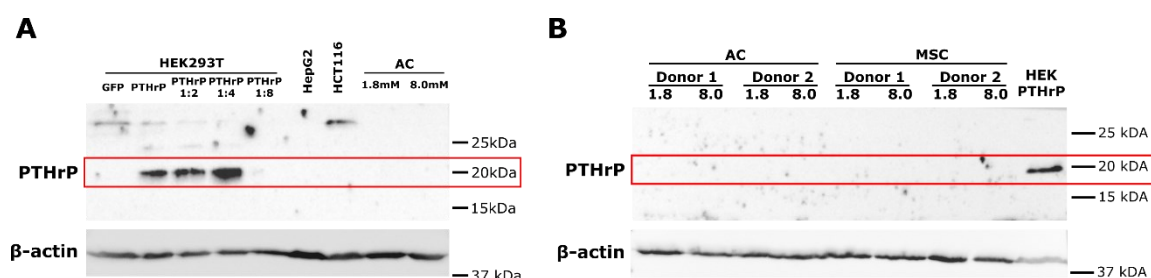


Figure 35 Detection of PTHrP protein levels using western blot. (A) HEK293T cells were transfected with PTHrP overexpression or GFP control plasmid for 24 hours. Cells were harvested 72 hours after transfection and cell lysate was immunoblotted against PTHrP. Serial dilutions of HEK^{PTHrP} lysate was prepared in water in order to determine detection sensitivity of the antibody. Endogenous PTHrP levels were evaluated from monolayer cultured HepG2 and HCT116 cell lines as well as AC TE-constructs cultured in chondrocyte differentiation medium for 35 days at 1.8 or 8.0 mM $[Ca^{2+}]_e$. **(B)** Immunoblotting against PTHrP in TE constructs from two separate AC and MSC donors on day 35. Immunoblotting against β -actin served as loading control.

4.2.11.3 Establishment of PTHrP protein detection via immunoradiometric assay

For this reason, a more sensitive detection method was needed. In clinical diagnostics, PTHrP can be detected in the blood serum of patients at levels as low as 0.5 pmol/L using immunoradiometric assay (IRMA). A flow chart describing the necessary steps for the establishment of PTHrP detection via IRMA is depicted in Figure 36. Since PTHrP IRMA is designed for analysis of human blood plasma, it was not clear whether ingredients of the lysis buffer used for protein isolation would interfere with the assay. Indeed, literature showed that cell culture medium or salt-based buffers like PBS create non-specific background signals in PTHrP IRMAs (Onda et al. 2010) and the authors suggested human blood plasma or 0.01 M EDTA as suitable solvents for samples to be analyzed by PTHrP IRMA. Therefore, first, a sample preparation protocol was developed to clear the lysate from unwanted residues of lysis buffer. The sample preparation protocol was then validated on lysates collected from HEK^{PTHrP} cells, to detect overexpressed PTHrP using Western blotting. Subsequently, it was confirmed whether the established sample preparation protocol was compatible with IRMA to detect overexpressed PTHrP. After establishment of a suitable sample preparation protocol, PTHrP levels were assessed in samples from calcium-treated AC- and MSC-based TE constructs using IRMA.

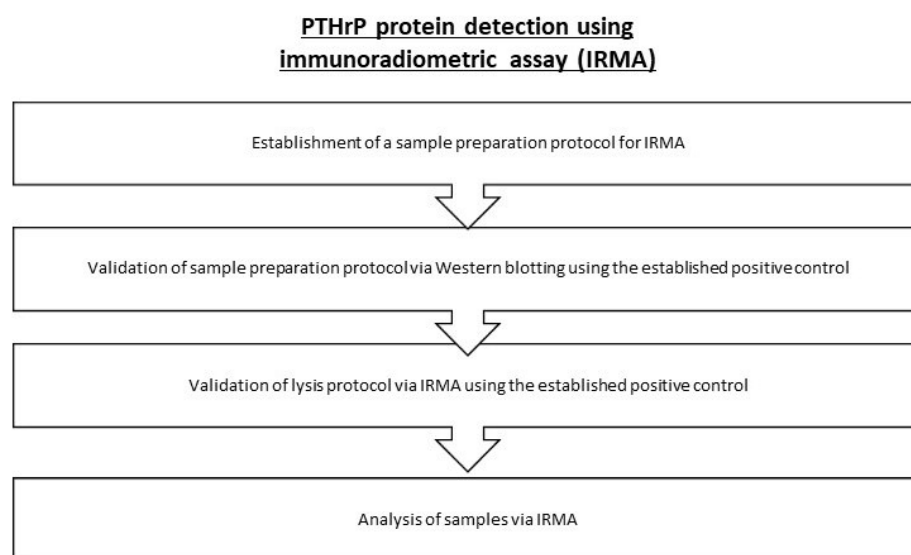


Figure 36 Flow chart of PTHrP protein detection using immunoradiometric assay. Overview of the main steps during the establishment of immunoradiometric assay (IRMA) as an analysis method to detect PTHrP protein levels.

To remove irrigating substances after lysis, routine protein lysis in phosphosafe[®] lysis buffer was followed by protein precipitation using ice-cold acetone. The resulting protein precipitate was subsequently resuspended in a desired solvent. To validate that protein precipitation and subsequent resuspension did not reduce PTHrP protein yield, the newly established acetone

precipitation protocol was compared to routine lysis in phosphosafe® buffer without precipitation using Western blotting. For this purpose, HEK^{PTHrP} cells were lysed and processed using the established acetone preparation protocol and the precipitated proteins were resuspended in an equal volume of either phosphosafe® buffer as positive control or 0.01 M EDTA as suggested by Onda et al. At this step, resuspension of protein precipitate in 0.01 M EDTA was chosen instead of resuspension in human blood plasma since excess amount of blood plasma proteins, such as albumin, would strongly interfere with Western blot detection. PTHrP protein detection by Western blot revealed no difference in band intensities between all lysis protocols (Figure 37). This indicated that protein precipitation using acetone resulted in similar PTHrP protein levels compared to lysis without precipitation.

Thus, protein lysis using phosphosafe® lysis buffer followed by protein precipitation using acetone and subsequent resuspension in 0.01M EDTA or human blood plasma was established as adjusted sample preparation protocol.

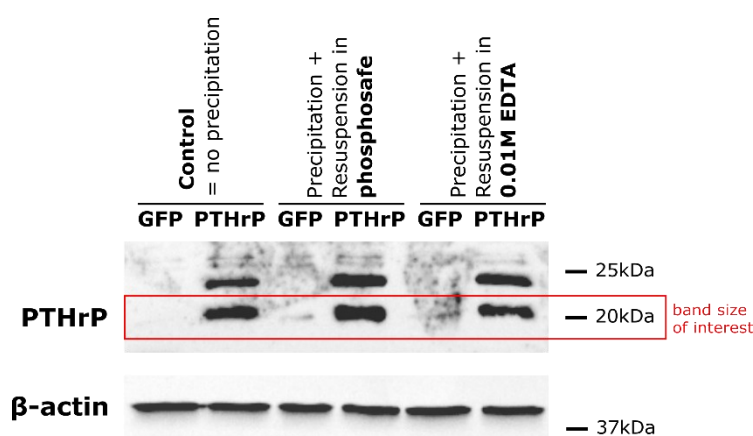


Figure 37 Validation of protein lysis protocols for PTHrP detection. HEK293T cells were transfected with PTHrP overexpression or GFP control plasmid for 24 hours. Cells were harvested 72 hours after transfection and cell lysate was immunoblotted against PTHrP. Cells were lysed via detergent-based lysis using phosphosafe® lysis buffer (lane 1+2), phosphosafe® lysis buffer followed by acetone protein precipitation and subsequent resuspension in phosphosafe® lysis buffer (lane 3+4) or phosphosafe® lysis buffer followed by acetone protein precipitation and subsequent resuspension in 0.01 M EDTA (lane 5+6). Immunostaining against β-actin served as loading control. Representative blot is shown for n=2 independent transfections.

To validate that the adjusted sample preparation protocol was also compatible with PTHrP detection using IRMA, protein lysates were generated from HEK^{PTHrP} cells. Since PTHrP IRMA is a highly sensitive detection method compared to Western blot, it was important not to exceed the working range of the IRMA assay by loading of too high amounts of overexpressed PTHrP in the assay. Therefore, to identify reasonable concentrations for IRMA establishment, the detection limit of PTHrP from HEK^{PTHrP} lysate using Western blotting was assessed in a dilution series. Using the modified sample preparation protocol, dilution experiments from Figure 35 A were extended

to dilutions of 1:4 to 1:256. After acetone precipitation, protein was resuspended in 0.01 M EDTA and water was used for dilution series. A dilution factor of 1:8 was determined as detection limit in the Western blot during initial experiments without protein precipitation (Figure 35 A). Using the modified sample preparation protocol, a PTHrP-positive band was detected at 1:16 dilution (Figure 38 A). Long-term exposure time of the membrane for up to 30 minutes during ECL detection even detected a faint band at 1:32 dilution, indicating 1:32 dilution as the lowest concentration for detection in Western blot (Figure 38 B).

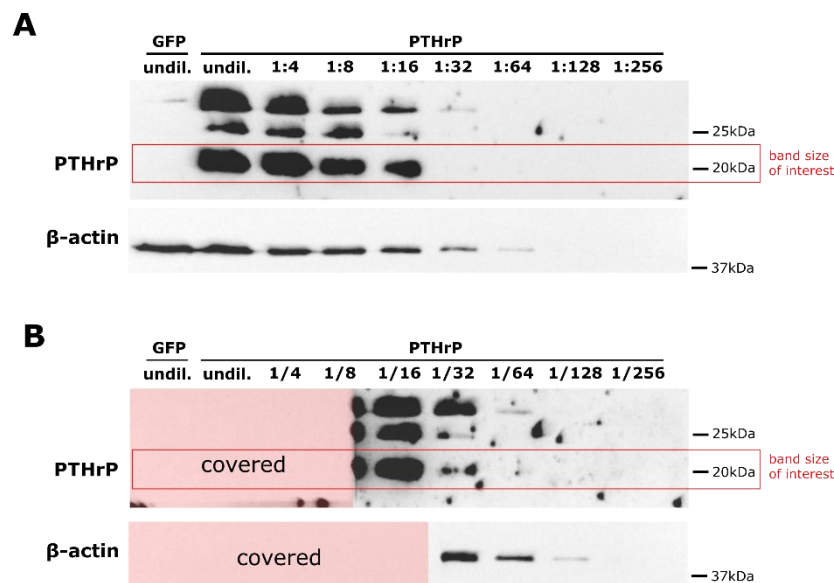


Figure 38 Establishment of PTHrP detection limit using western blot. HEK293T cells were transfected with PTHrP overexpression or GFP control plasmid for 24 hours. Cells were harvested 72 hours after transfection and cell lysate was immunoblotted against PTHrP. **A)** Cells were lysed via detergent-based lysis using phosphosafe[®] lysis buffer followed by protein precipitation using acetone and resuspension in 0.01 M EDTA. Serial dilutions of HEK^{PTHrP} lysate were prepared in water. Representative blot is shown for n=4 independent replicates **B)** Image of the same blot as in A), captured at long-term exposure time of 30 minutes to enhanced signal detection. Immunoblotting against β -actin served as loading control.

IRMA establishment using HEK^{PTHrP} lysate was therefore carried out at 1:32 dilution as the detection limit in western blot and 1:256 and 1:2048 dilution to functionally validate the readout of the assay in a dilution series. In order to most closely match the conditions of the PTHrP IRMA (i.e., analysis of human blood plasma samples), HEK^{PTHrP} and HEK^{GFP} cells were prepared using the modified sample preparation protocol and the acetone-precipitated protein pellets were resuspended in human blood plasma instead of 0.01 M EDTA. For the same reason, samples were diluted in human blood plasma instead of water. PTHrP IRMA was carried out by laboratory Dr. Limbach in Heidelberg. The results are summarized in Table 25. At a 1:32 dilution of HEK^{PTHrP} lysate, PTHrP levels were determined at 12.0 pmol/L. PTHrP levels declined to 10 or 4.2 pmol/L at higher

dilution of 1:256 or 1:2048, respectively. No signal was detected in HEK^{GFP} lysate at all dilutions, confirming the specificity of the detected signal.

Thus, protein lysis using phosphosafe® lysis buffer followed by protein precipitation using acetone and subsequent resuspension in human blood plasma was confirmed for the specific detection of PTHrP protein using IRMA.

Table 25 PTHrP IRMA analysis of lysates from HEK cells.

Sample	Dilution	PTHrP conc. [pmol/L]
HEK ^{PTHrP}	1:32	12.0
HEK ^{PTHrP}	1:256	10.0
HEK ^{PTHrP}	1:2048	4.2
HEK ^{GFP}	1:32	<0.50
HEK ^{GFP}	1:256	<0.50
HEK ^{GFP}	1:2048	<0.50

4.2.11.4 Effect of long-term extracellular calcium stimulation on PTHrP protein levels in AC and MSC-derived chondrocytes

After establishment of a suitable sample preparation protocol to detect genetically overexpressed PTHrP using IRMA, natural PTHrP protein levels were determined in AC- and MSC-based TE-constructs cultured at control or 8.0 mM [Ca²⁺]_e conditions for 35 days. In AC and MSC-derived chondrocytes cultured at control conditions, PTHrP levels were below detection limit, indicating low PTHrP in unstimulated cells (Table 26). After high extracellular calcium treatment, an induction of PTHrP was measured in lysates from 2 out of 4 AC donors. In samples from two other AC donors, PTHrP levels remained below detection limit and therefore no assumption about a general induction by calcium treatment can be made. In MSC-derived chondrocytes, PTHrP levels remained below detection limit after high calcium stimulation in samples from all donors. Thus, induction of PTHrP protein by high extracellular calcium stimulation in AC but not MSC-derived chondrocytes partly confirmed the AC-specific upregulation of *PTHrP* mRNA expression at the protein level.

Table 26 PTHrP IRMA analysis of lysates from AC and MSC-derived chondrocytes

Cell type	[Ca ²⁺] _e	Sample	PTHrP conc. [pmol/L]
AC	1.8 mM	Donor 1	<0.50
		Donor 2	<0.50
		Donor 3	<0.50
		Donor 4	<0.50
	8.0 mM	Donor 1	5.4
		Donor 2	2.5
		Donor 3	<0.50
		Donor 4	<0.50
MSC	1.8 mM	Donor 1	<0.50
		Donor 2	<0.50
		Donor 3	<0.50
		Donor 4	<0.50
	8.0 mM	Donor 1	<0.50
		Donor 2	<0.50
		Donor 3	<0.50
		Donor 4	<0.50

4.2.12 Effect of long-term extracellular calcium stimulation on cAMP levels in AC and MSC-derived chondrocytes

It was addressed next, whether, parallel to calcium-induced expression of *PTH1LH* and PTHrP protein in AC, calcium treatment also induced a differential regulation of the prominent PTHrP-induced downstream signaling molecule cAMP. Based on the described induction of *PTH1LH* mRNA and PTHrP protein after high calcium stimulation specifically in AC, cAMP induction was expected in AC but not in MSC-derived chondrocytes. To test this, constructs were cultured at control or elevated extracellular calcium concentration for 35 days and cAMP levels were determined in cell lysates from AC and MSC-derived chondrocytes using an ELISA. To enable cAMP measurement with the ELISA, cAMP needs to be stabilized in the cells. For this purpose, cells were pre-incubated with the phosphodiesterase inhibitor isobutylmethylxanthine (IBMX). On the last day of culture on day 35, constructs were pretreated with IBMX for 30 minutes and then exposed to fresh medium of the respective extracellular calcium concentration in the presence of IBMX to stabilize cAMP. As a positive control to reach high cAMP induction, control constructs were stimulated with 10 ng/ml recombinant human PTHrP₁₋₃₄, added at the time of medium exchange. cAMP levels in the cell lysate were determined 5 minutes and 30 minutes after the medium exchange. After application of PTHrP₁₋₃₄ peptide for 5 minutes or 30 minutes, mean cAMP levels were clearly

higher in AC and MSC-derived chondrocytes compared to controls without PTHrP₁₋₃₄. However, despite very strong induction after 30 minutes, this did not reach significance due to low sample size and large standard deviation (Figure 39). In AC and MSC-derived chondrocytes, high calcium treatment for 5 minutes and 30 minutes did not increase cAMP levels significantly (Figure 39 A+B) in this pilot experiment series and further experiments are now necessary to decide about a regulation of cAMP levels in AC and MSC-derived chondrocytes after high extracellular calcium stimulation.

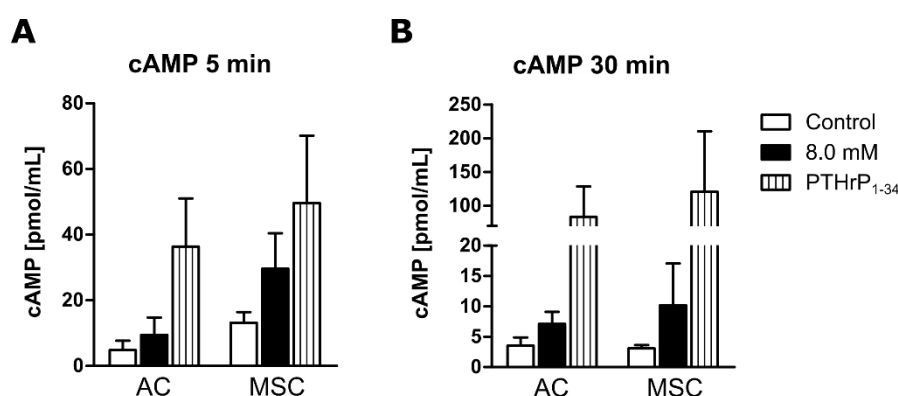


Figure 39 Effect of long-term extracellular calcium stimulation on cAMP levels in AC and MSC-derived chondrocytes. AC- or MSC-laden TE-constructs were cultured in chondrocyte differentiation medium for 35 days at control or 8.0 mM $[Ca^{2+}]_e$. A fresh pulse of control or high $[Ca^{2+}]_e$ medium was applied on day 35 and cAMP levels in the cell lysate were measured 5 minutes and 30 minutes after the medium change via cAMP ELISA. Cells were pre-treated for 30 minutes with IBMX, as well as during stimulation. Stimulation with 10 ng/ml PTHrP₁₋₃₄ at the time point of medium exchange served as positive control for cAMP induction. All data are expressed as mean \pm SEM for samples from n=3 AC and n=2 MSC donors. Paired Student's t-test, control vs. treatment.

4.2.13 Effect of PTHrP stimulation on differentiation marker expression, GAG synthesis and GAG deposition in AC-based TE constructs

With the intention to establish a causal relationship between PTHrP-induction and the calcium-mediated reduction in GAG synthesis and GAG deposition in AC-based TE-constructs, application of a PTHrP receptor antagonist is desired. It is known from preliminary work in our group that PTHrP₇₋₃₄ may allow some inhibition of the PTHrP signaling pathway, depending on the conditions. Unfortunately, here, PTHrP₇₋₃₄ did not inhibit the PTHrP₁₋₃₄-induced pathway activity in our model (data not shown) and, therefore, no inhibitory investigation of possible calcium-induced PTHrP effects on GAG synthesis and GAG deposition was possible in AC constructs.

Thus, in lack of potent PTHrP signaling inhibitors, the contribution of exogenous stimulation by PTHrP₁₋₃₄ on GAG synthesis and GAG deposition in AC constructs was further investigated directly. Specifically, it was asked whether PTHrP₁₋₃₄ supplementation could mimic the high calcium-mediated reduction of differentiation marker expression, GAG synthesis and GAG deposition in

AC constructs. Since calcium significantly induced *PTH LH* expression on day 21 and on day 35, but not on day 7, AC constructs were treated from day 21 to day 35 with 10 ng/ml human recombinant PTHrP₁₋₃₄. Parallel samples were exposed to constant calcium treatment at 8.0 mM [Ca²⁺]_e. As observed before, on day 35, calcium stimulation significantly reduced the expression of all three differentiation markers *COL2A1*, *ACAN* and *SOX9* and significantly decreased the GAG synthesis rate and GAG deposition in AC constructs compared to controls (Figure 40 A-C). This confirmed a reduction of differentiation marker expression and cartilage matrix formation after calcium treatment in AC in independent samples. PTHrP₁₋₃₄ stimulation from day 21 to day 35 significantly reduced the gene expression of *ACAN* and *SOX9* but did not change *COL2A1* expression (Figure 40 A). Mean GAG synthesis levels were lower after PTHrP₁₋₃₄ treatment compared to controls but this effect was not significant (Figure 40 B). GAG/DNA deposition was significantly reduced by PTHrP₁₋₃₄ stimulation (Figure 40 B+C).

Thus, PTHrP stimulation from day 21 to day 35 could partly reproduce the calcium-dependent suppression of cartilage ECM formation in AC-based TE constructs, inviting to speculate that a PTHrP-sensitive mechanism might contribute to this regulation.

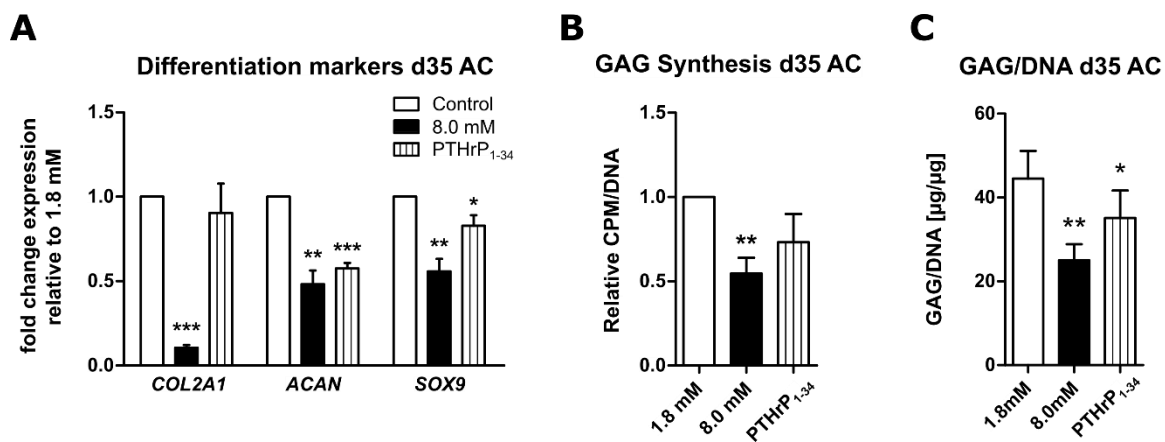


Figure 40 Effect of PTHrP₁₋₃₄ stimulation on cartilage matrix formation by AC. AC-laden TE-constructs were cultured in chondrocyte differentiation medium for 35 days at control or 8.0 mM [Ca²⁺]_e conditions. In the PTHrP-stimulation group, constructs were cultured at control conditions for 21 days and were treated with 10 ng/ml recombinant human PTHrP₁₋₃₄ from day 21 to day 35. **(A)** *COL2*, *ACAN*, and *SOX9* mRNA expression was determined by qPCR. Gene expression levels were normalized to the mean expression of reference genes *18S*, *GAPDH* and *RPL13*. **(B)** GAG synthesis rate measured as ³⁵S-sulfate incorporation during the last 24 hours of culture on day 35. Values were normalized to DNA-content and 1.8 mM [Ca²⁺]_e control samples were set to one. **(C)** GAG content measured by DMMB assay on day 35. Values were normalized to DNA-content. All data are expressed as mean ± SEM in samples from n=5 AC- and n=5 MSC donors. * p<0.05, ** p<0.01, *** p<0.001, vs 1.8 mM [Ca²⁺]_e, paired Student's t-test, control vs treatment.

4.2.14 Comparison of calcium sensing receptor levels in AC and MSC-derived chondrocytes

The cell surface-bound G-protein-coupled receptor, calcium sensing receptor (CaSR), is the primary cell sensor for extracellular calcium. Previous studies of CaSR expression and calcium-sensing in a rat chondrogenic cell line, RCJ3.1C5.18, demonstrated suppressive effects of extracellular calcium sensing via CaSR on GAG synthesis and *COL2A1* expression (Chang et al. 1999b; Chang et al. 2002). Moreover, calcium-induced regulation of *PTH1H* expression via CaSR was reported during chondrocyte differentiation in vitro (Burton et al. 2005) and in vivo (Cheng et al. 2020). This suggested CaSR as a potential candidate for a regulation of *PTH1H* expression in AC and MSC-derived chondrocytes. Therefore, it was investigated whether AC and MSC-derived chondrocytes exhibit different CaSR levels. In addition, it was tested whether CaSR levels were regulated by high calcium stimulation. For this purpose, AC and MSC-derived chondrocytes were cultivated for 35 days under control conditions or at 8.0 mM $[Ca^{2+}]_e$ and the CaSR levels were determined using Western blot. On day 35, high extracellular calcium stimulation slightly induced CaSR levels in samples from 2 out of 4 AC donors, while no such effect was observed in MSC-derived chondrocytes. Moreover, higher CaSR levels were detected in samples from 2 out of 4 AC donors compared to MSC-derived chondrocytes, irrespective of calcium treatment (Figure 41). Thus, due to inconsistent results and insufficient sample numbers, no final conclusion on the regulation of CaSR levels in AC and MSC-derived chondrocytes was possible.

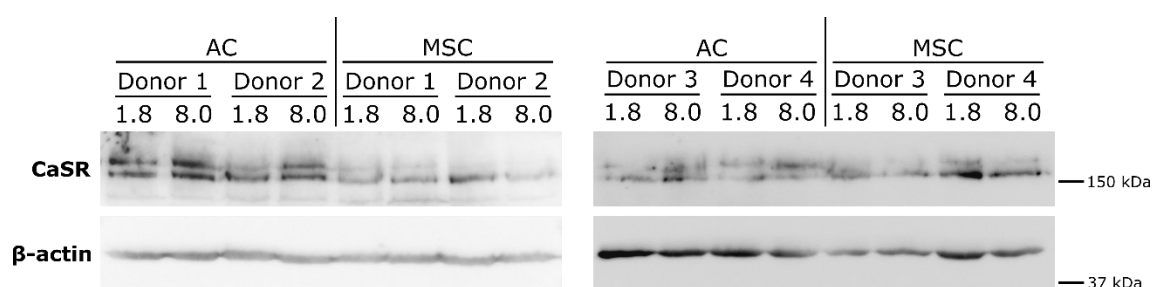


Figure 41 Effect of long-term extracellular calcium stimulation on CaSR levels in AC and MSC-derived chondrocytes. AC- or MSC-laden TE-constructs were cultured in chondrocyte differentiation medium for 35 days at control or high $[Ca^{2+}]_e$ conditions. Immunostaining against CaSR was performed on whole cell protein lysate from AC- and MSC-based TE constructs on day 35. Immunostaining against β -actin served as loading control. Blots are shown for samples from n=4 AC- and n=4 MSC donors.

Overall, in our model of human 3D-engineered cartilage, long-term hyperosmotic stimulation using calcium for 35 days compromised GAG synthesis and GAG deposition in AC- but promoted GAG synthesis and deposition in MSC-based TE constructs. Molecular characterization of AC and MSC-derived chondrocytes after long-term high calcium stimulation indicated a specific induction

of *S100A4* expression as well as PTHrP mRNA and protein levels in AC but not MSC-derived chondrocytes. Stimulation of AC with recombinant human PTHrP₁₋₃₄ protein partly reproduced the calcium-mediated reduction in differentiation marker expression and GAG deposition in AC constructs, suggesting a possible role for PTHrP on cartilage matrix formation in AC constructs. Importantly, the inverse regulation of GAG synthesis was specific to stimulation with CaCl₂. Thus, while long-term high extracellular calcium stimulation should be avoided during 3D cartilage engineering of AC, calcium stimulation provides a suitable stimulus to enhance the quality of MSC-based cartilage replacement tissue by enhancing GAG synthesis and GAG deposition in the construct.

5 Discussion

5.1 Effects of acute hyperosmotic stimulation on cartilage homeostasis

Osteoarthritis and cartilage defects are among the most prevalent disorders of the musculoskeletal system and due to the demographic changes in our society, the proportion of people with damaged cartilage is constantly increasing. At the same time, the low intrinsic regeneration capacity of cartilage requires regenerative approaches. However, current cartilage replacement tissues deposit insufficient GAG and type II collagen to resist the demanding mechanical conditions in the joint in the long-term. While mechanical compression protocols were suggested to enhance the GAG synthesis in cartilage replacement tissue, none of these studies addressed the contribution of mechano-induced physicochemical sub-stimuli to this response. Identifying the individual sub-parameter that contributes to load-induced stimulation of GAG synthesis may allow to optimize cartilage TE constructs easier and faster. Due to the relevance of osmotic pressure for the function of articular cartilage, acute hyperosmotic challenge appears as an important sub-parameter during acute load-induced stimulation of GAG synthesis. However, whether acute hyperosmotic pressure is a relevant sub-parameter for the stimulation of GAG synthesis was never investigated in a cartilage relevant model of pre-matured 3D engineered cartilage. Since load-induced stimulation of GAG synthesis changed with the GAG content of the tissue, investigation of the role of acute hyperosmotic stimulation as a sub-parameter of load-induced GAG synthesis should take the FCD into consideration.

This study provides interesting new insights into the response of pre-matured 3D-cultured human chondrocytes to acute hyperosmotic stimulation. It establishes p38, ERK1/2 and NFAT5 as osmo-response markers in pre-matured cartilage replacement tissue and shows that acute hyperosmotic stimulation reduced SOX9 and BMP signaling activity at high, but not at low FCD. However, this did not lead to changes in the mRNA levels of the ECM markers *COL2A1* and *ACAN*, nor was the GAG synthesis significantly altered at low FCD and at high FCD. Thus, FCD appears as a relevant factor only for the regulation of SOX9 protein and BMP pathway activity in chondrocytes after 3 to 24 hours of acute hyperosmotic stimulation. However, acute hyperosmotic conditions were no evident stimulus to enhance the GAG synthesis in cartilage TE constructs.

5.1.1 Establishment of AC-based cartilage TE constructs with low and high FCD

Previous studies indicated that the FCD of cartilage tissue may be relevant for the response of chondrocytes to external stimuli such as mechanical loading. Since we asked for the role of osmotic pressure as a sub-parameter of mechanical loading, it was important to establish the role

of acute hyperosmotic stimulation on GAG synthesis in a relevant model of pre-matured human 3D engineered cartilage that takes FCD into consideration. The generation of neocartilage using AC-seeded type I/III collagen scaffolds was previously established in our lab (Hecht et al. 2019; Lückgen et al. 2022; Praxenthaler et al. 2018; Scholtes et al. 2018). In these studies, after 35 days of redifferentiation, the newly formed tissue reached 89% of the hardness of native cartilage tissue and demonstrated a homogeneous GAG deposition in the constructs, reaching GAG/DNA levels of approximately 60-80 $\mu\text{g}/\mu\text{g}$ (Hecht et al. 2019; Lückgen et al. 2022; Praxenthaler et al. 2018). Due to the unavailability of native human cartilage tissue, this set up was used as a suitable model for the study of the mechano-response of chondrocytes. To explore the role of osmotic pressure as a sub-parameter of mechanical loading, this model of AC-seeded type I/III collagen scaffolds was used here. According to Safranin O staining on day 3 of pre-maturation, no visible signs of GAGs were detected in the constructs and GAG/DNA levels were as low as 8 $\mu\text{g}/\mu\text{g}$, indicating a low FCD in the tissue. On day 35 of pre-maturation, a mostly homogeneous distribution of GAGs was obvious in the constructs, resulting in significantly enhanced mean GAG/DNA levels of approximately 100 $\mu\text{g}/\mu\text{g}$, indicating a high FCD in the tissue. Thus, the GAG content of TE constructs in this study was comparable to that in previous studies from our group. Since a positive correlation between GAG content and FCD in the tissue was reported (Lu et al. 2004), conditions of low versus high GAG content correspond to a low versus high FCD. This way, cartilage TE constructs were obtained with a low or high FCD.

Since changes in chondrocyte morphology from small rounded cells in the native tissue (Bush and Hall 2003) towards a spread, fibroblast-like shape in monolayer culture (Benya et al. 1978) have significant impact on the response of chondrocytes to osmotic stimulation (Bush and Hall 2001; Urban et al. 1993) it was specifically relevant for this study that the cells maintain a typical chondrocyte-like morphology. As demonstrated in previous work from our group, the column-like orientation of type I/III collagen fibers in the here used scaffolds provided a comparable structural architecture compared to native cartilage tissue and allowed for a homogeneous distribution of the cells in the construct where cells maintained a chondrocyte-typical spheroid morphology (Scholtes et al. 2018). Thus, the here used model provided a cartilage-like niche for chondrocytes to maintain their typical spheroid shape and was therefore suited to study the hyperosmotic response of chondrocytes. Although others addressed the effect of acute hyperosmotic stimulation on 3D cartilage constructs, where cells maintained a typical spheroid phenotype (Erndt-Marino et al. 2019; Hopewell and Urban 2003; Peffers et al. 2010; Villanueva et al. 2009), all of these studies were performed without pre-maturation of the tissue, limiting the application

of these models to low FCD conditions as defined here. In addition, the use of hydrogels such as alginate or agarose limits the deposition of cartilage ECM in the construct to the pericellular regions of chondrocytes rather than inducing a homogeneous distribution throughout the construct (Dimicco et al. 2007; Ng et al. 2007). Thus, the here chosen 3D engineered cartilage represented a suitable model to study the influence of FCD on the osmo-response of human chondrocytes under standardized and cartilage-relevant 3D conditions.

5.1.2 Establishment of acute hyperosmotic response markers for engineered cartilage replacement tissue

To investigate the acute osmo-response of chondrocytes under such cartilage-relevant conditions, typical osmo-response markers were analyzed. Activation of the acknowledged osmo-response pathways p38 and ERK1/2 by hyperosmotic stimulation was so far never investigated in chondrocytes cultured under 3D conditions. It was here demonstrated that 3 hours of hyperosmotic stimulation induced p38 and ERK1/2 phosphorylation at osmolarities of 450-550 mOsm in 3D cultured chondrocytes. Interestingly, the osmolarity at which activation of p38 and pERK1/2 was observed here was comparable to previously reported p38 and ERK1/2 phosphorylation in monolayer-cultured chondrocytes at 450 mOsm (Tsai et al. 2007), 480 mOsm (Hdud et al. 2014) and 550 mOsm (Tew et al. 2009). An induction of p38 and ERK1/2 in monolayer culture and here in 3D culture, proposed their suitability as potent osmo-response markers independent of 2D versus 3D culture conditions.

Activation of p38 was so far never investigated at hyperosmotic stimulation times longer than 5 hours. This current study now demonstrates that acute hyperosmotic challenge at 550 mOsm induced p38 phosphorylation after 3 and 6 hours but not after 24 hours of stimulation and that this regulation was independent of the FCD content of the tissue. The here observed induction of p38 for up to 6 hours is in line with previously reported p38 phosphorylation after acute hyperosmotic stimulation at 550 mOsm in monolayer-cultured human articular chondrocytes for 10 minutes to 5 hours (Tew et al. 2009). This further demonstrates a cell adaptation when exposure lasts for 24 hours.

Activation of ERK1/2 was previously observed in isolated rat nucleus pulposus cells after hyperosmotic stimulation episodes for 5 minutes to 24 hours at 450 mOsm (Tsai et al. 2007) and in isolated porcine articular chondrocytes at slightly higher osmolarity of 600 mOsm for 6 hours (Racz et al. 2007). This is in agreement with the here observed ERK1/2 activation after 3 to 24 hours of hyperosmotic stimulation at 550 mOsm in 3D-cultured chondrocytes at low and at high

FCD. An adaptation like in the p38 pathway was, therefore, not obvious, qualifying ERK1/2 activity as the more robust indicator of an osmo-response.

Timing was also an issue for the osmo-sensitive transcription factor NFAT5 and its target genes *SLC5A3*, *S100A4* and *SLC6A12*. Acute hyperosmotic stimulation moderately enhanced *NFAT5* expression after 3 and 6 hours but not after 24 hours. In contrast, the expression of the NFAT5 target genes was strongly enhanced only after 24 hours of stimulation. Whether induction of NFAT5 target genes occurs delayed or is the result of long-term hyperosmotic stimulation, however, remained unclear. While induction of *NFAT5* and its target genes was previously described in monolayer-cultured human articular chondrocytes and murine ATDC5 cells after long-term hyperosmotic stimulation at 380 or 480 mOsm for several weeks (Caron et al. 2013; van der Windt et al. 2010), this is the first study that demonstrated their induction after acute hyperosmotic stimulation in 3D-cultured chondrocytes. Enhanced *Nfat5* mRNA stability was reported in murine kidney cells after hyperosmotic stimulation (Cai et al. 2005). Whether the mild increase in *NFAT5* mRNA in the present study may be due to post-transcriptional regulation of mRNA stability deserves further investigation. Moreover, the here observed mild induction of *NFAT5* gene expression is typical for the regulation of transcription factors, which often occurs by the rate of protein activity and promoter binding rather than changes in mRNA expression (Calkhoven and Ab 1996). Thus, future studies to evaluate the relevance of osmo-induced NFAT5 expression should definitely evaluate its translation into protein. Nevertheless, for the present work, *NFAT5* mRNA served as osmo-response marker and regulation of mRNA was sufficient for this purpose. NFAT5 response-genes *SLC5A3* and *SLC6A12* belong to a group of genes that encode for proteins that are involved in the volume regulation of cells in response to changes in the extracellular osmolarity via transport of ions and other osmolytes across the cell membrane (Hall 1995; Hall et al. 1996b). A late upregulation of the expression of these markers may suggest that chondrocytes start to adapt to disturbance in extracellular osmolarity after 24 hours in order to cope with the altered osmotic environment and maintain cellular functions. A similar time span of osmo-adaptation in chondrocytes was shown earlier for isolated chondrocytes (Urban et al. 1993) and chondrocytes in 3D alginate beads (Hopewell and Urban 2003).

Altogether, the data obtained here indicated for the first time that in pre-matured 3D-cultured chondrocytes, hyperosmotic stimulation activated p38 and ERK1/2 pathway activity and induced the expression of *NFAT5* and its target genes *S100A4*, *SLC5A3* and *SLC6A12*. Importantly, this regulation was independent of the FCD content in the construct. Thus, an FCD-independent regulation of the here investigated osmo-response markers in combination with their previously reported hyperosmotic induction in monolayer-cultured chondrocytes reinforced their use as

robust acute osmo-response markers in chondrocytes independent of FCD and surrounding ECM content.

5.1.3 Acute hyperosmotic regulation of pro-chondrogenic signaling pathways

While the induction of acute hyperosmotic response markers was independent of the FCD, this study further investigated whether the FCD affects the acute hyperosmotic regulation of prominent pro-chondrogenic signaling pathways, including SOX9, TGF β and BMP. Importantly, this is the first study examining acute hyperosmotic effects on pro-chondrogenic signaling molecules in pre-matured 3D-cultured chondrocytes.

In our 3D engineered cartilage model, hyperosmotic stimulation for 3, 6 and 24 hours had no effect on the expression of *SOX9* mRNA, irrespective of FCD. At the same time, SOX9 protein levels were inconsistently regulated at low FCD, but significantly reduced after hyperosmotic stimulation at high FCD. These data indicated that *SOX9* mRNA quantification was not predictive for the regulation of SOX9 protein levels. A differential regulation of *SOX9* mRNA and protein levels in chondrogenic cells was previously described by others (Diederichs et al. 2016), emphasizing the need to carefully interpret quantification of *SOX9* mRNA expression by confirmation of the corresponding protein levels. In previous studies, acute hyperosmotic stimulation enhanced the expression of *SOX9* in monolayer-cultured (Peffer et al. 2010; Tew et al. 2009) and in freshly embedded 3D-cultured chondrocytes (Erndt-Marino et al. 2019). Thus, while the data obtained here showed no change in *SOX9* mRNA expression, literature indicates an induction of *SOX9* mRNA in monolayer-cultured chondrocytes and in 3D-cultured chondrocytes without pre-maturation. So far, only one study investigated the effect of acute hyperosmotic stimulation on SOX9 at the protein level and found increased SOX9 protein levels after 5 hours of hyperosmotic stimulation at 550 mOsm (Tew et al. 2009). Interestingly, Tew et al. observed enhanced SOX9 mRNA stability after acute hyperosmotic stimulation. Their data therefore indicate that hyperosmotic stimulation can regulate SOX9 protein levels via post-transcriptional modification of its mRNA. Whether post-transcriptional regulation of *SOX9* mRNA may provide an explanation of the here observed reduction of SOX9 protein levels at unchanged mRNA expression needs further investigations in future studies.

Overall, the here observed specific reduction of SOX9 protein levels after hyperosmotic stimulation at high FCD was different to studies performed in monolayer. This indicates the importance of a cartilage-relevant 3D culture to investigate the response of chondrocytes to acute hyperosmotic stimulation. In addition, the differential regulation of SOX9 protein at low versus

high FCD in the present study indicated that FCD is a relevant factor for the regulation of SOX9 levels in chondrocytes after acute hyperosmotic stimulation.

So far, no studies investigated the regulation of TGF β -SMAD2/3 and BMP-SMAD1/5/9 signaling after acute hyperosmotic challenge in chondrocytes. Aiming to identify upstream regulators of acute osmo-induced changes in SOX9 protein levels, this study reported a co-regulation of BMP-SMAD1/5/9 signaling and SOX9 protein levels by acute hyperosmotic stimulation. Acute hyperosmotic stimulation for 3, 6 and 24 hours inconsistently regulated pSMAD1/5/9 levels at low FCD but consistently downregulated SMAD1/5/9 phosphorylation at high FCD. This suggests that hyperosmotic reduction of BMP signaling at high FCD is upstream of SOX9 protein levels. Furthermore, these data indicate that, similar to SOX9, FCD is a relevant factor for the regulation of BMP signaling after acute hyperosmotic stimulation. In addition, enhanced expression of BMP ligands *BMP2* and *BMP6* was specifically observed after hyperosmotic stimulation for 24 hours at low FCD but not at high FCD, which further demonstrates the relevance of FCD for the regulation of BMP signaling. Nevertheless, an induction of BMP ligand expression at low FCD occurred at unchanged SMAD1/5/9 pathway activity. Vice versa, enhanced BMP pathway activity at high FCD occurred in the absence of the induction of BMP ligand expression. This highlights the importance to validate mRNA levels at the protein and pathway activity level.

Unlike SOX9 protein and BMP pathway activity, pro-chondrogenic TGF β -SMAD2/3 signaling was reduced only after hyperosmotic stimulation for 24 hours. This regulation was observed at low and at high FCD, indicating that FCD is no relevant factor for the hyperosmotic regulation of TGF β -SMAD2/3 pathway activity. In addition, this indicates that TGF β -SMAD2/3 is likely no relevant upstream regulator of hyperosmotic effects on SOX9 protein.

Together, the here reported reduction of pro-chondrogenic TGF β signaling at low and high FCD and the reduction of SOX9 protein and BMP pathway activity at high FCD suggests an anti-chondrogenic effect of acute hyperosmotic stimulation on 3D-cultured chondrocytes, especially at high FCD. To this end, the here observed unchanged expression of *COL2A1* and *ACAN* expression after acute hyperosmotic stimulation at low and high FCD, was unexpected. Previous studies indicated a reduction of *COL2A1* and *ACAN* expression after acute hyperosmotic stimulation in monolayer (Palmer et al. 2001; Tew et al. 2009). Interestingly, despite reduced *COL2A1* mRNA expression, acute hyperosmotic stimulation enhanced *COL2A1* promoter activity in monolayer-cultured human articular chondrocytes (Tew et al. 2009), indicating increased transcriptional activity, but also enhanced turnover of *COL2A1* mRNA. This suggests a putative mechanism why *COL2A1* expression showed no net regulation after acute hyperosmotic stimulation in our model of 3D cultured chondrocytes. No change in *COL2A1* and *ACAN* expression was observed after acute

hyperosmotic stimulation in 3D-cultured chondrocytes without pre-maturation (Erndt-Marino et al. 2019). Thus, while this is in line with the here presented data at low FCD, this was the first study to demonstrate that hyperosmotic stimulation of 3D-cultured chondrocytes at high FCD does not change the expression of differentiation markers *COL2A1* and *ACAN*.

Overall, this study provided evidence that while FCD was no relevant factor for the regulation of osmo-response markers as well as TGF β pathway activity, the regulation of SOX9 protein levels and BMP pathway activity depended on the FCD. Therefore, FCD is a relevant factor during acute hyperosmotic stimulation studies and future studies should take this into consideration. Moreover, this study indicated unchanged SOX9 protein, BMP pathway activity and cartilage ECM-related gene expression after acute hyperosmotic stimulation at low FCD, which, concerning cartilage ECM-related genes, was in line with previous data on 3D-cultured chondrocytes without pre-maturation. Whether the reduced SOX9 and BMP pathway activity after acute hyperosmotic stimulation at high FCD ultimately leads to acute changes in cartilage matrix synthesis and to what extent acute hyperosmotic stimulation can thereby function as a sub-parameter of mechanical loading-induced GAG synthesis was therefore of interest.

5.1.4 The role of acute hyperosmotic stimulation as a sub-parameter of mechanical compression

The main goal of this study was to find out whether acute hyperosmotic challenge is a sub-parameter of mechanical compression capable to reproduce a load-induced stimulation of GAG synthesis in pre-matured 3D engineered cartilage. Importantly, this was the first study investigating the effect of acute hyperosmotic stimulation on GAG synthesis in a cartilage-relevant model of pre-matured 3D engineered cartilage. The here obtained data indicated that in adaptation to 3 hours of mechanical compression in our previous studies, three hours of acute hyperosmotic stimulation induced no significant regulation of GAG synthesis at low and at high FCD. Thus, unchanged GAG synthesis at low FCD was in line with unchanged pro-chondrogenic signaling molecules. Previous studies demonstrated in bovine articular chondrocytes cultured in 3D alginate gels without pre-maturation, that 4 hours of hyperosmotic stimulation at 550 mOsm reduced the GAG synthesis rate (Hopewell and Urban 2003). Others reported a stimulation of GAG synthesis after 24 hours of acute hyperosmotic stimulation using monolayer- and freshly embedded 3D-cultured chondrocytes (Urban et al. 1993; Villanueva et al. 2009). Unfortunately, derived from mechanical loading studies, GAG synthesis was only analyzed after 3 hours of acute hyperosmotic stimulation in this study. Thus, whether longer hyperosmotic stimulation for 24 hours at low FCD would also increase the GAG synthesis in our model is not clear.

So far, no studies investigated the regulation of GAG synthesis in pre-matured 3D-cultured chondrocytes at high FCD. The here observed unchanged GAG synthesis rate after acute hyperosmotic stimulation for 3 hours at high FCD was in accordance with an unchanged expression of cartilage matrix-related genes at the same time point. However, the data appeared somewhat surprising in the context of hyperosmotic reduction of pro-chondrogenic SOX9 and BMP signaling after 3 hours of hyperosmotic stimulation at high FCD. This indicates that pro chondrogenic SOX9 protein and BMP pathway activity at the end of acute hyperosmotic stimulation at high FCD are not the rate limiting parameters explaining changes in GAG synthesis over the following 24 hours. In a similar experimental set-up as here, our group previously described a load-induced reduction of GAG synthesis at low FCD and enhanced GAG synthesis at high FCD (Praxenthaler et al. 2018). The effects of mechanical stimulation on 3D-engineered human articular chondrocytes at low versus high FCD are therefore different to the observed regulation after hyperosmotic stimulation and may suggest that hyperosmotic stimulation is no major player during mechanical compression-related changes in GAG synthesis in chondrocytes. Comparing the observed effects after hyperosmotic stimulation with those after mechanical compression in our previous studies may further hint towards the contribution of osmotic stimuli to the mechanical loading response of chondrocytes. Interestingly, mechanical loading induced phosphorylation of ERK1/2 and slightly enhanced p38 activity in response to 3 and 24 hours of cyclic mechanical compression (Hecht et al. 2019; Lückgen et al. 2022; Praxenthaler et al. 2018). This indicates that p38 and ERK1/2 were induced by mechanical and hyperosmotic stimuli. In addition, mechanical loading studies suggested a set of robustly induced mechano-response genes, *FOS*, *FOSB*, *DUSP5* as well as *BMP2* and *BMP6* (Scholtes et al. 2018). Investigation of the expression of these genes after acute hyperosmotic stimulation demonstrated that their robust induction after mechanical loading was only partly reproduced by hyperosmotic stimulation. While *FOS* and *FOSB* qualified as early response genes after hyperosmotic stimulation, *DUSP5* showed only little regulation. Since *FOS* and *FOSB* are downstream targets of ERK1/2 signaling, the common induction of *FOS* and *FOSB* expression after mechanical and hyperosmotic challenge was in line with the described induction via the ERK1/2 pathway at both stimuli. However, it is not clear whether a common ERK1/2 - *FOS/FOSB* induction under both stimuli may be due to load-induced changes in osmolarity or is simply the sign of a similar cellular stress response under both stimuli. Importantly, load-induced alterations in tissue osmolarity are induced by a compression of the FCD in the tissue. Consequently, while mechanical loading at high FCD content induces changes in local osmolarity, no strong osmotic changes are exerted after mechanical compression at low FCD content in the tissue. Thus, an induction of ERK1/2 and *FOS/FOSB* after mechanical

loading at low FCD conditions are unlikely caused by load-induced changes in osmolarity. The analogous regulation of ERK1/2 and its downstream targets *FOS* and *FOSB* by mechanical and osmotic challenge, therefore, suggests the induction of general stress response mechanisms at both stimuli rather than an induction of osmotic signals by mechanical compression.

In contrast to *FOS* and *FOSB* expression, an upregulation of *BMP2* and *BMP6* expression was only observed after hyperosmotic stimulation for 24 hours at low FCD. Mechanical loading robustly enhanced the expression of BMP ligands after a 3 hour and a 24 hour mechanical loading protocol, independent of FCD (Hecht et al. 2019; Scholtes et al. 2018). This indicates that hyperosmotic effects may not be responsible for the induction of *BMP2* and *BMP6* expression after mechanical loading. Likewise, the here observed reduction of BMP signaling as well as SOX9 protein levels after 3 hours of hyperosmotic stimulation at high FCD was not observed after mechanical loading of chondrocytes, emphasizing the independent regulation of BMP pathway and SOX9 protein by mechanical and osmotic stimuli.

Overall, in the context of cartilage tissue engineering strategies, the current data imply that acute hyperosmotic pressure is not a suitable parameter to reproduce the loading related stimulation of GAG synthesis in cartilage TE constructs on its own. Interestingly, recent studies by our group demonstrated an importance of the cartilage ECM and its associated charged sugar molecules for the binding of growth factors and the induction of intracellular signaling cascades such as WNT, Indian hedgehog and BMP (Chasan et al. 2022; Gerstner et al. 2021). Release of growth factors from the ECM after mechanical loading was demonstrated (Annes et al. 2004; Vincent et al. 2004) and this growth factor release may be an alternate mechanism to explain FCD-dependent differences in cartilage matrix synthesis after loading.

5.2 Effects of long-term high extracellular calcium stimulation on cartilage matrix formation

While the here presented data indicated that acute hyperosmotic stimulation is likely no major player of the acute load-induced regulation of GAG synthesis, several studies suggested a stimulation of GAG synthesis and ECM deposition in 3D engineered cartilage from various animal species after moderate long-term hyperosmotic stimulation. However, the effect of long-term hyperosmotic stimulation on human 3D engineered cartilage was never investigated. To identify whether long-term hyperosmotic challenge can be a relevant stimulus to enhance the quality of cartilage replacement tissue, several studies highlighted the importance of the calcium microenvironment for cartilage ECM synthesis and deposition. Whether high extracellular calcium

stimulates or inhibits the cartilage ECM formation in cartilage TE constructs was so far unclear. Since AC and MSC are often used cell types for cartilage TE, the response of both cell types to long-term hyperosmotic stimulation using extracellular calcium was investigated. Thus, to elucidate whether long-term hyperosmotic calcium stimulation can enhance the GAG synthesis and ECM deposition in human 3D engineered AC- or MSC-based TE constructs, AC or MSC were matured for up to 35 days under standard or high extracellular calcium concentrations and cartilage matrix deposition and GAG synthesis rate were measured. Over 35 days of maturation, high extracellular calcium compromised the cartilage formation by AC, as evident by reduced expression of redifferentiation markers, lower GAG synthesis and GAG deposition. Opposite, in MSC, high calcium concentrations promoted GAG synthesis and GAG deposition significantly. Under high calcium conditions, AC did not mis-differentiate into a pro-hypertrophic phenotype and MSC hypertrophic differentiation was maintained but unaltered. While calcium had no influence on SOX9, TGF β and BMP signaling activity, *PTH LH* was specifically induced by calcium stimulation only in AC, but not in MSC. Stimulation of AC control constructs from day 21 to day 35 with recombinant human PTHrP₁₋₃₄ peptide partly reproduced the high calcium-mediated reduction of differentiation marker expression and GAG deposition in AC constructs. This suggests that AC acquired a higher sensitivity to elevated extracellular calcium concentrations compared to *in vitro* differentiated MSC via a PTHrP-sensitive signaling mechanism. Excitingly, long-term extracellular calcium stimulation provides a novel means to enhance the cartilage matrix content in MSC-based neocartilage.

5.2.1 Comparison of AC- and MSC-based cartilage TE constructs at control conditions

AC- and MSC-seeded type I/III collagen scaffolds were matured under standardized conditions for 35 days and the deposition of a cartilage-typic type II collagen- and PG-rich ECM was compared at the end of maturation. Previous data from our group demonstrated that AC- and MSC-based TE constructs deposited similar GAG/DNA over 35 days of maturation (Lückgen et al. 2022). Importantly, in earlier experiments, AC- and MSC-based constructs were attached to a β TCP-containing bone replacement material. An impact of calcium containing resorbable bone replacement material on cartilage ECM deposition was previously reported by others (Brocher et al. 2013; Sarem et al. 2018). Thus, to eliminate the effect of calcium, released from the resorbable β TCP material, no bone replacement phase was attached to the cartilage constructs in the present study. Compared to the previous studies from our group, here, in the absence of a bone replacement carrier, a similar deposition of type II collagen and GAG/DNA ratio was observed on day 35 in AC- and MSC-based TE constructs at control conditions.

Interestingly, at control conditions, AC- and MSC-based TE constructs revealed differences in DNA levels over the course of (re-)differentiation. At the start of (re)differentiation, on day 0, AC- and MSC-based constructs had a similar DNA content. While in control AC constructs DNA levels were increased after 35 days of redifferentiation compared to day 0, in MSC constructs no difference in DNA levels was observed before and after the differentiation. In previous experiments from our lab, chondrogenic pellet culture of MSC was characterized by a rapid loss of DNA in the initial 3 days of chondrogenesis. After this, DNA levels remained constant but lower than the initially seeded amount until the end of differentiation on day 42, indicating net cell loss (Fischer et al. 2018). Due to the selected time points for DNA measurement in this study, no assumption can be made about the initial cell loss in MSC constructs. At the end of differentiation on day 35, MSC constructs had similar DNA levels compared to day 0, which is different to pellet culture. This indicates that the type I/III collagen carrier may protect MSC from net cell loss over 35 days, presumably by providing a balance between cell death and proliferation. The increase in DNA levels in AC constructs indicates that AC underwent cell proliferation during redifferentiation. An induction of DNA levels in AC constructs and unchanged DNA-levels in MSC constructs was in line with previous studies from our lab (Lückgen et al. 2022). Thus, compared to pellet culture, the here used type I/III collagen carrier provided a niche for MSC-derived chondrocytes to deposit cartilage ECM without net cell loss. Under similar conditions, AC proliferated in the carrier. This is important for a potential clinical application of such constructs which indicates that the chosen carrier maintains cell viability in the construct.

Overall, the present study uses a 3D cartilage model allowing for high cartilage ECM deposition and maintained cell viability. Based on this, the effect of long-term hyperosmotic calcium stimulation on cartilage ECM formation was investigated.

5.2.2 Inverse regulation of cartilage ECM formation after long-term extracellular calcium stimulation

So far, 3D engineered cartilage tissue lacks a sufficiently high ECM content to withstand the demanding mechanical conditions in the joint in the long-term. Whether in our model of human 3D engineered cartilage the ECM deposition can be enhanced by long-term extracellular calcium stimulation was therefore addressed in the current study. It was demonstrated that calcium stimulation for 35 days inversely regulates GAG synthesis and GAG deposition in AC- and MSC-based engineered cartilage. Of note, in some of the samples, the measured GAG/DNA amount was not consistent with the results of histological staining for sulfated GAGs. While quantitative assessment of GAGs takes the entire construct into consideration, histological staining only

reflects the GAG distribution in a specific section of the tissue, which may account for the observed differences.

This was the first study to investigate the effect of long-term extracellular calcium stimulation on the ECM formation in human AC-based 3D engineered cartilage which presents an important novelty of this study. After maturation for 35 days under elevated extracellular calcium concentrations, GAG synthesis and GAG deposition were significantly reduced in AC constructs. Using monolayer-cultured bovine articular chondrocytes, previous studies indicated no regulation of GAG synthesis after extracellular calcium stimulation at 10 mM for 12 days (Koyano et al. 1996) which is different to the here observed results in 3D-cultured human AC.

Opposite to AC, long-term extracellular calcium stimulation significantly enhanced the GAG synthesis rate and GAG deposition in MSC-based TE constructs. Moreover, calcium treatment enhanced type II collagen deposition in the majority of MSC constructs but this effect did not reach significance due to limited sample numbers that were available. These results were unexpected as previous studies on human adipose tissue-derived MSC in pellet culture (Mellor et al. 2015) and bone marrow-derived MSC seeded in polyethylene terephthalate scaffolds (Sarem et al. 2018) reported reduced GAG and type II collagen deposition under 8.0 mM calcium conditions. A possible explanation for the observed differences is that in the study by Mellor et al., chondrogenic differentiation of adipose tissue-derived MSC was performed in the presence of BMP-6, which is not the case for bone marrow-derived MSC in our model. Considering the here observed higher BMP signaling activity in MSC-derived chondrocytes compared to AC, irrespective of calcium treatment, it might be hypothesized that the BMP signaling pathway plays a role during the inverse regulation of GAG formation by both cell types. BMP stimulation in the study by Mellor et al. may thus explain the observed differences between their results and those reported here. Sarem et al. reported reduced GAG deposition in 3D-cultured MSC stimulated with 8.0 mM extracellular Ca^{2+} for three weeks (Sarem et al. 2018). However, in their study, MSC were differentiated during the first two weeks under chondrogenic conditions using TGF β , followed by one week in hypertrophic medium with the addition of L-thyroxin. The induction of hypertrophic differentiation in their experimental setup presents a crucial difference to the here performed chondrogenic differentiation and may therefore explain the different results between both studies. In an early study that investigated the chondrogenic development of chicken limb bud mesenchymal cells in monolayer culture, a raise in extracellular calcium concentration to 3.3 mM for 72 hours enhanced the alcian blue-positive nodule formation and GAG synthesis rate (San Antonio and Tuan 1986), which is in line with the here reported results. In their study, the authors demonstrated that a calcium stimulation during the initial 24 hours was essential to induce the

observed effects and concluded that calcium may improve chondrogenic development via the promotion of mesenchymal cell aggregation. Although aggregation and nodule formation of MSC is of less relevance in the here used porous type I/III collagen carrier, it is conceivable that altered cell membrane properties induced by calcium could affect the cell shape of MSC to promote a cartilage typical round morphology. Indeed, a round cell shape was shown to promote the chondrogenesis of human MSC (Gao et al. 2010).

Importantly, the here observed inverse regulation of GAG synthesis by long-term extracellular calcium stimulation in AC and MSC-derived chondrocytes was not reproduced by control treatments using magnesium or sucrose. This indicates that the observed effects are specific to treatment with calcium and are no general hyperosmotic effect. Thus, long-term extracellular calcium treatment provides a suitable stimulus to enhance the quality of MSC-based cartilage TE constructs. In contrast, long-term calcium stimulation should be avoided during cartilage maturation of AC.

5.2.3 Role of anabolic and catabolic signaling mechanisms for calcium-regulated changes in GAG synthesis and cartilage ECM formation

To identify molecular signaling mechanisms that may underlie the calcium-induced inverse regulation of cartilage matrix production, this study found no differences in calcium-induced SOX9, TGF β and BMP signaling activity in both cell types, which was unexpected, considering the significant regulation of cartilage ECM formation in both cell types. In addition, unchanged SOX9, TGF β and BMP signals after long-term hyperosmotic stimulation are in contrast to reduced SOX9 protein and TGF β and BMP pathway activity after acute hyperosmotic stimulation. This may have several reasons, such as cell adaptations after long-term hyperosmotic challenge as well as markedly lower absolute changes in osmolarity.

While the enhanced GAG synthesis and GAG deposition in MSC-based TE constructs suggests a stimulation of pro-chondrogenic signaling pathways, the unchanged TGF β -SMAD2/3 activity in MSC-derived chondrocytes may be explained by the high TGF β supplementation in the culture medium which may restrict additional pathway activation. Nevertheless, this does not explain why SMAD2/3 pathways activity was not inhibited in AC, where high calcium stimulation reduced ECM formation and therefore suggested a reduction in pro-chondrogenic TGF β signaling. So far, no data are available in the literature regarding the regulation of TGF β pathway activity after long-term high extracellular calcium stimulation and the data obtained here suggest that TGF β signaling is not involved in calcium-mediated changes in cartilage matrix production by both cell types.

Since pro-chondrogenic BMP signaling was previously shown to be regulated by extracellular calcium during bone formation (Aquino-Martinez et al. 2017), it appeared as a promising candidate to mediate the calcium-dependent inverse regulation of cartilage matrix production in AC- and MSC-based constructs. Despite unchanged BMP-SMAD1/5/9 activity in response to high extracellular calcium levels, a higher BMP signaling activity was observed in MSC-derived chondrocytes compared to AC. A higher BMP1/5/9 signaling activity was supported by lower *GREM1* expression in MSC-derived chondrocytes compared to AC. In previous studies from our group, a differential BMP signaling activity between AC and MSC-derived chondrocytes was suggested during in vitro chondrocyte (re)differentiation in pellet culture (Dexheimer et al. 2016). In the former study, high initial BMP activity and endogenous BMP4 expression rapidly decreased during AC re-differentiation, whereas MSC-derived chondrocytes maintained high BMP pathway activity and upregulated *BMP4* and *BMP7* expression during chondrogenesis. It may be speculated that a higher BMP pathway activity in MSC-derived chondrocytes compared to AC may be involved in the differential regulation of cartilage matrix formation at high extracellular calcium concentrations by both cell types. This provides the basis for future studies to investigate whether stimulation of BMP pathway activity in AC may rescue the here observed calcium-dependent reduction in GAG synthesis and GAG deposition.

In the current study, the regulation of catabolic markers *S100A4* and *MMP13* was analyzed to identify whether differences in catabolic cell signaling are involved in the differential regulation of GAG synthesis and GAG deposition by AC and MSC-derived chondrocytes in response to long-term high extracellular calcium stimulation. This is the first study to show the upregulation of *S100A4* and *MMP13* expression by high extracellular calcium treatment in AC. In contrast, in MSC-derived chondrocytes high calcium stimulation showed no regulation of *S100A4* and *MMP13* expression. Enhanced *S100A4* (Yammani et al. 2006) and *MMP13* expression (Reboul et al. 1996) was previously associated with a catabolic OA phenotype in AC and the data further highlighted the role of *S100A4* as upstream regulator of *MMP13* expression. This suggests a possible mechanism of compromised cartilage formation by AC under high calcium conditions via upregulation of *S100A4* and *MMP13*. The essential role of *S100A4* for cartilage maturation was also demonstrated by the lack of (re)differentiation of AC and MSC, cultured in the presence of *S100A4* inhibitor Niclosamide. To gain further mechanistic understanding of the role of *S100A4* in calcium-induced cartilage matrix destruction, further studies are now needed to manipulate *S100A4* signaling in more elaborated short-term treatment studies or using valid inhibitors. A functional link between *S100A4* and *MMP13* was previously suggested via secretion of *S100A4* into the extracellular space

and signal activation via the receptor for advanced glycation end products (RAGE) to induce *MMP13* expression (Cipollone et al. 2003; Hofmann et al. 2002; Yammani et al. 2006). Therefore, future studies should also consider the use of specific RAGE-receptor inhibitors or antagonists. Nevertheless, the here presented data also showed that *MMP13* expression appeared by trend higher in MSC-derived chondrocytes compared to AC, regardless of calcium treatment. Although this effect did not reach significance, enhanced *MMP13* expression in MSC-derived chondrocytes is a well-established characteristic of their hypertrophic differentiation (Pelttari et al. 2006), confirming the hypertrophic phenotype of MSC in our model. This indicated that MSC-derived chondrocytes upregulate cartilage matrix synthesis and deposition despite a high *MMP13* expression. Whether calcium-induced increase in *MMP13* expression in AC leads to enhanced *MMP13* protein levels or a catabolic *MMP13* activity needs to be further addressed using ELISA and enzyme activity assays. Thus, the current data on high calcium-induced expression of *S100A4* and *MMP13* in AC encourages to determine their functional role for cartilage ECM formation by AC after long-term high extracellular calcium stimulation.

To further investigate the calcium-dependent regulation of catabolic signaling mechanisms, the catabolic signaling molecules *COX2* and *PGE₂* were analyzed. Since *COX2* and *PGE₂* were shown to have catabolic effects in OA chondrocytes (Attur et al. 2008) and their induction was demonstrated in response to high calcium stimulation in murine osteoblasts (Choudhary et al. 2004; Choudhary et al. 2003), their induction by high calcium levels was expected in AC. However, after 35 days of high extracellular calcium concentrations, *COX2* expression was unchanged in both cell types. In parallel, *PGE₂* secretion was enhanced by calcium treatment in MSC-derived chondrocytes. In AC, mean *PGE₂* secretion levels were almost doubled, but this did not reach significance. Nevertheless, a similar pattern of *COX2* and *PGE₂* regulation in both cell types challenges their role in mediating the observed inverse regulation of cartilage ECM production in AC- and MSC-based TE constructs in response to high calcium concentrations. In addition, clearly higher *PGE₂* secretion was observed in MSC-derived chondrocytes compared to AC, an effect that did not reach significance due to correction for multiple comparison but was previously reported in our model by others (Lückgen et al. 2022). Thus, in line with higher *MMP13* expression in MSC-derived chondrocytes, higher levels of catabolic *PGE₂* in MSC-derived chondrocytes indicate that MSC-derived chondrocytes upregulate cartilage matrix production in response to high extracellular calcium concentrations despite strong catabolic marker expression.

Another major finding of this study was that *PTH1H* expression was specifically upregulated by high calcium conditions in AC. Furthermore, PTHrP₁₋₃₄ stimulation reproduced the high calcium-

mediated reduction in *ACAN* and *SOX9* expression and GAG/DNA deposition in AC-based neocartilage. Using a similar experimental set up as performed here (i.e., type I/III collagen carrier-based cartilage TE constructs), J. Lückgen observed no differences in *PTH1R* expression between AC- and MSC-based TE constructs under standard (re)differentiation conditions (Lückgen, 2022). This is in line with the here reported observations at control conditions. Previous studies indicated higher PTHrP secretion into the culture supernatant during AC redifferentiation compared to MSC chondrogenesis (Fischer et al. 2010). In the current study, measurement of PTHrP secretion into the culture medium using ELISA was inconclusive (data not shown). Thus, whether AC and MSC-derived chondrocytes in our model secrete different levels of PTHrP is not known.

Using bovine articular chondrocytes in monolayer culture, Burton et al. indicated increased PTHrP secretion at high extracellular calcium concentration of 3 mM (Burton et al. 2005). Although PTHrP secretion was not investigated in the current study, this was in line with the here observed calcium induced upregulation of *PTH1R* mRNA and PTHrP protein in AC. Stimulation of AC with recombinant human PTHrP₁₋₃₄ partly reproduced the high calcium-mediated reduction of cartilage ECM related marker expression and GAG deposition in AC. PTHrP₁₋₃₄ is a truncated form of the full-length PTHrP peptide that only activates one branch of the typical PTHrP signaling response, namely signal transduction via PKA (Martin et al. 2021). To analyze whether calcium enhanced the expression of different PTHrP isoforms that signal via the PKC-dependent PTHrP signaling branch was technically not feasible in this study. Whether specific PTHrP isoforms would be able to fully reproduce the here observed calcium-induced reduction of cartilage matrix formation by AC is therefore an interesting topic for future studies.

Binding of PTHrP to its receptor, PTH1R, results in G-protein coupled signal transduction and subsequent cAMP production. The fact that the upregulation of PTHrP by high extracellular calcium in AC did not translate into differences in downstream cAMP levels suggests that calcium-induced PTHrP levels in AC may exert their effects in a PTH1R-independent fashion. In addition, low *PTH1R* expression in AC was previously demonstrated in our model (Lückgen, 2022), further emphasizing the involvement of PTH1R-independent actions. PTH1R-independent signal transduction of PTHrP was also reported during early chondrogenic MSC micromass pellet culture, where PTHrP secretion was high but *PTH1R* mRNA was not yet detected (Weiss et al. 2010) and data obtained here suggest similar actions for AC. PTHrP internalization and nuclear translocation was proposed as a possible mechanism of PTH1R-independent signal transduction (Clemens et al. 2001).

Overall, the here obtained data indicate for the first time that high extracellular calcium treatment differentially regulated PTHrP gene and protein levels in AC and MSC-derived chondrocytes. Since

PTHrP₁₋₃₄ stimulation from day 21 to day 35 partly reproduced the high calcium-mediated compromised cartilage matrix formation in AC, this encourages further studies of PTHrP ablation to elucidate the functional role of PTHrP during high calcium-induced cartilage matrix destruction in AC. While this would require the inhibition of PTHrP by a specific inhibitor, known inhibitors, such as PTHrP₇₋₃₄, proved not efficient to block PTHrP signaling in our model (data not shown). In addition, PTHrP₇₋₃₄ targets the PTH1R, and unchanged cAMP levels after calcium-stimulation suggested that calcium-induced PTHrP may exert receptor independent effects in AC. Identifying potent PTHrP inhibitors which also block the PTH1R-independent PKC-signaling branch of the PTHrP pathway may be used in future studies to investigate whether such inhibitors provide a promising tool to prevent cartilage matrix destruction under high extracellular calcium conditions in AC.

5.2.4 Influence of high extracellular calcium concentrations on the phenotype of AC and MSC-derived chondrocytes

Besides calcium-induced molecular signaling mechanism this study further studied whether long-term high extracellular calcium stimulation leads to changes in the phenotype of AC and MSC-derived chondrocytes. To this end, data from the current study demonstrated the absence of hypertrophic and osteogenic markers in AC at control and high extracellular calcium concentrations, indicating that AC did not mis-differentiate into a pro-hypertrophic phenotype at high extracellular calcium conditions. In MSC-derived chondrocytes, hypertrophic differentiation was confirmed by the detection of hypertrophic and osteogenic markers on gene and protein level. Interestingly, while some markers, such as *ALPL* mRNA and IBSP protein were upregulated by high calcium treatment, type X collagen protein levels were reduced by calcium stimulation in samples from 2 out of 3 MSC donors. The regulation of type X collagen by high extracellular calcium concentrations was previously investigated in studies using various MSC-like cells. In a study on monolayer-cultured chondrocytes isolated from 12 days old chicken embryos, extracellular calcium stimulation at 5-10 mM for 72 hours upregulated type X collagen (Bonen and Schmid 1991). Likewise, type X collagen levels were increased during monolayer culture of fetal bovine growth plate chondrocytes at 10 mM $[Ca^{2+}]_e$ for 12 days (Koyano et al. 1996). In human adipose tissue-derived MSC micromass pellets, high extracellular calcium concentrations of 8 mM for 28 days increased type X collagen levels (Mellor et al. 2015). While these studies reported an induction of type X collagen at elevated extracellular calcium concentrations, others found reduced *Col10a1* expression at high extracellular calcium concentrations. For example, in a model of murine growth plate chondrocytes cultured in monolayer at 3 mM $[Ca^{2+}]_e$ for two weeks, *Col10a1* expression was reduced compared to control cultures (Rodriguez et al. 2005). These data

indicate the importance to consider the model system when investigating effects of extracellular calcium concentration on the chondrogenic differentiation of MSC. Thus, the here selected 3D model of human articular cartilage TE constructs presents a valuable readout for the translation into clinical practice. In addition, the described discrepancies may be the result of slight variations in the stimulation protocol, highlighting the relevance of the here performed comparison of different cell types under standardized experimental conditions.

In the study by Rodriguez et al., reduced *Col10a1* expression was observed at increased expression of terminal differentiation markers osteopontin and enhanced mineralization. At the same time, *Acan* and *Col2a1* expression as well as alcian blue staining were reduced and the authors therefore concluded an enhanced differentiation of growth plate chondrocytes along the endochondral lineage at high extracellular calcium concentrations. Likewise, a reduction of extracellular calcium sensing by knock down of the extracellular calcium sensing receptor reduced the transition of chondrocytes into osteoblasts during callus maturation in a model of unfixed fracture healing in mice. Sarem et al. even suggested a shift from endochondral to intra membranous ossification in human bone marrow-derived MSC in the presence of a resorbable calcium hydroxyapatite carrier (Sarem et al. 2018). The here observed reduction of hypertrophic type X collagen in samples from two out of 3 MSC donors in combination with increased osteogenic *ALPL* expression and enhanced IBSP protein levels therefore may tempt to conclude a promoted differentiation along the endochondral lineage at high calcium conditions. However, the enhanced GAG deposition and induction of GAG synthesis in MSC samples at high $[Ca^{2+}]_e$ clearly challenges this hypothesis.

Overall, the presented data demonstrate that in our model of 3D-cultured human bone marrow-derived MSC, high calcium treatment enhanced the cartilage matrix formation at maintained hypertrophic differentiation.

5.2.5 Implications for osteochondral tissue engineering

As a main goal of this research, high extracellular calcium treatment was identified as a suitable stimulus to enhance the cartilage matrix formation in MSC-based TE constructs. This has important implications for the design of osteochondral tissue engineering constructs. During osteochondral TE, cartilage matrix formation occurs in close vicinity to resorbable calcified structures. For osteochondral TE approaches, it is therefore important to select cells that deposit high amounts of GAG and type II collagen in the presence of elevated extracellular calcium concentrations. In the present study, MSC-based TE constructs showed significantly higher type II collagen and GAG/DNA deposition under high calcium conditions compared to AC-based TE constructs. Thus, for the clinical application of AC or MSC during osteochondral defect treatment

this study suggests MSC as a more suitable cell source than AC for cartilage neogenesis in proximity to resorbable calcified structures like bone or bone mimetic replacement materials. Practical limitations of MSC-for cartilage TE are an undesired mineralization *in vivo*. Suppression of an undesired hypertrophic phenotype during *in vivo* chondrogenic differentiation of human MSC was recently accomplished by our group by seeding MSC into a heparin-augmented cartilaginous 3D hydrogel (Chasan et al. 2022). In this way, the use of MSC-based heparin-augmented hydrogels attached to resorbable calcium-containing bone replacement materials may present a valuable approach to generate stable articular cartilage for osteochondral tissue engineering constructs in the absence of undesired *in vivo* mineralization. Alternatively, an appealing approach for osteochondral TE may also be the design of multi-layered osteochondral constructs in which the chondral layer is connected to a bone replacement material via a transition zone of calcified cartilage. In such multilayered constructs, AC may be separated from calcified resorbable bone replacement structures via an intermediate layer of pro-hypertrophic MSC, prone to develop a layer of mineralized cartilage. Intriguingly, the importance of this intermediate mineralized cartilage layer for cartilage defect healing becomes evident as the use of non-zonal, purely chondral as well as biphasic osteochondral regeneration implants often revealed biomechanical failure at the bone-cartilage junction (Brun et al. 2008; LaPrade et al. 2008). Intriguingly, the benefit of a mineralized cartilage layer for cartilage defect repair in terms of tissue integration and mechanical stability was shown in several publications (Allan et al. 2007; Kandel et al. 2006; St-Pierre et al. 2012).

5.3 Limitations of the study

Although data from this study make an important contribution towards understanding the specific role of osmotic pressure as an important physicochemical stimulus during cartilage tissue engineering, it is important to note that the here performed experiments come with certain limitations.

One major advantage of this study compared to previous work is the used model of 3D-engineered human articular cartilage which closely resembles the structure of native cartilage tissue. Nevertheless, an inherent limitation of this study was the application of osmotic and calcium stimuli in the absence of surrounding connective tissue and other cell types. Although helpful to identify molecular signaling mechanisms in a precisely defined environment, *in vitro* studies do not fully recapitulate the *in vivo* situation. For example, extracellular calcium was shown to have

immunomodulatory properties, affecting the secretion of cytokines such as IL-1 β from immune cells (Ainscough et al. 2015) which in turn may interfere with cartilage matrix homeostasis.

Moreover, due to the limited availability of healthy articular cartilage, the here used model of articular cartilage tissue engineering constructs was based on the use of articular chondrocytes from OA joints. Therefore, it cannot be excluded that the OA background of the cells influences their signaling response. For this reason, the isolated chondrocytes were carefully harvested from areas of macroscopically intact articular cartilage. In addition, isolated chondrocytes were subjected to monolayer expansion upon which cells dedifferentiate and lose their OA phenotype. During subsequent redifferentiation protocols, chondrocytes develop a phenotype that is largely independent from its initial OA-background. Nevertheless, the influence of an OA phenotype in these cells cannot be completely neglected until comparative studies using cartilage tissue engineering constructs based on healthy articular chondrocytes are used for comparison.

During osmotic stimulation experiments, TE constructs were subjected to acute hyperosmotic stimulation episodes of 3-24 hours. Although this stimulation regime was designed to closely mimic mechano-induced changes in osmolarity, it is important to consider that load-induced changes in local tissue osmolarity are dynamic, including a hyperosmotic change upon compression, followed by a hypoosmotic change after unloading of the tissue. The relevance of dynamic osmotic changes for cartilage formation was demonstrated in previous studies where differences in *ACAN* mRNA expression were observed after static and dynamic osmotic stimulation (Palmer et al. 2001). Likewise, O'Connor et al. suggested that during cyclic osmotic stimulation of chondrocytes, cells primarily respond to hypoosmotic stimuli (O'Connor et al. 2014). Therefore, while this study provided no evidence that acute hyperosmotic stimulation is a promising means to stimulate ECM synthesis in cartilage TE constructs, further studies are needed to confirm this in cyclic osmotic stimulation experiments.

A potential flaw of this study is the investigation of acute hyperosmotic stimulation effects using only one specific osmolyte, NaCl. Although previous studies demonstrated no differences in GAG synthesis and ECM-related marker expression under ionic Na⁺, non-ionic sucrose and PEG as osmolytes (Erndt-Marino et al. 2019; Urban et al. 1993), the use of sucrose or PEG as additional osmotic controls would have provided a valuable confirmation about the osmotic nature of the observed effects.

An important finding from this study was that AC and MSC showed an opposite regulation of cartilage matrix formation in response to high extracellular calcium concentrations. Enhanced sensitivity of AC to extracellular calcium via a PTHrP-dependent mechanism was proposed a potential mechanism. However, to conclude about a causal relationship between PTHrP and

reduced cartilage matrix deposition, inhibitor studies are needed. Unfortunately, the here tested PTH1R antagonist PTHrP₇₋₃₄ did not prove as an effective inhibitor of PTHrP pathway activity. Therefore, more elaborated models for the loss of function of PTHrP are needed. In the last years, the use of induced pluripotent stem cells (iPSC) for cartilage tissue engineering, showed promising progress towards the differentiation of stem cells into stable articular chondrocytes. While transfection and knock down of genes was so far difficult to accomplish in primary articular chondrocytes, gene knock out in iPSC and subsequent differentiation into chondrocytes may be a suitable strategy for a reliable PTHrP ablation in chondrocytes.

In order to interpret these data in the context of osteochondral tissue engineering, another limitation of this study is the use of soluble extracellular calcium as a calcium source. While the addition of soluble calcium ions into the medium allows to precisely manipulate calcium concentrations in the culture medium, the release of calcium ions from resorbable bone replacement materials is variable. To understand the relevance of the here obtained data for osteochondral tissue engineering, experiments are needed to replace extracellular soluble calcium with resorbable bone replacement materials. For this purpose, special attention should be paid to the selection of an appropriate control. The choice of bone-replacement materials comes along, among others, with differences in porosity and stiffness of the material. The selection of an appropriate non-resorbable or non-calcium-based replacement material should therefore take this into consideration. In addition, while *in vitro* calcium resorption primarily depends on the passive dissolution of calcium ions into the interstitial fluid, in the joint, immune cells may affect the activity of osteoclast to enhance or reduce calcium resorption and thereby change the level of extracellular calcium.

Thus, besides certain inherent limitations of this project, the here performed experiments should encourage a series of follow-up experiments to further deepen our knowledge on the contribution of physicochemical stimuli to the successful formation of cartilage tissue engineering constructs.

5.4 Conclusion and outlook

With the aim to determine the role of acute hyperosmotic pressure as a sub-parameter of mechanical compression and to enhance the GAG synthesis of chondrocytes, this was the first study to apply acute hyperosmotic stimulation to mature human engineered cartilage. The here obtained data demonstrated that the known mechano-response markers p38, ERK1/2, *NFAT5*, *FOS* and *FOSB* are also valid response markers after acute hyperosmotic stimulation. Thereby this study indicated that mechanical and hyperosmotic challenge can induce similar signaling mechanisms. Nevertheless, the stimulation of GAG synthesis at enhanced SOX9 protein levels observed in the previous loading studies, was not reproduced by acute hyperosmotic stimulation under which pro-chondrogenic SOX9 protein and BMP pathway activity dropped, while GAG synthesis remained unaltered. Thus, although mechanical and hyperosmotic challenge partly triggered similar response pathways, short-term hyperosmotic pressure was no effective means to influence GAG synthesis. Further studies are now needed to evaluate the contribution of other load-induced sub-parameters to cartilage matrix synthesis.

While the main aim, to enhance the GAG synthesis in TE constructs, was not reached after acute hyperosmotic stimulation, the current data demonstrated that long-term hyperosmotic stimulation using soluble calcium chloride promoted the cartilage matrix formation in MSC-based engineered cartilage. Opposite, calcium compromised the cartilage matrix formation in neocartilage generated from AC. Thus, high calcium inversely regulated GAG synthesis and GAG deposition in AC- and MSC-based engineered cartilage. Investigation of pro- and anti-chondrogenic signaling mechanism that may underly the inverse regulation of cartilage matrix production revealed a differential regulation of anti-chondrogenic *S100A4* and *PTH1LH*, which were induced after calcium treatment only in AC. This encourages further studies to clarify their role for the calcium-mediated reduction of cartilage matrix formation in AC. An important observation of this study is that the inverse regulation of GAG synthesis was calcium-specific and not caused by general hyperosmotic effects. Thus, long-term extracellular calcium stimulation provides a novel means to enhance the cartilage matrix content in MSC-based cartilage replacement tissue whereas such conditions should be avoided during AC neocartilage formation. For the application in osteochondral tissue engineering, this implies that MSC should be the favored cell source for cartilage neogenesis in vicinity to calcified bone replacement materials. Further studies are now needed to confirm the here observed effects of soluble extracellular calcium using resorbable bone replacement material as a potential calcium source.

6 Summary

Due to the low regenerative capacity of articular cartilage, regenerative approaches are needed to treat cartilage defects and to restore the function of the tissue in the joint. However, a general drawback of current cartilage replacement tissues is an insufficient deposition of its main molecular components, type II collagen and proteoglycan. As a result, the tissue cannot withstand the demanding mechanical conditions in the joint. Recent studies of our group achieved an acute stimulation of cartilage matrix synthesis by a defined mechanical loading protocol which depended on the tissue's glycosaminoglycan (GAG)-content and its associated fixed charge density (FCD). However, to what extent mechano-induced physicochemical sub-stimuli contribute to cartilage matrix production remains unclear. Identifying the decisive sub-parameter that contributes to load-induced stimulation of cartilage matrix synthesis would provide an easily applicable stimulus to optimize the quality of cartilage replacement tissues. Due to the essential role of osmotic pressure for cartilage function, hyperosmotic challenge appears as an important sub-parameter of the loading-response. However, the contribution of acute hyperosmotic pressure to cartilage homeostasis is unclear and models that take a cartilage typical FCD into consideration are required. Interestingly, long-term maturation of animal chondrocytes under hyperosmotic conditions enhanced the matrix content of engineered cartilage but this was so far never investigated for human 3D-cultured chondrocytes. Thus, the aim of this study was to elucidate whether acute hyperosmotic stimulation, as a sub-parameter of mechanical compression, regulates cartilage matrix synthesis in a human engineered cartilage model at low and high FCD. In parallel, it was investigated whether long-term hyperosmotic stimulation can enhance the matrix synthesis and deposition of cartilage replacement tissue. To achieve these aims, human engineered cartilage was pre-matured for 3 or 35 days to develop a cartilage-like matrix of low or high FCD. Acute hyperosmotic stimulation on day 3 and on day 35 for 3 to 24 hours indicated that the known mechano-response markers ERK1/2, p38, *NFAT5*, *FOS* and *FOSB* are also immediate osmo-response markers, irrespective of the FCD content of the tissue. Opposite to previous results from mechanical loading studies, a downregulation of pro-chondrogenic SOX9 protein and BMP pathway activity indicated an anti-chondrogenic effect of short-term hyperosmotic stimulation on chondrocytes. However, this did not lead to changes in cartilage matrix synthesis at low and at high FCD. Thus, although acute hyperosmotic stimulation and mechanical compression partly triggered similar response pathways, short-term hyperosmotic pressure was no major player to influence the regulation of cartilage matrix synthesis.

In the context of long-term hyperosmotic stimulation, previous studies suggested a role of the extracellular calcium microenvironment for cartilage matrix synthesis and deposition. Since articular chondrocytes (AC) and mesenchymal stromal cells (MSC) are often used cell types for the design of cartilage replacement tissues, the response of both cell types to long-term hyperosmotic stimulation was investigated using extracellular calcium. Interestingly, the here obtained data revealed that long-term hyperosmotic calcium stimulation for 35 days compromised cartilage matrix formation in AC-based cartilage replacement tissue but promoted the cartilage matrix formation in neocartilage generated from MSC. Investigation of pro- and anti-chondrogenic signaling pathways after long-term calcium stimulation indicated a specific induction of catabolic *S100A4* and *PTH1LH* expression in AC. Stimulating AC with recombinant human PTHrP₁₋₃₄ peptide partly reproduced the calcium-mediated reduction of cartilage matrix deposition, suggesting a role of PTHrP for impaired cartilage matrix formation. Importantly, the inverse regulation of GAG synthesis in AC and MSC-derived chondrocytes was calcium-specific and not caused by general hyperosmotic effects. Long-term extracellular calcium stimulation, therefore, provides a novel means to enhance the cartilage matrix content of MSC-based engineered cartilage whereas such conditions should be avoided during AC neocartilage formation.

Overall, this study provides important information on the role of physicochemical stimuli for cartilage matrix formation in human engineered cartilage. It was demonstrated that acute hyperosmotic pressure was no effective stimulus to influence cartilage matrix synthesis, and further studies are now needed to determine the contribution other load-induced sub-parameter for GAG synthesis. Furthermore, this study indicated that long-term high extracellular calcium treatment provides a novel means to enhance the quality of MSC-based cartilage replacement tissue by stimulating GAG synthesis and GAG deposition. For the application in osteochondral tissue engineering approaches, this implies that MSC should be the first choice for cartilage matrix deposition in the vicinity of resorbable calcified bone replacement materials. However, studies are now needed to confirm the here observed effects of soluble extracellular calcium using resorbable bone replacement material as a potential calcium source.

7 Zusammenfassung

Aufgrund der geringen Regenerationsfähigkeit von Knorpelgewebe bedarf es regenerativer Ansätze um Knorpeldefekte zu behandeln und so die Funktion des Gewebes im Gelenk wiederherzustellen. Derzeit sind Knorpelersatzgewebe durch eine unzureichende Ablagerung von Typ II Kollagen und Proteoglykan, den Hauptbestandteilen des Gelenkknorpels, limitiert, wodurch das gezüchtete Gewebe den anspruchsvollen mechanischen Bedingungen im Gelenk auf Dauer nicht standhalten kann. In früheren Studien unserer Forschungsgruppe konnte die Knorpelmatrixsynthese mit Hilfe eines definierten mechanischen Belastungsprotokolls akut stimuliert werden, wobei die Induktion entscheidend vom Glykosaminoglykan (GAG)-Gehalt des Ersatzgewebes und der damit verbundenen Ladungsdichte (engl. fixed charge density, FCD) abhing. Bisher ist jedoch unklar, inwiefern belastungsinduzierte physikalisch-chemische Reize zu den beobachteten Effekten beitragen. Die Identifizierung des entscheidenden physikalisch-chemischen Subparameters der Belastungsantwort, der für die Induktion der Knorpelmatrixsynthese verantwortlich ist, würde es ermöglichen, Knorpelersatzgewebe mit einer einfach anwendbaren Stimulation gezielt zu verbessern. Aufgrund seiner Relevanz für die Funktion des Gelenkknorpels erscheint hyperosmotischer Druck als ein wesentlicher Subparameter der mechanischen Belastungsantwort. Da bisher allerdings unklar ist, inwiefern akuter hyperosmotischer Druck zur Knorpelhomöostase in reifem Knorpelersatzgewebe beiträgt, sind Studien notwendig, die dies unter Berücksichtigung einer knorpeltypischen FCD untersuchen. Interessanterweise wurde in Studien bereits gezeigt, dass eine langfristige hyperosmotische Stimulation den Knorpelmatrixgehalt in nicht-humanen Chondrozyten erhöht. Ob dies auch für humane Chondrozyten in 3D-Kultur der Fall ist wurde bisher jedoch nicht untersucht.

Das Ziel dieser Studie war es daher herauszufinden, ob eine akute hyperosmotische Stimulation, als Subparameter der mechanischen Kompression, die Knorpelmatrixsynthese in humanem Knorpelersatzgewebe bei niedriger und hoher FCD beeinflusst. Parallel dazu wurde getestet, ob eine langfristige hyperosmotische Stimulation die Matrixsynthese und Ablagerung von Knorpelersatzgewebe verbessern kann. Um diese Ziele zu erreichen, wurde humanes Knorpelersatzgewebe für 3 oder 35 Tage vorgereift, um eine knorpelähnliche Matrix mit niedrigem oder hohem FCD-Gehalt zu generieren. Die akute hyperosmotische Stimulation von Knorpelersatzgewebe für 3 bis 24 Stunden ergab, dass die bekannten mechanosensitiven Marker, ERK1/2, p38, *NFAT5*, *FOS* und *FOSB*, FCD-unabhängig auch als osmosensitive Marker fungieren. Im Gegensatz zu früheren Belastungsstudien allerdings deuteten reduzierte SOX9-Proteinspiegel und eine verringerte BMP-Signalwegaktivität auf eine anti-chondrogene Wirkung der hyperosmotischen

Stimulation auf Chondrozyten hin, wobei die Knorpelmatrixsynthese unverändert blieb. Somit konnte gezeigt werden, dass akute hyperosmotische Stimulation zwar einerseits ähnliche Signalwege induzierte wie mechanische Belastung, andererseits jedoch kein entscheidender Parameter für die Stimulation der Knorpelmatrixsynthese war.

Für eine langfristige hyperosmotische Stimulation zur Verbesserung von Knorpelersatzgewebe erscheint extrazelluläres Kalzium aufgrund früherer Studien besonders vielversprechend. Da artikuläre Chondrozyten (AC) und mesenchymale Stromazellen (MSC) häufig verwendete Zelltypen für die Herstellung von Knorpelersatzgeweben sind, wurde in der vorliegenden Arbeit die Reaktion beider Zelltypen auf eine langfristige hyperosmotische Kalzium-Stimulation untersucht. Nach 35-tägiger Kalzium-Behandlung war die Knorpelmatrixbildung in AC-basiertem Knorpelersatzgewebe reduziert, in MSC-basiertem Knorpelersatzgewebe allerdings erhöht. Die Untersuchung wichtiger pro- und anti-chondrogener Signalwege nach langfristiger Kalziumstimulation zeigte eine spezifische Induktion der katabolen *S100A4*- und *PTH1H*-Genexpression in AC. Die Behandlung von AC mit rekombinantem humanem PTHrP₁₋₃₄-Peptid konnte die kalziumabhängige Reduktion der Knorpelmatrixablagerung teilweise reproduzieren, was auf eine Rolle von PTHrP für die Beeinträchtigung der Knorpelmatrixbildung hindeutete. Bemerkenswert war außerdem, dass die inverse Regulation der Matrixsynthese in AC und MSC-basierten Chondrozyten kalziumspezifisch war und nicht durch allgemeine hyperosmotische Effekte verursacht wurde. Eine langfristige extrazelluläre Kalziumstimulation bietet daher einen vielversprechenden neuen Ansatz um den Knorpelmatrixgehalt in MSC-basiertem Knorpelersatzgewebe zu verbessern, wohingegen solche Bedingungen während der Knorpelbildung von AC kontraproduktiv sind.

Insgesamt liefert diese Studie wichtige Erkenntnisse, um den Einfluss physikalisch-chemischer Reize auf die Knorpelmatrixbildung zu verstehen. Da nachgewiesen wurde, dass akuter hyperosmotischer Druck kein relevanter Parameter zur akuten Stimulation der Knorpelmatrixsynthese ist, sind nun weitere Studien erforderlich, um den Beitrag anderer belastungsinduzierter Subparameter zur Matrixsynthese zu untersuchen. Des Weiteren deckte diese Studie auf, dass eine langfristige Behandlung mit erhöhtem extrazellulärem Kalziumgehalt einen vielversprechenden neuen Ansatz liefert, um die Qualität von MSC-basiertem Knorpelersatzgewebe durch erhöhte Knorpelmatrixsynthese und -ablagerung zu verbessern. Für die Anwendung im osteochondralen Tissue Engineering würde dies bedeuten, dass MSC in Kombination mit resorbierbaren kalzifizierten Knochenersatzmaterialien die favorisierte Zellquelle für die Herstellung von Knorpelgewebe sein sollten. In weiteren Studien müssen die hier beobachteten Effekte von löslichem extrazellulärem Kalzium nun unter Verwendung resorbierbarer Knochenersatzmaterialien als potenzielle Kalziumquelle bestätigt werden.

8 References

- Ainscough, J. S., Gerberick, G. F., Kimber, I. and Dearman, R. J. (2015). **Interleukin-1beta Processing Is Dependent on a Calcium-mediated Interaction with Calmodulin.** *J Biol Chem* *290* (52), 31151-31161, doi: 10.1074/jbc.M115.680694.
- Al Faqeh, H., Nor Hamdan, B. M., Chen, H. C., Aminuddin, B. S. and Ruszymah, B. H. (2012). **The potential of intra-articular injection of chondrogenic-induced bone marrow stem cells to retard the progression of osteoarthritis in a sheep model.** *Exp Gerontol* *47* (6), 458-464, doi: 10.1016/j.exger.2012.03.018.
- Albro, M. B., Cigan, A. D., Nims, R. J., Yeroushalmi, K. J., Oungoulian, S. R., Hung, C. T. and Ateshian, G. A. (2012). **Shearing of synovial fluid activates latent TGF-beta.** *Osteoarthritis Cartilage* *20* (11), 1374-1382, doi: 10.1016/j.joca.2012.07.006.
- Allan, K. S., Pilliar, R. M., Wang, J., Grynblas, M. D. and Kandel, R. A. (2007). **Formation of biphasic constructs containing cartilage with a calcified zone interface.** *Tissue Eng* *13* (1), 167-177, doi: 10.1089/ten.2006.0081.
- Angele, P., Yoo, J. U., Smith, C., Mansour, J., Jepsen, K. J., Nerlich, M. and Johnstone, B. (2003). **Cyclic hydrostatic pressure enhances the chondrogenic phenotype of human mesenchymal progenitor cells differentiated in vitro.** *J Orthop Res* *21* (3), 451-457, doi: 10.1016/S0736-0266(02)00230-9.
- Annes, J. P., Chen, Y., Munger, J. S. and Rifkin, D. B. (2004). **Integrin alphaVbeta6-mediated activation of latent TGF-beta requires the latent TGF-beta binding protein-1.** *J Cell Biol* *165* (5), 723-734, doi: 10.1083/jcb.200312172.
- Aquino-Martinez, R., Artigas, N., Gamez, B., Rosa, J. L. and Ventura, F. (2017). **Extracellular calcium promotes bone formation from bone marrow mesenchymal stem cells by amplifying the effects of BMP-2 on SMAD signalling.** *PLoS One* *12* (5), e0178158, doi: 10.1371/journal.pone.0178158.
- Arden, N. and Nevitt, M. C. (2006). **Osteoarthritis: epidemiology.** *Best Pract Res Clin Rheumatol* *20* (1), 3-25, doi: 10.1016/j.berh.2005.09.007.
- Attur, M., Al-Mussawir, H. E., Patel, J., Kitay, A., Dave, M., Palmer, G., Pillinger, M. H. and Abramson, S. B. (2008). **Prostaglandin E2 exerts catabolic effects in osteoarthritis cartilage: evidence for signaling via the EP4 receptor.** *J Immunol* *181* (7), 5082-5088, doi: 10.4049/jimmunol.181.7.5082.
- Bachrach, N. M., Mow, V. C. and Guilak, F. (1998). **Incompressibility of the solid matrix of articular cartilage under high hydrostatic pressures.** *J Biomech* *31* (5), 445-451, doi: 10.1016/s0021-9290(98)00035-9.
- Baltz, J. M. (2012). **Media composition: salts and osmolality.** *Methods Mol Biol* *912*, 61-80, doi: 10.1007/978-1-61779-971-6_5.
- Barradas, A. M., Fernandes, H. A., Groen, N., Chai, Y. C., Schrooten, J., van de Peppel, J., van Leeuwen, J. P., van Blitterswijk, C. A. and de Boer, J. (2012). **A calcium-induced signaling**

- cascade leading to osteogenic differentiation of human bone marrow-derived mesenchymal stromal cells.** *Biomaterials* 33 (11), 3205-3215, doi: 10.1016/j.biomaterials.2012.01.020.
- Barradas, A. M., Monticone, V., Hulsman, M., Danoux, C., Fernandes, H., Tahmasebi Birgani, Z., Barrere-de Groot, F., Yuan, H., Reinders, M., Habibovic, P., van Blitterswijk, C. and de Boer, J. (2013). **Molecular mechanisms of biomaterial-driven osteogenic differentiation in human mesenchymal stromal cells.** *Integr Biol (Camb)* 5 (7), 920-931, doi: 10.1039/c3ib40027a.
- Barrett-Jolley, R., Lewis, R., Fallman, R. and Mobasher, A. (2010). **The emerging chondrocyte channelome.** *Front Physiol* 1, 135, doi: 10.3389/fphys.2010.00135.
- Bassleer, C. T., Combal, J. P., Bougaret, S. and Malaise, M. (1998). **Effects of chondroitin sulfate and interleukin-1 beta on human articular chondrocytes cultivated in clusters.** *Osteoarthritis Cartilage* 6 (3), 196-204, doi: 10.1053/joca.1998.0112.
- Baumgarten, M., Bloebaum, R. D., Ross, S. D., Campbell, P. and Sarmiento, A. (1985). **Normal human synovial fluid: osmolality and exercise-induced changes.** *J Bone Joint Surg Am* 67 (9), 1336-1339.
- Behrens, P., Bitter, T., Kurz, B. and Russlies, M. (2006). **Matrix-associated autologous chondrocyte transplantation/implantation (MACT/MACI)--5-year follow-up.** *Knee* 13 (3), 194-202, doi: 10.1016/j.knee.2006.02.012.
- Benya, P. D., Padilla, S. R. and Nimni, M. E. (1978). **Independent regulation of collagen types by chondrocytes during the loss of differentiated function in culture.** *Cell* 15 (4), 1313-1321, doi: 10.1016/0092-8674(78)90056-9.
- Billingham, R. C., Dahlberg, L., Ionescu, M., Reiner, A., Bourne, R., Rorabeck, C., Mitchell, P., Hambor, J., Diekmann, O., Tschesche, H., Chen, J., Van Wart, H. and Poole, A. R. (1997). **Enhanced cleavage of type II collagen by collagenases in osteoarthritic articular cartilage.** *J Clin Invest* 99 (7), 1534-1545, doi: 10.1172/JCI119316.
- Binger, K. J., Gebhardt, M., Heinig, M., Rintisch, C., Schroeder, A., Neuhofer, W., Hilgers, K., Manzel, A., Schwartz, C., Kleinewietfeld, M., Voelkl, J., Schatz, V., Linker, R. A., Lang, F., Voehringer, D., Wright, M. D., Hubner, N., Dechend, R., Jantsch, J., Titze, J. and Muller, D. N. (2015). **High salt reduces the activation of IL-4- and IL-13-stimulated macrophages.** *J Clin Invest* 125 (11), 4223-4238, doi: 10.1172/JCI80919.
- Blaney Davidson, E. N., Remst, D. F., Vitters, E. L., van Beuningen, H. M., Blom, A. B., Goumans, M. J., van den Berg, W. B. and van der Kraan, P. M. (2009). **Increase in ALK1/ALK5 ratio as a cause for elevated MMP-13 expression in osteoarthritis in humans and mice.** *J Immunol* 182 (12), 7937-7945, doi: 10.4049/jimmunol.0803991.
- Bonen, D. K. and Schmid, T. M. (1991). **Elevated extracellular calcium concentrations induce type X collagen synthesis in chondrocyte cultures.** *J Cell Biol* 115 (4), 1171-1178, doi: 10.1083/jcb.115.4.1171.

- Bradford, M. M. (1976). **A rapid and sensitive method for the quantitation of microgram quantities of protein utilizing the principle of protein-dye binding.** *Anal Biochem* 72, 248-254, doi: 10.1006/abio.1976.9999.
- Brady, M. A., Waldman, S. D. and Ethier, C. R. (2015). **The application of multiple biophysical cues to engineer functional neocartilage for treatment of osteoarthritis. Part II: signal transduction.** *Tissue Eng Part B Rev* 21 (1), 20-33, doi: 10.1089/ten.TEB.2013.0760.
- Brittberg, M., Lindahl, A., Nilsson, A., Ohlsson, C., Isaksson, O. and Peterson, L. (1994). **Treatment of deep cartilage defects in the knee with autologous chondrocyte transplantation.** *N Engl J Med* 331 (14), 889-895, doi: 10.1056/NEJM199410063311401.
- Brocher, J., Janicki, P., Voltz, P., Seebach, E., Neumann, E., Mueller-Ladner, U. and Richter, W. (2013). **Inferior ectopic bone formation of mesenchymal stromal cells from adipose tissue compared to bone marrow: rescue by chondrogenic pre-induction.** *Stem Cell Res* 11 (3), 1393-1406, doi: 10.1016/j.scr.2013.07.008.
- Brun, P., Dickinson, S. C., Zavan, B., Cortivo, R., Hollander, A. P. and Abatangelo, G. (2008). **Characteristics of repair tissue in second-look and third-look biopsies from patients treated with engineered cartilage: relationship to symptomatology and time after implantation.** *Arthritis Res Ther* 10 (6), R132, doi: 10.1186/ar2549.
- Buckwalter, J. A. and Mankin, H. J. (1998). **Articular cartilage: tissue design and chondrocyte-matrix interactions.** *Instr Course Lect* 47, 477-486.
- Burton, D. W., Foster, M., Johnson, K. A., Hiramoto, M., Deftos, L. J. and Terkeltaub, R. (2005). **Chondrocyte calcium-sensing receptor expression is up-regulated in early guinea pig knee osteoarthritis and modulates PTHrP, MMP-13, and TIMP-3 expression.** *Osteoarthritis Cartilage* 13 (5), 395-404, doi: 10.1016/j.joca.2005.01.002.
- Bush, P. G. and Hall, A. C. (2001). **The osmotic sensitivity of isolated and in situ bovine articular chondrocytes.** *J Orthop Res* 19 (5), 768-778, doi: 10.1016/S0736-0266(01)00013-4.
- Bush, P. G. and Hall, A. C. (2003). **The volume and morphology of chondrocytes within non-degenerate and degenerate human articular cartilage.** *Osteoarthritis and Cartilage* 11 (4), 242-251, doi: 10.1016/s1063-4584(02)00369-2.
- Cai, Q., Ferraris, J. D. and Burg, M. B. (2005). **High NaCl increases TonEBP/OREBP mRNA and protein by stabilizing its mRNA.** *Am J Physiol Renal Physiol* 289 (4), F803-807, doi: 10.1152/ajprenal.00448.2004.
- Calkhoven, C. F. and Ab, G. (1996). **Multiple steps in the regulation of transcription-factor level and activity.** *Biochem J* 317 (Pt 2) (Pt 2), 329-342, doi: 10.1042/bj3170329.
- Caplan, A. I. (1991). **Mesenchymal stem cells.** *J Orthop Res* 9 (5), 641-650, doi: 10.1002/jor.1100090504.
- Caron, M. M., van der Windt, A. E., Emans, P. J., van Rhijn, L. W., Jahr, H. and Welting, T. J. (2013). **Osmolarity determines the in vitro chondrogenic differentiation capacity of progenitor cells via nuclear factor of activated T-cells 5.** *Bone* 53 (1), 94-102, doi: 10.1016/j.bone.2012.11.032.

- Chang, W., Tu, C., Bajra, R., Komuves, L., Miller, S., Strewler, G. and Shoback, D. (1999a). **Calcium sensing in cultured chondrogenic RCJ3.1C5.18 cells.** *Endocrinology* *140* (4), 1911-1919, doi: 10.1210/endo.140.4.6639.
- Chang, W., Tu, C., Chen, T. H., Komuves, L., Oda, Y., Pratt, S. A., Miller, S. and Shoback, D. (1999b). **Expression and signal transduction of calcium-sensing receptors in cartilage and bone.** *Endocrinology* *140* (12), 5883-5893, doi: 10.1210/endo.140.12.7190.
- Chang, W., Tu, C., Pratt, S., Chen, T. H. and Shoback, D. (2002). **Extracellular Ca(2+)-sensing receptors modulate matrix production and mineralization in chondrogenic RCJ3.1C5.18 cells.** *Endocrinology* *143* (4), 1467-1474, doi: 10.1210/endo.143.4.8709.
- Chasan, S., Hesse, E., Atallah, P., Gerstner, M., Diederichs, S., Schenker, A., Grobe, K., Werner, C. and Richter, W. (2022). **Sulfation of glycosaminoglycan hydrogels instructs cell fate and chondral versus endochondral lineage decision of skeletal stem cells in vivo.** *Advanced Functional Materials* *32* (7), 2109176, doi: <https://doi.org/10.1002/adfm.202109176>.
- Chen, C., Tambe, D. T., Deng, L. and Yang, L. (2013). **Biomechanical properties and mechanobiology of the articular chondrocyte.** *Am J Physiol Cell Physiol* *305* (12), C1202-1208, doi: 10.1152/ajpcell.00242.2013.
- Chen, C., Wei, X., Wang, S., Jiao, Q., Zhang, Y., Du, G., Wang, X., Wei, F., Zhang, J. and Wei, L. (2016). **Compression regulates gene expression of chondrocytes through HDAC4 nuclear relocation via PP2A-dependent HDAC4 dephosphorylation.** *Biochim Biophys Acta* *1863* (7 Pt A), 1633-1642, doi: 10.1016/j.bbamcr.2016.04.018.
- Chen, M., Sinha, M., Luxon, B. A., Bresnick, A. R. and O'Connor, K. L. (2009). **Integrin alpha6beta4 controls the expression of genes associated with cell motility, invasion, and metastasis, including S100A4/metastasin.** *J Biol Chem* *284* (3), 1484-1494, doi: 10.1074/jbc.M803997200.
- Cheng, Z., Li, A., Tu, C. L., Maria, C. S., Szeto, N., Herberger, A., Chen, T. H., Song, F., Wang, J., Liu, X., Shoback, D. M. and Chang, W. (2020). **Calcium-sensing receptors in chondrocytes and osteoblasts are required for callus maturation and fracture healing in mice.** *J Bone Miner Res* *35* (1), 143-154, doi: 10.1002/jbmr.3864.
- Chevront, S. N., Kenefick, R. W., Heavens, K. R. and Spitz, M. G. (2014). **A comparison of whole blood and plasma osmolality and osmolarity.** *J Clin Lab Anal* *28* (5), 368-373, doi: 10.1002/jcla.21695.
- Choudhary, S., Kumar, A., Kale, R. K., Raisz, L. G. and Pilbeam, C. C. (2004). **Extracellular calcium induces COX-2 in osteoblasts via a PKA pathway.** *Biochem Biophys Res Commun* *322* (2), 395-402, doi: 10.1016/j.bbrc.2004.07.129.
- Choudhary, S., Wadhwa, S., Raisz, L. G., Alander, C. and Pilbeam, C. C. (2003). **Extracellular calcium is a potent inducer of cyclo-oxygenase-2 in murine osteoblasts through an ERK signaling pathway.** *J Bone Miner Res* *18* (10), 1813-1824, doi: 10.1359/jbmr.2003.18.10.1813.
- Chowdhury, T. T., Salter, D. M., Bader, D. L. and Lee, D. A. (2004). **Integrin-mediated mechanotransduction processes in TGFbeta-stimulated monolayer-expanded**

- chondrocytes.** *Biochem Biophys Res Commun* 318 (4), 873-881, doi: 10.1016/j.bbrc.2004.04.107.
- Cipollone, F., Iezzi, A., Fazia, M., Zucchelli, M., Pini, B., Cuccurullo, C., De Cesare, D., De Blasis, G., Muraro, R., Bei, R., Chiarelli, F., Schmidt, A. M., Cuccurullo, F. and Mezzetti, A. (2003). **The receptor RAGE as a progression factor amplifying arachidonate-dependent inflammatory and proteolytic response in human atherosclerotic plaques: role of glycemic control.** *Circulation* 108 (9), 1070-1077, doi: 10.1161/01.CIR.0000086014.80477.0D.
- Clemens, T. L., Cormier, S., Eichinger, A., Endlich, K., Fiaschi-Taesch, N., Fischer, E., Friedman, P. A., Karaplis, A. C., Massfelder, T., Rossert, J., Schluter, K. D., Silve, C., Stewart, A. F., Takane, K. and Helwig, J. J. (2001). **Parathyroid hormone-related protein and its receptors: nuclear functions and roles in the renal and cardiovascular systems, the placental trophoblasts and the pancreatic islets.** *Br J Pharmacol* 134 (6), 1113-1136, doi: 10.1038/sj.bjp.0704378.
- Dantas, L. O., Salvini, T. F. and McAlindon, T. E. (2021). **Knee osteoarthritis: key treatments and implications for physical therapy.** *Braz J Phys Ther* 25 (2), 135-146, doi: 10.1016/j.bjpt.2020.08.004.
- Dexheimer, V., Gabler, J., Bomans, K., Sims, T., Omlor, G. and Richter, W. (2016). **Differential expression of TGF-beta superfamily members and role of Smad1/5/9-signalling in chondral versus endochondral chondrocyte differentiation.** *Sci Rep* 6, 36655, doi: 10.1038/srep36655.
- Diao, H. J., Fung, H. S., Yeung, P., Lam, K. L., Yan, C. H. and Chan, B. P. (2017). **Dynamic cyclic compression modulates the chondrogenic phenotype in human chondrocytes from late stage osteoarthritis.** *Biochem Biophys Res Commun* 486 (1), 14-21, doi: 10.1016/j.bbrc.2017.02.073.
- Diederichs, S., Gabler, J., Autenrieth, J., Kynast, K. L., Merle, C., Walles, H., Utikal, J. and Richter, W. (2016). **Differential regulation of SOX9 protein during chondrogenesis of induced pluripotent stem cells versus mesenchymal stromal cells: A shortcoming for cartilage formation.** *Stem Cells Dev* 25 (8), 598-609, doi: 10.1089/scd.2015.0312.
- Diederichs, S., Tonniere, V., Marz, M., Dreher, S. I., Geisbusch, A. and Richter, W. (2019). **Regulation of WNT5A and WNT11 during MSC in vitro chondrogenesis: WNT inhibition lowers BMP and hedgehog activity, and reduces hypertrophy.** *Cell Mol Life Sci* 76 (19), 3875-3889, doi: 10.1007/s00018-019-03099-0.
- Dimicco, M. A., Kisiday, J. D., Gong, H. and Grodzinsky, A. J. (2007). **Structure of pericellular matrix around agarose-embedded chondrocytes.** *Osteoarthritis Cartilage* 15 (10), 1207-1216, doi: 10.1016/j.joca.2007.03.023.
- Dominici, M., Le Blanc, K., Mueller, I., Slaper-Cortenbach, I., Marini, F., Krause, D., Deans, R., Keating, A., Prockop, D. and Horwitz, E. (2006). **Minimal criteria for defining multipotent mesenchymal stromal cells. The International Society for Cellular Therapy position statement.** *Cytotherapy* 8 (4), 315-317, doi: 10.1080/14653240600855905.

- Donato, R., Cannon, B. R., Sorci, G., Riuzzi, F., Hsu, K., Weber, D. J. and Geczy, C. L. (2013). **Functions of S100 proteins.** *Curr Mol Med* 13 (1), 24-57.
- Dreher, S. I., Fischer, J., Walker, T., Diederichs, S. and Richter, W. (2020). **Significance of MEF2C and RUNX3 regulation for endochondral differentiation of human mesenchymal progenitor cells.** *Front Cell Dev Biol* 8, 81, doi: 10.3389/fcell.2020.00081.
- Elder, B. D. and Athanasiou, K. A. (2008). **Synergistic and additive effects of hydrostatic pressure and growth factors on tissue formation.** *PLoS One* 3 (6), e2341, doi: 10.1371/journal.pone.0002341.
- Erickson, G. R., Alexopoulos, L. G. and Guilak, F. (2001). **Hyper-osmotic stress induces volume change and calcium transients in chondrocytes by transmembrane, phospholipid, and G-protein pathways.** *J Biomech* 34 (12), 1527-1535, doi: 10.1016/s0021-9290(01)00156-7.
- Erickson, G. R., Northrup, D. L. and Guilak, F. (2003). **Hypo-osmotic stress induces calcium-dependent actin reorganization in articular chondrocytes.** *Osteoarthritis Cartilage* 11 (3), 187-197, doi: 10.1053/s1063-4584(02)00347-3.
- Erndt-Marino, J., Trinkle, E. and Hahn, M. S. (2019). **Hyperosmolar potassium (K(+)) treatment suppresses osteoarthritic chondrocyte catabolic and inflammatory protein production in a 3-dimensional in vitro model.** *Cartilage* 10 (2), 186-195, doi: 10.1177/1947603517734028.
- Evans, C. H. (2013). **Advances in regenerative orthopedics.** *Mayo Clin Proc* 88 (11), 1323-1339, doi: 10.1016/j.mayocp.2013.04.027.
- Eyrich, D., Wiese, H., Maier, G., Skodacek, D., Appel, B., Sarhan, H., Tessmar, J., Staudenmaier, R., Wenzel, M. M., Goepferich, A. and Blunk, T. (2007). **In vitro and in vivo cartilage engineering using a combination of chondrocyte-seeded long-term stable fibrin gels and polycaprolactone-based polyurethane scaffolds.** *Tissue Eng* 13 (9), 2207-2218, doi: 10.1089/ten.2006.0358.
- Fahy, N., Alini, M. and Stoddart, M. J. (2018). **Mechanical stimulation of mesenchymal stem cells: Implications for cartilage tissue engineering.** *J Orthop Res* 36 (1), 52-63, doi: 10.1002/jor.23670.
- Farndale, R. W., Buttle, D. J. and Barrett, A. J. (1986). **Improved quantitation and discrimination of sulphated glycosaminoglycans by use of dimethylmethylene blue.** *Biochim Biophys Acta* 883 (2), 173-177, doi: 10.1016/0304-4165(86)90306-5.
- Farnsworth, N. L., Mead, B. E., Antunez, L. R., Palmer, A. E. and Bryant, S. J. (2014). **Ionic osmolytes and intracellular calcium regulate tissue production in chondrocytes cultured in a 3D charged hydrogel.** *Matrix Biol* 40, 17-26, doi: 10.1016/j.matbio.2014.08.002.
- Fischer, J., Aulmann, A., Dexheimer, V., Grossner, T. and Richter, W. (2014). **Intermittent PTHrP(1-34) exposure augments chondrogenesis and reduces hypertrophy of mesenchymal stromal cells.** *Stem Cells Dev* 23 (20), 2513-2523, doi: 10.1089/scd.2014.0101.

- Fischer, J., Dickhut, A., Rickert, M. and Richter, W. (2010). **Human articular chondrocytes secrete parathyroid hormone-related protein and inhibit hypertrophy of mesenchymal stem cells in coculture during chondrogenesis.** *Arthritis Rheum* 62 (9), 2696-2706, doi: 10.1002/art.27565.
- Fischer, J., Knoch, N., Sims, T., Rosshirt, N. and Richter, W. (2018). **Time-dependent contribution of BMP, FGF, IGF, and HH signaling to the proliferation of mesenchymal stroma cells during chondrogenesis.** *J Cell Physiol* 233 (11), 8962-8970, doi: 10.1002/jcp.26832.
- Fitzgerald, J. B., Jin, M., Chai, D. H., Siparsky, P., Fanning, P. and Grodzinsky, A. J. (2008). **Shear and compression-induced chondrocyte transcription requires MAPK activation in cartilage explants.** *J Biol Chem* 283 (11), 6735-6743, doi: 10.1074/jbc.M708670200.
- Flechtenmacher, J., Huch, K., Thonar, E. J., Mollenhauer, J. A., Davies, S. R., Schmid, T. M., Puhl, W., Sampath, T. K., Aydelotte, M. B. and Kuettner, K. E. (1996). **Recombinant human osteogenic protein 1 is a potent stimulator of the synthesis of cartilage proteoglycans and collagens by human articular chondrocytes.** *Arthritis Rheum* 39 (11), 1896-1904, doi: 10.1002/art.1780391117.
- Foley, S., Ding, C., Cicutini, F. and Jones, G. (2007). **Physical activity and knee structural change: a longitudinal study using MRI.** *Med Sci Sports Exerc* 39 (3), 426-434, doi: 10.1249/mss.0b013e31802d97c6.
- Fuchs, J., Kuhnert, R. and Scheidt-Nave, C. (2017). **12-month prevalence of osteoarthritis in Germany** (Robert Koch-Institut, Epidemiologie und Gesundheitsberichterstattung, doi: 10.17886/rki-gbe-2017-066, p. ^pp.
- Furumatsu, T., Tsuda, M., Taniguchi, N., Tajima, Y. and Asahara, H. (2005). **Smad3 induces chondrogenesis through the activation of SOX9 via CREB-binding protein/p300 recruitment.** *J Biol Chem* 280 (9), 8343-8350, doi: 10.1074/jbc.M413913200.
- Gahunia, H., Gross, A., Pritzker, K., Babyn, P. and Murnaghan, L. (2020). **Articular Cartilage of the Knee.** Health, Disease and Therapy Springer. Recuperado de: <https://www.springer.com/gp/book/9781493975853>. <https://doi.org/10.1007/978-1-4939-7587-7>.
- Gao, L., McBeath, R. and Chen, C. S. (2010). **Stem cell shape regulates a chondrogenic versus myogenic fate through Rac1 and N-cadherin.** *Stem Cells* 28 (3), 564-572, doi: 10.1002/stem.308.
- Garrigues, N. W., Little, D., Sanchez-Adams, J., Ruch, D. S. and Guilak, F. (2014). **Electrospun cartilage-derived matrix scaffolds for cartilage tissue engineering.** *J Biomed Mater Res A* 102 (11), 3998-4008, doi: 10.1002/jbm.a.35068.
- Gelber, A. C., Hochberg, M. C., Mead, L. A., Wang, N. Y., Wigley, F. M. and Klag, M. J. (2000). **Joint injury in young adults and risk for subsequent knee and hip osteoarthritis.** *Ann Intern Med* 133 (5), 321-328, doi: 10.7326/0003-4819-133-5-200009050-00007.
- Gerstner, M., Severmann, A. C., Chasan, S., Vortkamp, A. and Richter, W. (2021). **Heparan sulfate deficiency in cartilage: Enhanced BMP-sensitivity, proteoglycan production and an anti-apoptotic expression signature after loading.** *Int J Mol Sci* 22 (7), doi: 10.3390/ijms22073726.

- Getgood, A. M., Kew, S. J., Brooks, R., Aberman, H., Simon, T., Lynn, A. K. and Rushton, N. (2012). **Evaluation of early-stage osteochondral defect repair using a biphasic scaffold based on a collagen-glycosaminoglycan biopolymer in a caprine model.** *Knee* 19 (4), 422-430, doi: 10.1016/j.knee.2011.03.011.
- Glatt, V., Evans, C. H. and Stoddart, M. J. (2019). **Regenerative rehabilitation: The role of mechanotransduction in orthopaedic regenerative medicine.** *J Orthop Res* 37 (6), 1263-1269, doi: 10.1002/jor.24205.
- Goldring, M. B., Tsuchimochi, K. and Ijiri, K. (2006). **The control of chondrogenesis.** *J Cell Biochem* 97 (1), 33-44, doi: 10.1002/jcb.20652.
- Gotterbarm, T., Richter, W., Jung, M., Berardi Vilei, S., Mainil-Varlet, P., Yamashita, T. and Breusch, S. J. (2006). **An in vivo study of a growth-factor enhanced, cell free, two-layered collagen-tricalcium phosphate in deep osteochondral defects.** *Biomaterials* 27 (18), 3387-3395, doi: 10.1016/j.biomaterials.2006.01.041.
- Goyal, D., Keyhani, S., Lee, E. H. and Hui, J. H. (2013). **Evidence-based status of microfracture technique: a systematic review of level I and II studies.** *Arthroscopy* 29 (9), 1579-1588, doi: 10.1016/j.arthro.2013.05.027.
- Graceffa, V., Vinatier, C., Guicheux, J., Stoddart, M., Alini, M. and Zeugolis, D. I. (2019). **Chasing Chimeras - The elusive stable chondrogenic phenotype.** *Biomaterials* 192, 199-225, doi: 10.1016/j.biomaterials.2018.11.014.
- Grande, D. A., Pitman, M. I., Peterson, L., Menche, D. and Klein, M. (1989). **The repair of experimentally produced defects in rabbit articular cartilage by autologous chondrocyte transplantation.** *J Orthop Res* 7 (2), 208-218, doi: 10.1002/jor.1100070208.
- Guilak, F. (1995). **Compression-induced changes in the shape and volume of the chondrocyte nucleus.** *J Biomech* 28 (12), 1529-1541, doi: 10.1016/0021-9290(95)00100-x.
- Guilak, F., Alexopoulos, L. G., Upton, M. L., Youn, I., Choi, J. B., Cao, L., Setton, L. A. and Haider, M. A. (2006). **The pericellular matrix as a transducer of biomechanical and biochemical signals in articular cartilage.** *Ann N Y Acad Sci* 1068, 498-512, doi: 10.1196/annals.1346.011.
- Guilak, F. and Mow, V. C. (2000). **The mechanical environment of the chondrocyte: a biphasic finite element model of cell-matrix interactions in articular cartilage.** *J Biomech* 33 (12), 1663-1673.
- Guilak, F., Zell, R. A., Erickson, G. R., Grande, D. A., Rubin, C. T., McLeod, K. J. and Donahue, H. J. (1999). **Mechanically induced calcium waves in articular chondrocytes are inhibited by gadolinium and amiloride.** *J Orthop Res* 17 (3), 421-429, doi: 10.1002/jor.1100170319.
- Hall, A. C. (1995). **Volume-sensitive taurine transport in bovine articular chondrocytes.** *J Physiol* 484 (Pt 3), 755-766, doi: 10.1113/jphysiol.1995.sp020701.

- Hall, A. C. (2019). **The role of chondrocyte morphology and volume in controlling phenotype-implications for osteoarthritis, cartilage repair, and cartilage engineering.** *Curr Rheumatol Rep* 21 (8), 38, doi: 10.1007/s11926-019-0837-6.
- Hall, A. C., Horwitz, E. R. and Wilkins, R. J. (1996a). **The cellular physiology of articular cartilage.** *Exp Physiol* 81 (3), 535-545, doi: 10.1113/expphysiol.1996.sp003956.
- Hall, A. C., Starks, I., Shoults, C. L. and Rashidbigi, S. (1996b). **Pathways for K⁺ transport across the bovine articular chondrocyte membrane and their sensitivity to cell volume.** *Am J Physiol* 270 (5 Pt 1), C1300-1310, doi: 10.1152/ajpcell.1996.270.5.C1300.
- Han, S. K., Wouters, W., Clark, A. and Herzog, W. (2012). **Mechanically induced calcium signaling in chondrocytes in situ.** *J Orthop Res* 30 (3), 475-481, doi: 10.1002/jor.21536.
- Hdud, I. M., Mobasheri, A. and Loughna, P. T. (2014). **Effect of osmotic stress on the expression of TRPV4 and BKCa channels and possible interaction with ERK1/2 and p38 in cultured equine chondrocytes.** *Am J Physiol Cell Physiol* 306 (11), C1050-1057, doi: 10.1152/ajpcell.00287.2013.
- Healy, C., Uwanogho, D. and Sharpe, P. T. (1999). **Regulation and role of Sox9 in cartilage formation.** *Dev Dyn* 215 (1), 69-78, doi: 10.1002/(SICI)1097-0177(199905)215:1<69::AID-DVDY8>3.0.CO;2-N.
- Hecht, N., Johnstone, B., Angele, P., Walker, T. and Richter, W. (2019). **Mechanosensitive MiRs regulated by anabolic and catabolic loading of human cartilage.** *Osteoarthritis Cartilage* 27 (8), 1208-1218, doi: 10.1016/j.joca.2019.04.010.
- Heldin, C. H., Miyazono, K. and ten Dijke, P. (1997). **TGF-beta signalling from cell membrane to nucleus through SMAD proteins.** *Nature* 390 (6659), 465-471, doi: 10.1038/37284.
- Hellingman, C. A., Davidson, E. N., Koevoet, W., Vitters, E. L., van den Berg, W. B., van Osch, G. J. and van der Kraan, P. M. (2011). **Smad signaling determines chondrogenic differentiation of bone-marrow-derived mesenchymal stem cells: inhibition of Smad1/5/8P prevents terminal differentiation and calcification.** *Tissue Eng Part A* 17 (7-8), 1157-1167, doi: 10.1089/ten.TEA.2010.0043.
- Hoffmann, E. K., Lambert, I. H. and Pedersen, S. F. (2009). **Physiology of cell volume regulation in vertebrates.** *Physiol Rev* 89 (1), 193-277, doi: 10.1152/physrev.00037.2007.
- Hofmann, M. A., Drury, S., Hudson, B. I., Gleason, M. R., Qu, W., Lu, Y., Lalla, E., Chitnis, S., Monteiro, J., Stickland, M. H., Bucciarelli, L. G., Moser, B., Moxley, G., Itescu, S., Grant, P. J., Gregersen, P. K., Stern, D. M. and Schmidt, A. M. (2002). **RAGE and arthritis: the G82S polymorphism amplifies the inflammatory response.** *Genes Immun* 3 (3), 123-135, doi: 10.1038/sj.gene.6363861.
- Hopewell, B. and Urban, J. P. (2003). **Adaptation of articular chondrocytes to changes in osmolality.** *Biorheology* 40 (1-3), 73-77.
- Hoppe, A., Guldal, N. S. and Boccaccini, A. R. (2011). **A review of the biological response to ionic dissolution products from bioactive glasses and glass-ceramics.** *Biomaterials* 32 (11), 2757-2774, doi: 10.1016/j.biomaterials.2011.01.004.

- Howard, T. A., Murray, I. R., Amin, A. K., Simpson, A. H. and Hall, A. C. (2020). **Damage control articular surgery: Maintaining chondrocyte health and minimising iatrogenic injury.** *Injury* 51 Suppl 2, S83-S89, doi: 10.1016/j.injury.2019.10.072.
- Hu, J. C. and Athanasiou, K. A. (2006). **A self-assembling process in articular cartilage tissue engineering.** *Tissue Eng* 12 (4), 969-979, doi: 10.1089/ten.2006.12.969.
- Hunziker, E. B. (2009). **The elusive path to cartilage regeneration.** *Adv Mater* 21 (32-33), 3419-3424, doi: 10.1002/adma.200801957.
- Hurskainen, T. L., Hirohata, S., Seldin, M. F. and Apte, S. S. (1999). **ADAM-TS5, ADAM-TS6, and ADAM-TS7, novel members of a new family of zinc metalloproteases. General features and genomic distribution of the ADAM-TS family.** *J Biol Chem* 274 (36), 25555-25563, doi: 10.1074/jbc.274.36.25555.
- Jahr, H., van der Windt, A. E., Timur, U. T., Baart, E. B., Lian, W. S., Rolauffs, B., Wang, F. S. and Pufe, T. (2022). **Physosmotic induction of chondrogenic maturation is TGF-beta dependent and enhanced by calcineurin inhibitor FK506.** *Int J Mol Sci* 23 (9), doi: 10.3390/ijms23095110.
- Jeon, J. E., Schrobback, K., Hutmacher, D. W. and Klein, T. J. (2012). **Dynamic compression improves biosynthesis of human zonal chondrocytes from osteoarthritis patients.** *Osteoarthritis Cartilage* 20 (8), 906-915, doi: 10.1016/j.joca.2012.04.019.
- Johnstone, B., Hering, T. M., Caplan, A. I., Goldberg, V. M. and Yoo, J. U. (1998). **In vitro chondrogenesis of bone marrow-derived mesenchymal progenitor cells.** *Exp Cell Res* 238 (1), 265-272, doi: 10.1006/excr.1997.3858.
- Kandel, R. A., Grynopas, M., Pilliar, R., Lee, J., Wang, J., Waldman, S., Zalzal, P. and Hurtig, M. (2006). **Repair of osteochondral defects with biphasic cartilage-calcium polyphosphate constructs in a sheep model.** *Biomaterials* 27 (22), 4120-4131, doi: 10.1016/j.biomaterials.2006.03.005.
- Kim, Y. J., Sah, R. L., Grodzinsky, A. J., Plaas, A. H. and Sandy, J. D. (1994). **Mechanical regulation of cartilage biosynthetic behavior: physical stimuli.** *Arch Biochem Biophys* 311 (1), 1-12, doi: 10.1006/abbi.1994.1201.
- Kiviranta, I., Jurvelin, J., Tammi, M., Saamanen, A. M. and Helminen, H. J. (1987). **Weight bearing controls glycosaminoglycan concentration and articular cartilage thickness in the knee joints of young beagle dogs.** *Arthritis Rheum* 30 (7), 801-809, doi: 10.1002/art.1780300710.
- Kleinewietfeld, M., Manzel, A., Titze, J., Kvakan, H., Yosef, N., Linker, R. A., Muller, D. N. and Hafler, D. A. (2013). **Sodium chloride drives autoimmune disease by the induction of pathogenic TH17 cells.** *Nature* 496 (7446), 518-522, doi: 10.1038/nature11868.
- Knecht, S., Vanwanseele, B. and Stussi, E. (2006). **A review on the mechanical quality of articular cartilage - implications for the diagnosis of osteoarthritis.** *Clin Biomech (Bristol, Avon)* 21 (10), 999-1012, doi: 10.1016/j.clinbiomech.2006.07.001.

- Koyano, Y., Hejna, M., Flechtenmacher, J., Schmid, T. M., Thonar, E. J. and Mollenhauer, J. (1996). **Collagen and proteoglycan production by bovine fetal and adult chondrocytes under low levels of calcium and zinc ions.** *Connect Tissue Res* 34 (3), 213-225, doi: 10.3109/03008209609000700.
- Kreuz, P. C., Steinwachs, M. R., Erggelet, C., Krause, S. J., Konrad, G., Uhl, M. and Sudkamp, N. (2006). **Results after microfracture of full-thickness chondral defects in different compartments in the knee.** *Osteoarthritis Cartilage* 14 (11), 1119-1125, doi: 10.1016/j.joca.2006.05.003.
- Kunisch, E., Knauf, A. K., Hesse, E., Freudenberg, U., Werner, C., Bothe, F., Diederichs, S. and Richter, W. (2018). **StarPEG/heparin-hydrogel based in vivo engineering of stable bizonal cartilage with a calcified bottom layer.** *Biofabrication* 11 (1), 015001, doi: 10.1088/1758-5090/aae75a.
- Kusanagi, K., Inoue, H., Ishidou, Y., Mishima, H. K., Kawabata, M. and Miyazono, K. (2000). **Characterization of a bone morphogenetic protein-responsive Smad-binding element.** *Mol Biol Cell* 11 (2), 555-565, doi: 10.1091/mbc.11.2.555.
- Lai, W. M., Hou, J. S. and Mow, V. C. (1991). **A triphasic theory for the swelling and deformation behaviors of articular cartilage.** *J Biomech Eng* 113 (3), 245-258, doi: 10.1115/1.2894880.
- Langer, R. and Vacanti, J. P. (1993). **Tissue engineering.** *Science* 260 (5110), 920-926, doi: 10.1126/science.8493529.
- LaPrade, R. F., Botker, J., Herzog, M. and Agel, J. (2009). **Refrigerated osteoarticular allografts to treat articular cartilage defects of the femoral condyles. A prospective outcomes study.** *J Bone Joint Surg Am* 91 (4), 805-811, doi: 10.2106/JBJS.H.00703.
- LaPrade, R. F., Bursch, L. S., Olson, E. J., Havlas, V. and Carlson, C. S. (2008). **Histologic and immunohistochemical characteristics of failed articular cartilage resurfacing procedures for osteochondritis of the knee: a case series.** *Am J Sports Med* 36 (2), 360-368, doi: 10.1177/0363546507308359.
- Levorson, E. J., Raman Sreerekha, P., Chennazhi, K. P., Kasper, F. K., Nair, S. V. and Mikos, A. G. (2013). **Fabrication and characterization of multiscale electrospun scaffolds for cartilage regeneration.** *Biomed Mater* 8 (1), 014103, doi: 10.1088/1748-6041/8/1/014103.
- Li, H., Seitz, P. K., Selvanayagam, P., Rajaraman, S. and Cooper, C. W. (1996). **Effect of endogenously produced parathyroid hormone-related peptide on growth of a human hepatoma cell line (Hep G2).** *Endocrinology* 137 (6), 2367-2374, doi: 10.1210/endo.137.6.8641188.
- Liedtke, W. (2007). **TRPV channels' role in osmotransduction and mechanotransduction.** *Handb Exp Pharmacol* (179), 473-487, doi: 10.1007/978-3-540-34891-7_28.
- Litwic, A., Edwards, M. H., Dennison, E. M. and Cooper, C. (2013). **Epidemiology and burden of osteoarthritis.** *Br Med Bull* 105, 185-199, doi: 10.1093/bmb/lds038.

- Lodish, H., Berk, A., Zipursky, S., Matsudaira, P., Baltimore, D. and Darnell, J. (2000). **Osmosis, water channels, and the regulation of cell volume.** In: Molecular Cell Biology, ed. Freeman, W., 4th Edition. edn, New York, USA.
- Loeser, R. F. (2014). **Integrins and chondrocyte-matrix interactions in articular cartilage.** Matrix Biol 39, 11-16, doi: 10.1016/j.matbio.2014.08.007.
- Lopa, S. and Madry, H. (2014). **Bioinspired scaffolds for osteochondral regeneration.** Tissue Eng Part A 20 (15-16), 2052-2076, doi: 10.1089/ten.tea.2013.0356.
- Lopez-Rodriguez, C., Antos, C. L., Shelton, J. M., Richardson, J. A., Lin, F., Novobrantseva, T. I., Bronson, R. T., Igarashi, P., Rao, A. and Olson, E. N. (2004). **Loss of NFAT5 results in renal atrophy and lack of tonicity-responsive gene expression.** Proc Natl Acad Sci U S A 101 (8), 2392-2397, doi: 10.1073/pnas.0308703100.
- Lu, X. L., Sun, D. D., Guo, X. E., Chen, F. H., Lai, W. M. and Mow, V. C. (2004). **Indentation determined mechano-electrochemical properties and fixed charge density of articular cartilage.** Ann Biomed Eng 32 (3), 370-379, doi: 10.1023/b:abme.0000017534.06921.24.
- Lückgen, J. (2022) **Biologische Mechanokompetenz von humanem Knorpelersatzgewebe: die Rolle von Zellherkunft und Signalkaskaden.** Dissertation, Universität Heidelberg.
- Lückgen, J., Raque, E., Reiner, T., Diederichs, S. and Richter, W. (2022). **NFkappaB inhibition to lift the mechano-competence of mesenchymal stromal cell-derived neocartilage toward articular chondrocyte levels.** Stem Cell Res Ther 13 (1), 168, doi: 10.1186/s13287-022-02843-x.
- Luyten, F. P., Chen, P., Paralkar, V. and Reddi, A. H. (1994). **Recombinant bone morphogenetic protein-4, transforming growth factor-beta 1, and activin A enhance the cartilage phenotype of articular chondrocytes in vitro.** Exp Cell Res 210 (2), 224-229, doi: 10.1006/excr.1994.1033.
- Madej, W., van Caam, A., Blaney Davidson, E. N., van der Kraan, P. M. and Buma, P. (2014). **Physiological and excessive mechanical compression of articular cartilage activates Smad2/3P signaling.** Osteoarthritis Cartilage 22 (7), 1018-1025, doi: 10.1016/j.joca.2014.04.024.
- Maroudas, A. (1980). **6 - Physical chemistry of articular cartilage and the intervertebral disc.** In: The Joints and Synovial Fluid, ed. Sokoloff, L., Academic Press, pp. 239-291.
- Maroudas, A., Ziv, I., Weisman, N. and Venn, M. (1985). **Studies of hydration and swelling pressure in normal and osteoarthritic cartilage.** Biorheology 22 (2), 159-169, doi: 10.3233/bir-1985-22206.
- Maroudas, A. I. (1976). **Balance between swelling pressure and collagen tension in normal and degenerate cartilage.** Nature 260 (5554), 808-809, doi: 10.1038/260808a0.
- Martin, T. J., Sims, N. A. and Seeman, E. (2021). **Physiological and pharmacological roles of PTH and PTHrP in bone using their shared receptor, PTH1R.** Endocr Rev 42 (4), 383-406, doi: 10.1210/endrev/bnab005.

- Matta, C. and Zakany, R. (2013). **Calcium signalling in chondrogenesis: implications for cartilage repair.** *Front Biosci (Schol Ed)* 5, 305-324, doi: 10.2741/s374.
- McGlashan, S. R., Jensen, C. G. and Poole, C. A. (2006). **Localization of extracellular matrix receptors on the chondrocyte primary cilium.** *J Histochem Cytochem* 54 (9), 1005-1014, doi: 10.1369/jhc.5A6866.2006.
- Mellor, L. F., Mohiti-Asli, M., Williams, J., Kannan, A., Dent, M. R., Guilak, F. and Lobo, E. G. (2015). **Extracellular calcium modulates chondrogenic and osteogenic differentiation of human adipose-derived stem cells: A novel approach for osteochondral tissue engineering using a single stem cell source.** *Tissue Eng Part A* 21 (17-18), 2323-2333, doi: 10.1089/ten.TEA.2014.0572.
- Morancho, B., Minguillon, J., Molkenin, J. D., Lopez-Rodriguez, C. and Aramburu, J. (2008). **Analysis of the transcriptional activity of endogenous NFAT5 in primary cells using transgenic NFAT-luciferase reporter mice.** *BMC Mol Biol* 9, 13, doi: 10.1186/1471-2199-9-13.
- Mow, V. C., Wang, C. C. and Hung, C. T. (1999). **The extracellular matrix, interstitial fluid and ions as a mechanical signal transducer in articular cartilage.** *Osteoarthritis Cartilage* 7 (1), 41-58, doi: 10.1053/joca.1998.0161.
- Mueller, M. B., Fischer, M., Zellner, J., Berner, A., Dienstknecht, T., Kujat, R., Prantl, L., Nerlich, M., Tuan, R. S. and Angele, P. (2013). **Effect of parathyroid hormone-related protein in an in vitro hypertrophy model for mesenchymal stem cell chondrogenesis.** *Int Orthop* 37 (5), 945-951, doi: 10.1007/s00264-013-1800-1.
- Muhammad, H., Rais, Y., Miosge, N. and Ornan, E. M. (2012). **The primary cilium as a dual sensor of mechanochemical signals in chondrocytes.** *Cell Mol Life Sci* 69 (13), 2101-2107, doi: 10.1007/s00018-011-0911-3.
- Na, K. Y., Woo, S. K., Lee, S. D. and Kwon, H. M. (2003). **Silencing of TonEBP/NFAT5 transcriptional activator by RNA interference.** *J Am Soc Nephrol* 14 (2), 283-288, doi: 10.1097/01.asn.0000045050.19544.b2.
- Nebelung, S., Gavenis, K., Rath, B., Tingart, M., Ladenburger, A., Stoffel, M., Zhou, B. and Mueller-Rath, R. (2011). **Continuous cyclic compressive loading modulates biological and mechanical properties of collagen hydrogels seeded with human chondrocytes.** *Biorheology* 48 (5), 247-261, doi: 10.3233/BIR-2012-0597.
- Negoro, K., Kobayashi, S., Takeno, K., Uchida, K. and Baba, H. (2008). **Effect of osmolarity on glycosaminoglycan production and cell metabolism of articular chondrocyte under three-dimensional culture system.** *Clin Exp Rheumatol* 26 (4), 534-541.
- Ng, L., Hung, H. H., Sprunt, A., Chubinskaya, S., Ortiz, C. and Grodzinsky, A. (2007). **Nanomechanical properties of individual chondrocytes and their developing growth factor-stimulated pericellular matrix.** *J Biomech* 40 (5), 1011-1023, doi: 10.1016/j.jbiomech.2006.04.004.
- O'Connor, C. J., Case, N. and Guilak, F. (2013). **Mechanical regulation of chondrogenesis.** *Stem Cell Res Ther* 4 (4), 61, doi: 10.1186/scrt211.

- O'Connor, C. J., Leddy, H. A., Benefield, H. C., Liedtke, W. B. and Guilak, F. (2014). **TRPV4-mediated mechanotransduction regulates the metabolic response of chondrocytes to dynamic loading.** *Proc Natl Acad Sci U S A* *111* (4), 1316-1321, doi: 10.1073/pnas.1319569111.
- Onda, K., Yamaguchi, M., Ohashi, M., Sato, R., Ochiai, H., Iriki, T. and Wada, Y. (2010). **Modification of the analysis of parathyroid hormone-related protein in milk and concentrations of this protein in commercial milk and milk products in Japan.** *J Dairy Sci* *93* (5), 1861-1867, doi: 10.3168/jds.2009-2746.
- Palmer, G. D., Chao Ph, P. H., Raia, F., Mauck, R. L., Valhmu, W. B. and Hung, C. T. (2001). **Time-dependent aggrecan gene expression of articular chondrocytes in response to hyperosmotic loading.** *Osteoarthritis Cartilage* *9* (8), 761-770, doi: 10.1053/joca.2001.0473.
- Park, J. Y., Pillinger, M. H. and Abramson, S. B. (2006). **Prostaglandin E2 synthesis and secretion: the role of PGE2 synthases.** *Clin Immunol* *119* (3), 229-240, doi: 10.1016/j.clim.2006.01.016.
- Parkkinen, J. J., Ikonen, J., Lammi, M. J., Laakkonen, J., Tammi, M. and Helminen, H. J. (1993). **Effects of cyclic hydrostatic pressure on proteoglycan synthesis in cultured chondrocytes and articular cartilage explants.** *Arch Biochem Biophys* *300* (1), 458-465, doi: 10.1006/abbi.1993.1062.
- Peffer, M. J., Milner, P. I., Tew, S. R. and Clegg, P. D. (2010). **Regulation of SOX9 in normal and osteoarthritic equine articular chondrocytes by hyperosmotic loading.** *Osteoarthritis Cartilage* *18* (11), 1502-1508, doi: 10.1016/j.joca.2010.08.011.
- Pelttari, K., Lorenz, H., Boeuf, S., Templin, M. F., Bischel, O., Goetzke, K., Hsu, H. Y., Steck, E. and Richter, W. (2008). **Secretion of matrix metalloproteinase 3 by expanded articular chondrocytes as a predictor of ectopic cartilage formation capacity in vivo.** *Arthritis Rheum* *58* (2), 467-474, doi: 10.1002/art.23302.
- Pelttari, K., Winter, A., Steck, E., Goetzke, K., Hennig, T., Ochs, B. G., Aigner, T. and Richter, W. (2006). **Premature induction of hypertrophy during in vitro chondrogenesis of human mesenchymal stem cells correlates with calcification and vascular invasion after ectopic transplantation in SCID mice.** *Arthritis Rheum* *54* (10), 3254-3266, doi: 10.1002/art.22136.
- Peterson, L., Vasiliadis, H. S., Brittberg, M. and Lindahl, A. (2010). **Autologous chondrocyte implantation: a long-term follow-up.** *Am J Sports Med* *38* (6), 1117-1124, doi: 10.1177/0363546509357915.
- Phan, M. N., Leddy, H. A., Votta, B. J., Kumar, S., Levy, D. S., Lipshutz, D. B., Lee, S. H., Liedtke, W. and Guilak, F. (2009). **Functional characterization of TRPV4 as an osmotically sensitive ion channel in porcine articular chondrocytes.** *Arthritis Rheum* *60* (10), 3028-3037, doi: 10.1002/art.24799.
- Pittenger, M. F., Mackay, A. M., Beck, S. C., Jaiswal, R. K., Douglas, R., Mosca, J. D., Moorman, M. A., Simonetti, D. W., Craig, S. and Marshak, D. R. (1999). **Multilineage potential of adult**

- human mesenchymal stem cells.** *Science* 284 (5411), 143-147, doi: 10.1126/science.284.5411.143.
- Praxenthaler, H., Kramer, E., Weisser, M., Hecht, N., Fischer, J., Grossner, T. and Richter, W. (2018). **Extracellular matrix content and WNT/beta-catenin levels of cartilage determine the chondrocyte response to compressive load.** *Biochim Biophys Acta Mol Basis Dis* 1864 (3), 851-859, doi: 10.1016/j.bbadis.2017.12.024.
- Quinn, T. M., Grodzinsky, A. J., Buschmann, M. D., Kim, Y. J. and Hunziker, E. B. (1998). **Mechanical compression alters proteoglycan deposition and matrix deformation around individual cells in cartilage explants.** *J Cell Sci* 111 (Pt 5), 573-583, doi: 10.1242/jcs.111.5.573.
- Racunica, T. L., Teichtahl, A. J., Wang, Y., Wluka, A. E., English, D. R., Giles, G. G., O'Sullivan, R. and Cicuttini, F. M. (2007). **Effect of physical activity on articular knee joint structures in community-based adults.** *Arthritis Rheum* 57 (7), 1261-1268, doi: 10.1002/art.22990.
- Racz, B., Reglodi, D., Fodor, B., Gasz, B., Lubics, A., Gallyas, F., Jr., Roth, E. and Borsiczky, B. (2007). **Hyperosmotic stress-induced apoptotic signaling pathways in chondrocytes.** *Bone* 40 (6), 1536-1543, doi: 10.1016/j.bone.2007.02.011.
- Ramage, L., Nuki, G. and Salter, D. M. (2009). **Signalling cascades in mechanotransduction: cell-matrix interactions and mechanical loading.** *Scand J Med Sci Sports* 19 (4), 457-469, doi: 10.1111/j.1600-0838.2009.00912.x.
- Reboul, P., Pelletier, J. P., Tardif, G., Cloutier, J. M. and Martel-Pelletier, J. (1996). **The new collagenase, collagenase-3, is expressed and synthesized by human chondrocytes but not by synoviocytes. A role in osteoarthritis.** *J Clin Invest* 97 (9), 2011-2019, doi: 10.1172/JCI118636.
- Redini, F., Galera, P., Mauviel, A., Loyau, G. and Pujol, J. P. (1988). **Transforming growth factor beta stimulates collagen and glycosaminoglycan biosynthesis in cultured rabbit articular chondrocytes.** *FEBS Lett* 234 (1), 172-176, doi: 10.1016/0014-5793(88)81327-9.
- Responde, D. J., Lee, J. K., Hu, J. C. and Athanasiou, K. A. (2012). **Biomechanics-driven chondrogenesis: from embryo to adult.** *FASEB J* 26 (9), 3614-3624, doi: 10.1096/fj.12-207241.
- Richter, D. L., Schenck, R. C., Jr., Wascher, D. C. and Treme, G. (2016). **Knee articular cartilage repair and restoration techniques: A review of the literature.** *Sports Health* 8 (2), 153-160, doi: 10.1177/1941738115611350.
- Rodriguez, L., Cheng, Z., Chen, T. H., Tu, C. and Chang, W. (2005). **Extracellular calcium and parathyroid hormone-related peptide signaling modulate the pace of growth plate chondrocyte differentiation.** *Endocrinology* 146 (11), 4597-4608, doi: 10.1210/en.2005-0437.
- Rogers, B. A., Murphy, C. L., Cannon, S. R. and Briggs, T. W. (2006). **Topographical variation in glycosaminoglycan content in human articular cartilage.** *J Bone Joint Surg Br* 88 (12), 1670-1674, doi: 10.1302/0301-620X.88B12.18132.

- Sah, R. L., Kim, Y. J., Doong, J. Y., Grodzinsky, A. J., Plaas, A. H. and Sandy, J. D. (1989). **Biosynthetic response of cartilage explants to dynamic compression.** *J Orthop Res* 7 (5), 619-636, doi: 10.1002/jor.1100070502.
- Sampat, S. R., Dermksian, M. V., Oungouljian, S. R., Winchester, R. J., Bulinski, J. C., Ateshian, G. A. and Hung, C. T. (2013). **Applied osmotic loading for promoting development of engineered cartilage.** *J Biomech* 46 (15), 2674-2681, doi: 10.1016/j.jbiomech.2013.07.043.
- San Antonio, J. D. and Tuan, R. S. (1986). **Chondrogenesis of limb bud mesenchyme in vitro: stimulation by cations.** *Dev Biol* 115 (2), 313-324, doi: 10.1016/0012-1606(86)90252-6.
- Sarem, M., Heizmann, M., Barbero, A., Martin, I. and Shastri, V. P. (2018). **Hyperstimulation of CaSR in human MSCs by biomimetic apatite inhibits endochondral ossification via temporal down-regulation of PTH1R.** *Proc Natl Acad Sci U S A* 115 (27), E6135-E6144, doi: 10.1073/pnas.1805159115.
- Schneiderman, R., Keret, D. and Maroudas, A. (1986). **Effects of mechanical and osmotic pressure on the rate of glycosaminoglycan synthesis in the human adult femoral head cartilage: an in vitro study.** *J Orthop Res* 4 (4), 393-408, doi: 10.1002/jor.1100040402.
- Scholtes, S., Krämer, E., Weisser, M., Roth, W., Luginbühl, R., Grossner, T. and Richter, W. (2018). **Global chondrocyte gene expression after a single anabolic loading period: Time evolution and re-inducibility of mechano-responses.** *J Cell Physiol* 233 (1), 699-711, doi: 10.1002/jcp.25933.
- Schulze-Tanzil, G., de Souza, P., Villegas Castrejón, H., John, T., Merker, H. J., Scheid, A. and Shakibaie, M. (2002). **Redifferentiation of dedifferentiated human chondrocytes in high-density cultures.** *Cell Tissue Res* 308 (3), 371-379, doi: 10.1007/s00441-002-0562-7.
- Seguin, C. A. and Bernier, S. M. (2003). **TNF α suppresses link protein and type II collagen expression in chondrocytes: Role of MEK1/2 and NF-kappaB signaling pathways.** *J Cell Physiol* 197 (3), 356-369, doi: 10.1002/jcp.10371.
- Sheikh-Hamad, D. and Gustin, M. C. (2004). **MAP kinases and the adaptive response to hypertonicity: functional preservation from yeast to mammals.** *Am J Physiol Renal Physiol* 287 (6), F1102-1110, doi: 10.1152/ajprenal.00225.2004.
- Shoback, D. M., Thatcher, J. G. and Brown, E. M. (1984). **Interaction of extracellular calcium and magnesium in the regulation of cytosolic calcium and PTH release in dispersed bovine parathyroid cells.** *Mol Cell Endocrinol* 38 (2-3), 179-186, doi: 10.1016/0303-7207(84)90116-3.
- Shulman, H. J. and Opler, A. (1974). **The stimulatory effect of calcium on the synthesis of cartilage proteoglycan.** *Biochem Biophys Res Commun* 59 (3), 914-919, doi: 10.1016/s0006-291x(74)80066-5.
- Sieber, S., Michaelis, M., Guhring, H., Lindemann, S. and Gigout, A. (2020). **Importance of osmolarity and oxygen tension for cartilage tissue engineering.** *Biores Open Access* 9 (1), 106-115, doi: 10.1089/biores.2020.0009.

- St-Pierre, J. P., Gan, L., Wang, J., Pilliar, R. M., Gryn timer, M. D. and Kandel, R. A. (2012). **The incorporation of a zone of calcified cartilage improves the interfacial shear strength between in vitro-formed cartilage and the underlying substrate.** *Acta Biomater* 8 (4), 1603-1615, doi: 10.1016/j.actbio.2011.12.022.
- Steadman, J. R., Rodkey, W. G., Singleton, S. B. and Briggs, K. K. (1997). **Microfracture technique for full-thickness chondral defects: Technique and clinical results.** *Operative Techniques in Orthopaedics* 7 (4), 300-304, doi: [https://doi.org/10.1016/S1048-6666\(97\)80033-X](https://doi.org/10.1016/S1048-6666(97)80033-X).
- Stockwell, R. A. (1967). **The cell density of human articular and costal cartilage.** *J Anat* 101 (Pt 4), 753-763.
- Stockwell, R. A. (1991). **Cartilage failure in osteoarthritis: Relevance of normal structure and function. A review.** *Clinical Anatomy* 4 (3), 161-191, doi: <https://doi.org/10.1002/ca.980040303>.
- Stroud, J. C., Lopez-Rodriguez, C., Rao, A. and Chen, L. (2002). **Structure of a TonEBP-DNA complex reveals DNA encircled by a transcription factor.** *Nat Struct Biol* 9 (2), 90-94, doi: 10.1038/nsb749.
- Tan Timur, U., Caron, M., van den Akker, G., van der Windt, A., Visser, J., van Rhijn, L., Weinans, H., Welting, T., Emans, P. and Jahr, H. (2019). **Increased TGF-beta and BMP Levels and improved chondrocyte-specific marker expression in vitro under cartilage-specific physiological osmolarity.** *Int J Mol Sci* 20 (4), doi: 10.3390/ijms20040795.
- Tanabe, T. and Tohnai, N. (2002). **Cyclooxygenase isozymes and their gene structures and expression.** *Prostaglandins Other Lipid Mediat* 68-69, 95-114, doi: 10.1016/s0090-6980(02)00024-2.
- Tew, S. R., Peffers, M. J., McKay, T. R., Lowe, E. T., Khan, W. S., Hardingham, T. E. and Clegg, P. D. (2009). **Hyperosmolarity regulates SOX9 mRNA posttranscriptionally in human articular chondrocytes.** *Am J Physiol Cell Physiol* 297 (4), C898-906, doi: 10.1152/ajpcell.00571.2008.
- Thielen, N. G. M., van der Kraan, P. M. and van Caam, A. P. M. (2019). **TGFbeta/BMP signaling pathway in cartilage homeostasis.** *Cells* 8 (9), doi: 10.3390/cells8090969.
- Toyoda, T., Seedhom, B. B., Kirkham, J. and Bonass, W. A. (2003). **Upregulation of aggrecan and type II collagen mRNA expression in bovine chondrocytes by the application of hydrostatic pressure.** *Biorheology* 40 (1-3), 79-85.
- Tsai, T. T., Guttapalli, A., Agrawal, A., Albert, T. J., Shapiro, I. M. and Risbud, M. V. (2007). **MEK/ERK signaling controls osmoregulation of nucleus pulposus cells of the intervertebral disc by transactivation of TonEBP/OREBP.** *J Bone Miner Res* 22 (7), 965-974, doi: 10.1359/jbmr.070322.
- Urban, J. P., Hall, A. C. and Gehl, K. A. (1993). **Regulation of matrix synthesis rates by the ionic and osmotic environment of articular chondrocytes.** *J Cell Physiol* 154 (2), 262-270, doi: 10.1002/jcp.1041540208.

- van Beuningen, H. M., Glansbeek, H. L., van der Kraan, P. M. and van den Berg, W. B. (1998). **Differential effects of local application of BMP-2 or TGF-beta 1 on both articular cartilage composition and osteophyte formation.** *Osteoarthritis Cartilage* 6 (5), 306-317, doi: 10.1053/joca.1998.0129.
- van Beuningen, H. M., van der Kraan, P. M., Arntz, O. J. and van den Berg, W. B. (1994). **Transforming growth factor-beta 1 stimulates articular chondrocyte proteoglycan synthesis and induces osteophyte formation in the murine knee joint.** *Lab Invest* 71 (2), 279-290.
- van der Kraan, P., Vitters, E. and van den Berg, W. (1992). **Differential effect of transforming growth factor beta on freshly isolated and cultured articular chondrocytes.** *J Rheumatol* 19 (1), 140-145.
- van der Windt, A. E., Haak, E., Das, R. H., Kops, N., Welting, T. J., Caron, M. M., van Til, N. P., Verhaar, J. A., Weinans, H. and Jahr, H. (2010). **Physiological tonicity improves human chondrogenic marker expression through nuclear factor of activated T-cells 5 in vitro.** *Arthritis Res Ther* 12 (3), R100, doi: 10.1186/ar3031.
- Villanueva, I., Bishop, N. L. and Bryant, S. J. (2009). **Medium osmolarity and pericellular matrix development improves chondrocyte survival when photoencapsulated in poly(ethylene glycol) hydrogels at low densities.** *Tissue Eng Part A* 15 (10), 3037-3048, doi: 10.1089/ten.TEA.2009.0001.
- Vincent, T. L., Hermansson, M. A., Hansen, U. N., Amis, A. A. and Saklatvala, J. (2004). **Basic fibroblast growth factor mediates transduction of mechanical signals when articular cartilage is loaded.** *Arthritis Rheum* 50 (2), 526-533, doi: 10.1002/art.20047.
- Visser, A. W., de Mutsert, R., le Cessie, S., den Heijer, M., Rosendaal, F. R., Kloppenburg, M. and Group, N. E. O. S. (2015). **The relative contribution of mechanical stress and systemic processes in different types of osteoarthritis: the NEO study.** *Ann Rheum Dis* 74 (10), 1842-1847, doi: 10.1136/annrheumdis-2013-205012.
- Watts, B. A., 3rd, Di Mari, J. F., Davis, R. J. and Good, D. W. (1998). **Hypertonicity activates MAP kinases and inhibits HCO-3 absorption via distinct pathways in thick ascending limb.** *Am J Physiol* 275 (4), F478-486, doi: 10.1152/ajprenal.1998.275.4.F478.
- Weiss, S., Hennig, T., Bock, R., Steck, E. and Richter, W. (2010). **Impact of growth factors and PTHrP on early and late chondrogenic differentiation of human mesenchymal stem cells.** *J Cell Physiol* 223 (1), 84-93, doi: 10.1002/jcp.22013.
- Whitfield, J. F. (2008). **The solitary (primary) cilium--a mechanosensory toggle switch in bone and cartilage cells.** *Cell Signal* 20 (6), 1019-1024, doi: 10.1016/j.cellsig.2007.12.001.
- Wilusz, R. E., Sanchez-Adams, J. and Guilak, F. (2014). **The structure and function of the pericellular matrix of articular cartilage.** *Matrix Biol* 39, 25-32, doi: 10.1016/j.matbio.2014.08.009.
- Winter, A., Breit, S., Parsch, D., Benz, K., Steck, E., Hauner, H., Weber, R. M., Ewerbeck, V. and Richter, W. (2003). **Cartilage-like gene expression in differentiated human stem cell**

- spheroids: a comparison of bone marrow-derived and adipose tissue-derived stromal cells.** *Arthritis Rheum* 48 (2), 418-429, doi: 10.1002/art.10767.
- Wu, M., Chen, G. and Li, Y. P. (2016). **TGF-beta and BMP signaling in osteoblast, skeletal development, and bone formation, homeostasis and disease.** *Bone Res* 4, 16009, doi: 10.1038/boneres.2016.9.
- Xu, J., Wang, W., Clark, C. C. and Brighton, C. T. (2009). **Signal transduction in electrically stimulated articular chondrocytes involves translocation of extracellular calcium through voltage-gated channels.** *Osteoarthritis Cartilage* 17 (3), 397-405, doi: 10.1016/j.joca.2008.07.001.
- Xu, X., Urban, J. P., Tirlapur, U. K. and Cui, Z. (2010). **Osmolarity effects on bovine articular chondrocytes during three-dimensional culture in alginate beads.** *Osteoarthritis Cartilage* 18 (3), 433-439, doi: 10.1016/j.joca.2009.10.003.
- Yammani, R. R., Carlson, C. S., Bresnick, A. R. and Loeser, R. F. (2006). **Increase in production of matrix metalloproteinase 13 by human articular chondrocytes due to stimulation with S100A4: Role of the receptor for advanced glycation end products.** *Arthritis Rheum* 54 (9), 2901-2911, doi: 10.1002/art.22042.
- Yoo, J. U., Barthel, T. S., Nishimura, K., Solchaga, L., Caplan, A. I., Goldberg, V. M. and Johnstone, B. (1998). **The chondrogenic potential of human bone-marrow-derived mesenchymal progenitor cells.** *J Bone Joint Surg Am* 80 (12), 1745-1757, doi: 10.2106/00004623-199812000-00004.
- Yuan, H., Fernandes, H., Habibovic, P., de Boer, J., Barradas, A. M., de Ruyter, A., Walsh, W. R., van Blitterswijk, C. A. and de Bruijn, J. D. (2010). **Osteoinductive ceramics as a synthetic alternative to autologous bone grafting.** *Proc Natl Acad Sci U S A* 107 (31), 13614-13619, doi: 10.1073/pnas.1003600107.
- Zawel, L., Dai, J. L., Buckhaults, P., Zhou, S., Kinzler, K. W., Vogelstein, B. and Kern, S. E. (1998). **Human Smad3 and Smad4 are sequence-specific transcription activators.** *Mol Cell* 1 (4), 611-617, doi: 10.1016/s1097-2765(00)80061-1.
- Zhang, L., Hu, J. and Athanasiou, K. A. (2009). **The role of tissue engineering in articular cartilage repair and regeneration.** *Crit Rev Biomed Eng* 37 (1-2), 1-57, doi: 10.1615/critrevbiomedeng.v37.i1-2.10.
- Zhang, Z., McCaffery, J. M., Spencer, R. G. and Francomano, C. A. (2004). **Hyaline cartilage engineered by chondrocytes in pellet culture: histological, immunohistochemical and ultrastructural analysis in comparison with cartilage explants.** *J Anat* 205 (3), 229-237, doi: 10.1111/j.0021-8782.2004.00327.x.
- Zhou, Y., David, M. A., Chen, X., Wan, L. Q., Duncan, R. L., Wang, L. and Lu, X. L. (2016). **Effects of osmolarity on the spontaneous calcium signaling of in situ juvenile and adult articular chondrocytes.** *Ann Biomed Eng* 44 (4), 1138-1147, doi: 10.1007/s10439-015-1406-4.
- Zimmerman, B. K., Nims, R. J., Chen, A., Hung, C. T. and Ateshian, G. A. (2021). **Direct osmotic pressure measurements in articular cartilage demonstrate nonideal and concentration-dependent phenomena.** *J Biomech Eng* 143 (4), doi: 10.1115/1.4049158.

EIGENANTEIL AN DER DATENERHEBUNG UND -AUSWERTUNG

Die Arbeit wurde mit Ausnahme der Etablierung des PTHrP IRMA Assays in Abschnitt 4.2.11.2 zu 100% von mir selbst durchgeführt. Die Etablierung des PTHrP IRMA Assays fand in Zusammenarbeit mit Dr. Justyna Buchert statt. Aufgrund thematischer Überschneidung beider Projekte und um die Etablierung zügig voranzutreiben, wurde in den entsprechenden Versuchen die Zellkulturarbeit aufgeteilt. Die Aufarbeitung der Proben fand gemeinsam statt. Die Analyse der Zellen mittels Western Blot wurde von mir durchgeführt.

Die Positivkontrolle eines in vivo mineralisierten MSC pellets in Figure 16 E wurde von Dr. Simon Dreher zur Verfügung gestellt.

Diese Daten wurden in keiner anderen Doktorarbeit verwendet.

EIGENE VERÖFFENTLICHUNGEN UND BEITRÄGE

Kongressbeiträge:

Hammersen, T., Zietzschmann, S., Richter, W.

Inverse regulation of Cartilage Matrix production by High Extracellular Calcium in Articular Chondrocytes and Mesenchymal Stroma Cells

Poster presentation, Annual Meeting of the Orthopaedic Research Society (ORS), February 2022, Tampa, FL, US

Hammersen, T., Zietzschmann, S., Richter, W.

Inverse Effects of Calcium on Cartilage Matrix Production by Articular Chondrocytes versus Mesenchymal Stroma Cells: Implications for Osteochondral Cartilage Engineering

Poster presentation, 6th World Congress Tissue Engineering and Regenerative Medicine International Society (TERMIS), November, 2021, Maastricht, NL

Hammersen, T., Zietzschmann, S., Richter, W.

Extracellular calcium differentially regulates cartilage matrix production by articular chondrocytes and mesenchymal stroma cells

Oral presentation, 29th Annual Meeting of the European Orthopaedic Research Society (EORS), September 2021, Rome, IT

Abstract publiziert:

Hammersen, T., Zietzschmann, S. & Richter, W. (2021, November). *Extracellular calcium differentially regulates cartilage matrix production by articular chondrocytes and*

mesenchymal stroma cells. In Orthopaedic Proceedings (Vol. 103, No. SUPP_13, pp. 41-41). The British Editorial Society of Bone & Joint Surgery, doi: 10.1302/1358-992X.2021.13.041

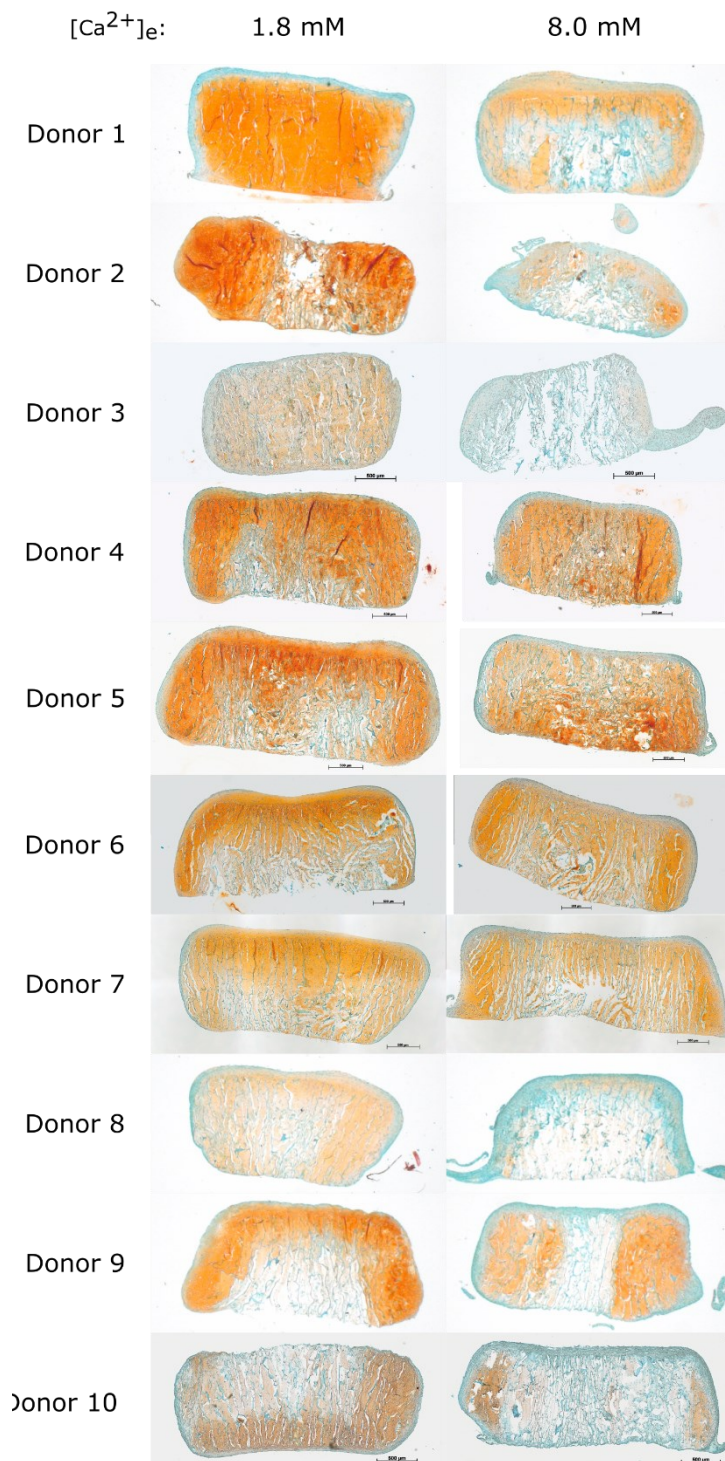
Hammersen, T., Zietzschmann, S., Richter, W.

Inverse effects of calcium on cartilage matrix production by articular chondrocytes versus mesenchymal stroma cells

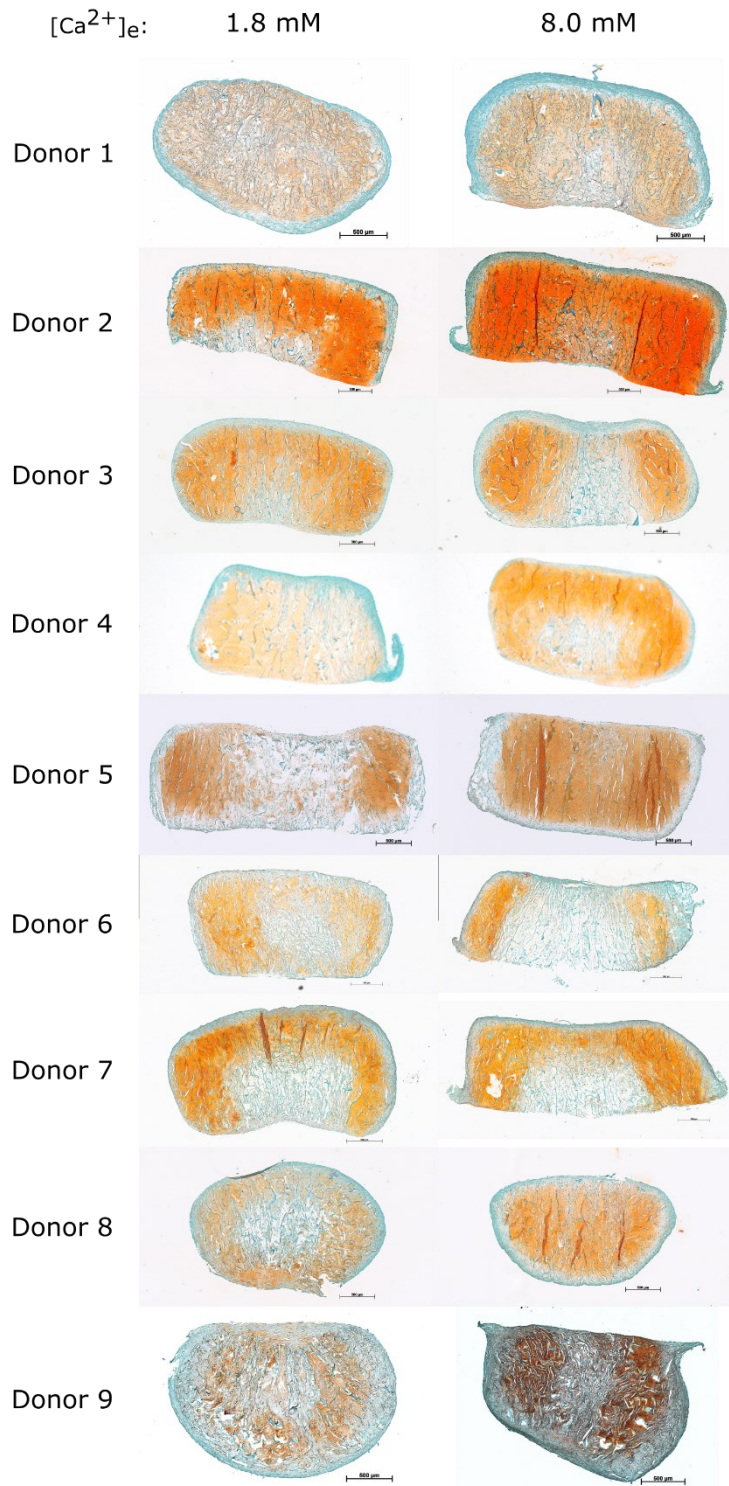
Rapid Fire Presentation, Joint Meeting of the French and German Societies for Matrix Biology, May 2021, Online

APPENDIX

Safranin O staining AC d35



Appendix Figure 1 Safranin O staining of AC-based TE constructs on day 35. Histological Safranin O staining for samples from all AC donor populations considered for the analysis of Figure 19. See the caption of Figure 19 A for details.

Safranin O staining MSC d35

Appendix Figure 2 Safranin O staining of MSC-based TE constructs on day 35. Histological Safranin O staining for samples from all MSC donor populations considered for the analysis of Figure 20. See the caption of Figure 20 A for details.

LEBENS LAUF

Persönliche Daten

Vorname: Tim Dieter
Nachname: Hammersen
Geburtsdatum: 07.08.1990
Geburtsort: Frankfurt a.M. (Höchst)
Nationalität: Deutsch

Universitärer Werdegang

Seit 12/2017: Annahme als Doktorand an der Medizinischen Fakultät der Ruprecht Karls-Universität Heidelberg (Heidelberg, Deutschland)

09/2017 – 05/2022: Wissenschaftlicher Mitarbeiter am Universitätsklinikum Heidelberg (Heidelberg, Deutschland)
Promotion am Zentrum für Orthopädie, Unfallchirurgie und Paraplegiologie, Forschungszentrum für Experimentelle Orthopädie
Leitung: Prof. Dr. Wiltrud Richter

09/2015 – 08/2017: Masterstudium an der VU University Amsterdam (Amsterdam, Niederlande)
Abschluss: Master of Science (Human Movement Science – Research Master)
Masterarbeit am MOVE Research Institute Amsterdam
Betreuer: Prof. Dr. Richard Jaspers

10/2011 – 09/2015: Bachelorstudium an der Eberhard Karls Universität Tübingen (Tübingen, Germany)
Abschluss: Bachelor of Science (Biologie)
Bachelorarbeit am Institut für Medizinische Genetik und Angewandte Genomik
Betreuer: Dr. Nicolas Casadei

Schulischer Werdegang

08/2000 – 06/2010 Eichendorffschule mit gymnasialer Oberstufe Immanuel Kant (Kelkheim, Deutschland)

June 18, 2010 Abitur (Allgemeine Hochschulreife)

DANKSAGUNG

Insbesondere geht mein Dank an Prof. Dr. Wiltrud Richter, für die Bereitstellung der Mittel und für die Möglichkeit, dass ich an diesem spannenden Thema forschen und meine Doktorarbeit verfassen konnte. Liebe Wiltrud, danke für die hochwertige wissenschaftliche Ausbildung, die ich von Dir erhalten habe, sowie für Deine große fachliche Expertise, auf die ich mich immer verlassen konnte. Ich habe viel von Dir gelernt und Du hast es geschafft, dass ich immer wieder über mich hinauswachsen konnte. Danke auch dafür, dass Du es mir ermöglicht hast an zahlreichen internationalen Kongressen teilzunehmen, auf denen ich neben viel Erfahrungen auch neue Kontakte knüpfen konnte.

Danke an die vielen Ärztinnen und Ärzte für die Aufklärung der Patientinnen und Patienten, sowie die Entnahme von Knorpelproben und Knochenmarkaspiraten. Ohne Ihre Hilfe und die gesammelten Proben wäre meine Forschung nicht möglich gewesen.

Mein Dank geht auch an PD Dr. Solvig Diederichs. Danke Solvig, dass Du deine wissenschaftliche Expertise mit mir geteilt hast und immer bereit warst mir bei Fragen zu helfen, meine Ergebnisse mit mir zu diskutieren und als Ansprechperson bereit zu stehen.

Ich bedanke mich außerdem bei Dr. Justyna Buchert für die Unterstützung bei der Etablierung des PTHrP IRMA, für die kurze Einführung in die Welt der iPS Zellkultur, sowie für die ständige Hilfsbereitschaft bei Fragen im Laboralltag. Des Weiteren danke ich Dr. Svitlana Melnik und Dr. Safak Chasan für die große wissenschaftliche Expertise und die vielen kleinen und großen Tipps bei der Versuchsplanung und im Laboralltag.

Ich danke auch Birgit Frey für die Hilfe bei allen Fragen rund um histologische Untersuchungen. Danke auch an Petra Glück und Tetyana Fragnito, dass ihr euch so herzlich und aufmerksam um all das gekümmert habt, was den Laboralltag so reibungslos funktionieren lässt.

Vielen Dank auch an alle Kolleginnen und Kollegen, die mich während der Doktorarbeit begleitet haben. Ihr habt eine Arbeitsatmosphäre geschaffen, in der ich mich immer wohl gefühlt habe und in der es Spaß gemacht hat zu arbeiten. Danke für eure Unterstützung bei allen wissenschaftlichen Problemen, für die vielen lustigen Momente, im Labor und außerhalb, für die entstandenen

Freundschaften und besonders für die vielen schönen Erinnerungen an meine Zeit als Doktorand, die immer auch mit Erinnerungen an Euch verbunden sein werden.

Insbesondere möchte ich mich bei meinen ehemaligen Mitdoktorandinnen Dr. Janine Lückgen und Dr. Ursula Kreuser bedanken. Danke, Janine, für deine Freundschaft, sowie für deine fachliche und emotionale Unterstützung besonders in den schwierigen Phasen der Doktorarbeit. Liebe Ursula, dir danke ich besonders für alle Unterstützung in den letzten Jahren, fachlich und privat. Danke für deine aufmerksame und humorvolle Art. Ich freue mich, dass du deine anfängliche Skepsis gegen „den neuen im Büro“ zügig ablegen konntest und bin dir dankbar für die schöne Freundschaft, die entstanden ist.

Einen großen Dank auch an Isolde, Sophia und Georg Klampfleuthner, dass ihr mich so herzlich in die Familie aufgenommen habt und nicht nur während der Doktorarbeit immer für uns da seid, uns motiviert und an uns denkt.

Ich möchte mich ganz besonders bei meiner ganzen Familie für die kontinuierliche Unterstützung bedanken, allen voran meinen Eltern, Isa und Dirk. Mama und Papa, nicht nur während der Doktorarbeit wart ihr immer für mich da, sondern mein Leben lang konnte ich mich immer auf euch verlassen. Ihr habt mich zu dem Menschen gemacht, der ich heute gerne bin. Dafür bin ich euch sehr dankbar.

Liebe Feli, von Anfang an warst du ein fester Bestandteil meines Laboralltags und ich bin sehr glücklich, dass du inzwischen auch fester Bestandteil meines Lebens bist. Neben so vielen Dingen, für die ich dir danken will, möchte ich dir hier besonders für deine Zuversicht und deinen Antrieb während der Doktorarbeit danken. Dich um mich zu haben und zu wissen, dass du da bist, ist ein schönes Gefühl, das mir nicht nur während der Doktorarbeit immer wieder Kraft und Freude gibt.

EIDESSTATTLICHE VERSICHERUNG

1. Bei der eingereichten Dissertation zu dem Thema

“Physicochemical stimuli to enhance the quality of human engineered cartilage: The role of osmolarity and calcium”

handelt es sich um meine eigenständig erbrachte Leistung.

2. Ich habe nur die angegebenen Quellen und Hilfsmittel benutzt und mich keiner unzulässigen Hilfe Dritter bedient. Insbesondere habe ich wörtlich oder sinngemäß aus anderen Werken übernommene Inhalte als solche kenntlich gemacht.
3. Die Arbeit oder Teile davon habe ich bislang nicht an einer Hochschule des In- oder Auslands als Bestandteil einer Prüfungs- oder Qualifikationsleistung vorgelegt.
4. Die Richtigkeit der vorstehenden Erklärungen bestätige ich.
5. Die Bedeutung der eidesstattlichen Versicherung und die strafrechtlichen Folgen einer unrichtigen oder unvollständigen eidesstattlichen Versicherung sind mir bekannt. Ich versichere an Eides statt, dass ich nach bestem Wissen die reine Wahrheit erklärt und nichts verschwiegen habe.

Ort und Datum

Unterschrift